Nanostructured vectors for the transport of active molecules through biological membranes for pharmaceutical and nutraceutical applications

Sabrina Bochicchio

Department of Industrial Engineering

*Corso di dottorato in Ingegneria Industriale-
curriculum Ingegneria Chimica
(XV ciclo)*

Nanostructured vectors for the transport of active molecules through biological membranes for pharmaceutical and nutraceutical applications

Supervisor
*Prof. Anna Angela Barba*

Ph.D. student
Sabrina Bochicchio

Scientific Referees
Prof. Gaetano Lamberti
Prof. Sotiris Missailidis
Prof. Gabriele Grassi

Ph.D. Course Coordinator
Prof. Ernesto Reverchon

To my family

Publications

(Inherent the Ph.D. project)

International Journals

- **Bochicchio S.**; Dapas B.; Russo I.; Ciacci C.; Piazza O.; De Smedt S.; Pottie E.; Barba A.A.; Grassi G.; "In vitro and ex vivo delivery of tailored siRNA-nanoliposomes for E2F1 silencing as a potential therapy for colorectal cancer"; *IJP - International Journal of Pharmaceutics*, 2017, in press

- **Bochicchio S.**; Dalmoro A.; Recupido F.; Lamberti G.; Barba A.A.; "Nanoliposomes production by a protocol based on a simil-microfluidic approach"; accepted as publication in "Lecture Notes in Bioengineering (LNBE)", Springer Ed., 2017

- **Bochicchio S.**; Dalmoro A.; Barba A.A.; D'Amore M.; Lamberti G.; "New preparative approaches of micro and nano drug delivery carriers"; *Current Drug Delivery*, 2017, 14(2), 203-215

- Dalmoro A.; Abrami M.; Galzerano B.; **Bochicchio S.**; Barba A.A.; Grassi M.; Larobina D.; "Injectable chitosan/b-glycerophosphate system for sustained release: gelation study, structural investigation, and erosion tests"; *Current Drug Delivery,* 2017, 14(2), 216-223

- Piazza O.; Russo I.; **Bochicchio S.**; Barba A. A.; Lamberti G.; Zeppa P.; Di Crescenzo V.; Carrizzo A.; Vecchione C.; Ciacci C.; "Cyclin D1 Gene Silencing by siRNA in ex vivo human tissues cultures"; *Current Drug Delivery,* 2017, 14(2), 246-252

- D'Apolito R.; **Bochicchio S.**; Dalmoro A.; Barba A. A.; Guido S.; Tomaiuolo G.; "Microfluidic investigation of the effect of liposome surface charge on drug delivery in microcirculation"; *Current Drug Delivery*, 2017, 14(2), 231-238

- **Bochicchio S.**; Barba A.A.; Grassi G.; Lamberti G.; "Vitamin delivery: carriers based on nanoliposomes produced via ultrasonic irradiation"; *LWT - Food Science and Technologies*, 2016, 69, 9 -16

- **Bochicchio S.**; Dalmoro A.; Barba A.A.; Grassi G.; Lamberti G.; "Liposomes as siRNA delivery vectors"; *Current Drug Metabolism*, 2015, 15, 882-892

- Barba A.A.; **Bochicchio S.**; Lamberti G.; Dalmoro A.; "Ultrasonic energy in liposome production: process modelling and size calculation"; *Soft Matter*, 2014, 10 (15), 2574 – 2581

Technical Journals

- **Bochicchio S.**; Barba A.A.; Lamberti G.; "Nanovettori per il rilascio di farmaci antitumorali a base di acidi nucleici"; ICF- Chemical and Pharmaceutical Industry italian journal, n. 2, 2015

- Dalmoro A., **Bochicchio S.**, Lamberti G., d'Amore M., Barba A.A.; "Intensificazione di processo per nuove formulazioni"; AIDIC news, n. 3, 2016

Work submitted:

- **Bochicchio S.**; Sala M.; Spensiero A.; Scala M.C.; Gomez-Monterrey I.M.; Lamberti G.; Barba A.A.; "On the design of tailored liposomes for peptide delivery"

Book Chapters

- **Bochicchio S.**; Lamberti; Barba A.A.; "Phenomenological and formulation aspects in tailored nanoliposomes production" chapter in book Liposomes, InTech Ed., 2016, in press

- Barba A.A.; **Bochicchio S.**; Dalmoro A.; Caccavo D.; Cascone S.; Lamberti G.; "Polymeric and lipid-based systems for controlled drug release: an engineering point of view; submitted as chapter in book to Pharmaceutical Nanotechnology, Volume IX: Sustained and controlled delivery systems, 2017

Work in preparation:

- Russo I.; **Bochicchio S.**; Piazza O.; Lamberti G.; Barba A.A.; Carrizzo A.; Vecchione C.; Zeppa P.; Iovino P.; Bucci, C.; Ciacci C.; "Control of inflammation progression in inflammatory bowel disease by suitable systems for cyclin d1 and e2f1 sirna delivery"; 2017

Proceedings

International

- Russo I.; **Bochicchio S.**; Piazza O.; Barba A.A.; Lamberti G.; Carrizzo A.; Zeppa P.; Vecchione C.; Iovino P.; Bucci, C.; Ciacci C.; "Evaluation of efficacy of new vectors for siRNA CYCLIN D1 and E2F1 delivery in control of cancer progression in inflammatory bowel disease" presented to 12th Congress of European Crohn's and Colitis organization 15-18/02/2017, Barcelona (Spain)

- **Bochicchio S.**; Dalmoro A.; Recupido F.; Lamberti G.; Barba A.A.; "Nanoliposomes production by a protocol based on a simil-microfluidic approach", presented to WIVACE 2016/BIONAM 2016 workshop, 4-7/10/2016, University of Salerno, Fisciano (SA) (Italy) and in proceedings on "Lecture Notes in Bioengineering (LNBE)", Springer Ed.

- Sala M.; **Bochicchio S.**; Spensiero A.; Scala M. C.; Gomez-Monterrey I. M.; Dalmoro A.; Lamberti G.; Campiglia P.; Barba A. A.; "Drug delivery system of peptide KRX 29 for treatment of chronic heart failure", 15th Naples Workshop on Bioactive Peptides, 23-25 June 2016 Naples (Italy)

- D'Apolito R.; **Bochicchio S.**, Tomaiuolo G.; Guido S.; Dalmoro A; Barba A.A.; "Liposomes as drug delivery system: effect of superficial charge on margination in blood flow", 14th European Symposium on Controlled Drug Delivery, 13-15/04/2016 Egmond aan Zee (Holland)

- **Bochicchio S.**; Sala M.; Spensiero A.; Scala M.C.; Gomez-Monterrey I.M.; Campiglia P.; Dalmoro A.; Lamberti G.; Barba A.A.; "Liposomal structures design for peptide delivery in heart failure therapy", 14th European Symposium on Controlled Drug Delivery, 13-15/04/2016, Egmond aan Zee (Holland)

- **Bochicchio S.**; Dalmoro A.; Cavallaro G.; Craparo F.; Sardo C.; Giammona G.; Lamberti G.; Barba A.A.; "Nanoparticle based PHEA-DETA-PLA copolymer for NABDs delivery", 14th European Symposium on Controlled Drug Delivery, 13-15/04/2016, Egmond aan Zee (Holland)

- Barba A.A.; **Bochicchio S.;** Lamberti G; Sala M.; Campiglia P.; "Ultrasonic assisted production of nanoliposomes as peptide delivery vectors", 42nd Annual Meeting & Exposition of the Controlled Release Society CRS 2015, 26-29/07/2015, Edinburgh (Scotland)

- Cascone S.; **Bochicchio S.;** Lamberti G.; Titomanlio G.; Barba A.A.; "In vitro and in silico models in pharmacokinetic studies", 42nd Annual Meeting & Exposition of the Controlled Release Society CRS 2015, 26-29/07/2015, Edinburgh (Scotland)

- Caccavo D.; Cascone S.; **Bochicchio S.;** Lamberti G.; Dalmoro A.; Barba A.A.; "Hydrogels-based matrices behavior: experimental and modeling description", 42nd Annual Meeting & Exposition of the Controlled Release Society CRS 2015, 26-29/07/2015, Edinburgh (Scotland)

- **Bochicchio S.;** Dalmoro A.; Cascone S.; Lamberti G.; Barba A.A.; "dsDNA encapsulating in nanoliposomal structures towards gene therapies", 1st International Congress of the Controlled Release Society-Greek local chapter 2015, 27-28/05/2015, Athens (Greece)

- Dalmoro A.; **Bochicchio S.;** Apicella P.; d'Amore M.; Barba A.A.; "Micro and nano structured vectors for the drug delivery", 21st International Congress of Chemical and Process Engineering CHISA 2014, 23-27/08/2014, Praga (Czech Republic)

- **Bochicchio S.;** Dalmoro A.; Grassi G.; Lamberti G.; Barba A.A. "Vectors for vitamins delivery: nano liposomes production via ultrasonic irradiation", 13th European Symposium on Controlled Drug Delivery, 16-18/04/2014, Egmond aan Zee (Holland)

- Dalmoro A.; **Bochicchio S.;** Lamberti G.; d'Amore M.; Barba A.A. "Vectors for vitamins delivery: shell-core microparticles production via ultrasonic atomization and microwave stabilization", 13th European Symposium on Controlled Drug Delivery, 16-18/04/2014, Egmond aan Zee (Holland)

- Barba A.A**.; Bochicchio S.**; Dalmoro A.; Lamberti G. "Liposomal SUVs preparation by ultrasonic energy: a new approach based on a conventional technique", 8th World Meeting on Pharmaceutics, Biopharmaceutics and Pharmaceutical Technology, 31/03-03/04/2014, Lisbona (Portugal)

National

- **Bochicchio S.**; Dalmoro A.; Lamberti G.; d'Amore M.; Barba A.A. "Chemical Engineering approaches in the production of dedicated systems for the dosage of active molecules" Microwaves and ultrasound as process intensification tools for drug carriers production, national convention GRICU 2016, 12-14/09/2016, Anacapri (NA), Italy

- Barba A.A.; Lamberti G.; Dalmoro A.; **Bochicchio S.**; d'Amore M. "Nuovi sviluppi della terapia genica: approcci multidisciplinari al dosaggio controllato di siRNA", National Workshop, 14-15/09/2015, University of Salerno, Fisciano (SA), Italy

- d'Amore M.; Dalmoro A.; **Bochicchio S.**; Lamberti G.; Barba A.A. "Produzione di sistemi di rilascio ottimali per i Nucleic Acid Based Drugs in terapie antitumorali", Le Giornate del Farmaco, I edizione , 12/04/2013 University of Salerno, Fisciano (SA), Italy

Contents

Figures index

VIII

IX

Tables index

Abstract

Purpose of the PhD thesis was to develop dedicated lipid nanostructured vectors with tailored features (in terms of size, surface charge, load capability, stimuli responsive ability and stability) through the design of novel production processes expressly developed for nutraceutical and therapeutic agents encapsulation.

The preliminary performed review of the main processes used for liposomes production have underlined that the majority of the conventional and more innovative methods adopted show a number of drawbacks such as few product volumes in output (directly linked to the impossibility in scaling up the process), high energy consumption, long times of production together with the use of toxic solvents and other process drastic conditions. To the light of these literature findings and with the aim to produce nanostructured vectors through more sustainable processes, two novel techniques, sharing the ultrasound technology as process intensification tool used in particles size reduction and homogenization operations, were designed and developed to respond to the needs of a better process performance, improving its efficiency and cutting down energy consumption.

At first, based on the use of ultrasound as alternative energy resource, a solid particles size reduction process was developed and coupled with the bench scale conventional Thin Film Hydration (TFH) method. This technique provides the generation of a lipid film which is formed after solvents evaporation through the use of a rotary evaporator. The dried film is then hydrated, spontaneously producing micrometric vesicles characterized by the presence of several bilayers. Then the method was revisited by adding the ultrasound assisted step developed in order to produce, in a versatile manner, structures with the desired dimension (on micro/nano scale), starting from the micrometric ones.

Four are the main sections composing the set-up to apply this innovative protocol: a feeding section, a solvent evaporation section, a liposomes production/homogenization section and a recovery section. In particular, the homogenization section is composed of a 3 mm sonication tip (operative frequency 20 kHz) which acts on micrometric vesicles sample aliquots.

Subsequently to the realization of the production bench scale apparatus, the phenomenology connected to the vectors constitution was investigated and a dynamic model able to describe the curvature of a lipid bilayer under the effect of ultrasonic energy was then proposed and tested.

In that regard, starting from micrometric vesicles, the ultrasound energy is used to break the lipid bilayer into smaller pieces, then these pieces close themselves in spherical structures producing small vesicles. Moreover the role of several process parameters were also elucidated.

Once established its reliability and due its great potential in reducing time spent, without compromising the integrity of the liposomal systems produced (in terms of structure and load), the ultrasound intensification tool was also used for liposomes homogenization operation during vesicles production through a simil-microfluidic approach.

As a matter of fact, in order to produce higher volumes of lipid vectors, potentially on production scale, directly with nanometric size, a simil-microfluidic apparatus was expressly designed and fabricated, overcoming the limitations of the small output volumes typical of the conventional bench scale techniques.

There are five main sections composing the realized apparatus: a feeding section, a pumping section, a production section, an homogenization section and a recovery section. In particular the homogenization section is composed of a 6 mm sonication tip (operative frequency 20 kHz) directly immersed in the entire hydroalcholic solution containing nanoliposomes.

As previously done, the phenomenological aspects involved in vectors constitution were investigated for this new adopted set-up. In particular, the reproduction of the phenomenology connected to the vesicles formation through a microfluidic approach was achieved by the use of constructive expedients (millimetric diameter of tubes, peristaltic pumps, injection needle). Particularly, nanostructured vectors formation happens at the interfaces between the alcoholic and water phases, when they start to interdiffuse in a direction normal to the liquid flow stream; changes in flow conditions result in size variations of the insertion section of the organic phase reflecting on the vesicles dimensional features.

In that regards, taking into account that size and size distribution are key parameters determining liposomes performance as carrier systems in both pharmaceutical and nutraceutical applications, a control on the produced nanoliposomes dimensional features was demonstrated by tuning the volumetric flow rates and the lipids concentration process parameters. In particular, it was understood that increasing the ratio between the water volumetric flow rate to the lipids-ethanol volumetric flow rate the liposomes dimensional distibution increases; on contrary, ultrasonic energy enhances the homogenization of the hydroalcoholic bulk and, as expected on the bases of previous studies conducted on smaller volumes, its duty cycle application efficaciously promoted a better vesicles dimensional distribution. This result

was also confirmed by working at equal flow rates but at different lipid concentrations. Finally, the developed simil-microfluidic apparatus, working at room conditions and in absence of toxic solvents, makes nanoliposomes production a safe and low cost process, highly productive due to the use of ultrasound which was demonstrated to be a scalable means for process intensification. By using the two developed experimental set-up, several classes of liposomal structures were formulated and produced to respond to specific requests of nutraceutical and pharmaceutical applications. Through the ultrasound assisted tool at first coupled with the conventional THF method and subsequently used as integrant part of the homogenization section of the simil-microfluidic apparatus, different active molecules were successfully encapsulated in lipid nanostructured vectors solving the critical issues linked to their naked administration and transport through biological membranes. In particular, nanoliposomes containing vitamins with different hydrophobicity (α-tocopherol, ergocalciferol, vitamin B12) and ferrous sulfate, with highly interesting features for nutraceutical market, were produced achieving stable loaded nanoliposomes with high encapsulation efficiencies and good dimensional features.

In details, for vitamins-nanoliposomes productions, neuter vesicles with micrometric size, ranging from 2.9 μm to 5.7 μm, were produced, obtaining, after sonication in duty cycle, small vesicles in the average range of 40 nm to 51 nm in size. High encapsulation efficiency (e.e.) was obtained in both micrometric vesicles, with a e.e. % of 72.0 ± 00 % for vitamin B12, 95.0 ± 7.07 % for α-tocopherol and 81.5 ± 2.12 % for ergocalciferol, and small vesicles, with an e.e. % of 56.2 ± 8.51 % for vitamin B12, 76.3 ± 14.02 % for α-tocopherol and 57.5 ± 13.9 % for ergocalciferol (the higher the vitamin hydrophobicity, the higher the encapsulation efficiency). Finally, a comparison between vitamin B12 load achievable with the developed technique and the vitamin load achievable by breaking unloaded preformed liposomes (conventional approach) showed an increase of encapsulation efficiency in small vesicles from 40% to 56.2 %, confirming the effectiveness of the pointed out technique.

Regarding the ferrous sulfate-nanoliposomes, their massive production was possible due to the simil-microfluidic approach with a precise control on particles size and size distribution. In particular, the effect of different weight ratios of iron to the total formulation components (0.06, 0.035, 0.02 and 0.01 iron/total components weight ratio) on the final vesicles encapsulation efficiency was investigated obtaining with the last formulation an high encapsulation efficiency (up to 97%).

In general, ferrous sulfate loaded nanoliposomes, negative charged, with good dimensional features (127-135 nm for not sonicated and 48-76 nm for sonicated liposomes) were successfully produced through the use of the simil-microfluidic method developed, obtaining an elevated process yield if

compared to the classical bench scale techniques (THF and Ethanol Injection).

For pharmaceutical purposes, anionic nanoliposomes containing a new synthetized peptide (KRX29) for a not conventional heart failures therapy and new, cutting edge, nucleic acids based therapeutics agents (NABDs), used in gene therapy, were successfully produced.

Regarding KRX29-nanoliposomes production, micrometric particles of 7.2-11.7 μm were obtained and sized with the use of the developed ultrasound assisted process thus achieving 22 – 35 nm vesicles. The effect of liposomes charge on both peptide encapsulation and recovery efficiencies was at first studied, showing an higher encapsulation efficiency (about 100%) achieved (both in small and large vesicles) by using the higher charge ratio formulation (13:1 (-/+)). Viceversa, the ability to recover the entrapped peptide was obtained for loaded systems (both in small and large vesicles) at the lower charge ratio formulation (1:1 (-/+)). As the charge ratio, also the peptide concentration showed influence on the liposomes encapsulation efficiency.

For NABDs complexes production, at first preliminary experiments in which dsDNA was used to simulate the structure of siRNA molecule were done by testing different dsDNA/DOTAP lipid charge ratio (3:1, 5:1 and 7:1 (+/-)) in order to achieve the higher dsDNA encapsulation efficiency in the smaller carrier possible. DOTAP phospholipid was used due to its positive charge. The performed activities have confirmed the versatility of the ultrasound assisted technique for producing micro (2.2 – 2.9 μm) and nano lipid vectors (28 - 56 nm) encapsulating NABDs. In particular, the charge ratio (+/-) variation from 3:1 to 7:1 (+/-) by changing the amount of positive lipid (DOTAP) used in liposome preparation have allowed to an improved e.e. wich was 64 % and 100 % respectively for small and large vesicles by using the 7:1 (+/-) charge ratio.

Starting from these preliminary tests, siRNAs-nanoliposomes complexes were produced for the inhibition of E2F1 protein expression, studied as a potential way to treat colorectal cancer associated to Inflammatory Bowel Diseases. By the TFH/sonication technique nanoliposomes with 33-38 nm range size and 100% siRNA encapsulation efficiency were obtained. The produced loaded nanoliposomes demonstrated a very low cytotoxicity in cells when compared with the commercial transfection agent Lipofectamine® 2000 and an excellent uptake in the cultured human colon mucosa tissues. A remarkable anti-E2F1 expression effect after siE2F1-1324-nanoliposome samples transfection has been demonstrated also in a dynamic human model such the colon tissue microenvironment (i.e. an 80.5% reduction of E2F1 expression respect to the basal tissue was achieved in patient 4), a clear tendency to respond in a patient-dependent way was observed.

All the achieved results highlight the potentiality of the purposely designed nanoliposomes in deliver, in a controlled manner, different active molecules for both pharmaceutical and nutraceutical purposes. The formulative and the chemical engineering approaches adopted in this thesis for nanostructured vectors production respectively enhance the product quality (nanoparticles with tailored features) and make the process more attractive in terms of improved safety and reduced costs.

1. Topic and aims

This chapter underlines the reason why the necessity of nanostructured vectors for the transport of active molecules through biological membranes is of critical importance. Moreover the aims of the thesis and the research organization plan to reach the aims are described.

Keywords

Nanostructured vectors; Advanced Drug Delivery Systems (DDSs); Active molecules; Controlled release; Therapeutic agents

1.1 Nanostructured vectors

Advanced Drug Delivery Systems (DDSs) production is one of the main challenges in the development of effective pharmacological therapies as well as in the growth of new nutraceutical products. Main purposes of an ideal DDSs are: to protect loaded active molecules from degradation in physiological environments; to deliver them in a controlled manner (time period and releasing rate) and towards a specific organ or tissue (targeted drug delivery); to allow the maintenance of the drug level in the body within therapeutic window. Smart features, such as to respond to physiological stimuli and to trigger active molecules release, are also desirable. To achieve all these properties, delivery systems material, size, charge, affinity with entrapped active molecules – biological membranes, play a crucial role. Being characterized by a promising pharmacokinetic and a favorable safety profile, liposomes are ideal carriers of relevant active molecules classes: important micronutrients, such as vitamins and minerals, and powerful and cutting-edge therapeutic agents, such as Nucleic Acid Based Drugs (NABDs) and novel synthetized active ingredients.

1.2 Aims of this thesis

Aims of this research project are: to develop dedicated nanostructured vectors with tailored features (in terms of size, surface charge, load capability, stimuli responsive ability) and the relative suitable characterization procedures; to investigate the mechanisms that regulate vectors constitution and release of the loaded active molecules to propose mathematical descriptions of the main physical phenomena; to study the role of the main process parameters optimizing both production stages and loading/stability – in physiological environments – features of produced nanovectors.

1.3 Planned activities

Gantt

Main activity / Year / Detail / Quadrimester	2014			2015			2016		
	I	II	III	I	II	III	I	II	III
Literature review									
Developed vectors for the transport of active molecules through biological membranes. Nature, structure and size.	█	█	█	█	█	█	█		
Conventional and emerging technologies to produce micro-, nano- structured lipid carrier	█	█	█	█					
Bench scale production of lipidic micro-nano- vectors									
Ultrasonic energy in lipid vectors production (bench scale experimental set-up apparatus)	█								
Characterization protocols (morphology, structure, size)	█	█							
Lipid bilayers refolding phenomena study, modeling size prediction	█	█		█					
Loaded lipid carriers production by ultrasonic assisted technique (with active model molecules); process parameters optimization	█	█		█					
Characterization protocols (morphology, structure, size, encapsulation efficacy, loading)	█	█		█					
In vitro testing (stability, realease properties)		█		█					
Vitamins / Peptides / NABDs loaded vectors in ex-vivo tissues testing									
Vitamins / Peptides / NABDs loaded vectors production (dsDNA as model NABDs, siRNA for specific diseases)	█	█	█	█					
Vitamins / Peptides / NABDs loaded vectors characterization			█	█	█				
Vitamins / Peptides / NABDs loaded vectors transfection in ex vivo tissues				█	█	█			
Relevant transport phenomena Relevant formulative and process parameters tuning	█			█	█				
Design and realization of a semi-continuous experimental set-up									
Component selection, plant layout design				█	█		█		
Set up realization, fluid dynamic investigation, testing					█		█	█	█
Tailored (in loading, size and structures) lipid vector production							█	█	█

During the first year, the research activity was focused on the literature review concerning the nanostructured vector for the transport of active molecules through biological membrane and the techniques relatives to their production. At first, based on the use of ultrasound as alternative energy resource, a particles size reduction process was developed and coupled with the bench scale conventional Thin Film Hydration (TFH) method for nanoliposomes production. In particular, the phenomena which take place during liposome formation after sonication were analyzed and a mathematical model for the prediction of the final liposomes size was proposed. Then the activity was focused on the production of nanostructured liposomal vectors, loaded with vitamins, peptides and dsDNA (simulating siRNA structure), through the ultrasound assisted technique developed. In the second year the literature review has been continued and nanostructured vectors able to encapsulate siRNA, for their transfection in cells and ex vivo human tissue, have been produced. The relevant transport phenomena have been analyzed along with the relevant formulative and process parameters tuning. Furthermore, the design of a semi-continuous experimental set-up for a larger scale lipid vectors production, including the component selection and plant layout design, has been started and continued during the third year. In this year the research activity concerns the realization and testing of a simil-microfluidic experimental apparatus for the production of nanostructured vectors with tailored features, in terms of size, charge and load capability was done and the relevant phenomena have been analyzed again along with the formulative and process parameters tuning. Finally, the developed semi-continuous experimental set-up was applied to ferrous sulfate nanostructures vectors production for nutraceutical applications.

1.4 Outline of the thesis

An introduction on the importance of microencapsulation and liposomes as drug delivery systems (Chapter two) is followed by the review of the literature concerning conventional and emerging technologies to produce micro- and nano- structured lipid carrier systems (Chapter three). Then, two developed techniques for liposomes production, the ultrasound-assisted Thin Film Hydration technique and the simil-microfluidic method developed, are shown and their layout, principles and phenomenological aspects are described (Chapter four). Afterwards, all the applications concerning the encapsulation of active molecules for nutraceutical (vitamins and ferrous sulfate) and pharmaceutical (NABDs and peptides) purposes through the ultrasound-assisted Thin Film Hydration technique and the simil-microfluidic apparatus developed are presented (Chapter five). The conclusive part endorses the usefulness of the novel techniques for lipid nanostructured vectors production, based on an ultrasound assisted size reduction/homogenization process used as powerful intensification tool

(Chapter six). Finally, the abstracts relative the main pubblications inherent the Ph.D. project are reported (Appendix).

Table 1. *Thesis map*

Chapter 2	Liposomes generalities
Chapter 3	State of art of liposomes production
Chapter 4	Experimental set-up: design and realization Phenomenological aspects
Chapter 5	Applications – each of them is self-standing
Chapter 6	Conclusive remarks about the main findings of this PhD research project
Appendix	Abstracts of the main publications inherent the PhD project

Chapter Two

2. Introduction

This chapter outlines the importance of microencapsulation processes with their related critical issues. Moreover the features and the advantages of liposomes as carrier systems for therapeutic and nutraceutical agents delivery are presented along with the necessity of their inclusion in nanostructured vectors.

Keywords

Microencapsulation; Liposome; Controlled Drug Delivery; Pharmaceutical agent; Nutraceutical agent

2.1 Importance of microencapsulation processes

Microencapsulation is a process by which solid, liquid or gaseous active ingredients are packaged within a second material for the purpose of shielding the active ingredient from the surrounding environment (Dubey, 2009). Nanoencapsulation is similar to microencapsulation but at sizes on the nano scale. Microparticles are particles with a diameter of 1-1000 μm, while nanopaticles are <1 μm in size. Micro/nanoencapsulation process has a lot of applications such as in medical, pharmaceutical, cosmetic, food and beverages and agriculture fields. Encapsulation in micro or nanoparticles can be used to protect molecules from the environment, to convert liquid active components into a dry solid system, to mask undesired properties of the active components, to control release of the active components for timed release and/or sustained release (Bansode et al., 2010). In the food sector particles as liposomes have great potential as packaging material and represent an efficient way for controlling nutraceutical delivery and improving and promoting the growth of the nanofood industry (Teixeira et al., 2008). In medical field the delivery of drug at the right time, in the target where it is needed, is essential to realize the full potential of therapeutic molecules (Orive et al., 2005); this can be achieved encapsulating drugs in suitable carriers. Micro and nanoparticles as controlled drug delivery systems can minimize active molecules degradation and loss and, at the same time, reduce side effects and prevent collateral and toxic effects; can increase drug absorbance and bioavailability improving drug biodistribution and penetration in cellular compartment, overcoming the biological membrane barrier.

2.1.1 Critical issues in microencapsulation

There are a large number of microencapsulation processes and the selection of the preferred once is not always a simple task and depends on the active molecules dimension and solubility, the solvents employed, the delivery systems desired size, the process and product economics (Nack, 1970). What is common to the most of the methods certainly is the difficult concerning technical problems such as to control the final properties of the produced carriers in terms of size, stability, drug encapsulation efficiency, all issues becoming more pronounced as particle size is reduced. In particular, bioactive molecules, especially those of new biotechnological production to be used as therapeutic agents, are usually high degradable and sensitive to heat and organic solvents, available only in small quantities and very expensive. Therefore, the stability and the biological activity of the drugs should be not affected during the microencapsulation process, moreover the drug yield and its encapsulation efficiency as well as its stability should be high. Vectors final features and quality should be good and reproducible and

the process should be easy and cheap, useful at an industrial scale. Moreover the process should ensure a residual level of organic solvent lower than the limit value imposed by the European Pharmacopeia (Benita, 2006).

Unfortunately, most of the conventionally used methods to produce active molecules delivery systems are too expensive, not energy-efficient and with any consideration for the source of materials used and manufacturing waste.

A process intensification is required in order to achieve a process miniaturization, reduce the capital cost, improve safety and energy efficiency and improve product quality.

To the light of these difficulties affecting the conventionally used techniques, novel microencapsulation processes including simpler scale-up procedures should be developed, which may also increase the scope of commercial products reducing its costs and improving their quality. In that regard the ultrasonication is the key process intensification tool adopted in this thesis for nanostructured vectors production, its principles and benefits will be in dept discussed in 4.1.1.1 paragraph.

2.1.2 Materials of vectors

Micro and nanoparticles, included several reservoirs, such as micro/ nanocapsules, micro/nano-spheres and lipid micro/ nanoparticles, have attracted wide attention of researchers in various areas as they can be structured starting from a variety of materials whose nature can be organic or inorganic. Inorganic structures include magnetic particles, quantum dots, carbon nanotubs and gold particles whereas organic complexes include lipid and polymer conjugated particles (Yildirimer et al., 2011).

Among them, lipidic and polymeric micro and nanoparticles are the most important ones reflecting not only the functions but also the main features of an ideal drug delivery system (Bochicchio et al., 2016b).

In particular, polymeric particles can be prepared from both natural polymers (e.i., chitosan) and synthetic biodegradable and biocompatible polymers (e.i., poly-lactic-co-glycolic acid (PLGA)) (Hadinoto et al., 2013), due to their high structural integrity, stability during storage, and controlled release capability have been widely used as therapeutic delivery vehicles (Peer et al., 2007). Compared to polymeric carriers, the lipid once, which can be prepared from both natural and synthetic phospholipids, have been considered as the more ideal drug delivery vehicles because of their superior biocompatibility and similarity to biological membranes (Figure 1). However, the choice between them is highly dependent on the chemico-physical properties of the active molecules to be encapsulated and on the usage.
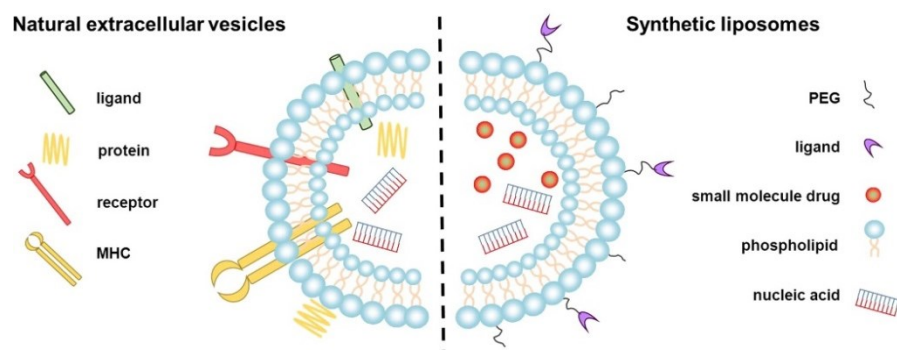
Figure 1. *Cellular mimetic behaviour of liposomes as delivery systems (van der Meel et al., 2014)*

Taking into account that each application requires a particular carrier features in term of size, surface charge, and other specific characteristics such as stimuli responsive ability (i.e. mucoadhesion), the evaluation of the starting material which will constitute the carrier is of fundamental importance.

2.2 Lipid carrier systems for therapeutic and nutraceutical agents delivery: liposomes

Among the several vectors used or the use of which has been explored/is under investigation, the main role is played by lipid carriers for their advantages of higher degree of biocompatibility and versatility. Lipid-based Drug Delivery Systems (DDSs) are safety and efficacy carriers which can be eaisily tailored to meet different disease conditions, route of administrations, costs, product stability, toxicity and efficacy (Attama et al., 2012). Lipid DDSs can assume disparate structures. Solid Lipid Nanoparticles (SLNs) are lipid-based DDS and represent an evolution of emulsions, the oil of the fat emulsion is replaced by solid lipids giving a solid at room temperature. SLN are stable and can give protection of the incorporated drug from degradation assuring drug controlled release and low cytotoxicity (Weber et al., 2014). These particles can be prepared without the use of organic solvents and a large scale production through high pressure homogenization can be obtained, however the drug loading capacity of conventional SLN is limited by the solubility of drug in the lipid melt and its rapid loss due to the structure of the lipid matrix. To overcome these limits Nanostructured Lipid Carriers (NCLs) have been proposed. These particles are similar to the SLN but are composed of different fatty acids mix, this composition increases the drug loading and prevents drug expulsion (Mukherjee et al., 2009). Lipid Nanocapsules (LNCs) are also lipid particles characterized by a core-shell structure, with a liquid oil core and an external solid lipid layer. These

particles can be produced through the phase inversion temperature (PIT) method (all the production techniques are described in chapter 3).

Finally, there are liposomes, the lipid vesicles object of study of this thesis, whose main features are below discussed.

Liposomes

Liposomes are closed vesicular structures, constituted by one or more phospholipid bilayers, which are formed when membrane lipids are dispersed in an excess of water. Differently from micelle, in the liposomes both the internal and the external regions are aqueous.

According to their lipophilicity, active molecules can be encapsulated in liposomes by different ways: inside the lipid bilayer, in the aqueous volume, or at the interface between the lipid bilayer and the aqueous volume (Figure 2).
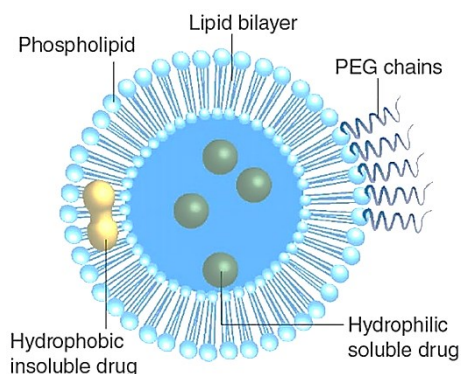
Figure 2 *Liposomes representation (Deshpande et al., 2013)*

In addition liposomes are highly biocompatible and biodegradable carriers known to possess low intrinsic toxicity and immunogenicity (Sawant and Torchilin, 2012). Liposomes are also versatile systems in terms of size and chemical modifications. They can be easily reduced in size and coated with different polymers and their surface can be chemically modified with specific ligands to give active targeting. These characteristics together with their similarity to biological membranes make them vectors of great interest when compared with the more common polymer-based vectors, even if the polymeric vectors can be intelligent carriers due to the stimuli-responsive behaviours (Cascone et al., 2012, Dalmoro et al., 2010, Dalmoro et al., 2012, Barba et al., 2013).

Liposomes can be classified on the basis of their size and their composition (Coelho et al., 2010), as detailed in Table 2.

Table 2 *Liposomes classification by size / structure (Coelho et al., 2010, Samad et al., 2007)*

Liposome	Essential description
Liposome classification by size	
SUV (**Small Unilamellar Vesicle**)	Size: from about 20 to 200 nm. They have only one lipid bilayer. They are thermodynamically instable with tendency to fusion; are not rapidly degraded by the RES (Reticuloendothelial System), thus have a long half-life in the blood stream.
LUV (**Large Unilamellar Vesicle**)	Size: from about 200 nm to 1 μm. They have only one lipid bilayer. They can carry hydrophilic drugs and macromolecules and have a short half-life in the blood stream.
GUV (**Giant Unilamellar Vesicle**)	Size: bigger than 1 μm. They are constituted by one phospholipid bilayer.
OLV (**Oligo Lamellar Vesicle**)	Size: from 100 nm to 1 μm. They are constituted by several concentric phospholipid bilayers (approximately 5 lipid bilayers).
MLV (**Multi Lamellar Vesicle**)	Size: bigger than 0.5 μm. They are constituted by several concentric phospholipids bilayer membranes (5-25 lipid bilayers). Both lipophilic and hydrophilic drugs can be encapsulated. They are stable structures and are easily eliminated by the Reticuloendothelial System (RES).
MVV (**Multi Vesicular Vesicle**)	Size: bigger than 1 μm. They are similar in size to MLVs but are multi compartmental structures constituted by vesicles surrounded by other vesicles.
Liposome classification by composition	
Conventional liposome	Composed by neutral or anionic phospholipids and cholesterol; quickly adsorbed by the RES.
pH-sensitive liposome	Characterized by the carboxyl group of cholesteryl hemisuccinate or oleic acid; they release their content in acidulous environment.
Cationic liposome	Characterized by cationic phospholipids; able to carry big molecules with negative charges such as DNA or RNA.
Long-circulating liposome	Composed by neutral phospholipids and cholesterol; they have a long circulation time in blood (half-life 40 h).
Immunoliposome	Characterized by the presence of antibodies on their surface which increase their specificity.

Due to their unic features, liposomes can be used as delivery systems in many fields of application such as pharmaceutical, medical, nutraceutical and cosmoceutical. In particular, in nutraceutical field liposomes are used as packaging material to deliver many bioactive ingredients such as vitamins, proteins and other micronutrients (i.e. iron) (LIU et al., 2013). On the other hand, in pharmaceutical field, the flexibility of liposomes to couple with site-specific ligands to achieve active targeting makes them increasingly important to deliver NABDs for gene therapy and different kind of peptides for new treatments (Smith et al., 1997, Immordino et al., 2006). In that regards, liposomes protect molecules by the action of degrading agents present in the blood stream and prevent their elimination by the immune system, solving the problem of therapeutic molecules short half-life.

2.2.1 Critical issues in therapeutic and nutraceutical agents delivery

During recent years, new therapeutic strategies, such as gene therapy, have been introduced into clinical practice. The discovery of NABDs, for instance, such as siRNA molecules, has definitely opened new therapeutic perspectives, however their use is still very limited due to their low stability, their limited membrane-permeability and their short half-life in the circulatory system. Indeed, the delivery of genetic material in vivo is the major obstacle in siRNA therapies and a number of intracellular and extracellular barriers must be overcome. SiRNAs, as well as all nucleic acid structures, are hydrophilic and negatively charged molecules. In normal conditions, the double phospholipid layer, which forms the cell plasma membrane, represents an impermeable barrier to polar and big macromolecules (Bochicchio et al., 2014). At physiological pH, the phosphate groups of the RNA backbone are deprotonated, therefore negatively charged, and the diffusion of these poly-anions is particularly difficult in the cells. Moreover, nucleic acids have a short half-life in the circulatory system indeed they are easily degraded by endo- or exo-nucleases and, subsequently, they are eliminated by the kidneys. Another problem regards siRNA immune response activation and, because immune reactions can vary among different cell types, it is difficult to anticipate all in vivo response based on in vitro work. In Table 3 the main problems related to "naked" siRNA administration are shortly summarized.

Table 3. *Problems of naked siRNA for clinical uses (David et al., 2012)*

Naked siRNA	
Problems	Causes
Short half life	- Serum nuclease susceptibility - Rapid renal clearance - Phagocyte uptake
Reduced uptake by cells	- Anionic nature - Too large to pass membrane

To solve these issues, the current strategy is the encapsulation of these macromolecules not only to reduce their toxicity, to improve their pharmacokinetics properties and to improve the stability of the drugs, but also to increase their efficiency (Miele et al., 2012).

The increasingly knowledge about the mechanisms involved in cell signaling pathways and their communication systems has allowed to identify new therapeutic targets which can involve such the use of molecules already know, but never used before for treatment of that disease, as the use of new chemically manufactured active-molecules. In addition to the NABDs, there are many different molecules which can have therapeutic properties such as protein, peptides, vitamins and antibody.

Peptides are molecules of great interest in therapeutic field as, along with proteins, are key regulators of biological functions and, as therapeutic agents, offer high biological activity associated with high specificity and low toxicity (Funke and Willbold, 2012). Protein engineering has revolutionized the therapeutic field by providing new tools to customize existing proteins or to create novel ones for specific clinical applications (Carter, 2011). New synthetized molecules can be for example copies or optimized versions of endogenous human proteins which can be used for receptors inibition or can be themselves overexpressed in order to treat the deseases. In medical field these molecules suffer from the same problems seen for NABDs, concerning their delivery in naked form through biological membranes, this step is particularly difficult for high molecular weight and hydrophilic peptides. Furthermore, their susceptibility to enzymatic degradation makes peptidic structures high degradable, characterized by in vitro and in vivo instability, immunogenicity and short half-life (Pisal et al., 2010). Encapsulation is an effective approach which can be used to prolong the shelf life and improve the bioavailability of peptides such as a wide variety of other molecules (Ulrich, 2002).

The situation is not different for micronutrients, such as vitamins and iron, which have great beneficial effects both when used in strictly medical field that if used in nutraceutical once but, due to their low stability, it is essential to encapsulate these molecules in suitable nanostructured vectors (LIU et al., 2013). Indeed, antioxidant nutraceutical products have received considerable

interest due to their safety profile and their potential therapeutic effects against cardiovascular diseases (CVD), cancer, diabetes and obesity (Rajasekaran et al., 2008) but it is essential to wrap this micronutrients in protective materials in order to prevent their deterioration.

Moreover, during food processes such as pasteurization and sterilization, vitamins and micronutrients such as iron are exposed to adverse thermal degradation, in this case packaging material represent an efficient way for controlling nutraceutical delivery and improving and promoting the growth of the nanofood industry.

It is important to underline that a market insight report on liposomes, divided into Therapeutic, Cosmetic and Other fields of applications, covering more then 330 companies that are engaged in liposomes research/supply, worldwide Patents, partnership, collaborations, mergers and acquisitions, shows a tremendous growth of this carriers in all the application fields and all over the world. The report gives a global market estimation and prediction of liposomes trend for the 2005-2020 time period (*RITMIR028: Liposomes – A Market Insight Report, July 2013 © RI Technologies - www.researchimpact.com*).

3. Liposomes production: State of the art

This chapter analyzes the literature related to the different techniques for lipid and liposomes nanostructured vector preparation. The recent developments in liposomes production techniques are also presented.

Keywords

Drug delivery systems; Lipid carriers; Liposomes; Production techniques; Nanoparticles

3.1 Lipid carrier production

Nowadays there is a vast array of possibilities to produce lipid-based drug delivery systems. The choice of the preparation method is influenced by several factors, the main of which to be considered are:

1. the physicochemical characteristics of both the molecule to be encapsulated and the lipid material used in carrier formulation;
2. the application and its involved processes;
3. the nature of the medium in which the lipid vesicles are dispersed.

Different are the methods that have been described in the literature for the production of lipid nanoparticles and are discussed along, with their advantages and disadvantages.

3.1.1 Methods for lipid nanoparticles production

Different are the methods used for the production of lipid nanoparticles, the main used are: High Pressure Homogenization, Microemulsion, Emulsification-Solvent Evaporation and Phase Inversion Technique, along described.

3.1.1.1 High Pressure Homogenization

High Pressure Homogenization technique was introduced by Siekmann and Westesen in 1992 for lipid nanoparticles dispersion production (Siekmann and Westesen, 1992) and then the technique was developed by Müller and Lucks, in 1996, for solid lipid nanoparticles (SLNs) production. This method is widely used for SLN, nanostructured lipid carriers (NLC) and lipid-drug conjugates (LDC) preparation (How et al., 2013, Mukherjee et al., 2009, Üner, 2006) as well as for downsizing large lipid vesicles in order to achieve nanometric liposomes (Pupo et al., 2005, Barnadas-Rodríguez and Sabés, 2001).
In High Pressure Homogenization method lipids are pushed with high pressure (100–2000 bar) through a narrow gap of few micron ranges (Singhal et al., 2011). The fluid accelerates on a very short distance to very high velocity (over 1000 Km/h) and the high shear stress and cavitation forces generated in the homogenizer cause the distruption of lipid particles to submicron range (Chaturvedi and Kumar, 2012). There are Hot and Cold High Pressure Homogenization. In the first technique the lipid nanoparticle dispersion is achieved using temperatures above the melting point of the lipid used. The drug to be loaded and lipids are dispersed, under stirring by a high-shear mixing device, in a hot surfactant solution. The pre-emulsion formed is then homogenized by using a piston-gap homogenizer or a jet-stream homogenizer in order to produce a hot colloidal emulsion. This o/w

nanoemulsion is cooled down to room temperature to recrystallize the lipids leading to nanoparticles formation. The process produces nanoparticles on large scale but the technique presents some disadvantages: increasing the homogenization leads to an increases of the particle size due to the coalescence which occurs because of the high kinetic energy of the particles (Mukherjee et al., 2009). Furthermore, high temperature lead to degradation of active compounds and hence loss of drug into the aqueous phase during homogenization. Finally, the tecnique is not appropriated for hydrophilic drugs, infact during the homogenization of the melted lipid phase the drug will partition to the water phase resulting in a too low encapsulation rate (Chaturvedi and Kumar, 2012). Cold High Pressure Homogenization has been developed to overcome some of problems of the hot homogenization. The first preparatory step is the same as in the hot homogenization, the lipid formulation is melted above its melting point and drug is dissolved in it. Then the system is rapidly cooled down using dry ice or liquid nitrogen to minimize the thermal exposure of the sample. After solidification, the lipid mass is grounded using mortar milling to yield lipid microparticles in a range between 50 and 100 μm. Then the lipid microparticles are dispersed in a cold surfacatant solution obtaining a cold pre-suspension of micronized lipid particles. This suspension is passed through an high pressure homogenizer at/or below room temperature and the microparticles are broken down to nanoparticles (Bleve et al., 2011). Large particles can be achieved but drug can be expulsed during storage (Shah et al., 2015).

High pressure homogenization is a process that can be used for large scale production of lipid nanoparticles and to downsize lipid vesicles, however, this technique require extremely high energy inputs, such as pressure, heat and shear forces.

3.1.1.2 Microemulsion

In 1943 Hoar and Shulman introduced the concept of microemulsion, they prepared the first oil in aqueous surfactant solution, adding an alcohol as a cosurfactant (Hoar and Schulman, 1943). Microemulsion technique can be used for lipid nanoparticle production. In particular, this method is used for solid lipid nanoparticles production using microemulsion dilution technique (Gasco, 1993). In this method water, co-surfactant and surfactant are mixed and heated to the same temperature as the lipids, the mixture is then added, uder stirring, to the lipids, obtaining a microemulsion. The hot microemulsion is then diluted into an excess of cold water and this reduction in temperature causes breaking of the microemulsion, converting it into nanoemulsion, which upon recrystallization of lipid phase produces lipid particles (Chaturvedi and Kumar, 2012). In order to incapsulate hydrophilic molecule, a multiple w/o/w microemulsion can be prepared and lipophilic drug can be added in it. Microemulsion technique offers different advantages which include no need for specialized equipment, low energy inputs and it

can be used for scale-up the production of lipid nanoparticles. The major limitation in using this method is that additional efforts are needed to remove the surfactant, which can be toxic, using additional steps such as ultrafiltration, ultracentrifugation or dialysis (Battaglia et al., 2014).

3.1.1.3 Emulsification-Solvent Evaporation

In 1992 Sjöström and Bergenståhl described solid lipid nanoparticles production using Emulsification-Solvent Evaporation technique (Sjöström and Bergenståhl, 1992). In this method lipids are dissolved in a water-immiscible organic solvent and emulsified in an aqueous phase. Then the organic solvent is evaporated under mechanical stirring at room temperature and reduced pressure, living lipid precipitates nanoparticles (Mehnert and Mäder, 2001, Bouchemal et al., 2004). Hydrophilic drugs can be incorporated by this techniques preparing a w/o/w emulsion and dissolving the drug in the internal water phase (Yassin et al., 2010). The solvent evaporation must be fast in order to avoid particles aggregation. Particles of 100 nm can be produced with no sophisticated equipment however different are the limits of this technique. First of all the solubility of some lipids in organic materials lead to dilute dispersions with low lipid particles content. The diluited dispersion need to be concentrate by different processes such as ultra-filtration, evaporation and lyophilization. On the other hand increasing lipid content the efficiency of homogenization decreases due to the high viscosity of the dispersed phase (Mehnert and Mäder, 2001).

3.1.1.4 Phase Inversion Technique

Phase Inversion is a common technique used for nanoemulsion preparation. In 2002 Heurtault and his research group adapted this method for lipid nanoparticles preparation (Heurtault et al., 2002) and in 2009 Huynh and coworkers used this method for the preparation of LNCs (Lipid Nanocapsules) (Huynh et al., 2009).
This tecnique takes advantage of polyethoxylated surfactants ability to modify their affinities for water and oil as a function of the temperature. The inversion take place at the temprature know as Phase Inversion Temperature (PIT) which concept was introduced in 1964 by Shinoda and Arai (Shinoda and Arai, 1964). Above the PIT an oil/water emulsion will change to a water/oil emulsion (Das and Kinsella, 1990). At first lipid, surfactant and water are mixed in the right ratio, the sample is then exposed to thermal treatment after which the inversion of emulsion is generated. The last step is the dilution with cold water which induced a thermal irreversible shock leading to the formation of nanometric lipid particles.

3.1.2 Methods for liposomes production

Since their discovery in 1965, many techniques and methodologies have been envolved for the manufacture of liposomes on small and large scales, for different applications (Mozafari, 2005). There are three main classes of liposomes conventional production methods, classified on the bases of the three principal liposome production steps: 1) lipid hydration; 2) regulation of liposome size; 3) removal of non-encapsulated drug (Samad et al., 2007). Lipid hydration step includes mechanical methods, methods based on organic solvents and methods based on detergent removal. After the lipid hydration step liposome size have to be regulated and the non-encapsulated drug have to be removed.

In recent years new techniques have been introduced for liposomes formulation such as Membrane Contactor Technique, Supercritical Fluid methods, Heating method, Spray Drying, Freeze Drying, Microfluidic channel method, Dense Gas technique and Cross Flow Injection technique, these methods along with the conventional once are discussed below.

3.1.2.1 Lipid hydration techniques

The first step in liposome production is the lipid hydration which can be achieved through mechanical methods, methods based on organic solvents and methods based on detergent removal.

Mechanical methods

Thin film hydration

The thin film hydration was the first mechanical method, introduced by Bangham and coworkers, for liposome preparation and nowadays is one of the most widely used technique for liposome production (Meure et al., 2008, Bangham and Horne, 1964). A rotating evaporator is used in these methods. Lipids are firstly dissolved in an organic solvent such as chloroform or methanol. The organic solution is then evaporated and the wall of a rotating vessel covered by a thin lipid layer. The layer is then hydrated, under adequate stirring, by an aqueous buffer solution containing the hydrophilic drug to be loaded. The temperature of the hydrating medium should be above the gel-liquid crystal transition temperature (Tc or Tm) (Dua et al., 2012). If the drug have hydrophobic nature it can be mixed with the organic solvent and lipid formulation. The process allows the formation of Multilamellar Vesicles (MLVs), which can be reduced in size to produce Small Unilamellar Vesicles (SUVs). The process can be optimized by using glass beads which allow the generation of thinner lipid layers by increasing their surface, thinner layers increase the efficiency of hydration and drug entrapment. One of the main advantages in using this methods lies in its easiness to perform and low cost, in addition all different kinds of lipid mixtures can be used and high encapsulation rates of hydrophobic and

hydrophilic molecules can be achieved (Wagner and Vorauer-Uhl, 2010). On the other hand the method is not scalable and toxic solvent traces could be remain in the final formulation. To overcome this limitation Ran and Yalkowsky have used halothane, a commonly inhalation anesthetic, in place of either chloroform or ether, to prepare liposomal formulations (Ran and Yalkowsky, 2003).

Methods based on organic solvents

Double emulsion

Double emulsion involves lipids dissolution in a water/organic solvent mixture, the aqueous phase will form droplets in the organic solvent. Then the organic solution, containing water droplets, is introduced into an excess of aqueous medium followed by mechanical dispersion. By this way water-in-oil-in-water (W/O/W) double emulsion is achieved. After mechanical vigorous shaking, part of the water droplets collapse giving Large Unilamellar Liposomes (LUVs) (Dwivedi and Verma). In 1994 Zengh and coworkers have utilized the double emulsion technique for the microencapsulation of hemoglobin in liposomes using a film dehydration/rehydration approach (Zheng et al., 1994). In 2006 Wang and coworkers have described a double emulsion based method for the preparation of unilamellar liposomes containing disaccharides as lyoprotectants in both the inner and outer aqueous phase. In 2008 a novel method for fabricating phospholipid vesicles with high encapsulation efficiency using controlled double emulsions was described by Shum and his research group. With this approach a W/O/W double emulsion is generated in a glass microcapillary device where the size of the capillaries used and the flow rates of the different phases are controlled. The solvent is removed through evaporation at low rate giving 20 μm to 150 μm liposome vesicles with high encapsulation efficiency (Shum et al., 2008).

Solvent injection

In solvent injection methods there are two miscible phases, one of which contains dissolved lipids, which are mixed together leading to lipids aggregation to form liposomes. The most studied solvent injection methods includes Ether Infusion and Ethanol Injection methods. In the first step of *Ether diffusion method* lipids are dissolved in diethyl ether or ether/methanol mixture and slowly injected to an aqueous solution mantained at 55-65 °C or under reduced pressure. If the drug to be encapsulated is hydrophilic it can be dissolved in this aqueous solution. The second step consists in the removal of ether under vacuum which leads to the formation of liposomes 70-190 nm in size (Riaz, 1996). The *Ethanol Injection method* was described in 1973 by Batzry and Korn (Batzri and Korn, 1973) and then by Kremer and coworkers in 1977 (Kremer et al., 1977). In this method lipids are dissolved in ethanol then the rapid injection of the lipid solution into the

aqueous media allows to the formation of liposomes 30-110 nm in size. Many variants of this technique have been made by several reaserch groups (Phapal and Sunthar, 2013). In 2001 Maitani and coworkers modified this method to produce liver targeting liposomes. At first, phosphatidylcholine, cholesterol, β-sitosterol β-D glucoside and oleic acid were mixed in warm absolute ethanol in a round bottom flask at about 60 °C and then 70 °C water was added rapidly to the lipid-ethanol solution. After liposomes formation the ethanol was removed by evaporation uder reduced pressure. They have obtained 150-160 nm liposomes (Maitani et al., 2001). By the same method in 2007 they have produced cationic liposomes rich in DOPE, containing DNA, in order to improve the efficacy of liposomes as vector systems for gene delivery (Maitani et al., 2007). Hauschild and collaborators have developed a modern variation of ethanol injection method: the inkjet method. They used an inkjet printer to inject a phospholipid solution into water, achieving 50-200 nm SUVs with efficient encapsulation of drugs (Hauschild et al., 2005, Meure et al., 2008). In general, the ethanol injection, being a bulk technique, does not allow to have a strict control on liposomes final size and the product volumes in output are small. Although, considering its simplicity, low cost and rapid execution, some aspects of this technique have been resumed in this thesis and coupled with the microfluidic principles (Chapter 4; 4.2 section), overcoming the limitations of ethanol injection method linked to low volumes in output and the impossibility in having particles dimensional features control.

Cross-flow Injection
Wagner and coworkers in 2002 have developed the cross-flow injection system. Based on the ethanol injection method, they developed a scalable production technique of liposomes to overcame some of limitation of the precedent technique (Wagner et al., 2002a). They invented the crossflow injection apparatus consisting of the crossflow injection module, vessels for the polar phase (PBS-buffer solution) and ethanol/lipid solution and a nitrogen pressure device. At first lipids are dissolved in 95% ethanol at 55 °C. The aqueous solution is pumped with a peristaltic pump; while pumping the polar phase through the crossflow injection module the ethanol/lipid solution is injected into the polar phase with varying pressures applied by a nitrogen pressure device. By varying different parameters such as the injection pressure, buffer flow rates and lipid concentration they demonstrated that parameters such as the injection hole diameter do not influence the vesicle forming process in contrast with lipid concentration and the injection pressures which instead strongly influence vesicles size distribution (Wagner et al., 2002b).

Reverse Phase Evaporation (REV)
In 1978 Szoka and Papahadjopoulos described the reverse phase evaporation (REV) method for unilamellar liposome production (Szoka and

Papahadjopoulos, 1978). In this technique phospholipids are dissolved in organic solvent, usually diethylether, isopropylether or a mixture of isopropyl ether and chloroform and aqueous buffer. The resulting two-phase system is sonicated briefly until the mixture becomes a clear one-phase dispersion. The organic solvent is then evaporated under reduced pressure leading to liposome formation. This technique has been used to encapsulate different large and small hydrophilic molecules (Pidgeon et al., 1987, Canova-Davis et al., 1986). In 2014 Oliveira and coworkers utilized this method to produce diminazene aceturate loaded liposomes for the treatment of trypanosomosis (Oliveira et al., 2014). As for the other techniques also for this method some variations have been developed by different research groups. Otake and coworkers in 2003 have described the Supercritical Reverse Phase Evaporation Method (scRPE) (Otake et al., 2003). They used a mixture of L-a-dipalmitoylphosphatidylcholine (DPPC), supercritical carbon dioxide ($scCO_2$) and ethanol for the preparation of liposomes with high trapping efficiency for water-soluble substances, examining the effects of phospholipid structure, preparation pressure, and amount of ethanol used on liposomes physicochemical properties.

Methods based on detergent removal

In this technique detergents, such as bile salts or alkylglycosides, are utililized to solubilize lipids (Wagner and Vorauer-Uhl, 2010). Detergents are amphiphilic molecules which are soluble in its monomeric form until they reach their critical micellar concentration (CMC). Above CMC, they aggregate to form micelles. Lipids are mixed with detergents at their critical micellar concentrations leading to the formation of mixed lipid-detergent micelles. When the detergent is removed micelles become increasingly richer in lipids and finally spontaneous form LUVs. The size and properties of the produced liposomes depend on several factors such as the chemical nature of the detergent, its elimination rate, the temperature and the ionic strength. By this method the production of liposomes, homogeneous in sizes, can be carried out but detergents may denature macromolecules and may form aggregates with smaller compounds (Schubert, 2002). The removal of detergents may be difficult, many different techniques are used for its elimination such as dialysis, gel-permeation chromatography, contact with non-ionic polystrene beads. The choice of the method to be employed depends on the detergent nature. One of the main application of detergent removal method is the model membrane reconstitution, in 1995 Rigaud and coworkers described a strategy for proteoliposome preparation that involves the use of detergents. In such preparation proteins are solubilized with phospholipids and detergent which is then removed, resulting in the formation of bilayer vesicles with incorporated proteins (Rigaud et al., 1995).

3.1.2.2 Liposome size reduction

Sonication, extrusion through polycarbonate membranes and High-pressure homogenization are the main methods used for liposomes size reduction.
Sonication technique is a simple and efficient method to reduce liposomes size (Huang et al., 2010, Woodbury et al., 2006). The cavitation phenomena induced by sonication can break up MLVs turning them into SUVs with diameters in the range of 20-100 nm. Being the ultrasounds used in this work as tool for liposomes size reduction and homogenization, this technique, along with the phenomenological aspects, will in detail described in Chapter four (4.1 section). In general, it is possible to adopt two different sonication technique on the basis of the sonicator type: probe sonication and bath sonication (Dwivedi et al., 2014). With the first method the tip of a sonicator is directly immersed into the liposomes dispersion while in the second method the liposomes sample is immersed in a bath and ultrasound are applied.
The extrusion technique is the process whereby multilamellar liposomes are forced through filters with defined pore sizes to obtain a liposome population with a mean diameter reflecting that of the filter pore (Hope et al., 1993). Due to the pressure forces generated when liposomes are passed through the membrane, SUVs are produced from MLVs (Cho et al., 2013). The great number of passages of liposomes through polycarbonate filters in order to obtain monodispersal sample makes this technique laborious. Furthermore, a freezing and thawing process prior to extrusion have to be made in order to increases the unilamellarity and the entrapment efficiency of the liposomes. With high-pressure homogenization technique is also possible to reduce in size liposomes in order to obtain SUVs as already described in paragraph 3.1.1.1.

3.1.2.3 Removal of non-encapsulated drugs

To remove non-encapsulated drugs different techniques can be adopted and the choice depends on the properties of both liposomes and molecules which have to be separate. Ultracentrifugation, for example, is a convenient and rapid technique but the high forces generated can be traumatic for the physical properties of liposomes. If the liposomes and the encapsulated molecules are characterized by an opposite charge a ionic-exchange resins can be used (Lasic and Papahadjopoulos, 1998). The size exclusion chromatography (SEC) is also a well know technique to separate small solutes from liposomes but is very laborious when an high quality separation is wanted due to the column pre-treatments which are required (Ruysschaert et al., 2005). Finally, a dialysis membrane, with the right characteristic depending on the molecules to be separate, can be easily used (Wallace et al., 2012).

3.1.2.4 Liposomes stabilization

The Freeze-Drying (FD) is a well know method used to ensure the long-term stability of liposomes and is the most used method to store liposomes in the dried state. To overcame the stresses associated with freeze-drying, carbohydrates can be added to lipid solution as lyoprotectants before the lyophilization. Three main steps characterize the FD process: the freezing of liposomes, the primary drying, which is a sublimation process, and the secondary drying, which is a desorption process (Chen et al., 2010). The freezing step can be obtained by different way such as freezing liposomes in liquid nitrogen or freezing down the liposomes to −45 °C at 0.6–1 °C/min or at 1 °C/min, in all cases the primary freezing temperature and the freezing rate have a key role in determining the liposomes morphology and stability. Other factors influencing the formulation stability are the properties of drugs, the composition of lipid bilayers, the particle size, the composition in lyoprotectants, the dry mass ratio of lyoprotectant/lipid. These and other factors have to be optimized in order to improve liposome lyophilization. Many new techniques for liposomes production have included lyophilization as a foundamental step in their processes. In 2014, Yin and collaborators have described the ultrasonic Spray Freeze-Drying (SFD) technique for protein-loaded liposomal production in order to obtain transdermal delivery of human epithelial growth factor (Yin et al., 2014). Li and Deng have utilized the freeze drying of monophase solutions to achieve sterile and pyrogen-free submicron liposomes (Li and Deng, 2004) while Wang and coworkers have prepared submicron unilamellar liposomes by freeze-drying double emulsions (Wang et al., 2006).

3.1.2.5 Recent development in liposomes production techniques

Dual asymmetric centrifugation

In 2008 Massing and collaborators proposed the Dual Asymmetric Centrifugation (DAC) method for the production of liposomes (Massing et al., 2008). This technique differs from the usual centrifugation because the sample is undergone, during the normal centrifugation process, to an additional rotation around its own vertical axis. By this way an efficient homogenization is achieved due to the two overlaying movements of the sample generated: the sample is pushed outwards, as in a normal centrifuge, and it is pushed to the center of the vial due to the additional rotation. At first, mixing hydrogenated phosphatidylcholine, cholesterol (55:45 mol%) and 0.9% NaCl-solution, they achieved a viscous vesicular phospholipid gel (VPC) which is then diluted to obtain liposomal dispersion. Liposome size can be regulated by optimizing DAC speed, lipid concentration and homogenization time. Glass beads can be also used to mix lipids. In optimized conditions, Massing and his research group have achieved 60 ± 5 nm liposomes with a trapping efficacy of $56 \pm 3.3\%$ for calcein. The year

later they prepared also small amounts of sterile siRNA-liposomes, about 109 nm in size, with high entrapping efficiency, ranging from 43 to 81%, depending on batch size (Hirsch et al., 2009). In 2011, also Adrian and collaborators have used the DAC method to produce liposomes containing siRNA, targeting the particles surface with an antibody for selective interaction with neuroblastoma cells, achieving 190 to 240 nm particles with a siRNA encapsulation efficiency up to 50% (Adrian et al., 2011). By this technique, in only one step, SUVs in a highly reproducible manner can be prepared.

Spray Drying

Spray drying is a continuous single step process which leads to both particle formation and drying and it was proposed for scaling up the liposome production process. Atomization of the sample, drying of the spray droplets and collection of the solid product are the main steps involved in this method (Shaji and Bhatia, 2013). At first lipids are mixed in organic solvents and the dispersion is pumped into the drying chamber through a spray nozzle leaving the sample atomized. Then the sample is dried in a concurrent air flow and collected in a reservoir. The dried lipids powder have to be hydrated in order to obtain multilamellar liposomes. Despite the numerous advantages in using this technique in terms of time and energy consuming, many are the difficulties in achieving stable liposomes. Different research groups have used this technique to produce loaded drug liposomes successfully, other have found many problems with respect to their stability. Silva and collaborators have obtained two populations of beta-carotene loaded liposomes, with average particle sizes around 300 and 1500 nm (Silva et al.). Sweeney and coworkers have used efficiently Spray-freeze-dried method to produce liposomal ciprofloxacin powder for inhaled aerosol drug delivery (Sweeney et al., 2005). Instead, Karadag and coworkers have recently confirmed the difficulty in prepare functional liposomal powders using conventional wall materials. In order to avoid thermal and environmental liposomes instability they adopted the "Layer-by-Layer" (LbL) depositing method, coating the surface of anionic lecithin liposomes with a cationic chitosan and adding maltodextrin as wall material to facilitate spray drying. When liposome were coated no liposomes aggregation or breakdown was observed and stable vesicles about 500 nm were achieved (Karadag et al., 2013).

Membrane Contactor

Membrane contactor technique have already been used for the preparation of polymeric and lipidic nanoparticles and, most recently, it has been proposed for the preparation of liposomes. In 2011 Jaafar-Malej and coworkers have described a new method for liposome preparation based on both the principles of the ethanol-injection and membrane contactor methods. They

prepared liposomes 150-286 nm in size by mixing lipids in ethanol and pressing the obtained phase, at temperatures above the melting point of the lipids, through a membrane with a specified pore size, allowing the formation of multiple microflow streams. An aqueous phase flowed tangentially to the membrane surface leading to the formation of vesicles as the two miscible phases interdiffuse, hydrating the phospholipids (Jaafar-Maalej et al., 2011). In 2012 Laouini and coworkers have utilized this technique to produce 100 nm spironolactone loaded liposomes achieving an encapsulation efficiency of 93 % (Laouini et al., 2012a).

Heating method

This method consists in mixing lipids and glycerol with aqueous solution, along with the material to be encapsulated, in a heat-resistant flask at a temperature above the Tc of the lipids and under an inert atmosphere. Has been demonstrated that liposomes and nanoliposomes can be formed by the heating method (HM) which have been successfully employed for gene transfer applications (Mozafari et al., 2002). Mozafari, in 2005, had modified the HM improving liposome monodispersity and storage stability. The variation apported to the so called "Mozafari method" consists in add lipids to a preheated mixture of nisin and a polyol such as glycerol in a heat-resistant flask. The suspension is then leaved to stabilize at temperatures above the Tc under an inert atmosphere (Mozafari, 2010). Glycerol acts as isotonising and disperdant agent stabilizing liposomes and there is no need to remove it from the preparation. The particle size depends on the phospholipid nature, charge, the speed of the stirring and the shape of the reaction vessel thus the liposome dimension can be controlled (Laouini et al., 2012b).

Microfluidic method

Microfluidic method is a relatively new technology used for the production of liposomes, this technique gives the possibility to control the lipid hydration process. The method can be classified in continuous-flow microfluidic and droplet-based microfluidic methods, according to the way in which the flow is manipulated (Yu et al., 2009). In 2004, Jahn and collaborators have described a microfluidic hydrodynamic focusing (MHF) method which operates in a continuous flow mode. In this technique a stream of isopropyl alcohol containing the dissolved lipids is hydrodynamically focused in a microchannel cross junction between two aqueous buffer streams. Monitoring the flow rates, thus controlling the lipids solution/buffer dilution process, dimension of liposomes can be controlled. They determined also that the liposomes size can be controlled by altering the ratio of the flow rate in the side inlet channels compared to the center inlet channel (Jahn et al., 2004). In 2006, Tan and coworkers have described a microfluidic based method to control liposome vesicles formation. The

method is based on a microfluidic device in which channel junctions are used in order to generate droplets which sizes is controlled by monitoring the flow rate. An expanding nozzle is used to control the breakup location of the droplet generation process. By this way monodispersed submicron droplets were achieved (Tan et al., 2006). Many variants of microfluidic method have been described in literature (Pradhan et al., 2008) such as 3D microfluidic hydrodynamic focusing in a concentric capillary array described in 2014 by Hood and collaborators (Hood et al., 2014). In this thesis the microfluidic method has been coupled with the ethanol injection method and a simil-microfluidic apparatus has been developed as detailed in Chapter 4 (4.2 section).

Supercritical Fluid method

In recent years dense gas technique was proposed for liposomes manufacturing in order to overcome the issues of both conventional techniques (i.e. use of organic solvent, use of multiple steps, problems associated to the stability of the final liposomal product) and new techniques such as the heating method and the membrane contactor which used high temperature (Meure et al., 2008). Great interest has been directed to the use of supercritical fluid (SCF) technology as new way to produce liposomes. SCF-CO_2 is a not toxic and not inflammable solvent which has low critical temperature (31 °C) and pressure (7.38 MPa) (Parhi et al.) thus it can be used to avoid the degradation of thermolabile substances to be encapsulated. In 1997 Frederiksen and collaborators used supercritical carbon dioxide for the preparation of liposomes containing fluorescein isothiocyanate-dextran (FITC-dextran) and zinc phthalocyanine tetrasulfonic acid (TSZnPc) choosed as water soluble model substances. They used an apparatus consisting of two main parts: the high-pressure and the low-pressure sections. First lipids were dissolved under pressure in supercritical carbon dioxide, and then exposed to a low-pressure in which the solution is expanded and simultaneously mixed with the aqueous phase. The addiction of 7% absolute ethanol to carbon dioxide at controlled temperature and pressure resulted in the production of liposomes encapsulating the water soluble molecules, of 200 nm in size (Frederiksen et al., 1997). There are many different methods in utilizing SCF (Sekhon, 2010), as the scRPE above mentioned as a variation of REV technique for liposome production (Zhao et al.).

4. Novel developed techniques for liposomes production

In this chapter two novel developed techniques, the Ultrasound assisted Thin Film Hydration method and a Simil-microfluidic approach for lipid nanostructured vectors production are presented along with their layout, principles and main phenomenological aspects involved in liposomes formation.

4.1 Ultrasound assisted Thin Film Hydration: layout, principles and phenomenological aspects

4.1.1 Generalities

As seen in Chapter 2, the use of liposomes in several fields of biotechnology, as well as of pharmaceutical and food sciences, is continuously increasing: they could be used as carriers for drugs and other active molecules of industrial relevance. Among other characteristics, one of the main relevant features to their target applications is the liposome size. From a pharmaceutical point of view liposomes dimensions influence liposomes time of circulation in the blood stream and/or their permeability through membrane fenestration in tumour blood vessels, from a nutraceutical point of view nanometric liposomes are able to improve taste, flavor, stability, absorption and bioavailability of nutients.

On this basis, a versatile and reliable technique able to produce liposomes of different sizes to be used for disparate applications has been developed. In that regard, the Thin Film Hydration method (discussed in Chapter 3, 3.1.2.1 paragraph), which produce micrometric structures, was revisited by adding an ultrasound assisted step in order to prepare, in a versatile manner, nanometric structures with the desired dimensions.

In particular, the size of liposomes is determined during the production process, decreasing due to the addition of ultrasound energy. The energy is used to break the lipid bilayer into smaller pieces, then these pieces close themselves in spherical structures.

Here, the mechanisms of rupture of the lipid bilayer and of the sphere's formation was studied and modeled accounting for how the energy, supplied by ultrasounds, is stored within the layers, as elastic energy due to the curvature and as energy due to the edge, and accounting for the kinetics of bending phenomenon. An algorithm to solve the model equations was designed and the relative calculation code was written. A dedicated preparation protocol, which involves active periods during which the energy is supplied and passive periods during which the energy supply is set to zero, was defined and applied. The model predictions compares nicely with the experimental results, by using the energy supply rate and a time constant as fitting parameters. Working with liposomes of different sizes as starting point of the experiments, the key parameter is resulted to be the ratio between the energy supply rate and the initial surface area.

4.1.1.1 Principles of the ultrasound process and benefits

Ultrasound is a mechanical vibration phenomenon having a frequency above the range of human hearing (> 20 KHz). When ultrasound is adsorbed by a media, acustic vibrations increase kinetic energy, producing an instantaneous

temperatures and pressures rise. The explanation of the process can be found in cavitation-wave hypothesis, proposed in 1960. According to this hypothesis, when pressure changes, there is a formation of cavities at liquid-gas intarface. The collapse of these cavities generate shock waves bubbles capable of resonance vibration and producing vigorous eddying or microstreaming. The stresses associated with the propagation of ultrasonic waves may be converted into thermal energy or into chemical energy. Ultrasound assisted processes can be used for a disparate industrial applications, i.e. to homogenize, atomize, disperse, deagglomerate and sizing particles, emulsify, disintegrate cells and extracting protein or enzymes from them, to increase reaction speed, to clean, to degass liquids. For example ultrasonic atomization take advantage by ultrasound-phenomenon to break up a liquid film into fine droplets. In this case the phenomenology of the droplets formation process can be explained with cavitation-wave hypothesis or with the capillary wave hypothesis (Avvaru et al., 2006) which analyze the behaviour of a liquid on the solid surface vibrating basing on Taylor instability criteria (Kull, 1991). When the vibration have a frequency of 30 Hz, above a threshold value of amplitude, on the liquid surface capillary waves, made of crests and troughs, are formed. At higher values of amplitude liquid droplets, separated from the waves crest, are formed (Abramov, 1999).

In general, ultrasonication is an easy and scalable process which shows competitive energy costs, applicable in a vast range of fields and for disparate applications.

Regardig the particles size reduction, it takes advantage from ultrasound process ability to break up lipid structures. In case of nanoliposomes the energy is used to break the lipid bilayer into smaller pieces, then these pieces close themselves in spherical structures producing SUVs. In comparison with other sizing techniques, the ultrasonic once shows great potential due to reducing time spent and easiness in use. Ultrasonic process not need a number of passages of liposome suspension through a membrane such as extrusion method and not high pressure have to be used (see 3.1.2.2 paragraph). Furhermore, the final dimension of particles are not fixed to the pore size of the membrane but it is possible to change the vesicles size according to the application requirements. This is possible controlling the duty cycle, the discontinuous process by which the liquid sample is sonicated in periodic time intervals followed by switch off in energy supply. Finally, due to the critical importance to have a sterile environment during loaded SUVs production, another advantage is that sonotrode tip is simpler to clean and sterilize.

The process parameters influencing the sizing process are the ultrasonic amplitude (%), the power (W), the number of sonication cycles and the time of sample exposure to ultrasound, as below detailed.

4.1.2 Experimental section

4.1.2.1 Materials

L-a-Phosphatidylcholine (PC) from egg yolk (CAS no. 8002-43-5), L-a-phosphatidyl-DL-glycerol sodium salt (PG) from egg yolk lecithin (more than 99% pure), cholesterol (CHO) (CAS no. 57-88-5), potassium phosphate monobasic (CAS no. 7778-77-0) and sodium hydroxide (CAS no. 1310-73-2) were purchased from Sigma Aldrich (Milan, Italy) as dried powders and used without further purification. All the other chemicals and reagents such as chloroform (CAS no. 67-66-3), ethanol (CAS no. 64-17-5), methanol (CAS no. 67-56-1) (Sigma Aldrich – Milan, Italy) used were of analytical grade.

4.1.2.2 Layout

Figure 3 shows a schematization of nanoliposomes production process through the ultrasound assisted Thin Film Evaporation technique developed.

D-1	Rotavapor
D-2	Mixing/sonication tank
Z-1	Sonicator
1	Lipid/Solvent (and hydrophobic molecule) feed line
2	Solvent evaporation line
3	Dried Lipid feed line
4	Hydration solution (and hydrophilic molecule) feed line
5	Nanoliposomes suspension
	Key to abbreviations
US	Ultrasounds source
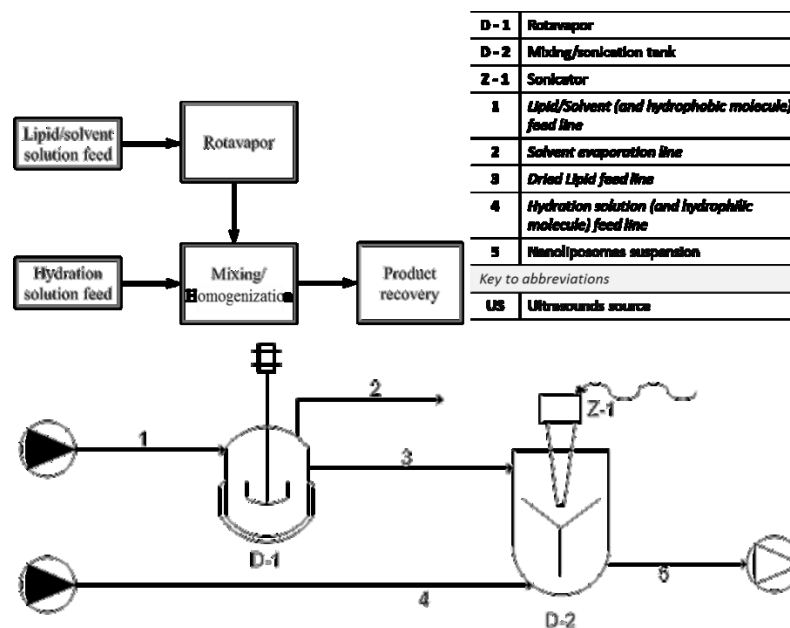
Figure 3. *Process schematization of nanoliposomes production through the ultrasound assisited Thin Film Hydration method; the main steps are reported: lipids/organic solvent solution (1) is introduced in a rotary evaporator (D-1) where solvents are evaporated (2) leading to the formation of a dryied lipid film (3) which is then hydrated (4) and stirred (D-2) After this step a suspension containing MLVs is produced and submitted to a duty cycle sonication process (Z-1) thus producing SUVs (5), finally recovered*

The set-up is composed by four main sections: a feeding section, a solvent evaporation section, a liposomes production section and a recovery section. In particular the production section is constituted by a rotary evaporator (Heidolph, Laborota 4002 Control), where micrometric vesicles are prepared, and an ultrasonic source (VCX 130 PB Ultrasonic Processors of Sonics & Materials Inc., CT, USA; maximum power 130 W; frequency 20 kHz; sonotrode tip length 137 mm; sonotrode tip diameter 3 mm), which gives nanoliposomes as output product.

For liposomes production at nanometric scale at first lipids are dissolved in organic solvents (chloroform/methanol) eventually containing the hydrophobic drug to be encapsulated; after mixing, the solution is vacuum dryied for 3 houres at 50 °C while rotating at 30 rpm in a water bath. The dried lipid film which is generated is then hydrated at room temperature with water or other hydration solution eventually containing the hydrophilic drug to be encapsulated and continuously stirred at 60 rpm. A suspension containing MLVs is produced, maintained at room temperature for 2 hours and then sonicated (treated volume: 1 mL) by applying a duty cycle purposely developed. The duty cycle is a discontinuous process by which the liquid sample is sonicated in periodic time intervals followed by switch off in energy supply. It consists in 2 ten-second irradiation rounds (amplitude 45%), each followed by a twenty-second pause in order to prevent thermal vesicle disruption thus obtaining large vesicles, on micrometric scale, smaller then the starting once. In particular, taking into account their size and the phenomenology at the base of liposomes formation (detailed in 4.1.2.4 paragraph), in this thesis, the large vesicles obtained from the first two rounds of duty cycle sonication will be named Large Unilamellar Vesicles (LUVs) due to the presumed presence of one lipid layer composing their structures. The sample is then stored overnight at 4°C and protected from light in order to stabilize the produced LUVs. Subsequently, in order to obtain SUVs, after the stabilization phase, the sample is sonicated again, at 45% amplitude (percentage of maximum deliverable power), up to four more rounds as detailed in the next paragraph.

4.1.2.3 Liposomes preparation

SUVs were prepared by using the ultrasound assisted Thin Film Hydration technique and applying a dedicate protocol of sonication as before described. Briefly, unloaded liposomes were prepared dissolving PC (40 mg), CHO (16 mg) and PG (4 mg) at 10:8:1 (mol:mol) ratio into 1 mL of chloroform/methanol 2:1 (vol/vol) solvent mixture. After vigorous pipetting, the solvent mixture was removed by evaporation in a rotary evaporator (Heidolph, Laborota 4002 Control) and the achieved lipid film was vacuum-dried for 3 hours at 50°C in a water-bath. The dried lipid film was then hydrated at room temperature with 7 mL of PBS (pH 7.4), pre-warmed until 50 °C, and adequately stirred. To prepare phosphate buffer solution (PBS)

potassium phosphate monobasic 0.2 M and sodium hydroxide 0.2 M were dissolved in distilled water to obtain a pH 7.4 PBS final solution. After hydration, a solution of Multi Lamellar Vesicles (MLVs), was obtained. The sample was maintained at room temperature for 2 hours and then 1 mL of the solution was subjected to a sonication step in order to get Large Unilamellar Vesicles (LUVs). Then, the LUVs sample was stored at 4°C for one night, protected from light, in order to allow vesicles stabilization. In order to obtain Small Unilamellar Vesicles (SUVs), more sonication steps were carried out. Design variables of this protocol are the number of sonication steps as well as the "amplitude" of sonication, i.e. the power level at which the ultrasound applicator was activated. Both the LUVs and the SUVs productions therefore involved sonication steps. Each sonication step was designed by this way: the ultrasounds were applied to 1 mL of solution for ten seconds, followed by twenty seconds of time during which the ultrasound applicator was switched off, in order to allow the sample cooling and to avoid thermal degradation. Liposomes size was measured by Photon Correlation Spectroscopy (PCS) using the Zetasizer Nano ZS instrument (Malvern, UK) that incorporates noninvasive backscatter (NIBS) optics. A detection angle of 173 degrees was used to permit size measurements of turbid samples like liposomes suspensions. The resulting particle size distribution was plotted as number of liposomes versus size. All the measurements were performed in triplicate, thus the results were expressed as average values.

4.1.2.4 Modelling

In order to describe what happens to the double layer of lipids which constitutes the liposomes, both the thermodynamics as well the kinetics of the process have been studied and thus modeled. From the energetic point of view (thermodynamic) the free energy of the membrane is mainly given by two fractions: the elastic energy due to membrane curvature and the tension energy due to the edge of the layer. Indeed, at the boundary of a bilayer the polar heads have to be arranged as a semi-circle, in order to connect the two monolayers (Helfrich, 1974). The elastic energy has been estimated by Helfrich (Helfrich, 1973) as proportional to the second power of twice the mean surface curvature, $1/R$, and to Gaussian surface curvature, $1/R^2$; through the main elastic moduli, k_c and $\bar{k}_c$; the edge energy are assumed to be proportional to the length of the bilayer edge (Helfrich, 1973, Fromherz, 1983), by the edge tension parameter, γ. On the basis of simple geometrical reasoning (Fromherz, 1983); a disc initially of radius ρ_D, with a surface area $A_D = \pi \rho_D^2$, which is (partially) bended toward forming a sphere (equivalent in area, then with a sphere radius $R_S = \rho_D/2$), has an edge length equal to $L = (2\pi \rho_D^2)\sqrt{1 - (\rho_D^2/4R^2)}$. Summarizing, for N vesicles with a mean curvature $1/R$, the total free energy could be estimated by equation (4.1):

$$g = N(g_{elastic} + g_{edge}) =$$

$$= N\left\{\left[\frac{1}{2}\left(k_c + \frac{1}{2}\bar{k}_c\right)\frac{4\pi\rho_D^2}{R^2}\right] + \left[\gamma(2\pi\rho_D)\sqrt{1 - \frac{\rho_D^2}{4R^2}}\right]\right\} \qquad (4.1)$$

Therefore, the thermodynamic of the process ("how much" the liposome formation is possible) could be described once the number and the size of the starting discs, N and ρ_D, as well as the curvature of the vesicle, $1/R$, are known; after the estimation of the material parameters $(2k_c + \bar{k}_c)$ and γ.

The kinetic of the process ("how fast" the discs bends, "how fast" they're broken, and "how fast" the spheres were opened and flattened) could be described taking into account for the rate of energy addition as well as considering the bending process (during which the free energy decreases) as a first order phenomenon (Fromherz, 1983), in which the radius of curvature changes proportionally to the difference between actual curvature and the minimum curvature (corresponding to a closed sphere of radius R_S). In formulas, this means that the energy change is described by:

$$\frac{dg}{dt} = \dot{g} \qquad (4.2)$$

And the radius change is described by:

$$\frac{dR}{dt} = -\frac{R - R_S}{\tau_c} \qquad (4.3)$$

The rate of energy addition, $\dot{g}$, and the time-constant of the bending process, τ_c, are process parameters to be determined. The energy supplied to a sphere causes the sphere to open and to flatten (a decreases in curvature, an increase in radius R). When energy is supplied to a flat disc, which is characterized by an infinite radius of curvature, this energy is no more used to decrease the curvature, but to break up the disc giving rise to smaller flatten bilayer fragments.
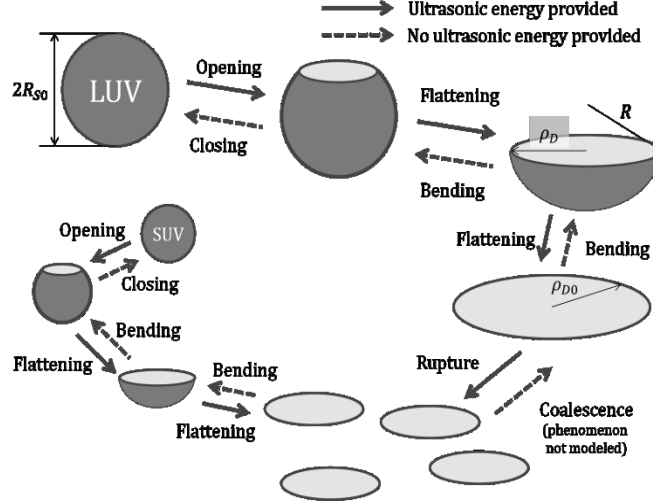
Figure 4. *The phenomena which take place during liposome formation*

Summarizing, the phenomena which take place during liposome formation are depicted in Figure 4, whereas the process of modelling is reported as the flow-sheet in Figure 5. In Figure 4 the phases in which ultrasonic energy is supplied are described by full line arrows; the phases "of relaxation" during which no energy is supplied are described by dashed line arrows. The coalescence phenomenon, which causes small disks to give large disks, is not modelled since it should take place on a time scale considerably longer than the one observed here. The full duration of the process is divided in several time-steps, Δt, and then the integration of the ODEs (4.2 and 4.3) was numerically carried out, accounting for the duty-cycle of energy supplying. The energy for flat bilayer fragments break-up was indeed supplied in a non-continuous mode, allowing alternate phases of disc break-up, heat dissipation and membrane bending. The process modelling requires to calculate, for each time-step, the free energy, g, the disc radius, ρ_D, curvature, R, and the numbers of liposomes, N.

> ➤ The process is considered to start from a single ($N_0 = 1$) LUV (Large Uni-lamellar Vesicle) of radius R_{S0} (corresponding to a total area $A_0 = 4\pi R_{S0}^2$). Under this condition the initial radius of curvature is equal to the sphere radius ($R_0 = R_{S0}$); the disc equivalent (with the same area) to the sphere, will have the initial radius $\rho_{D0} = \sqrt{4R_{S0}^2} = 2R_{S0}$; and the free energy, given by equation 4.1, is only due to elastic energy, $g_0 = \frac{1}{2}\left(k_c + \frac{1}{2}\bar{k}_c\right)\frac{4\pi\rho_{D0}^2}{R_{S0}^2} = \frac{16\pi}{2}\left(k_c + \frac{1}{2}\bar{k}_c\right)$.

➢ During the phase in which no energy is supplied, the curvature increases and the radius of curvature R decreases, according with eq. 4.3 (in Figure 5, the ODE is numerically solved according an Euler's scheme. Since the model is not given only by a couple of ODEs, but it requires also several choices regarding the calculation path, the simplest numerical scheme, the Euler's one, has to be selected. Anyway, the stability and the accuracy of the scheme have been tested reducing the time-step size until the solution remained unchanged). In this phase, the disc radius and the number of liposomes remain constant, whereas the free energy is calculated by eq. 4.1.

➢ When the energy is supplied, first of all eq. 4.2 has to be solved (once more, in Figure 5 the ODE is numerically solved according to an Euler's scheme). Then, two different paths have to be followed according to the actual curvature.

➢ If the configuration is not planar (curvature different from zero, radius of curvature finite), the spheres open, i.e. the curvature decreases (the radius of curvature increases). The radius of curvature has to be calculated by eq. 4.1. Again, during this phase the disc radius and the number of liposomes remain constant.

➢ At last, in presence of planar configuration, the energy supplied is used to increase the edge length. The length of the edge could be calculated from the eq. 4.1, therefore $L = 2N\pi\rho_D = g/\gamma$. Since the total surface area remains constant, $A_0 = A = N\pi\rho_D^2$; the disc radius and the number of liposomes could be obtained from these two last equations: $\rho_D = 2A\gamma/g$ and $N = A/(\pi\rho_D^2)$, as reported in Figure 5.

The process is then described by repeating the calculation scheme for each time step, on the basis of the duty cycle imposed to the sample ($\dot{g} = \dot{g}(t)$).
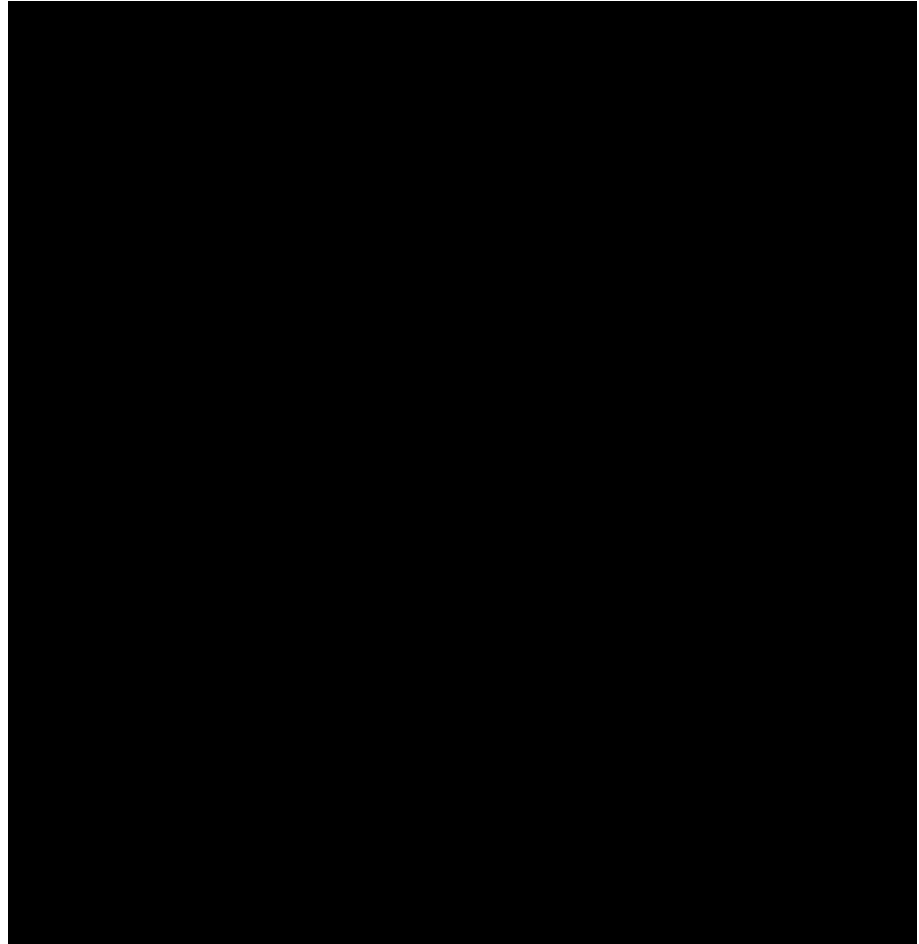
Figure 5. *The model calculation flow-sheet*

4.1.3 Results and discussion

4.1.3.1 Part 1: Model testing

First of all, the response of the model to external stimuli has been checked by applying a fictitious ultrasound duty cycle. The duty cycle is built applying a power term, $\dot{g}_0$, for ten seconds, followed by a "pause" in energy supply for other twenty seconds. The cycle is repeated twice (for a total of ninety seconds). There is the need for periods during which the energy supply is switched off in order to avoid a continuous heating of the sample. In the proposed model the power is intended to be fully delivered to the membrane, therefore actually it is a (very small) fraction of the energy supplied by ultrasound applicator to the sample.
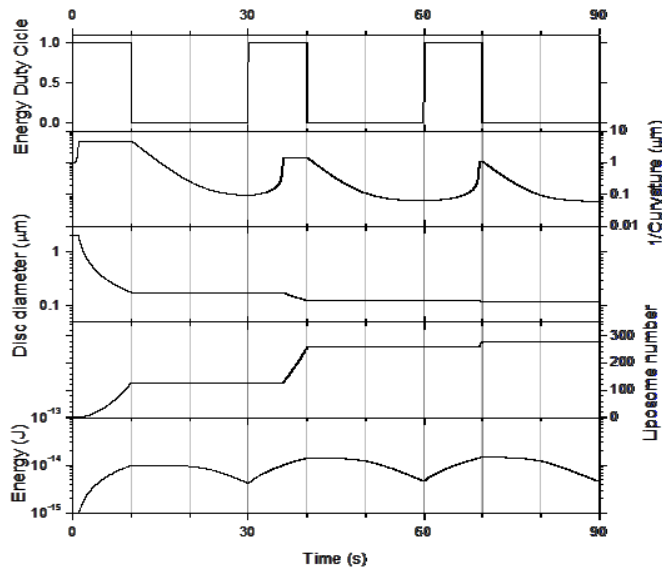
Figure 6. *Output of the calculation model for the simulated test*

The dimensionless forcing term, $\dot{g}(t)/\dot{g}_0$, is reported in Figure 6 as the first graph starting from the top: it is depicted with a behavior as a square wave, even if actually the transition between on and off is somewhat more slow and less stiff. Starting from the top, in Figure 6 these graphs have been reported: the already discussed duty cycle; the radius of curvature, R in μm; the radius of the disc equivalent to the sphere, ρ_D in μm; the number of liposomes, N; and the total free energy, g in J. In order to perform the simulation, the material parameters have been taken from literature to be k_c=2.3·10^{-19}J; $\bar{k}_c$=0 J; γ=7.0·10^{-20} J/nm. The initial radius of the LUV was taken to be R_{S0} =1 μm, giving an initial equivalent disk radius of ρ_{D0}= 2 μm. The initial energy of the structure with these choice results $g_0 = 8\pi k_c = $

$5.8 \cdot 10^{-18}$ J. The two parameters which need to carry out the simulation were arbitrarily chosen to be $\dot{g}_0 = 10^{-15}$ W and $\tau_c = 3$ s.

> At the beginning of the simulated test, roughly for a second the radius of curvature increases (as it is visible in the second graph), meaning that the initial LUV is being opened. In this period, the supplied energy was used just to increase the free energy of the membrane (the elastic energy actually decreases, while the edge energy increases), therefore the equivalent disc does not change its size, and the number of liposomes remains constant as well on its initial value (which is one). The third and the fourth graphs (from the top in Figure 6) then show two constant value initial segments (since the abscissa is just one second, these segments are just recognizable in the graphs). During this phase, the total free energy, reported in the fifth graph from the top, increases from its initial value, g_0 which is of the order of 10^{-18} J, toward values within the range reported in the fifth graph. The rate of this first phase is dictated by the value of the power parameter $\dot{g}_0$ (the higher the power, the faster the de-bending of the sphere).

> During the following nine seconds, while the energy is being supplied, it is possible to see that: from the second graph, the radius of curvature remains constant on a very high value (actually the membrane is flat, the radius of curvature should be infinite); from the third graph, the radius of the equivalent disc starts to decrease and, from the fourth graph, the number of structures increases, both these phenomena are due to the fact that the membrane is being disrupted by the ultrasound energy; from the fifth graph, the total free energy increases, being stored in the structures as edge energy. The magnitude of the phenomena which happen during this phase are also dictated by the value of the power parameter $\dot{g}_0$ (the higher the power, the higher the number of discs produced and the smaller their size).

> At the end of first ten seconds of energy supply, roughly $N = 130$ discs with a radius $\rho_D = 176$ nm have been obtained (the radius of the sphere equivalent to the disc being $R_S = \rho_D/2 = 88$ nm), and the energy has reached a maximum roughly equal to 10^{-14} J. During the following twenty seconds the relaxation process starts, and the discs bend themselves toward the spherical configuration, since the total free energy in that configuration is lower (the elastic contribution being lower than the edge contribution). During this phase, thus, the radius of curvature decreases (the curvature increases) and the total free energy decreases. The kinetic of such process being dictated by eq. 4.3 and by the value of the time-constant parameter τ_c (the smaller the time-constant, the faster the bending process). As

expected, during the bending phase no more entities were produced and their size remains constant (N and ρ_D are constants).

➢ Starting from the thirtieth seconds, the cycle starts again. During about the first five seconds (up to 35 s), the discs open (R increases), the entities do not change number and size (N and ρ_D remain constants), the total free energy increases.

➢ During the remaining of supply-energy phase (about five more seconds), the entities were flat discs, and then the energy was used to disrupt them: the curvature does not change, the number of entity increases and their size decreases. The total free energy still increases.

➢ From forty to sixty seconds, the relaxation phase takes place: the discs bend toward sphere, thus the radius of curvature decreases, and the total free energy decreases, too. The number and the size of entities remain constant. During this phase, the diameter of the attainable liposomes is roughly equal to 124 nm (during the corresponding first phase it was 176 nm), their number is increased to about 250.

➢ Once more, starting from the sixtieth seconds, the cycle starts again. This time the energy supplied was almost all used to open the spheres (they're a lot and very small now, and thus they require a lot of energy to be opened), and thus just a little decrease in entity's size (and a little increase in entity's number) was attained. Roughly, 280 liposomes with a diameter of 120 nm were obtained.

Even if fictitious, this "experiment" is a lot informative and useful to understand both the role and the relevance of the model parameter as well as the behavior of the real systems. For example, it is evident that – if this situation was real – a second cycle of ultrasound application is useful in order to reduce liposome size, but a third cycle could be avoided. Of course, with the aim of point out a real and useful model, a comparison of its calculation against real experimental data is mandatory.

4.1.3.2 Part 2: Experimental results description and interpretation

Two different tests were designed and carried out in order to validate the proposed model.

1. For the first kind of test (identified as the Run 1), the starting point was a solution containing LUVs, with a diameter within the micrometric scale (D_{D0} = 1.4 micron), obtained starting from the hydrated lipid bilayer (the MLVs solution), by a single step of sonication. The LUVs solution, after the night of rest (see Experimental section for preparation details) was then subjected to further one, two or three steps of sonication, in order to produce

SUVs, for a total time of sonication of ten, twenty or thirty seconds of application. These three tests (identified as Run 1.a, 1.b and 1.c) were carried out at a constant level of power (amplitude 45%, nominal power 58 W).
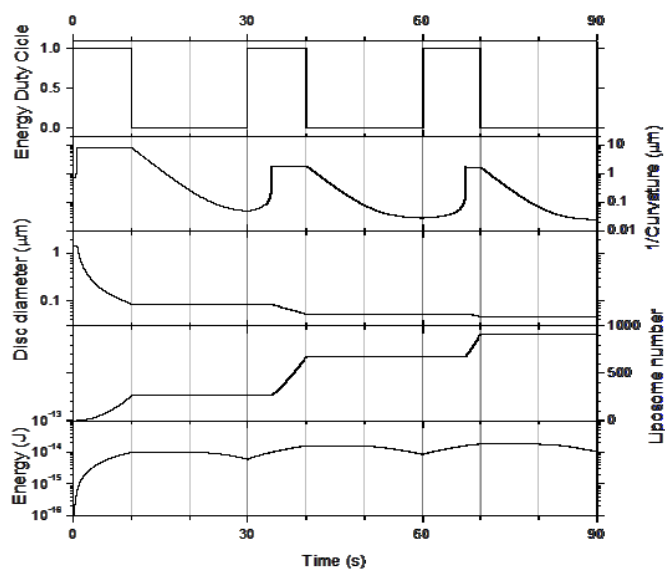
Figure 7. *Output of the calculation model for real test Run 1*

2. For the second kind of test (Run 2), the starting point was a solution containing SUVs, therefore with a diameter already within the nanometric scale, even if in presence of a large standard deviation, which can be interpreted as a large distribution of initial diameters (D_{D0} = 70 nm ± 40 nm). This initial SUVs solution, working at three different levels of power (Runs 2.a, 2.b and 2c), was subjected to further one, two or three steps of sonication (Runs 2.x1, 2.x2 and 2.x3 with x = a, b or c); all relevant parameters, including power levels and obtained liposome diameters, are reported in Table 4. It is worth to note that: i) the level of used power does not affect significantly the size of the liposome; and ii) increasing the number of ultrasound application cycles changes a little the liposome size, whereas decrease the standard deviation of experimental data (i.e., the repetition of the ultrasound application causes the narrowing of the size distribution).

Table 4. *Summary of experimental results*

	Initial diameter	U.S. Amplitude	Nominal power	Number of cycle(s)	Final diameter
	nm	%	W	#	nm
Run 1.a	1400	45	58	1	86
Run 1.b	1400	45	58	2	51
Run 1.c	1400	45	58	3	49
Run 2.a1	70 ± 40	30	39	1	64 ± 35
Run 2.a2	70 ± 40	30	39	2	66 ± 21
Run 2.a3	70 ± 40	30	39	3	44 ± 6
Run 2.b1	70 ± 40	45	58	1	69 ± 27
Run 2.b2	70 ± 40	45	58	2	72 ± 16
Run 2.b3	70 ± 40	45	58	3	59 ± 8
Run 2.c1	70 ± 40	60	78	1	67 ± 20
Run 2.c2	70 ± 40	60	78	2	75 ± 6
Run 2.c3	70 ± 40	60	78	3	37 ± 3

Results of the simulation of the Run 1 are reported in Figure 7, which organized the same way of Figure 6, showing (from the top) the ultrasound duty cycle, the liposome radius, the radius of the equivalent disc, the number of liposomes and the energy for each liposome/disc of lipid bilayer. The general behavior of each variable is the same already discussed for Figure 6. The simulation has been carried out using the same values for parameters already listed in the simulation of Part 1 ($k_c = 2.3 \cdot 10^{-19}$ J; $\bar{k}_c = 0$ J; $\gamma = 7.0 \cdot 10^{-20}$ J/nm), and using the remaining two ($\dot{g}_0$ and τ_C) as fitting parameters, by comparison of the calculation results with the final diameters of the observed liposome, as reported in Table 4. The value obtained are: $\dot{g}_0 = 1 \cdot 10^{-15}$ W, $\tau_C = 2.8$ s. The comparison between experimental data and calculated values is reported in Figure 8, which shows a nice agreement between the two series of data. It is worth to note that, even if the use of fitting parameters could drive the model toward the correct prediction of experimental data, the model itself is robust enough to account for the unexpected experimental observed behavior: the first ultrasound cycle causes a large decrease in sphere size (from 1400 nm to 86 nm), the second cycle causes another noticeable decrease (from 86 nm to 51 nm), whereas the third cycle does not change the size (51 nm is very close to 49 nm, within the measurement error). This could lead to the conclusion that the model is able to reproduce all the physical phenomena which take place during the process.
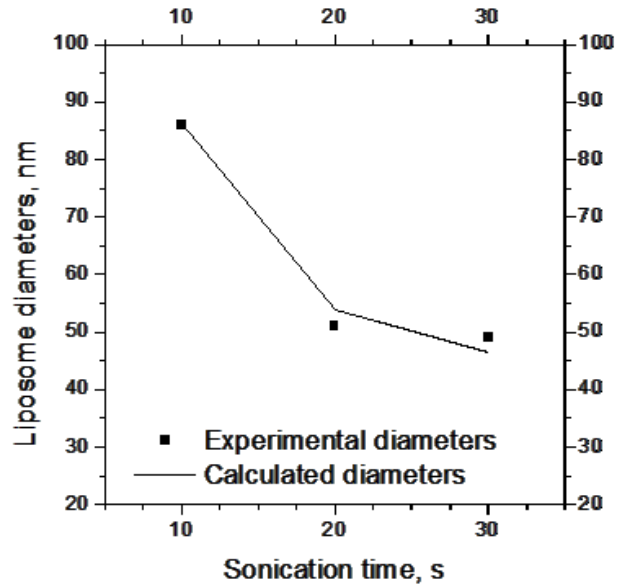
Figure 8. *Experimental and calculated liposome diameters for Run 1*

The calculations related to the Run 2 (precisely the data of Run 2.a, i.e. the test performed using the ultrasound amplitude of 30%, corresponding to nominal power of 39 W) are summarized in Figure 9, which is organized the same way of Figure 6 and Figure 7.
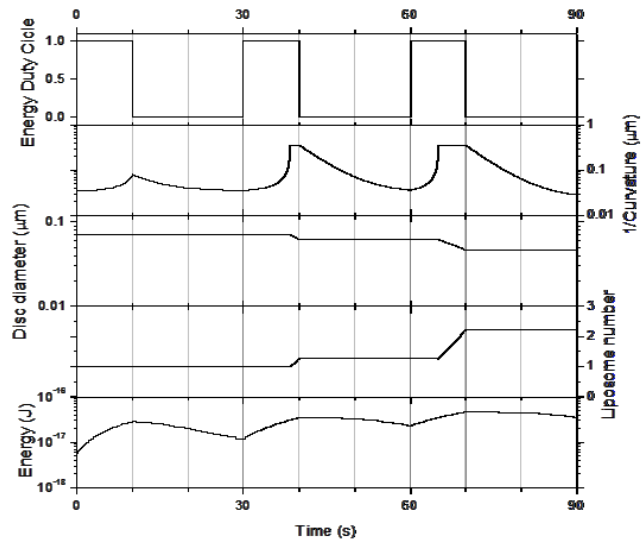
Figure 9. *Output of the calculation model for the real test Run 2.a*

The comparison between calculated values and experimental data is reported in Figure 10 for Run 2.a, and once more it shows a nice agreement between the two series of data: the calculated values falls well inside the confidence range given by standard deviation of experimental data. The fitting parameters value are $\dot{g}_0 = 2.3 \cdot 10^{-18}$ W and $\tau_C = 4.8$ s. Since the level of power resulted to not affect the liposome size, there is no need for further optimization/comparison with the results of Run 2.b and/or 2.c.
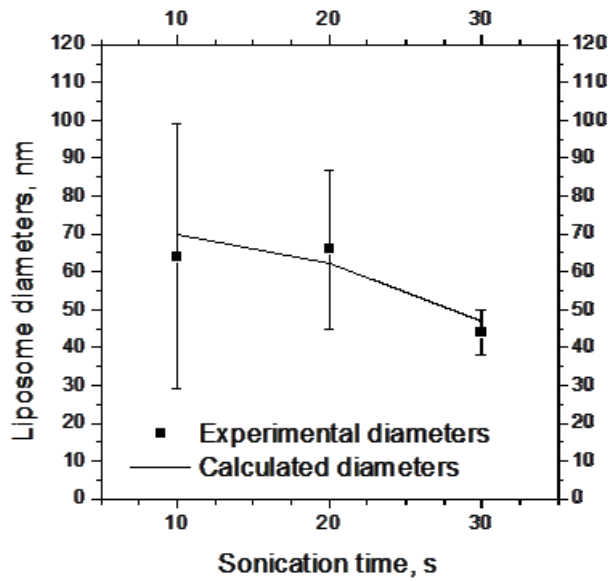
Figure 10. *Experimental and calculated liposome diameters for Run 2.a*

While the fitted values for the time constant, τ_C, are of the same order of magnitude (2.8 s for Run 1 and 4.8 s for Run 2), the fitted values for the rate of energy supply, $\dot{g}_0$, is quite different (roughly three orders of magnitude). Actually, the relevant parameter should be not the rate of energy supply but its ratio with the surface area of the lipid bilayer, A_0. For Run 1, this value is $\dot{g}_0/A_0 = 1.6 \cdot 10^{-4}$ W/m^2; for Run 2, this value is $\dot{g}_0/A_0 = 1.5 \cdot 10^{-4}$ W/m^2. It is evident that a single value of this parameter, $\dot{g}_0/A_0$, can describe both the tests.

As far as observed until now, the model is *descriptive*, i.e. it is able to describe how the size of liposome – made of the materials used in this thesis – changes if the ultrasonic energy duty cycle is varied. In order to point out a fully *predictive* model, a deeper knowledge of the parameters nature is required. I.e., the physical meaning of the ratio $\dot{g}_0/A_0$ as well as of the time constant, τ_C, have to be clarified and the effects of process parameters (sample volume, ultrasonic probe size and efficiency, amplitude and power of the US source, nature of the lipid bilayer) on the model parameters ($\dot{g}_0/A_0$ and τ_C) have to be investigated.

4.1.4 Remarks

A versatile and reliable technique able to produce liposomes of different sizes to be used for disparate applications has been developed. The Thin Film Hydration method was successfully revisited by adding an ultrasound assisted step in order to produce nanometric structures, with the desired dimensions, starting from the micrometric ones.

The phenomenological aspects involved in vectors constitution have been highlighted along with the mechanisms of bilayer rupture/nanovesicles formation. In that regard, a dynamic model able to describe the curvature of a lipid bilayer under the effect of ultrasonic energy was proposed and tested. The model is based on the calculation of bilayer free energy due to the curvature (elastic contribution) and due to the layer limits (edge contribution). The supply of energy by sonication exposure can cause the spherical vesicles opening or the disc rupture (increasing of the edge length). During the rest phase, while no ultrasonic energy is supplied, the bilayer curves toward the spherical form in order to minimize the free energy. The dynamic of such processes was described as a first order phenomenon and the model was numerically solved using the rate of energy supply, $\dot{g}_0$, and a time constant, τ_C, as fitting parameters. The fitting was carried out by comparison with experimental data produced by a preparation protocol detailed on purpose. The model was found able to calculate successfully size of spherical vesicles (liposomes), on the nano-metric scale, produced by cycles of sonication. Two different groups of tests, performed starting from LUVs (Large Uni-Lamellar Vesicles) and from SUVs (Small Uni-Lamellar Vesicles), allowed to identify as key parameters the time constant and the rate of energy supply for unit of bilayer surface area, $\dot{g}_0/A_0$. The model, because of the presence of fitting parameters, cannot be defined as a predictive tool, but it was found able to reproduce all the observed features of the real preparation process.

Due to its easiness, reliability, versatility and its great potential in reducing time spent, the ultrasound process developed and modelled was also used for liposomes homogenization operation during vesicles production through a simil-microfluidic approach detailed in the next section. In that regard, a simil-microfluidic apparatus was developed in order to produce higher volumes of lipid vectors, potentially on production scale, directly with nanometric size.

Finally, different active molecules of industrial relevance were encapsulated in nanoliposomes through the developed technique as detailed in the "Applications" section.

Part of this work has been reported in:
Barba A.A., Bochicchio S., Lamberti G., Dalmoro A., "Ultrasonic energy in liposome production: process modelling and size calculation", Soft Matter, 2014, 10 (15), 2574 – 2581.

4.2 Simil-microfluidic liposome preparation method: layout, principles and phenomenological aspects

4.2.1 Generalities

Due to their biocompatibility**,** safety and delivery efficacy, the demand of liposomes based products to be used in pharmaceutical and nutraceutical field has risen together with the need of large-scale and low environmental impact techniques capable to produce significant amounts of liposomes in a short time and without the use of drastic conditions. Indeed, according to the Paris Agreement on climate change (Abeysinghe and Barakat, 2016), innovation must go hand in hand with the developing of green products, improving the business processes and scaling-up investments through greater energy and material efficiencies (Burck et al., 2014). The energy efficiency and emissions reduction in the industrial sectors are the crucial point.

As seen in "State of the art" section, nowadays there is a wide set of possibilities to produce lipid-based drug delivery systems through the use of conventional or more recently discovered techniques (Meure et al., 2008, Wagner and Vorauer-Uhl, 2010, Bangham and Horne, 1964). However, despite the leaps and bounds made with the novel technologies in the last few years, the majority of these methods are characterized by high energy request, long times of process, the use of toxic solvents together with a low productivity. In particular, the most used techniques, such as the Ethanol Injection (Pons et al., 1993) or the Thin Film Hydration method discussed in the previous section, are bench-scale techniques characterized by bulk discontinuous processes. Microfluidics is a relatively new technology used for the production of liposomes on nanometric scale (Yu et al., 2009). This last gives the possibility to produce, in a continuous manner, Small Unilamellar Liposomes (SUVs) with a precise control on liposomes dimensional features by modulating the flows at micrometric scale, anyway the method is characterized by elevated costs of microfabrication and low product volumes in output.

To overcome these limitations, in this thesis microfluidics based methods, which are expensive for special devices needed and microfabrication costs, have been transposed to a millimeter scale and coupled with the Ethanol Injection method, drastically reducing the production costs and increasing the yields.

With the aim to have a control on flow, typically chaotic in a bulk phase which is instead laminar, and thus controllable, in a microfluidic system, starting from a work of Pradhan and collaborators (Pradhan et al., 2008), in which a syringe pump driven microfluidic device was used to produce liposomes, the design and the developement of a new semicontinuous bench scale apparatus for a massive nanoliposomes production, overcoming the limits imposed by the syringe volumes, has been done. The process basically

consists in the realization of a contact between two flows, lipids/ethanol and water solutions, inside a tubular device, where interdiffusion phenomena allow the formation of lipid vesicles. Furthermore in this thesis, taking into account that size and size distribution are key parameters determining liposomes performance as carrier systems in both biomedical applications (i.e. influencing liposomes time of circulation in the blood stream and/or their permeability through membrane fenestration in tumour blood vessels (Sawant and Torchilin, 2012)) and nutraceutical applications (i.e. improving taste, flavor, stability, absorption and bioavailability of nutraceuticals (Reza Mozafari et al., 2008, Bochicchio et al., 2016a) similarly as done by Jahn and collaborators for a microfluidic hydrodynamic focusing (MHF) platform (Jahn et al., 2004), a dimensional control of the produced nanoliposomes was demonstrated by tuning not only the flow rates, as done by Jahn research group, but also the lipids concentration. In the light of what previously explored and modelled (4.1 section), ultrasonic energy, and its developed duty cycle protocol (Barba et al., 2014), was used as intensification tool in nanoliposomes production through the simil-microfluidic apparatus. The duty cycle sonication process was successfully scaled up and used for particles homogenization operation as below described.

4.2.2 Experimental section

4.2.2.1 Materials

L-α-Phosphatidylcholine (PC) from soybean, Type II-S, 14-23% choline basis (CAS n. 8002-43-5) and ethanol of analytical grade (CAS n. 64-17-5) were purchased from Sigma Aldrich (Milan, Italy).

4.2.2.2 Layout

Figure 11 shows a schematization of nanoliposomes production process through the semicontinuous simil-microfluidic apparatus fabricated. The set-up is constituted by five main section: a feeding section, a pumping section a production section, an homogenization section and, finally, a recovery section.
In particular, the feeding section consists in two lines: the first is made up by a stirred tank filled with a lipids/ethanol solution (number 1 of Figure 11), in which is eventually dissolved an hydrophobic active principle, conveyed in a silicon tube (667-8441 RS Components, Northants, UK). This latter has an internal diameter of 1.6 mm and a length of 610 mm, is made of silicone and is suitable for food and pharmaceutical applications (operating temperature range from -50 to 200° C).
The second line includes a stirred tank filled with the hydration solution (number 4 of Figure 11), which can be pure water or an aqueous solution

containing the hydrophilic active principle, conveyed in a flexible silicone tube (00392400, RS Components, Northants, UK) with an internal diameter and length of 5 mm and 360 mm, respectively.

The pumping section is composed by two single head peristaltic pumps (Verderflex OEM mod. Au EZ) indicated as elements G-1 and G-2 in Figure 11 with a polyamide, acetal and stainless steel pump head and a permanent magnet gear-motors.

In particular, among the several pumping systems (gear pumps, piston pumps, syringe pumps, gravity systems, pressurized canisters), peristaltic pumps were chosen for their several advantages: they are able to pump different kinds of fluid; the treated fluid does not interact directly with the pump components thus the cleaning and the maintenance operations are easily performed; they are able to modulate large amount of fluids and to keep them constant; finally they are suitable for large-scale processes (Dalmoro et al., 2014).

The lipids/ethanol solution tube ends with a 0.6 mm internal diameter needle (Eurospital Spa, mod. Euroset 34 Fly 23G Latex Free) inserted into a silicon tube of 3 mm internal diameter and 185 mm length (00392200, RS Components, Northants, UK) which is an extension of the water tube. This is the production section sketched in Figure 11 and indicated as element I-1. In this section an interdiffusion of the two pushed liquids occurs leading to the formation of liposomes on nanometric scale.

Briefly, the process starts when lipids/ethanol and water solutions are pushed through peristaltic pumps into the production section, where liposomal vesicles are formed directly on nanometric size. The formed hydroalcoholic solution is recovered in a tank and stirred. Finally, in order to homogenize the vesicles for a better particles size distribution, aliquots of the liposomal suspension are subjected to the duty cycle sonication process previously developed and modelled (Barba et al., 2014), by applying a duty cycle consisting of 5 ten-second irradiation rounds each followed by a 20 second pause in order to prevent thermal vesicle disruption. In particular, a 3 mm probe was used in the homogenization process by treating 1 ml sample aliquots at 45 % amplitude of sonication in duty cycle (130 W, 20 kHz) as before done for nanoliposomes production through the ultrasound assisted Thin Film Hydration method (4.1 section).

In that regard, the homogenization section was subsequently scaled up by using a titanium probe of 6 mm diameter acting directly on 110 ml sample production batch and changing some of the sonication key parameters as detailed in 4.2.2.5 paragraph. Figure 11 shows exactly the apparatus plant configuration directly with the integration of the ultrasound assisted homogenization section scaled up.

D-1	Lipid/ethanol solution (*and hydrophobic molecule*) feed tank
D-2	Hydration solution (*and hydrophilic molecule*) feed tank
D-3	Mixing/sonication tank
G-1	Pump for lipid/ethanol solution
G-2	Pump for hydration solution
I-1	Lipid/ethanol solution injection
Z-1	Sonicator
1-2-3	*Lipid/Ethanol feed line*
4-5-6	*Hydration solution feed line*
7-8	Nanoliposomes suspension
Key to abbreviations	
US	Ultrasounds source

Figure 11. *Process schematization of nanoliposomes production through the semicontinuous simil-microfluidic apparatus; the main sections are reported: feeding, pumping, production, homogenization and recovery. From the tanks (D-1, D-2) lipids/ethanol and water solutions are pushed through peristaltic pumps (G-1, G-2) to the production section (I-1) were nanometric vesicles are formed. The hydroalcoholic solution (7) is recovered in a tank (D-3) and subjected to a duty cycle sonication process (Z-1). Finally the suspension (8) is recovered and characterized*

Flow regime evaluation

First of all, taking into account that a microfluidic system is characterized by a laminar flow regime, the fluid dynamic nature of the simil-microfluidic apparatus was evaluated.

In the simil-microfluidic set up developed, through the use of constructive expedients (millimetric tubes, peristaltic pumps, injection needle) the reproduction of the laminar flow regime was possible being all the Hagen-Poiseuille assumptions satisfied (Bird et al., 2007) as detailed in the results section (4.2.3.1 paragraph).

At first the Reynolds number was found for all the conditions used. In particular, for all the volumetric flow rates tested (10:1, 15:1, 20:1 and 40:1 Vhs/Vls), the Reynolds number (*Re*) of the organic and the polar phases was calculated as follows:

$$Re = \frac{4 \cdot \rho \cdot \dot{V}}{\mu \cdot D} \qquad (4.4)$$

where ρ is the fluid density, *V* is the volumetric flow rate of the fluid, μ is its dynamic viscosity and *D* is the diameter of the tube. For the determination of the fluid dynamic conditions some approximations were done: the organic phase was referred only to ethanol, the polar phase only to water and the liposomal suspension was referred to a water-alcohol solution, their chemical-physical and transport properties (density and viscosity) were determined at room temperature. In detail, for the polar phase a tube diameter of 5 mm was considered and the density and the viscosity of the water were taken equal to 103 kg/m^3 and 10^{-3} Pa·s, respectively. For the organic phase, a 1.6 mm diameter tube was considered and the density and the viscosity of the ethanol at room temperature were considered to be equal to 789 kg/m^3 and to 1.2·10^{-3} Pa·s, respectively. For the hydroalcholic suspension the liposomal section production tube of 3 mm was considered and the chemical-physical and transport properties of the mixture were approximated to those of the water being the concentration of ethanol in the suspension very small for all the volumetric flow rates ratio (Vhs/Vls) tested, with a maximum of 9 % v/v of ethanol for the 10:1 Vhs/Vls up to the 2.5 % v/v of ethanol used at 40:1 Vhs/Vls.

Moreover, in order to neglect the end effects and thus fulfill another assumption of Hagen-Poiseuille, the "entrance length" (*Le*), after the lipid/ethanol tube entrance in that of water, was calculated as $Le = 0.035 \cdot D \cdot Re$. In particular, the Le was calculated taking into account the lower and the higher Reynolds numbers obtained and the 3 mm diameter of the tube where the hydroalcholic solution streams. Notably, a certain entrance region is needed for the buildup to the parabolic profile thus the piping length, in which the two phases interdiffuse, has to be longer than the "entrance length".

4.2.2.3 Liposomes preparation

Once defined the geometric parameters, those of process such as the volumetric flow rates, the lipid concentration and the sonication conditions adopted were investigated in order to establish their control on the nanoliposomes dimensional features. For this purpose samples of unloaded liposomes were produced at different conditions and then characterized. The morphological characterization was performed by using optical microscopy (Axioplan 2- Image Zeiss) for fluorescence imaging, a 100 X oil immersion objective was used to visualize the vesicles. Rhodamine B was used for microscope fluorescence observations.

Dimensional characterization of vesicles was performed by Dynamic Light Scattering analysis (Zetasizer Nano ZS, Malvern, UK). The resulting particle size distribution was plotted as number of liposomes versus size. The Polydispersity Index (PDI) was calculated for all the preparations. Statistical analysis of experimental data (size and PDI) were analyzed using Student's t-test and one-way analysis of variance (ANOVA), and differences were considered statistically significant at $p < 0.05$.

Volumetric flow rate ratio modulation

In order to study the influence of the lipid concentration and the volumetric flow rate ratio on liposomes size and size distribution, liposomes were at first prepared by maintaining constant the PC concentration in the hydroalcoholic solution at 0.15 mg/ml and varying the volumetric flow rates. This latter, defined as the hydration solution volumetric flow rate (Vhs) to the lipid solution volumetric flow rate (Vls), was varied (10:1, 15:1, 20:1 and 40:1 Vhs/Vls) maintaining constant the Vls at 4 ml/min and changing the Vhs (40 ml/min, 60 ml/min; 80 ml/min and 160 ml/min). Briefly, for this purpose, 16.5 mg of PC were dissolved in 10 ml of ethanol to achieve the lipid solution, while deionized water (100 ml) was used as hydration solution. The two liquids were pushed into their respective silicon tubes through the use of peristaltic pumps following the process previously described and schematized in Figure 11.

Lipid concentration modulation

After the volumetric flow rate ratio optimization, maintaining constant at 10:1 the Vhs/Vls ratio, the lipid concentration in the final hydroalcoholic solution was changed (0.15, 1, 4 and 5 mg/ml) and the liposomes size and size distribution were analyzed again.

Aliquots (1 ml) from all the produced samples were then taken and subjected to the homogenization process (Barba et al., 2014).

The effects of volumetric flow rate ratio and PC concentration on liposomes size and size distribution were studied with and without the ultrasound contribution.

4.2.2.4 Process productivity evaluation

In order to have an idea of the productivity of the process through the simil-microfluidic apparatus developed, liposomes number for unit volume of solution obtained at different operative conditions was evaluated. In particular the number of vesicles formed for unit volume in the final hydroalcoholic solution, at the different volumetric flow rates ratio tested and PC concentrations used, was valued for sonicated and not sonicated samples. The number of liposomes for unit volume (N_{lip}) was analytically calculated as done by *Encapsula Nanosciences*, a liposome formulator and manufacturer pharmaceutical company, considering the equation below:

$$N_{lip} = \frac{M_{lip} \cdot N_a}{N_T \cdot 1000}$$ (4.5)

where M_{lip} is the PC concentration (mol/ml), N_α is the Avogadro number $(6.022 \cdot 10^{23}/mol)$, N_T (nm^2/nm^2) is the number of lipids present in one liposome depending on liposomes diameter and determined by using the relation:

$$N_T = \frac{[4 \cdot \pi \cdot (\frac{d}{2})^2 + 4 \cdot \pi \cdot (\frac{d}{2} - h)^2]}{a}$$ (4.6)

where *d* is the vesicles diameter size (nm), *h* is the thickness of the bilayer (nm) and *a* is the hydrophilic portion surface area (nm^2).
For unilamellar vesicles made from phosphatidylcholine the bilayer thickness is about 5 nm while the hydrophilic portion surface area is equivalent to 0.71 nm^2 thus the equation 4.6 can be simplified as follows:

$$N_T = 17.69 \cdot [\left(\frac{d}{2}\right)^2 + \left(\frac{d}{2} - 5\right)^2]$$ (4.7)

where 17.69 is equal to $4 \cdot \frac{\pi}{a} = 4 \cdot \frac{\pi}{0.71}$, expressed in $1/nm^2$.

4.2.2.5 Scale up of the ultrasound assisted homogenization process

To move from a production scale of a few milliliters to a greater production batches (of the order of hundred milliliters) the homogenization section was scaled up. In particular, the 3 mm sonotrode tip was replaced by a 6 mm tip acting directly on the entire volume of the liposomal suspension (110 ml per batch), thus the plant configuration described in 4.2.2.2 paragraph was adopted.
In particular, in order to obtain, with the new plant configuration, the same final nanoliposomes dimensional features previously achieved by sonicating 1 mL aliquots of sample, keeping constant the duration of each cycle (10 s) and the time in which the ultrasound is not applied (20 s) and operating with

an amplitude of 100%, the ultrasound power and the number of cycles required to sonicate a 110 ml volume of liposomal suspension were determined. In particular, starting from a volume of unloaded nanoliposomes suspension of 1 ml, using an amplitude of 100 %, the energy supply by one sonication cycle of 10 seconds was determined. Considering the linearity between the power and the volume of sonication, the power required to sonicate 110 ml of liposomal suspension was determined, then the number of duty cycle sonication rounds able to provide the necessary power has been obtained experimentally. In particular, unloaded nanoliposomes were produced by mantaining constant the optimized conditions (10:1 Vhs/Vls; 5 mg/ml lipids/final hydroalcoholic solution) and by submitting the samples to different sonication rounds: 0, 15, 30 and 60 duty cycle rounds were applied, then vesicles were characterized in terms of size and size distribution.

4.2.3 Results and Discussion

4.2.3.1 Simil-microfluidic apparatus

A new semicontinuous bench scale apparatus for nanoliposomes production was successfully designed and developed, overcoming the limits imposed by the conventionally used techniques. In particular, by coupling the ethanol injection method with the microfluidic principle and transposing them on a micrometric scale it was possible to achieve a massive nanoliposomes output in an easy and cheap way. In a work of Pradhan and collaborators (Pradhan et al., 2008) a syringe pump driven microfluidic device was developed to produce nanoliposomes, in this thesis the semicontinuous bench scale apparatus was designed by replacing the syringe pumps by the peristaltic once, allowing the production of larger volumes and by injecting the lipid phase directly into the polar phase without the help of any tubes connection systems. Moreover, microfluidics based methods, such as the MHF platform made by Jahn et al. (Jahn et al., 2004), which are expensive for special devices needed and microfabrication costs, have been transposed to a millimeter scale, drastically reducing the production costs and increasing the yields.

The simil-microfluidic approach had also permitted to overcome the limit of bulk phase methods in which is difficult to control the liposomes dimensional features instead carefully modulated in this thesis with a further ultrasound assisted homogenization step. Finally, the simil-microfluidic apparatus had allowed to successfully produce ferrous sulfate loaded nanoliposomes to be used in nutraceutical application as detailed in "Application" section (Chapter 5).

Flow regime evaluation and phenomenological aspects

Like in a microfluidic system, due to the millimetric scale of the channels and the low volumetric flow rates, the flow in the simil-microfluidic

apparatus developed is laminar in opposition to the chaotic onces characterizing the bulk phases. Indeed, results obtained relatively to the flow regime evaluation have shown that all the Hagen-Poiseuille assumptions were satisfied (Bird et al., 2007). First of all Reynolds number results are reported in Table 5.

Table 5. *Reynolds number relative to the polar phase, the organic phase and the hydroalcholic solution at the different volumetric flow rates ratio tested*

V, ml/min	R_e
Polar Phase	
40	169.7
60	254.6
80	339.5
160	679.0
Organic Phase	
4	34.9
Hydroalcholic Phase	
44	311.4
64	452.6
84	594.5
164	1160

For all the conditions tested, the polar and the organic phases exhibit a laminar flow regime in the feeding section, likewise the hydroalcholic phase in the production section. In particular, the Reynolds number, which was found to be less than 2100 for all the volumetric flow rates conditions tested, changes from 311.4 to 1160 moving from 10:1 Vhs/Vls to 40:1 Vhs/Vls. This result shows that the blending between the two phases is governed by diffusion mechanisms.

Apart from the Reynolds number, the other Hagen-Poiseuille assumptions were also satisfied. In particular, operating at constant temperature and pressure, the fluids were considered incompressible and the flow was considered to be steady being, except for the startup moment, the volumetric flow rates mantained constant during the entire production process. Moreover, the fluid is considered Newtonian because the behavior of the hydroalcholic suspension was approximated to that of water which is a Newtonian fluid.

Finally, the piping length in which the two phases interdiffuse is longer than the "entrance length" needed to buildup the parabolic profile. In particular a 32.7 mm and a 121.8 mm entrance lengths were found at the lower and the higher Reynolds number tested, respectively. This lengths are lower than that of the pipe (150 mm) where interdiffusion phenomena occured.

From a phenomenological point of view, liposomes formation is governed by the molecular diffusion between two phases: the organic solvent, in which the lipids are solubilized, and the water; this latter simultaneously diffuses into the organic solvent in order to reduce its concentration below the critical value required for the lipids solubilization. During the diffusion process, lipid vesicles on nanometric scale start to form through a mechanism called "self-assembly", according to the theory of Lasic et al. (1988): lipids dissolved in an organic solvent are in the form of bilayer fragments (Phospholipid Bilayer Fragments, BPFs), the interdiffusion of the water and the organic solvent reduces the solubility of the lipids in the solvent causing thermodynamic instability of BPFs edges, inducing the curvature and the closure of bilayer fragments which allow the formation of liposomal vesicles (Lasic and Papahadjopoulos, 1998). In particular, for a microfluidic system, liposomes formation happens at the interfaces between the alcoholic and water phases, when they start to interdiffuse in a direction normal to the liquid flow stream. Changes in flow conditions result in a size variations of the insertion section of the organic phase reflecting on the vesicles dimensional features. In particular, increasing the volumetric flow rates ratio, the size of the insertion section of the organic phase decreases; this leads to a major dilution of the organic phase limiting the formation of long BPFs thus inducing the production of liposomal structures of small dimensions. In general, it was shown that the variation in shear forces at the interface of the two fluids have no conseguence on liposomes structure. In particular, mantaining constant the volumetric flow rates ratio and changing both the buffer and the lipids alcoholic solutions volumetric flow rates, Jahn and collaborators have demonstrated that is not the magnitude of the shear forces between the parallel layered stream in having significant impact on liposomes size and size distribution as the stream width (which depends on the volumetric flow rates ratio) (Jahn et al., 2007). In Figure 12 a schematic representation of the liposome formation process through the microfluidic approach is presented.
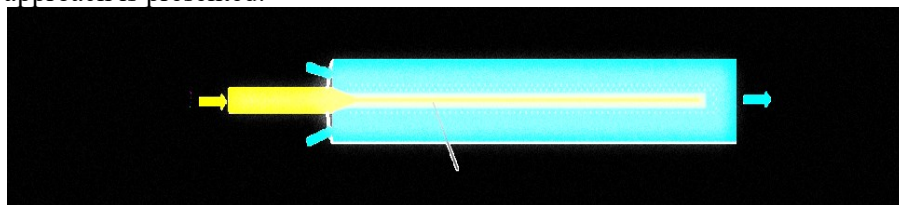
Figure 12. *Representation of the liposome formation process by a microfluidic approach*

In general, local fluctuations of the lipid concentration in a bulk solution make difficult to control the size and the polydispersity of the produced vesicles. On the contrary, the presence of intubated laminar flows with the relative matter diffusive transport allows to minimize the fluctuations of the lipid concentration inside the tubes and to modulate the size and the size distribution of the final vesicles.

4.2.3.2 Unloaded nanoliposomes production: process parameters effect on dimensional features

Small Unilamellar Vesicles (SUVs) directly on a nanometric scale were produced through the developed simil-microfluidic apparatus, without the use of any toxic solvents and drastic conditions (i.e. high temperature and/or pressure). In Figure 13 the SUVs obtained are shown. In particular, to the light of nanoliposomes size obtained (detailed in the next subparaghaph) vesicles presented in the fluorescence microscopy images are called SUVs even if aggregates and/or large vesicles produced together with SUVs, although few, are well and more visible in the captured images.
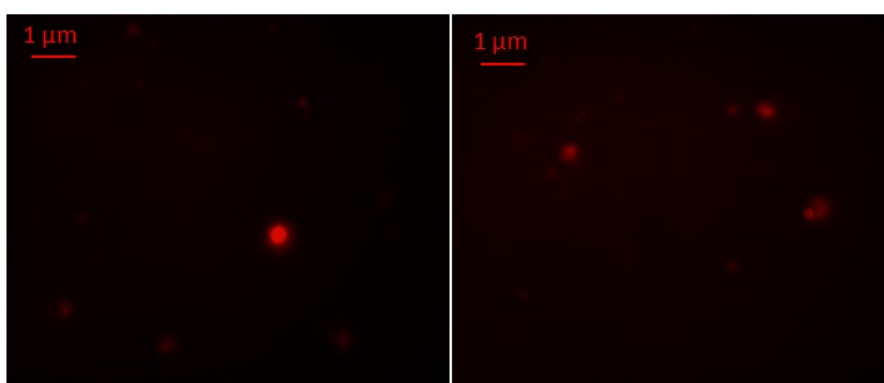
Figure 13. *Fluorescence microscopy images of lipid vesicles labelled with Rhodamine B dye and visualized with a 100 X objective*

Effect of volumetric flow rate ratio
The volumetric flow rate ratio exerts a strong influence on the final vesicles dimensional features as also found by Jahn and collaborators for a microfluidic hydrodynamic focusing platform (Jahn et al., 2004).
In fact, it was shown that increasing the ratio between the water volumetric flow rate to the lipids-ethanol volumetric flow rate the liposomes dimension, reported in Figure 14 A, do not change in a statistical manner ($p > 0.05$) while the PDI value increases as showed in Figure 14 B.
In particular, for not sonicated samples, PDI is worsened when flow rate ratio increases from 20 to 40 (it is kept statistically constant between 10 and 20); for sonicated samples, PDI is worsened going from a flow rate of 10 to 15; for higher flow rates it is kept constant.

Specifically, not sonicated liposomes of 49 nm in size were obtained by operating with a 10:1 Vhs/Vls ratio and vesicles even smaller were achieved with a 15:1 and 20:1 Vhs/Vls, up to a diameter of 33 nm for liposomes obtainined by using a 40:1 Vhs/Vls, the higher volumetric flow rate ratio tested. An opposite trend is visible for the PDI of not sonicated samples, whose 0.36 value obtained from the 10:1 Vhs/Vls becomes 0.73 when a 40:1 Vhs/Vls ratio was used, index, the latter, of an highly polydispersed sample. The ultrasound assisted process applied reduces the liposomes PDI for all the flow rates explored except for the 15:1. The duty cycle sonication has a key role in the liposomes homogenization by reducing the polydispersity of the sample, optimizing the size distribution; i.e. for the 40:1 Vhs/Vls the PDI is nearly halved (Figure 14 B).
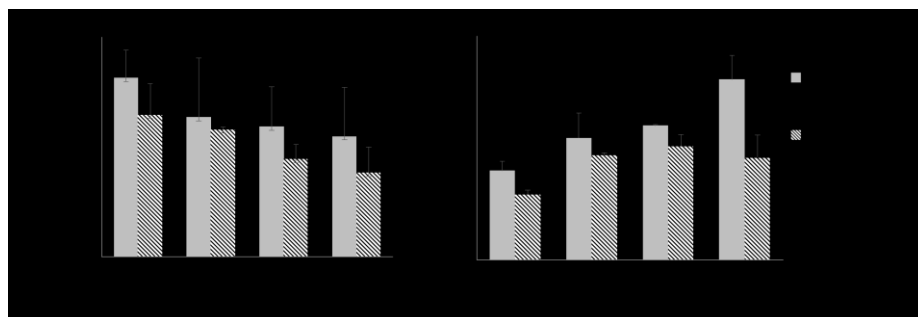
Figure 14 *A) Sonicated and not sonicated liposomes diameter size at different volumetric flow rates ratio. B) Polydispersity Index (PDI) of sonicated and not sonicated liposomes at different volumetric flow rates ratio. Results are expressed as average of three determinations and reported along with the standard deviation*

Effect of lipid concentration
It was observed that at equal flow rates ratio, when the lipids concentration increases the liposomes size (Figure 15 A) and PDI values (Figure 15 B) remain statistically constant (p > 0.05); just for sonicated samples, PDI is worsened when concentration increases from 0.15 to 1, then it is kept constant. The sonication process has confirmed to be efficacy for liposomes homogenization ameliorating liposomes dimensional distribution for concentrations 4 and 5 mg/ml (values statistically significant, p<0.05); i.e. for the 5 mg/ml concentration, after the homogenization step, the PDI decreases from 0.32 to 0.29 (Figure 15 B).
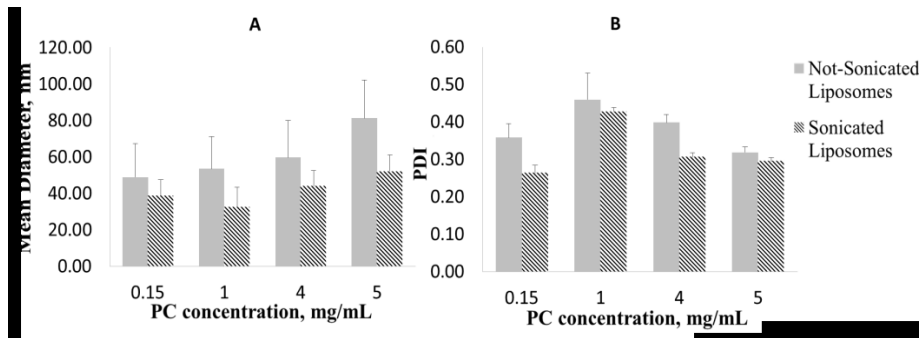
Figure 15 *A) Sonicated and not sonicated liposomes diameter size at different PC concentrations in the hydroalcoholic solution. B) Polydispersity Index (PDI) of sonicated and not sonicated liposomes at different PC concentrations in the hydroalcoholic solution. Results are expressed as average of three determinations and reported along with the standard deviation*

4.2.3.3 Productivity of the process

The number of liposomes for unit volume, index of the productivity of the process, was calculated for all the conditions tested. It was demonstrated that the number of liposomes increases for sonicated samples. It is important to note that the sonication always enhances the productivity of the process with a maximum of 57 % more liposomes produced with a 40:1 Vhs/Vls ratio (Figure 16 A) and a plus of 67 % considering the 5 mg/ml PC concentration (Figure 16 B).
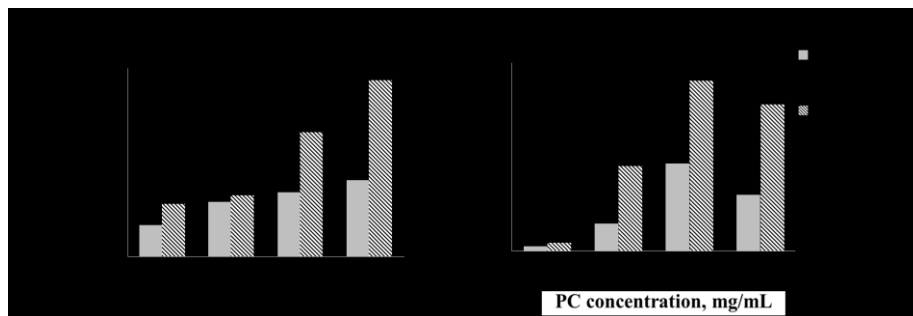
Figure 16 *A) Sonicated and not sonicated liposomes number (Nlip) for unit volume of solution obtained at different volumetric flow rates ratio. B) Sonicated and not sonicated liposomes number (Nlip) for unit volume of solution obtained at different PC concentrations in the hydroalcoholic solution*

Summerizing, the results relative to the unloaded vesicles production have shown that the liposomal vesicles with the best size distribution were produced by using a volumetric flow rate ratio of 10:1 Vhs/Vls and a

concentration of lipids equal to 5 mg/ml. The duty cycle sonication process was effective in homogenize the vesicles as well as to increase the productivity of the process as showed for all the operative conditions tested.

4.2.3.4 Scale up of the ultrasound assisted homogenization process

In order to scale up the ultrasound assisted homogenization process, keeping constant the duty cycle irradiation time and using the 6 mm tip with a 100% amplitude, the power to be delivered and thus the number of sonication cycles able to amplifying the sound wave on the entire batch volume produced (110 ml) generating the same dimensional features founded for sonicated sample aliquots (1 ml) was found.

In particular, being the power of sonication equal to 4.7 W for 1 ml of sample volume and considering the linearity between the power and the number of sonication rounds at fixed volume (Figure 17), the power theoretically required to sonicate 110 ml was about 500 W; such power has been operatively obtained by using 15 rounds of duty cycle sonication.
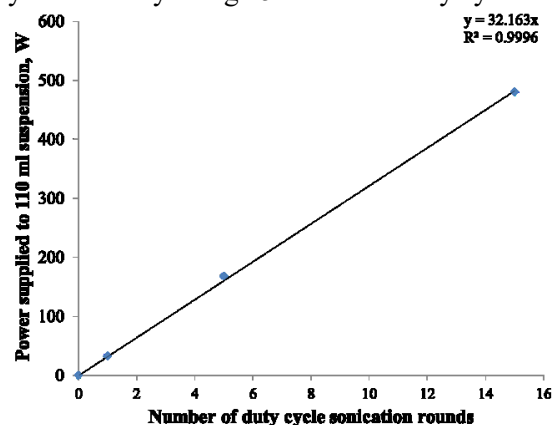
Figure 17. *Linearity between the number of duty cycle sonication rounds applied and the power supplied to 110 ml nanoliposomes suspension*

The effect of different times of sample exposure to ultrasound on the vesicles dimensional features was studied after 0, 15, 30 and 60 rounds of duty cycle sonication, results are reported in Figure 18.
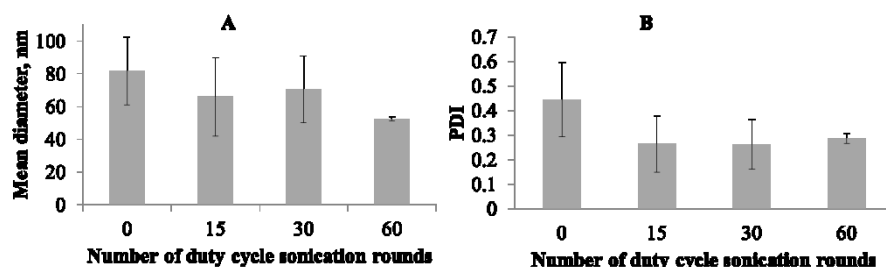
Figure 18 *A) Liposomes diameter size after different number of duty cycle sonication rounds. B) Polydispersity Index (PDI) of liposomes after different number of duty cycle sonication rounds. Results are expressed as average of three determinations and reported along with the standard deviation*

As a result of the homogenization process scale-up, it was possible to observe a reduction of both liposomes diameter size (Figure 18 A) and PDI (Figure 18 B) as an effect of sonication. In particular, starting from 82 nm not sonicated vesicles (0 rounds) the average size was reduced to 66, 70 and 52 nm respectively after 15, 30 and 60 duty cycle sonication rounds. With regard to the polydispersity index, the sonication was always effective in homogenize the liposomal suspensions for all the operating conditions tested. In particular, samples obtained by using 60 rounds of duty cycle sonication (52.4 ± 1.05 nm; 0.29 ± 0.01 PDI) showed a significant reduction of the standard deviation and can be compared with those obtained on a small scale, operating with 1 ml sample aliquot and the 45% amplitude, having an average size of 52.18 ± 8.93 nm and a PDI of 0.29 ± 0.01 (4.2.3.2 paragraph). However, depending on the application requirements, 15 rather than 60 duty cycle rounds can be used.

In conclusion, the homogenization step has proved to be an effective and easily scalable method therefore was included in the production process by using the simil-microfluidic apparatus configuration as schematized in Figure 19.
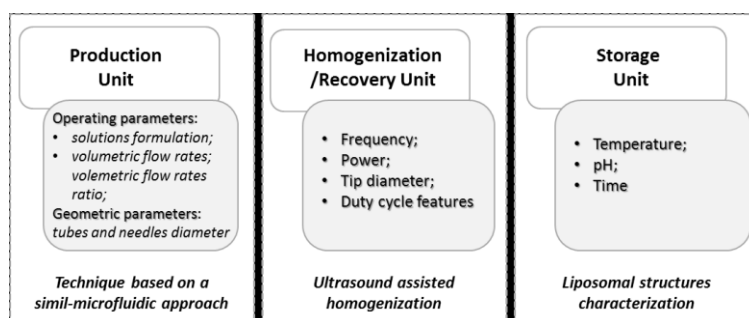
Figure 19. *Three main units of the simil-microfluidic set-up: a production unit according to the simil-microfluidic approach, an ultrasound assisted homogenization and recovery unit, a storage unit*

4.2.4 Remarks

A massive production of nanoliposomes is possible due to the developed simil-microfluidic bench scale apparatus with a precise control on particles dimensional distribution by varying the liquids volumetric flow rate ratio. In particular, increasing the ratio between the water volumetric flow rate to the lipids-ethanol volumetric flow rate the liposomes PDI increases; at equal flow rates, when the lipids concentration increases the liposomes PDI is kept constant. Ultrasonic energy was used to enhance homogenization of the hydroalcoholic bulk and, as expected on the bases of previous studies, its duty cycle application efficaciously promoted vesicles disaggregation. The ultrasound assisted homogenization has also proved to be a reliable and scalable process intensification tool. The simil-microfluidic apparatus developed is ables to produce nanoliposomes through a sustainable large scale process, avoiding the use of toxic solvents and drastically reducing process time and costs.

Part of this work has been reported in:
Bochicchio S.; Dalmoro A.; Recupido F.; Lamberti G.; Barba A.A.; "Nanoliposomes production by a protocol based on a simil-microfluidic approach", accepted as publication in "Lecture Notes in Bioengineering (LNBE)", Springer Ed. (2016)

5. Applications

In this chapter, all the applications concerning the use of the Ultrasound assisted Thin Film Hydration method and the Simil-microfluidic technique developed are presented. The aim is focused on the production of nano-liposomal carriers loaded with different kinds of active molecules: micronutrients (vitamins and ferrous sulfate) for nutraceutical applications and therapeutic agents (peptide and NABDs) for pharmaceutical applications. Each application is briefly described introducing the appliance field, describing the materials and the obtained results.

Keywords

5.1 Liposomal vectors for vitamins delivery

5.1.1 Generalities

Liposomes are efficient nutrient delivery systems which are able to ensure a controlled and targeted release to foodstuffs due to their thermodynamic stability (Fernández-García et al., 2007, Kwak, 2014, deAssis et al., 2014). The possibility of producing nanostructured materials for controlling the bioavailability of nutrients with strong biological activity has great industrial relevance for optimizing product formulation (food supplements, vitamin dosage systems) and processing, thus contributing to people's health and well-being (Sanguansri and Augustin, 2006, Lopez-Rubio et al., 2006, Soottitantawat et al., 2005, Emamifar et al., 2010, deAssis et al., 2012, deAssis et al., 2014).

Recently, much attention has been paid to using the nanoliposomes as carriers of bioactive ingredients in food and nutrition for encapsulating antioxidants (Azevedo et al., 2013, LIU et al., 2013, Isailović et al., 2013, Gupta and Abu-Ghannam, 2011, Toniazzo et al., 2014). In fact, using liposomes as antioxidant vitamin carriers represents a promising approach for developing new functional food formulations and solving the vitamin stability issues which strongly hinder their application.

Vitamin B12, α-Tocopherol and Vitamin D2 were used due to their great antioxidant potential and different hydrophilic-lipophilic and solubility properties.

Few are the information regarding the encapsulation of ergocalciferol and vitamin B12 in liposomes, a little bit more can be found in literature for α-tocopherol encapsulated in liposomes (Rovoli et al., 2013) but data are completely missing in relation to the production of liposomes smaller than 80-100 nm in size encapsulating vitamins.

In this thesis nanoliposomal vectors (NLV) with high encapsulation efficiency of vitamins were produced for a controlled release purposes. Taking into account the benefits in obtaining the smallest nanoliposome with the highest vitamins encapsulation efficiency, the ultrasound assisted Thin Film Hydration method developed (4.1 section) was used. The main challenge of this approach was to test the versatility of the developed preparative protocol to achieve tailored liposomes in terms of size and encapsulation efficiency in relation to three used vitamins, different in size and solubility. By using the developed technique (Barba et al., 2014) the production of 40-50 nm SUVs containing ergocalciferol, vitamin B12 and α-tocopherol was performed emphasizing that vitamins encapsulation efficiency for NLV smaller than 50 nm was never tested before.

5.1.2 Materials

L-α-Phosphatidylcholine (PC) from egg yolk (CAS n. 8002-43-5), Cholesterol (CHO) (CAS n. 57-88-5), L-αPhosphatidyl - DL glycerol sodium salt (PG) from egg yolk lecithin (over 99% pure), vitamin B12, B12, (CAS n. 68-19-9), α-tocopherol, TC (CAS n. 10191-41-0), ergocalciferol, D2, (CAS n. 50-14-6), potassium phosphate monobasic (CAS n.7778-77-0) and sodium hydroxide (CAS n. 1310-73-2) were purchased from Sigma Aldrich (Milan, Italy) as dried powders and used without further purification. All the other chemicals and reagents such as chloroform (CAS n. 67-66-3), ethanol (CAS n. 64-17-5), methanol (CAS n. 67-56-1) (Sigma Aldrich, Milan, Italy) used were of analytical grade.

5.1.3 Methodology and sperimental set-up

5.1.3.1 Preparation of MLVs and SUVs loaded with vitamin B12

Unilamellar liposome vesicles were prepared by means of the Thin Film Hydration method (Meure et al., 2008, Bangham and Horne, 1964) by sonication. In short, PC (40 mg), CHO (16 mg) and PG (4 mg) at 10:8:1 (mol:mol) ratio were dissolved at 50 °C in 2 mL of chloroform/methanol 2:1 (vol/vol). The solvent was removed by evaporation in a rotary evaporator (Heidolph, Laborota 4002 Control) and the lipid film produced was vacuum-dried for 3 hours at 50°C in a water bath. The dried lipid film was then hydrated at room temperature with 2 mL of pre-warmed PBS (pH 7.4) containing vitamin B12 (14.32 mg) and continuously stirred at 60 rpm. The molar ratio of vitamin to the total amount of lipids was 1:10 (mol:mol). A phosphate buffer solution (PBS) was prepared by dissolving potassium phosphate monobasic 0.2 M and sodium hydroxide 0.2 M in distilled water thus obtaining a pH 7.4 PBS final solution. This buffer solution was used for carrying out liposome production and vitamin load and stability tests.

The preparation containing MLVs was maintained at room temperature for 2 hours. Part of this sample was used to assay morphology, size and entrapment efficiency of MLVs. Most of the sample was then sonicated at 45% amplitude (treated volume: 1 mL) by applying a duty cycle consisting in 2 ten-second irradiation rounds (amplitude 45%), each followed by a twenty-second pause in order to prevent thermal vesicle disruption thus obtaining Large Vesicles (LVs). The sample was stored overnight at 4°C and protected from light to stabilize the produced LVs. In order to obtain SUVs, after the stabilization phase, the sample was then sonicated at 45% amplitude (percentage of maximum deliverable power) for four more rounds.

The above-described sonication protocol was carried out with VCX 130 PB Ultrasonic Processors of Sonics & Materials Inc., CT, USA instrument (maximum power 130 W, frequency 20 kHz; sonotrode tip length 137 mm; sonotrode tip diameter 3 mm) as described in 4.2.2.2 paragraph. The

dedicated protocol of duty cycle sonication is schematized in Figure 20 A, and the process parameters in MLV and SUV preparation are summarized in Table 6.
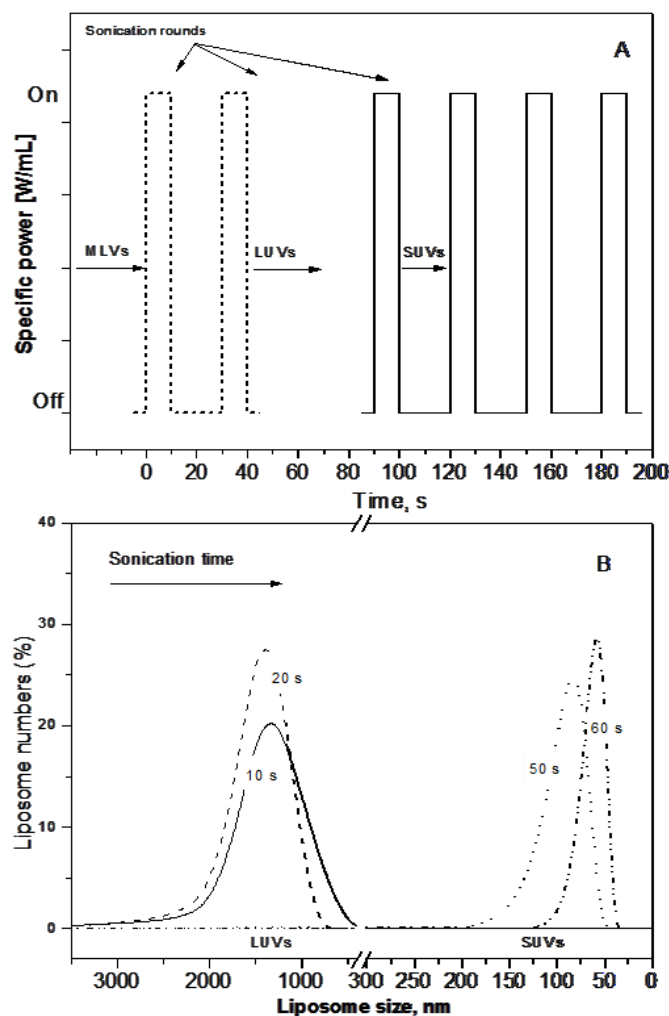
Figure 20. *Ultrasonic irradiation protocol (duty cycle, A) and its effect on liposomal structures size (from Multilamellar Vesicles –MLVs- to Small Unilamellar Vesicles –SUVs-, B). In Figure A, starting with MLVs, following two irradiation rounds (all irradiation rounds are of 10 seconds and are all followed by a 20-second pause) Large Unilamellar Vesicles-LUVs with micrometric diameter size are obtained as showed by LUVs size distribution in Figure B. In Figure A, starting with LUVs, after three and four more irradiation rounds (50 and 60 seconds), SUVs of nanometric size are obtained as showed by SUVs size distribution in Figure B.*

Table 6. *Process parameters adopted in Multiamellar Vesicles (MLVs) and Small Unilmellar Vesicles (SUVs) preparation, achieved loading and encapsulation efficiency. Results are expressed as average of three determinations; SD is the standard deviation*

Process parameter	MLV	SUV
Sonication duty cycle (s)		2 + 4 irradiation rounds
Fraction of maximum power (%)		45
Frequency (KHz)		20
Treated volume (mL)	2	1
Encapsulation efficiency (%) and Standard Deviation (SD)		
Vitamin B12 (%, SD)	72.0 ± 0.00	56.2 ± 8.51
α-Tocopherol (%, SD)	95.0 ± 7.07	76.3 ± 14.20
Ergocalciferol (%, SD)	81.5 ± 2.12	57.5 ± 13.9
Theoretical load (%)		
Vitamin B12 (%)	19.2	19.2
α-Tocopherol (%)	2.9	2.9
Ergocalciferol (%)	19.9	19.5
Effective load achieved (%)and Standard Deviation (SD)		
Vitamin B12 (%)	14.6 ± 0.65	11.76 ± 3.67
α-Tocopherol (%)	2.8 ± 0.70	2.2 ± 0.12
Ergocalciferol (%)	16.8 ± 1.23	11.9 ± 4.11

5.1.3.2 Preparation of MLVs and SUVs loaded with vitamin α-tocopherol

The preparation of SUVs containing α-tocopherol was carried out using the Thin Film Hydration method followed by sonication, as above described. In short, PC (120 mg) and CHO (3 mg) at 20:1 molar ratio and α-tocopherol (3.70 mg) were dissolved in 2 mL of chloroform/methanol 2:1 (vol/vol). The solvent was removed by evaporation and the dried lipid film was hydrated with 3 mL of PBS (pH 7.4) at room temperature and adequately stirred. The molar ratio of α-tocopherol to the total amount of lipids was 1:20 (mol:mol). The preparation containing MLVs was treated by applying the duty cycle described above for vitamin B12-containing liposomes.

5.1.3.3 Preparation of MLVs and SUVs loaded with vitamin ergocalciferol

The lipid composition used for SUVs loaded with ergocalciferol was PC (60 mg) and CHO (1.5 mg) at 20:1 molar ratio. The molar ratio of ergocalciferol (14.92 mg) to the total amount of lipids was 1:2 (mol:mol). The Thin Film Hydration method followed by sonication was used for producing ergocalciferol loaded SUVs as described for the other vitamins.

5.1.3.4 Physicochemical characterization of vesicles

Bright field imaging
The morphological and dimensional characterizations of MLVs were performed with optical microscopy (Axioplan 2- Image Zeiss) for bright field imaging. A 100 X oil immersion objective was used to visualize the vesicles.

Particle sizes
A dimensional analysis of microscope images, performed with the software *ImageJ* was combined with a Dynamic Light Scattering analysis for MLV and SUV dimensional characterization. In particular, Dynamic Light Scattering analysis were performed by using the ZetasizerNano ZS (Malvern, UK) which incorporates noninvasive backscatter (NIBS) optics. The detection angle of 173 degrees, able to measure the particles size of the concentrated, turbid sample was used. The resulting particle size distribution was plotted as the number of liposomes versus size. All the measurements were performed in triplicate. The results were expressed as average values.

5.1.3.5 Evaluation of vitamins encapsulation and stability test

Encapsulation efficiency and load
With the aim to measure the encapsulated vitamin, liposomes were lysed by ethanol and the entrapped vitamin was assayed by UV spectroscopy. In short, a given amount of each kind of loaded liposomes, prepared as above described, was washed three times with PBS and centrifuged. The recovered precipitates (loaded liposomes) were added with ethanol to promote the lysis of the liposomal bilayers and the suspension was undergone to UV spectrophotometric assay performed using Lambda 25 UV/VIS Spectrophotometer (PerkinElmer, Monza, Italy). An absorption spectrum from 200 nm to 600 nm was always investigated for all vitamins formulations and the maxima wavelengths, typical for each loaded vitamin: at $\lambda=361$nm for liposomes containing vitamin B12, at $\lambda=290$ nm for liposomes containing α-tocopherol and at $\lambda=265$ nm for liposomes containing ergocalciferol, was considered. The vitamins amounts were determined using a calibration curve prepared for all kinds of vitamins in the

different solvent used. A control with unloaded liposomes in the same absorption spectrum was performed.

For all formulations, encapsulation efficiency (e.e.) was determined as the percentage of detected encapsulated vitamin in liposomes to the initial amount of vitamin included in the formulation; it was calculated using the following equation:

$$e.e.\,(\%) = \left(\frac{encapsulated\ vitamin,\ mg}{initial\ vitamin\ amount, mg}\right) \times 100 \qquad (5.1)$$

Vitamin loads were determined through the ratio:

$$load\,(\%) = \left(\frac{encapsulated\ vitamin,\ mg}{total\ mass\ of\ loaded\ liposomes,\ mg}\right) \times 100 \qquad (5.2)$$

In particular, the *theoretical load* is referred to the initial amount of vitamin included in the formulation (divided by the total mass); the *effective* one is referred to the assayed vitamin amount (divided by the total mass).

Stability test

In order to evaluate the ability of the liposomal structures to retain their loading outside the cell environment, stability tests were performed observing vitamins release in PBS solution (pH 7.4) at 37°C (investigated time: about 10 days). In short, given amounts of loaded liposomes were put in measured volumes of PBS solution, then aliquots were removed from each sample at given time and centrifuged at 13000 rpm for 30 minutes at 4°C (Beckman Coulter Avanti J-25I, Ramsey, Minnesota, USA) to precipitate the liposomes. After centrifugation the supernatant was carefully removed without disturbing the pellet and the precipitated liposomes were washed three times with PBS solution in order to be sure that all un-encapsulated vitamins were removed. After each centrifugation and wash steps the supernatants were collected for UV spectrophotometric analysis. Vitamin B12 in supernatant was determined by carrying out a UV spectrophotometric analysis using PBS as blank, while α-tocopherol and ergocalciferol in supernatant were determined using 90 mL/100 mL ethanol as blank. The recovered pellet was re-suspended in ethanol in order to lyse the liposomes and the entrapped vitamin contained in the precipitated liposomes was assayed, via UV spectrophotometric analysis, using ethanol as blank. All the measurements were performed in triplicate.

5.1.4 Results

5.1.4.1 MLVs production from lipidic film via ultrasonic irradiation: loading and characteristics

Bright field imaging

Bright field imaging was used in order to clarify the structure of vitamin B12, α-tocopherol and ergocalciferol loaded MLVs. As shown in Figure 21, spherical, separated and defined liposomes were obtained for each formulation.

vitamin B12 liposomal vesicles   α-tocopherol liposomal vesicles   ergocalciferol liposomal vesicles
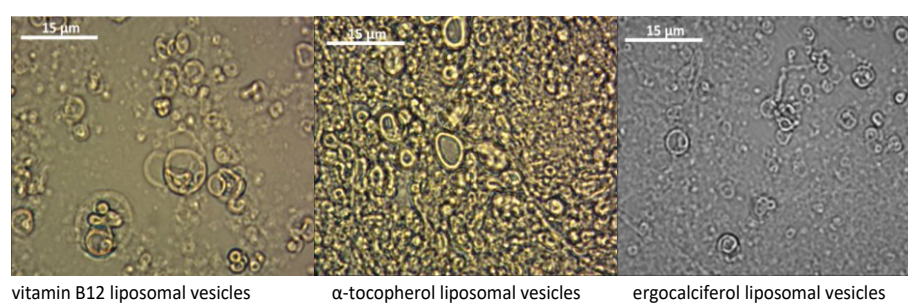
Figure 21. *Optical microscope pictures (in bright field, Obj. 63X) of loaded MLVs*

Particle sizes measurement

The dimensional analysis of microscope images prior to vesicle sonication showed micrometric MLVs in all samples. The diameter sizes were 5.77 ± 1.23 μm for vitamin B12-liposomes, 3.89 ± 1.72 μm for α-tocopherol-liposomes and 2.96 ± 1.97 μm for ergocalciferol-liposomes as summarized in Table 7.

Table 7. *Structures size of loaded Multilamellar Vesicles (MLVs) and Small Unilamellar Vesicles (SUVs). Results are expressed as average of three determinations; SD is the standard deviation*

Sample	Vitamin B12 - liposome mean diameter size ± SD	α-Tocopherol - liposome mean diameter size ± SD	Ergocalciferol - liposome mean diameter size ± SD
MLVs	5.770 μm ± 1.23	3.890 μm ± 1.72	2.960 μm ± 1.97
SUVs	0.051 μm ±0.028	0.040 μm ±0.009	0.048 μm ± 0.037

Determination of MLVs encapsulated vitamin B12, α-tocopherol and ergocalciferol

For all formulations high effective loads (the theoretical load can be taken in account as reference) were obtained. The results of MLVs loads determination are reported in Table 6.

For all formulations, high encapsulation efficiencies were obtained; in particular, e.e. achieved for MLVs were 72.0 ± 00 % for vitamin B12, 95.0 ± 7.07 % for α-tocopherol and 81.5 ± 2.12 % for ergocalciferol. The results of MLV encapsulation efficiency are also summarized in Table 6 (and compared with vitamin e.e. in SUVs).

Stability test and evaluation of vitamin B12, α-tocopherol and ergocalciferol release

Liposomes loaded with vitamin B12, α-tocopherol and ergocalciferol underwent a stability test to evaluate the timing of drug release in similar conditions to the intracellular environment. Liposomes were found to be stable at 37°C in PBS (pH 7.4) media release over a 10-day period.

5.1.4.2 SUVs production from lipidic film via ultrasonic irradiation: loading and characteristics

Particle sizes

A Dynamic Light Scattering analysis carried out after six total sonication rounds showed nanometric SUVs with diameter size of 51 ± 28 nm for vitamin B12-liposomes, 40 ± 9 nm for α-tocopherol-liposomes and 48 ± 37 nm for ergocalciferol-liposomes (Table 7).

Determination of SUVs encapsulated vitamin B12, α-tocopherol and ergocalciferol

For all formulations high effective loads (the theoretical load can be take in account as reference) were obtained. The results of SUVs loads determination are reported in Table 6.

The encapsulation efficiency achieved for SUVs was 56.2 ± 8.51 % for vitamin B12, 76.3 ± 14.02 % for α-tocopherol and 57.5 ± 13.9 % for ergocalciferol. The results of SUVs encapsulation efficiency are summarized in Table 6.

Evaluation of vitamin B12, α-tocopherol and ergocalciferol release (stability test)

SUVs loaded with vitamin B12, α-tocopherol and ergocalciferol underwent a similar stability test to MLVs under the same physiological conditions described above. SUVs were found to be stable over a 10-day period as shown in Figure 22. Retained vitamin profiles show that the encapsulated molecules are well confined in the nanoliposomal structures (pellet).
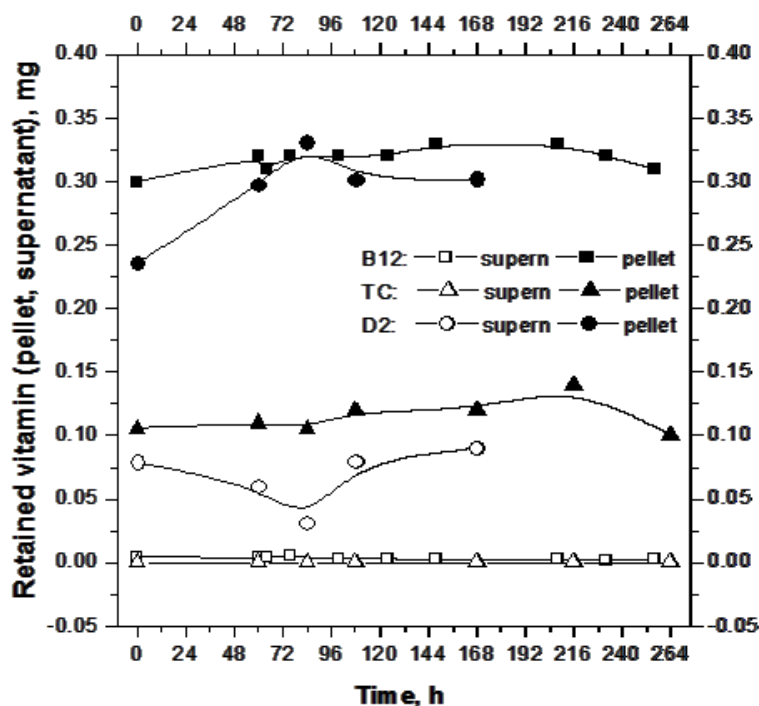
Figure 22. *Vitamins retention in nanoliposomes (SUVs) and released in PBS. Full symbols: squares, triangles and circles are referred to B12, tocopherol and ergocalciferol, respectively, and represent vitamin retained in the pellet. Open symbols: squares, triangles and circles are referred to B12, tocopherol and ergocalciferol, respectively, and represent the vitamin losses in phosphate buffer solution*

5.1.5 Discussion

5.1.5.1 Thin film hydration technique assisted by ultrasonic irradiation

Stable, highly loaded liposomal structure were carried out by means of an efficient ultrasound-assisted procedure. The rupture of the MLV lipid bilayer with ultrasonic energy produces smaller pieces which enclose themselves in nanometric liposomal structures (the process is shown in Figure 4 of 4.1 section) whose size depends on irradiation time, amplitude, frequency and on the volume of the sample treated.

As shown in Table 8, liposome diameter sizes are correlated to the number of sonication rounds applied: starting with MLVs, following two irradiation rounds (all irradiation rounds are of 10 seconds and are all followed by a 20-

second pause) LUVs with 1.416 ± 0.117 μm diameter size are obtained. Starting with LUVs, following two more sonication rounds, SUVs of 86 ± 33 nm in size are produced; after three more sonication rounds and four more irradiation rounds, SUVs of 51 ± 28 nm and 49 ± 26 nm are obtained, respectively.

Table 8. *Large Unilamellar Vesicles (LUVs) and Small Unilamellar Vesicles (SUVs) mean diameter size and Standard Deviation (SD) after sequential sonication rounds. Triplicate measurements were performed*

Sample		Mean diameter size ± SD
LUVs: 2 *Starting batch*		1.416 μm ± 0.117
SUVs:	*Batch 2*	86 nm ± 33
	Batch 3	51 nm ± 28
	Batch 4	49 nm ± 26

In Figure 20 the ultrasonic irradiation protocol used (Figure 20 A) is compared with the liposome size measurements carried out after sample irradiation (Figure 20 B). In Figure 20 A, the first two duty cycle sonication rounds which produce LUVs, correspond to the first two curves in Figure 20 B; the last two irradiation rounds which produce SUVs, correspond to the last two curves in Figure 20 B. As previously reported, one of disadvantages of size reduction process by sonication is the poor control in size-uniformity of SUVs. This is due to the dimensional heterogeneity of MLVs produced by the Thin Film Hydration technique.

The main advantage of the duty cycle sonication, applied in association with the traditional TFH method, is that there is no fixed constraint to the pore size of the membrane and the size of the vesicles can be changed according to the application requirements. SUVs of the right size can be obtained in a few seconds by simply modulating the duty cycle starting from micrometric liposomes. Furthermore, due to the importance of producing SUVs in a sterile environment, another advantage is that sonotrode tips are easier to clean and sterilize compared to membranes.

In this thesis SUVs with 40-51 nm in size containing vitamins with elevated encapsulation efficiency were obtained in a few seconds by modulating the duty cycle (irradiation protocol) starting from micrometric liposomes. This is possible applying the dedicated radiative protocol developed defining several operative parameters (power of ultrasound, amplitude, number of rounds and their duration) as described in 4.2 section (Barba et al., 2014). Moreover, if it is compared with similar liposomes production methods, the developed protocol is more easy and rapid. For example, nanoliposomes

production process used by Mohammadi and coworkers (Mohammadi et al., 2014) is similar to that used in this study but involves three stages (thin film hydration - homogenization – sonication) and gives particles of 82–90 nm in size entrapping D3, vitamin with similar features to those of ergocalciferol.

On the basis of all these advantages duty cycle sonication method can be easily scaled up to industrial scale for control the mean size of liposomes for SUVs production without affecting their load efficiency. This is what was done in the second part of the PhD project as described in *"Scale up of the ultrasound assisted homogenization process"*, 4.2.3.4 paragraph.

Moreover, the high encapsulation efficiency of both hydrophilic and hydrophobic vitamins found in MLVs decreases but in a not considerable manner after the size reduction process, making this ultrasound-assisted technique useful for obtaining highly loaded nanoliposomes.

Finally, in order to carry out a comparison between the vitamins load achievable with the developed technique and the vitamin load achievable by breaking unloaded preformed liposomes (classic encapsulation approach), vitamin B12 was encapsulated within liposomes by producing unloaded MLVs, hydrating the lipidic film with PBS without vitamin B12 and then irradiating the sample (with the same parameters and duty cycle sonication protocol described above) in a PBS solution containing vitamin B12. Using this second approach the vitamin B12 encapsulation efficiency in SUVs was 40%, which was much lower compared to the value of 56.2 % achieved for B12 encapsulation with the ultrasound-based TFH technique. Therefore the new approach appears to be a promising technology for obtaining highly loaded nanoliposomal formulations, boosting bioactive antioxidant delivery and providing process optimization in terms of possibilities of size range and production times.
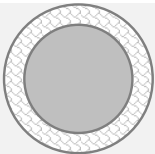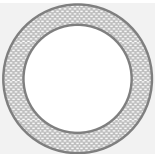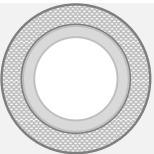
5.1.5.2 Vitamins solubility and SUVs load analysis

Both hydrophilic and hydrophobic vitamins are easily destabilized by variations in temperature, oxygen, light and humidity (Azevedo et al., 2013). The encapsulation in liposome enables us to improve the stability of water-soluble vitamins and assure the bioavailability of liposoluble vitamins with absorption limitations, at the same time thus protecting them during storage and in the physiological environment as mentioned in 2.2.1 paragraph regarding the critical issues in nutraceutical agents delivery.

Liposomes are able to incorporate hydrophilic and hydrophobic vitamins: hydrophilic vitamins can be encapsulated in the interior aqueous compartment, while lipophilic and amphiphilic vitamins can be incorporated into the liposome bilayer. As shown in Table 9, since vitamin B12 is hydrophilic it is mainly entrapped in the liposome aqueous core while α-tocopherol and ergocalciferol, hydrophobic molecules, are entrapped in the liposome lipid bilayer. Both the incorporation and the release of hydrophilic and hydrophobic vitamins (the main features of used vitamins and obtained

SUVs are summarized in Table 9) are influenced by the lipid composition of SUVs resulting in various levels of drug incorporation efficiency.

Table 9. *Main vitamins properties and Small Unilamellar Vesicles characterization*

Properties	Vitamin B12	α-Tocopherol	Ergocalciferol
Average mass (Da)*	1355.36	430.71	396.65
Stokes radius (nm)*	0.85	0.43	0.46
Solubility in H_2O (mg/mL)*- 20°C -	12.5	0.021	0.050
Encapsulation Efficiency (%)	56.2 ± 8.51	76.3 ± 14.2	57.5 ± 13.9
Total mass of vitamin (mg) in supernatant and pellet	14.32 ± 1.08	3.70 ± 0.41	14.92 ± 3.29
Mass of vitamin (mg) in supernatant	6.70 ± 1.36	0.92 ± 0.44	6.56 ± 3.48
Mass of vitamin (mg) in pellet	7.62 ± 1.24	2.78 ± 0.22	8.36 ± 0.19
Vitamin retention area (grey filling) in the liposomal structures			

*Source: ChemSpider Search and share chemistry at http://www.chemspider.com

Cholesterol plays an important role in liposome formulations for bilayer stability; in Tabandeh & Mortazavi (Tabandeh and Mortazavi, 2013) it was observed that drug encapsulation efficiency is also directly related to cholesterol molar ratio due to its competition with α-tocopherol. The composition of the lipid bilayer as well as the incorporation of the right amount of cholesterol are essential for the encapsulation efficiency of hydrophobic molecules. In particular, a study on encapsulation efficiency of α-tocopherol in MLVs produced by the TFH method was done by varying the molar ratio of *α*-tocopherol and that of cholesterol (Tabandeh and Mortazavi, 2013). In this thesis 1:20 molar ratio of α-tocopherol to egg lecithin was selected as the optimum amount for the production of MLVs with the highest encapsulated amount of α-tocopherol in its active form. Moreover, among the different molar ratios of cholesterol investigated by Tabandeh & Mortazavi (1:20, 1:10, 1:1 cholesterol to lecithin mol:mol), 1:20

molar ratio of cholesterol was selected as the optimum formulation. Using these optimum ratios of cholesterol and α-tocopherol and the thin film hydration method they have obtained MLVs with 86 % e.e. but not in small unilamellar vesicles.

In this thesis, starting from 1:20 molar ratio of α-tocopherol to the total amount of lipids and maintaining at 1:20 the molar ratio of cholesterol to phosphatidylcholine, MLVs of 3.9 μm in size with an e.e. of 81.5 % have been produced, obtaining high encapsulation efficiency in agreement with Tabandeh & Mortazavi.

In another study, based on thin-film hydration-sonication method, Mohammadi and coworkers (Mohammadi et al., 2014) have encapsulated in nanoliposomes the hydrophobic active molecule vitamin D3. In particular, in contrast with what has been said about the key role of cholesterol in hydrophobic vitamins encapsulation, they have showed that changing the lecithin to cholesterol ratio (60:0, 50:10, 40:20, 30:30 w/w) the encapsulation efficiency does not change for nanoliposomes encapsulating vitamin D3. In their study the e.e. was more than 93%, in liposomes of 82–90 nm in size, for all formulations tested and they showed that changes in cholesterol amount have an effect only on the stability, in particular, on the zeta potential of empty liposomes.

In the present study it has been shown that α-tocopherol and ergocalciferol hydrophobic vitamins can be encapsulated with high encapsulation efficiency in SUVs with a diameter range of 40-48 nm using phosphatidylcholine and cholesterol at 20:1 molar ratio. The SUVs range size obtained, which can be easy achieved by the two operative steps, thin film hydration - sonication, could be particularly interesting for intravenous vitamin therapy.

In the production of MLVs and SUV encapsulating vitamin B12 has been used 1:4 w/w ratio of vitamin B12 to the total amount of lipids taking into account the best vitamin/lipids ratio find in a work of Liu and Park (Liu and Park, 2010) in which ascorbic acid (vitamin C), another water-soluble vitamin, was encapsulated in chitosan-coated nano-size liposomes with a maximum loading efficiency about 96.5% when 1:1 weight ratio of vitamin C to the total amount of lipids was used.

It is important to note that the applied sonication duty cycle does not affect vitamins stability but plays a role, as above discussed, on the encapsulation efficiency and in turn on vitamin loads.

In Table 9 it is shown that the initial amount of each vitamin (total mass of vitamin) was perfectly assayed in supernatant (mass of vitamin in supernatant) and pellet (mass of vitamin in pellet) phases collected at the end of sonication procedure from MLVs to SUVs (a purposely test of mass balance was performed).

In Table 9 it is shown the effect of sonication action on encapsulation efficiency and on vitamin loads for the prepared MLVs and SUVs. The

sonication, inducing a cyclic opening and closing of liposomal bilayer, involves vitamin losses in the sonication bulk in amount related to the features of the entrapped vitamin (mainly the solubility).

The SUVs obtained in this thesis are stable and did not release significant amounts of vitamins in PBS throughout the study period. The main consequence is that they may have a longer shelf life (i.e., a commercial product based on this formulation can be kept for long periods without deteriorating or releasing active components).

5.1.6 Remarks

Liposomes can be a highly efficient delivery system which is able to maintain accessible vitamin sources for new pharmaceutical and food industry applications. The high encapsulation efficiency of both hydrophilic and hydrophobic vitamins into SUVs and the obtainable nano-size by means of the developed ultrasonic assisted approach make liposomes optimal carriers biocompatible, stable and easy to reduce in size.

In this study the new developed procedure, based on thin film hydration method followed by sonication cycles, was applied to prepare liposomes loaded with three vitamins with different hydrophobicity. All the kinds of liposomal structures produced were characterized in terms of encapsulation efficiency, size and stability in a relatively long period. The liposomes were obtained with tailored size ranging from 2.9 μm to 5.7 μm for MLVs obtaining, after sonication in duty cycle, SUVs in the average range of 40 nm to 51 nm in size. High encapsulation efficiency was obtained in both MLVs, with a e.e. % of 72.0 ± 00 % for vitamin B12, 95.0 ± 7.07 % for α-tocopherol and 81.5 ± 2.12 % for ergocalciferol, and SUVs, with a e.e. % of 56.2 ± 8.51 % for vitamin B12, 76.3 ± 14.02 % for α-tocopherol and 57.5 ± 13.9 % for ergocalciferol (the higher the vitamin hydrophobicity, the higher the encapsulation efficiency). A comparison between vitamin B12 load achievable with the developed technique and the vitamin load achievable by breaking unloaded preformed liposomes (conventional approach) showed an increase of encapsulation efficiency in SUVs from 40% to 56.2 %, confirming the effectiveness the of pointed out technique.

Part of this work has been reported in:
Bochicchio S.; Barba A.A.; Grassi G.; Lamberti G.; "Vitamin delivery: carriers based on nanoliposomes produced via ultrasonic irradiation"; *LWT - Food Science and Technologies*, 2016, 69, 9 -16

5.2 Nanoliposomes vectors for ferrous sulfate delivery

5.2.1 Generalities

As in depth previously discussed for vitamins delivery (5.1 section), due to their unique properties of biocompatibility, biodegradability, low intrinsic toxicity and versatility, liposomes uses has been rapidly grown as new technology for food fortification (Kosaraju et al., 2006). In particular, size and size distribution are key parameters determining liposomes performance as delivery systems in nutraceutical applications by improving taste, flavor, stability, absorption and bioavailability of bioactive compounds, all features which are meliorate if the micronutrient is nanoencapsulated (Reza Mozafari et al., 2008, Srinivas et al., 2010, Putheti, 2015, Bochicchio et al., 2016a). Compared with micrometre-sized systems produced by traditional microencapsulation techniques, nanoparticles have a larger interfacial surface area and have the potential to improve the solubility, enhance the bioavailability and improve the controlled release of the bioactive principle (Singh, 2016). Moreover, nanoparticles may also have an elongated retention time in the small intestine when compared to the larger structures (Huang, 2012).

Food enrichment process was introduced with iron micronutrient in order to combat anemia, one of the most widespread nutritional deficiencies, affecting globally two billion people (Mellican et al., 2003). In 1993 the Special Commission for Enrichment of Foods was created by the Venezuela Government and, in the same year, a fortification program began in which maize and wheat flours were enriched with 20 and 50 mg of iron (as ferrous fumarate)/kg flour, respectively (Layrisse et al., 1996). Despite the success of iron fortification in addressing the prevalence of iron deficiency anemia, particularly in developing countries, this has been limited by the lack of a robust, simple, and easy-to-transfer fortification technology (Mehansho, 2006). Regarding the supplementary micronutrient products present on market in the form of tablet or capsules their quality and variety have to be improved, increasing the availability and access of supplements in the commercial sector (Mora, 2002).

In order to meliorate the supplementary iron products currently on the market, often composed by micrometric particles, sometimes containing the less absorbable ferric form of iron and obtained, in the most of the cases, by using ineffective production processes and drastic conditions, ferrous sulfate nanoliposomes were produced in this thesis by using the simil-microfluidic bench scale apparatus developed, presented in 4.2 section.

With the aim to give a contribution in the development of both an improved iron-nanoliposomal formulation and a simple, low cost and sustainable production method, at first the effect of different weight ratios of iron to the total formulation components (0.06, 0.035, 0.02 and 0.01 iron/total components weight ratio) on the final vesicles encapsulation efficiency was investigated. Then, a comparison in terms of vesicles final properties (mean diameter size, polidispersity index, zeta potential, charge and encapsulation efficiency) and the yields of the processes was realized between liposomes obtained by using the simil-microfluidic set up and the ones obtained by using the Ethanol Injection and the ultrasound assisted Thin Film Hydration method, at the same operative conditions.

5.2.2 Materials

L-α-Phosphatidylcholine (PC) from soybean, Type II-S, 14-23% choline basis (CAS n. 8002-43-5), Cholesterol (CHO) (CAS n. 57-88-5), Rhodamine B dye (CAS 83-68-9-Sigma-Aldrich, Milan, Italy), ferrous sulfate heptaidrate (CAS n. 7782-63-0), ascorbic acid (CAS n. 50-81-7), ethanol of analytical grade (CAS n. 64-17-5), Triton X100 (CAS n. 9002-93-4), hydrochloric acid (CAS n. 7647-01-0), hydroxylamine hydrochloride (CAS n. 5470-11-1), ammonium acetate (CAS n. 631-61-8), glacial acetic acid (CAS n. 64-19-7) and 1,10-Phenantroline (CAS n. 66-71-7) were purchased from Sigma Aldrich (Milan, Italy).

5.2.3 Methodology and sperimental set-up

5.2.3.1 Preparation of iron loaded nanoliposomes

Production through the simil-microfluidic apparatus
Ferrous sulfate loaded nanoliposomes were produced by using the simil-microfluidic bench scale apparatus developed whose layout and main process steps are described in 4.2 section.
The optimized conditions of 10:1 (Vhs/Vls) volumetric flow rate ratio and 5 mg/ml lipids in the final hydroalcoholic solution were used for liposomes preparation. Briefly, a lipid/ethanol solution was obtained by dissolving 470 mg of PC and 94 mg of cholesterol in 10 ml of ethanol. Cholesterol was used at 2.5:1 (mol/mol) PC/CHOL ratio and was added to the formulation in order to stabilize the loaded vesicles. Ferrous sulfate heptaidrate and ascorbic acid were dissolved in 100 ml of deionized water which was used as hydration solution. Ascorbic acid was added as an anti-oxidant to preserve the ferrous ion against oxidation in a ferrous/acorbic acid weight ratio of 1:6 (w/w). It has been shown that the co-addition of ascorbic acid and iron in a 2:1 molar ratio (6:1 weight ratio) increases iron absorption from foods 2- to 3-fold in adults and children (Stekel et al., 1986b, Stekel et al., 1986a, Lynch and

Stoltzfus, 2003). In particular, four different formulations were produced which differ from each other for the ferrous sulfate/total formulation components (lipids, ascorbic acids and ferrous sulfate) weight ratio (w/w) used. Starting from a 0.06 ferrous sulfate/total components weight ratio, selected from Xia et Xu (2005) (Xia and Xu, 2005), nanoliposomes were also produced by using a 0.035, 0.02 and 0.01 ferrous sulfate/total components (w/w) ratio and maintaining constant all the other chemical and process parameters adopted. In order to have a comparison with the ferrous sulfate loaded particles, unloaded nanoliposomes were produced by adoperating the same formulation and process conditions but using, as hydration solution, pure deionized water without the addition of ascorbic acid and iron.

Production through the classical bench scale techniques
The conventional Ethanol Injection (EI) method (3.1.2 section) and the ultrasound assisted Thin Film Hydration (TFH) technique developed (4.1 section) were adopted for the production of ferrous sulfate loaded nanoliposomes in order to have a comparison in terms of productivity with those achieved by the use of the simil-microfluidic semicontinuous apparatus fabricated. In particular, the fourth formulation with a 0.01 ferrous sulfate/total components (w/w) ratio was produced with both the techniques.

Ethanol Injection
Using the EI technique, ferrous sulfate loaded and unloaded nanoliposomes were prepared by dissolving 470 mg of PC and 94 mg of cholesterol in 10 ml of ethanol. After stirring, the ethanol/lipid solution was sprayed by means of a 10 ml syringe (needle of 0.8 mm) in a 100 ml of deionized water containing ferrous sulfate (5.64 mg) and ascorbic acid (33.8 mg) at 6:1 (w/w) to achieve loaded nanoliposomes. Liposomes suspension was stirred for 10 min and left stabilize at room temperature for two hours. Finally, aliquots (1 ml) of the obtained vesicles were subjected to the duty cycle sonication size reduction process, according to the procedures previously described (4.1.2.2 paragraph). By this way nanoliposomes were produced by maintaining at 5 mg/ml the lipid concentration in the final hydroalcoholic solution and at 10:1 (v/v) the volume ratio between the hydration solution to the lipid solution as done by using the simil-microfluidic apparatus in optimized conditions.

Ultrasound assisted Thin Film Hydration
The ultrasound assisted TFH method was also used to produce nanoliposomes maintaining constant the lipid concentration. Briefly 47 mg of PC and 9.4 mg of CHOL at 2.5:1 (mol/mol) ratio were dissolved in 1 mL of chloroform/methanol at 2:1 (vol/vol). The solvent was removed by evaporation at 50 °C for 3 h in a rotary evaporator (Heidolph, Laborota 4002 Control, Bergamo, Italy) under reduced pressure until a lipid film was

produced. The dried lipid film was then hydrated at room temperature with 11 mL of deionized water containing ferrous sulfate (0.62 mg) and ascorbic acid (3.72 mg) at 6:1 (w/w). The preparation containing Multilamellar Vesicles (MLVs) was maintained at room temperature for 2 h and, subsequently, sample aliquots (1 mL) were subjected to the ultrasound assisted size reduction process, in the mode previously described for the other production techniques adopted.

5.2.3.2 Physicochemical characterization of vesicles

Morphology
The morphological characterizations of unloaded and ferrous sulfate loaded nanoliposomes were performed with optical microscope in fluorescence field (Axioplan 2- Image Zeiss, Jena, Germany) equipped with a software to capture the images. The Rhodamine B dye was used to visualize lipid vesicles. A 100 x oil immersion objective was used.

Size and zeta potential
Size and zeta potential determinations of unloaded and ferrous sulfate loaded vesicles were performed by using the Zetasizer Nano ZS (Malvern, UK) with noninvasive backscatter (NIBS) optics. The detection angle of 173 degrees was used. The resulting particle size distribution was plotted as number of liposomes versus size. The Polydispersity Index (PDI) was calculated for all the preparations. All the measurements were performed in triplicate. The results were expressed as average values.

5.2.3.3 Evaluation of iron encapsulation and stability test

Encapsulation efficiency (EE)
From all the samples produced, aliquots were taken and spectrophotometrically analyzed in order to measure the real encapsulated and the unencapsulated amount of ferrous sulfate. For this purpose 2 ml aliquots were centrifuged at 30000 rpm (Beckman Optima L-90K, SW 55 Ti rotor) for 1 h at 4 ° C in order to remove the supernatant from the precipitated nanoliposomes (pellet). The supernatant volume, stored for the subsequent ferrous sulfate determination, was measured and replaced with the same volume of Triton X100 at 1% (v/v) in order to lyse the nanoliposomes pellet and to analyze the encapsulated ferrous sulfate.
Iron determination was performed by the 1,10-Phenanthroline assay. Briefly, to 400 μl aliquot of supernatant, 200 μl of 37 % (v/v) hydrochloric acid were added to acidified the solution together with 100 μl of 10 % (v/v) hydroxylamine hydrochloride used as a reducing agent. After 10 minutes, 1 ml of ammonium acetate buffer solution, previously prepared by dissolving 50 g of ammonium acetate in 30 ml of deionized water and 140 ml of glacial acetic acid, was added together with 200 μl of 1,10-Phenantroline at 0.5 %

(v/v). The steps were repeated for the pellet dissolved in Triton X 100. The total volume for each test tube was then increased to 10 mL with deionized water. Blanks reagents were prepared in the same manner but using pure water or Triton X100 in place of the samples. An absorption spectrum from 200 nm to 600 nm was investigated for all the samples and the maximal wavelength of 510 nm, typical of the 1,10-Phenantroline-Fe^{2+} ions complex, was considered. The iron amounts was determined by using a ferrous sulfate calibration curve previously prepared with the same 1,10-Phenantroline colorimetric determination. The UV spectrophotometric assay was performed by using Lambda 25 UV/VIS Spectrophotometer (PerkinElmer, Monza, Italy).

The encapsulation efficiency (e.e.) was determined as the percentage of ferrous sulfate encapsulated in nanoliposomes to the initial amount of ferrous sulfate included in the formulation and was calculated using the equation 5.3:

$$e.e.\,(\%) = \left(\frac{Fe\ in\ the\ pellet, mg}{Fe\ in\ the\ pellet + Fe\ in\ the\ supernatant, mg} \right) \times 100 \quad (5.3)$$

Iron loads were determined through the ratio:

$$Load, \% = \frac{Fe, mg}{Fe + ascorbic\ acid + lipids, mg} \times 100 \qquad (5.4)$$

In particular, the theoretical load is referred to the initial amount of iron included in the formulation and divided by the total mass while the effective one is referred to the iron amount effectively presents in the nanoliposomes (pellet) divided by the total mass.

Stability test
The stability of the produced nanoliposomes with the best iron encapsulation efficiency (fourth formulation) was tested in conditions simulating those of food storage. The samples were maintained at 4 °C for a period of about 15 days in deionized water and the mass of iron present in the supernatant and in the pellet was quantified at established time. Briefly, given amounts of loaded nanoliposomes were put in measured volumes of deionized water. Subsequently, after 6 h, 22 h, 46 h, 70 h, 130 h e 346 h sample aliquots were taken and centrifuged under the same operating conditions described for the encapsulation efficiency determination. The mass of iron present in both the supernatant and the pellet solutions were determined, at each time, by the 1, 10-Phenantroline method through UV spectrophotometric assay. All the measurements were performed in triplicate.

5.2.4 Results and Discussion

5.2.4.1 Iron loaded nanoliposomes production

Simil-microfluidic apparatus production process

The simil-microfluidic bench scale apparatus developed has allowed to successfully produce iron loaded nanoliposomes in the desired range size by using the optimized conditions. The method has permitted to produce ferrous-sulfate nanostructured vectors without the use of drastic conditions, such solvents and/or high pressure, currently used in literature and also at industrial scale for iron-particles manufacturing by using discontinuous processes such Reverse Phase Evaporation, Thin Film Hydration and Homogenization-Freeze Thawing methods, this last used for the commercial microencapsulated iron Biofer® (Lipotech) production (Kosaraju et al., 2006, Xia and Xu, 2005, Abbasi and Azari, 2011, De Paoli and Hager, 1996). A part of the drastic conditions used, limits in the output volumes of final product, usually ranging from 10 to 60 mL with the above mentioned techniques, represent another crucial problems directly linked with high commercial costs of supplemental products which, for this reason, are not jet widely used as a very proper therapies. With the simil-microfluidic set up developed, by using the ultrasound as tool for the process intensification, it is possible to obtain a massive output with the minimum of energy, costs and time: one batch of 110 mL iron-liposomal suspension can be produced in few minutes with the possibility to restart the process in a semi-continuous manner. Once again the chemical engineering approach of process intensification together with the use of not drastic condition has led to the production of suitable nanovector.

Formulation efficacy

Scientific works about iron encapsulation in lipid particles for nutraceutical applications show some failing in terms of formulation such an unbalanced ascorbic acid/iron (AA/Fe) weight ratio compared to that recommended by the World Health Organization (WHO) (Dary and Hurrell), which is the 6:1 w/w used in this thesis, and the frequent use of the less absorbable form of iron: the ferric form (Santiago, 2012).

For example, a 1:15 weight ratio of ascorbic acid to ferrous sulfate was used by Xia and Xu (Xia and Xu, 2005) and also by Abbasi and Azari (Abbasi and Azari, 2011) while a 1:1.5 AA/Fe weight ratio was used in another work by Kosaraju and collaborators (Kosaraju et al., 2006). Even if referring to the products already on the market and most frequently used for the treatment of iron deficiencies it can be note that formulations are unbalanced in iron/ascorbic acid ratio, for example SunActive®, a TAIYO International product for iron fortification, contains a 4:1 w/w A.A./Fe, furthermore the ferric pyrophosphate is used in this formulation. Biofer®, a Lipotech microencapsulated iron product, contains 1:15 AA/Fe w/w. Sideral and

Sideral Forte, a Pharmanutra products, are formulated with the less absorbable ferric pyrophosphate form and contains from 1:4 to 1:2 w/w Fe/A.A, this last used in Sideral Forte, for the treatment of severe anemias.

Moving from the nutraceutical field towards the food sector, the optimized formulation containing the liposomal ferrous form could be used also for food fortification. In that regard iron food fortification is recognized as a strategy to control childhood anemia: i.e. the frequent use of cow's milk in Latin America, including Brazil, during infancy, and iron fortification of this vehicle is an inexpensive alternative to increase iron levels in children (Lamounier et al., 2010), about that Torres and collaborators have observed a decreases of anemia when 1 liter/day of fluid milk fortified with 3 mg of chelate amino acid iron were administered to children (Torres et al., 1996).

Considering to enrich a milk with the ferrous sulfate nanoliposomes produced through the use of the simil-microfluidic apparatus developed, and considering the formulation with the maximum e.e. achieved (Table 11), it would be possible to obtained in just few minutes (one batch) a milk suspension with an iron concentration of 56.4 mg/L that would be enough to meet the daily requirement of iron for an entire family. Indeed, the Recommended Dietary Allowances (RDAs) for iron considering an adult is of 8 mg for males and of 18 mg for females (Food and Board, 2002) thus 250 ml of enriched milk daily would be sufficient for one person.

5.2.4.2 Iron loaded nanoliposomes characterization

Morphology

In order to obtain information about morphology, fluorescence imaging was used. As showed in Figure 23 spherical and separated liposomes were achieved with all the formulations tested.
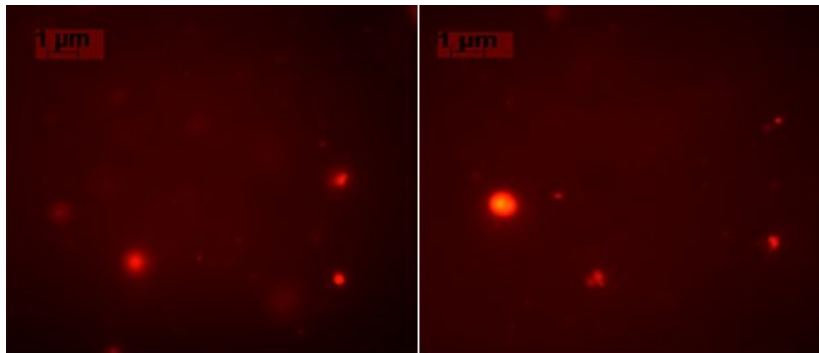
Figure 23. *Fluorescence microscopy images of ferrous sulfate lipid vesicles labelled with Rhodamine B dye and visualized with a 100 X objective*

Size and zeta potential

The objective of a fortification technology development is to deliver bioavailable active molecule, such iron, via commonly consumed foods and

beverages without compromising their taste, appearance and stability. In particular, the iron solubility is very dependent on the size and the shape of the iron-particles complexes, characteristics which are governed by the manufacturing process (Mehansho, 2006). In that regard, particles of nanometric scale are required to maintain the transparency of clear beverages during enrichment: carrier have to be small enough so as not to scatter light and be detected by naked eye (Danino et al., 2014). The nano-scale plays a crucial role also for other forms of iron supplementation such oral formulations, the first choice to replace normal iron levels. In this case, the size of nanoparticle systems has a remarkable influence on carriers uptake after their administration: in many works has been proved that nanostructured delivery systems yield an increases in drug uptake, enhancing the intestinal absorption of the active principle (Desai et al., 1996, Hussain et al., 2001). Despite the crucial role of particle size in iron delivery is confirmed by several studies, few are those in which dimensional features are clearly showed while the major of works not provide this information; also the commercial products not specify the carriers dimensions. In this thesis an accurate analysis of iron-vesicles dimensional features and surface charge, produced by the simil-microfluidic apparatus, was done and the results obtained from the sonicated and not sonicated samples are presented in Table 10.

Table 10. *Sonicated and not sonicated liposomes diameter size, polydispersity index (PDI) and zeta potential produced at different weight ratio of ferrous sulfate to the total formulation components. Results are expressed as average of three determinations and reported along with the standard deviation (SD)*

	Unloaded vesicles	0.06 w/w	0.035 w/w	0.02 w/w	0.01 w/w
Not sonicated samples size and PDI					
Size (nm) ± SD	71.81 ± 6.97	127.01 ± 36.64	154.08 ± 15.95	103.64 ± 29.09	135.33 ± 11.2
PDI ± SD	0.41 ± 0.03	0.45 ± 0.04	0.76 ± 0.034	0.69 ±0.08	0.40 ± 0.03
Sonicated samples size and PDI					
Size (nm) ± SD	50.52 ± 19.7	47.80 ± 6.46	53.4 ± 19.16	65.16 ± 15.48	76.29 ± 16.4
PDI ± SD	0.22 ± 0.01	0.38 ± 0.01	0.52 ± 0.004	0.63±0.12	0.37 ± 0.029
Samples zeta potential					
Zeta Potential (mV) ± SD	-57.87 ± 1.13	-41.05 ±0.7	-20 ±1.16	- 19±0.55	-35.87 ± 2.05

In reference to the not sonicated samples, it can be observed that the diameter size of unloaded nanoliposomes (about 72 nm) is smaller than the ferrous sulfate loaded form. The increases of loaded vesicles average dimension, which is about 103-154 nm range in size, is indicative of the fact that a certain amount of iron and ascorbic acid is encapsulated within the vesicles. Regarding the polydispersity index of the samples it was remained almost unchanged for the unloaded vesicles and for the 0.06 (w/w) and the 0.01 (w/w) formulations (PDI about 0.4) while some aggregates were founded for the 0.035 (w/w) and the 0.02 (w/w) samples with a PDI value of about 0.7 (Table 10). Considering the sonicated samples it can be note that the sonication has a crucial role in reducing the size of the iron loaded liposomes confirming what previously seen for the unloaded structures: i.e. the average liposomes diameter size of the first formulation (0.06 w/w) is decreased of about the 44 % after the ultrasound assisted step (from 127 nm to about 48 nm in size). This is true for all the tested samples. With regard to the polydispersity index, the sonication is effective again: ever taking into account the first iron-loaded formulation the PDI, initially of 0.45, becomes 0.38 after the ultrasound assisted homogenization step. The reduction in vesicles size and PDI by passing from the not sonicated to the sonicated samples was always found for all the samples tested (Table 10).

Moreover, it is important to note that size and PDI values obtained for the not sonicated unloaded liposomes with the addition of cholesterol (72 nm; 0.4 PDI) are near to the value obtained for the not sonicated unloaded nanoliposomes formulated with only PC, without cholesterol, (81 nm size; 0.32 PDI) by using the same process conditions: 10:1 Vhs/Vls and a 5 mg/ml PC concentration in the final hydroalcholic solution. The same comparable values were found for the PC-CHOL sonicated unloaded samples (50 nm size and a 0.2 PDI) and the PC sonicated unloaded sample (52 nm in size and a 0.3 PDI) (4.2 section). This comparison point out the reliability and the reproducibility of the developed set-up and the operating conditions used.

Another important parameter to take into account in the development of drug delivery systems to be used in nutraceutical applications is the zeta potential (ζ), a stability index of the nanoliposomes suspensions. In order to avoid the nanostructures aggregation, resulting in a precipitation and loss of product stability, carriers should have a $|\zeta| > 30$ mV, when the zeta potential drops below this value the system becomes unstable and begins forming larger complexes as the attractive forces prevails (Schatzlein, 2013). Here, negatively charged vesicles were produced for all the iron/total formulation components (w/w) ratio tested (0.06, 0.035, 0.02 and 0.01 weigh ratio). In particular, the zeta potential value for unloaded liposomes was negative (-57.87 ± 1.13 mV) due the presence of polyunsaturated fatty acids (linoleic and olei acids) composing the phosphatidylcholine vesicles. Moreover, being the negative charges of the liposomal bilayer able to trap the cationic ferrous sulfate by electrostatic interactions, as a consequence of the presence of

positive charged iron ions, the vesicles surface becomes less negative for loaded liposomes (Table 10). In particular it seems that for the 0.035 (w/w) and for the 0.02 (w/w) formulations the electrostatic interactions have conrned more the outer vesicles surface then the inner part, being the zeta potential less negative (about -20 mV) respect to the other formulations (from -36 to - 41 mV ζ range) where iron is mostly entrapped in the liposomes core (see Table 10).

Encapsulation efficiency (EE)

Due to its rapid oxidation-reduction (redox) reactions, iron administration is almost always accompanied by undesired effects related to taste, appearance, and bioavailability. In order to develop an effective iron fortification technology or iron supplement therapy it is of critical importance border the micronutrient into the liposomes aqueous core so as to limit the components that cause undesirable organoleptic properties and influence iron bioavailability.

In order to make iron unreactive during its administration and storage, ferrous sulfate was isolated from the external environment and oxidizing agents by encapsulation in nanoliposomal structures produced by using different weight ratio of iron to the total formulation components. According with Xia and Xu, it was observed that increasing ferrous ion concentration there is a decreases of encapsulated ferrous ion amount when deionized water is used as hydrating medium (Xia and Xu, 2005). Nevertheless, it is important to underline that by using the Reverse-Phase Evaporation (REV) method and maintaining the same hydration medium and iron species used in this thesis, they have obtained an e.e. of about 5% and 16 % respectively for a 0.06 and a 0.04 w/w iron/total components used. As visible from Table 11, in this thesis a 22 % e.e. and a 42 % e.e. were achieved by using respectively a 0.06 and a 0.035 w/w iron/total formulation components through the use of the simil-microfluidic apparatus developed. In general, the decreases in iron e.e. by increasing the ferrous sulfate concentration can be explained by the fact that the ferrous sulfate is a strong electrolyte and for major load values the ionic strength, defined as the concentration of ions present in a solution, increases, resulting in a reduction of the encapsulation capacity in the aqueous phase (solution of iron and ascorbic acid) [56]. In virtue of these considerations, loaded nanoliposomes characterized by higher iron/total formulation components weight ratios were studied observing an increased e.e. in particular of 52 % by using a 0.02 w/w iron/total components and of about the 97 % with the 0.02 w/w iron/total components formulation (Table 11).

Table 11. *Theoretical load, effective load and encapsulation efficiency (e.e.) of sonicated liposomes produced at different weight ratio of ferrous sulfate to the total formulation components. Results are expressed as average of three determinations and reported along with the standard deviation (SD)*

	0.06 w/w Fe/total components	0.035 w/w Fe/total components	0.02 w/w Fe/total components	0.01 w/w Fe/total components
Theoretical load ± SD (%)	4.23 ± 0	3.41 ± 0	2.3 ± 0	0.98 ± 0
Effective load ± SD (%)	0.99 ± 0.031	1.28 ± 0. 32	1.22 ± 0. 2	0.93 ± 0.13
e.e. ± SD (%)	22.33 ± 0.58	42.14 ± 6.74	52.2 ± 1.41	96.63 ± 2.7

In general, better e.e. results respect to the literature works has been obtained by the use of a simple and rapid technique and just deionized water as hydration medium. Indeed, by means of the last formulation, it was possible to obtain stable liposomes with a diameter of 76 nm and an encapsulation efficiency of 97 %. In a work of Kosaraju and collaborators a preparation of Fe/AA-loaded liposomes below 250 nm in size was obtained for Fe/AA concentrations of 7.5/5 % (w/w) by using Emultop ® obtaining a maximum of 57 % e.e. with an homogenization process (Kosaraju et al., 2006). In some cases, higher ferrous sulfate e.e. were obtained in liposomes by using citric acid sodium phosphate buffer solution as hydration medium and Tween 80 in the lipid formulation but the liposomes dimensions are in the micrometer scale (Abbasi and Azari, 2011).

Regarding the ferrous sulfate loads achieved, from Table 11 it can be observed that the 0.035 w/w Fe/total components formulation showed the major effective load, about the 1.3 %, along with an encapsulation efficiency of about 42 %.

Stability test

The stability of the produced iron loaded nanoliposomes with the best encapsulation efficiency (0.01 w/w Fe/total formulation components) was tested in conditions simulating those of iron enriched food (such milk or fruit juice) storage. The samples, maintained at 4 °C for a period of about 15 days in deionized water, were found to be stable as can be observed from the Figure 24.
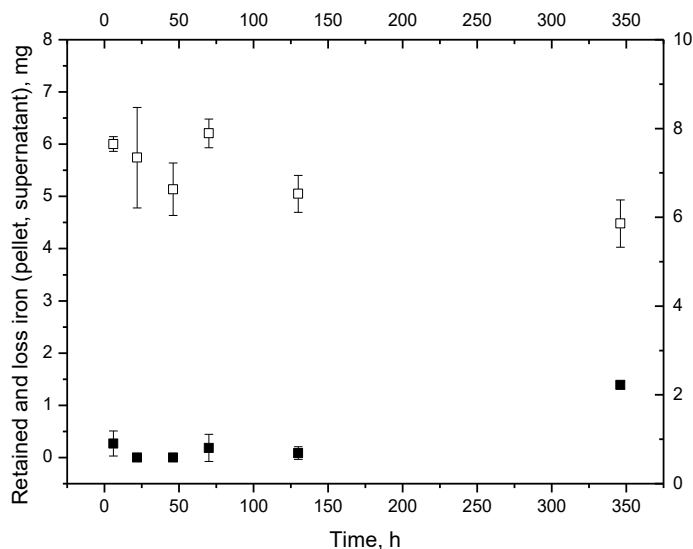
Figure 24. *Iron retained in nanoliposomes and released in deionized water. The open symbols are referred to the ferrous sulfate mass retained in the pellet, the full symbols represent the iron losses in deionized water*

The trend of the mass of iron presents in the pellet and in the supernatant at different time remains constant during an observation period of 130 h (about 6 days). At the last observation, after 346 h (about 15 days), approximately the 24 % of the total ferrous sulfate was released in the supernatant, probably due to oxidation phenomena occurred to lipids. In general, liposomal structures showed a good ability in retain the iron mass in their core structures, proving to be useable for food iron enrichment application.

5.2.4.3 A comparison between the simil-microfluidic apparatus and the classical bench scale techniques

Iron liposomes produced with the simil-microfluidic set-up were compared with ferrous sulfate loaded vesicles produced with the conventional techniques by using the same operating conditions and the 0.01 w/w Fe/total components formulation. In Table 12 the results relative to structures size, PDI, zeta potential and encapsulation efficiency of iron-nanoliposomes are presented for the tree methods adopted.

Table 12. *Size, PDI, zeta potential and encapsulation efficiency (e.e.) of ferrous sulfate loaded nanoliposomes produced adopting the 0.01 w/w Fe/total components formulation*

	Simil-microfluidic set-up	Thin Film Hydration	Ethanol Injection
Size (nm) ± SD	76.29±16.4	49.85±1.79	74.53±9.81
PDI ± SD	0.37±0.029	0.30±0.021	0.52±0.039
Zeta Potential (mV) ± SD	-35.87±2.05	-30.2±1.27	-37.27±2.26
e.e. ± SD (%)	96.63± 2.7	97.98± 2.17	100±0

The liposomal dimensional features are comparable except for a slight reduction in liposomes size observed by using the ultrasound assisted Thin Film Hydration method and an increases in PDI by using the Ethanol Injection method. Zeta potential values as well as the encapsulation efficiencies remains high and mostly similar, with a 100 % of e.e. by using the EI technique. The strength of the simil-microfluidic apparatus resides therefore in the process time and yield, in the use of not drastic conditions (toxic solvents or high pressure/temperature are avoided), in the controllable final liposomes dimensional features by modulating the starting flow conditions.

In particular, the conventional Thin Film Hydration method (Bangham and Horne, 1964) followed by the ultrasound assisted size reduction process (Barba et al., 2014), used in this thesis also for the production of SUVs encapsulating different kind of vitamins (5.1 section), peptides (5.3 section) and Nucleic Acid Based Drugs (NABDs) (5.4 and 5.5 sections), despite giving the possibility in achieving liposomes on nanometric scale due to the versatility of the size reduction process developed, with high loads for the most of the active molecules used, suffers of the impossibility to scale up the process. The volumes in output are small with long process times. Indeed, also if considering the higher capacity of a standard size round bottom flask commercially available, the resulting volume of product obtainable in a given time (usually 3-4 hours are necessary just to the solvent evaporation step) is small and finite, the situation is not different for the ethanol injection technique which, despite being a more rapid method, presents a maximum syringe volume of 50 ml, moreover the process is discontinuous and not controllable. The semicontinuous apparatus developed has not limits in the production, in particular in just 2.5 minutes it is possible to produce 110 ml of iron-nanoliposomes solution. As visible in Table 13, through the use of

the developed apparatus the yield of the process, intended as the ratio of the number of liposomes produced in one batch for unit volume (see 4.2.2.4 paragraph, eq. 4.5) to the time spent for their production, is about $2.3 * 10^{14}$ (1/ml h) while with the conventional technique the yield decreases becoming about $9*10^9$ (1/ml h) and $5.4*10^{11}$ (1/ml h) respectively when the Thin Film Hydration and the Ethanol Injection methods are adopted.

Table 13. *A comparison in terms of process yield between the use of the simil-microfluidic set-up and the classical bench scale methods in nanoliposomes production. A volumes of 110 ml (one batch volume), 3000 ml (maximum round bottom flask volume) and 50 ml (maximum sysringe volume) were considered for Simil microfluidic set-up, ultrasound assisted TFI and the EI techniques, respectively with a production time of 2.5 min, 10 min and 24 h*

	Simil-microfluidic set-up	Thin Film Hydration	Ethanol Injection
Maximum volume producible, ml	No limits	3000	50
Yield for a batch, 1/(ml h)	$2.27*10^{14}$	$8.98 * 10^9$	$5.42 * 10^{11}$

5.2.5 Remarks

A massive production of nanoliposomes is possible due to the developed apparatus with a precise control on particles size and size distribution by varying the liquids volumetric flow rate ratio or lipids concentration. Ferrous sulfate loaded nanoliposomes with high encapsulation efficiencies (up to 97 % e.e.) and good dimensional features (127-135 nm for not sonicated and 48-76 nm for sonicated liposomes) were successfully produced through the use of the simil-microfluidic apparatus developed, obtaining an elevated process yield if compared to the classical bench scale techniques. Taking into account that "less waste" and "less energy" are the central topics of food manufacturers, the apparatus developed could will make iron-nanoliposomal based nutraceutical products cheaper due to a more efficient and sustainable production process, avoiding the use of toxic solvents and drastic conditions. The simil-microfluidic apparatus developed could have a great impacts on the nutraceutical-processing industries reducing process time and costs.

Part of this work has been reported in:
Bochicchio S.; Lamberti, Barba A.A., "Phenomenological and formulation aspects in tailored nanoliposomes production", chapter in book Liposomes, InTech Ed, 2017, in press.

5.3 Nanoliposomes vectors for peptide delivery

5.3.1 Generalities

The use of peptides in the development of new therapeutic strategies is becoming increasingly important due to their multifunctionality. Indeed, peptides can be used as vaccines, as cell-penetrating molecules or as new therapeutics for a lot of different diseases. In paticular, in 2015 the results relative to a Phase IIB Trial of BLP25 Liposome Vaccine have been published (Fosgerau and Hoffmann, 2015). As therapeutics agents, peptides could be used for the cure of a vast array of diseases but the lack of effective vectors limits their use (Tan et al., 2010). The susceptibility to enzymatic degradation make peptides high degradable molecules, characterized by in vitro and in vivo instability, immunogenicity and short half-life (Patel et al., 2014b).

The developement of suitable drug delivery systems is a key to improve peptides pharmacokinetic properties and to achieve a controlled and targeted release which resuts in a revolutionary new clinical approach for the treatment of different diseased states as cancer, multiple sclerosis, diabetes, hepatitis, rheumatoid arthritis, leukemia, infectious diseases and Heart Failure (HF) (Huang and Wang, 2006, Patel et al., 2014a, Li et al., 2012, Park et al., 2011).

In that regard, G protein-coupled receptor kinase 2 (GRK2) is a kinase which role is relevant in the physiology of various organs/tissues including the heart and blood vessels (Carotenuto et al., 2013). It was demonstrated that GRK2 levels are increased in HF (Carotenuto et al., 2013, Iaccarino et al., 2005) thus the inhibition of this kinase represents a potential way to treat several cardiovascular pathologies (Harding et al., 2001).

The KRX29 is a novel small cyclic peptide designed on the HJ loop of GRK2, where its kinase activity resides. It inhibited potently and selectively the GRK2 activity, being more active than its linear precursor. In a cellular system, this peptide confirms the beneficial signaling properties of a potent GRK2 inhibitor.

Although its small dimension (8 amino acids) KRX29 low absorption, instability in physiological environments and short half-life requires the encapsulation in suitable carriers in order to overcome these limits. In this thesis, with the aim to increase the potential therapeutic of the KRX29 peptide, tailored nanoliposomes as suitable delivery vectors for this GRK2 inhibitor have been designed and produced.

Three different liposomal formulations, by changing the charge ratio (-/+) between the negative charged phosphatidilglicerol and the positive charged peptide KRX29, were investigated. In particular, the liposomal vectors were designed using a 1:1, 7:1 and 13:1 (-/+) charge ratios and produced by the thin film hydration method followed by the sonication sizing process, the

new method described in 4.1 section (Barba et al., 2014), in order to achieve nanoliposomes with predictable and reproducible size distributions. The liposomes charge effect on both peptide encapsulation and recovery efficiencies was studied through an analytical HPLC protocol expressly developed for this purpose. Moreover, the peptide loading on encapsulation and recovery efficiencies in the produced liposomes was also tested together with the stability of peptide-liposome complex in Tris-HCl solution simulating extracellular conditions. This study thus represents a mile stone for future in-vivo investigations to prove the effectiveness (and its performance as inhibitor) of the encapsulated peptide.

5.3.2 Materials

Peptide KRX29, which main properties can be found in Table 14, was manufactured as described in the next paragraph. L-α-Phosphatidylcholine (PC) from egg yolk (CAS n. 8002-43-5), Cholesterol (CHO) (CAS n. 57-88-5), L-αPhosphatidyl - DL glycerol sodium salt (PG) from egg yolk lecithin (over 99% pure), Tris(hydroxymethyl)aminometane hydrochloride (CAS n.42861) and sodium chloride (CAS n. S9888) were purchased from Sigma Aldrich (Milan, Italy) as dried powders and used without further purification. All the other chemicals and reagents such as chloroform (CAS n. 67-66-3), ethanol (CAS n. 64-17-5), methanol (CAS n. 67-56-1)(Sigma Aldrich- Milan, Italy), used were of analytical grade.

5.3.3 Methodology and sperimental set-up

5.3.3.1 Peptide KRX29 synthesis

Peptide KRX29 synthesis was performed according to the solid phase approach using standard Fmoc methodology in a manual reaction vessel (Atherton, 1989). Nα-Fmoc-Asp(Allyl)-OH and Nα-Fmoc-Lys(Alloc)-OH were used as lactam precursors .The first amino acid was linked on to the Rink resin (0.75 mmol/g) previously deprotected by a 25% piperidine solution in DMF for 30 min. The following protected amino acids were then added stepwise. Each coupling reaction was accomplished using a 3- fold excess of amino acid with HBTU and HOBt in the presence of DIPEA (6 equiv). The Nα-Fmoc protecting groups were removed by treating the protected peptide resin with a 25% solution of piperidine in DMF and the deprotection protocol was repeated after each coupling step.
After linear assembly, cyclization was performed as described in literature (Grieco et al., 2001). The N-terminal Fmoc group was removed and the peptide was released from the resin with TFA/iPr3SiH/H2O (90:5:5) for 3 h. The crude peptides were purified by preparative RP-HPLC and purity monitored by analytical HPLC. Molecular weights were confirmed by ESI-

MS.

Table 14. *Peptide KRX29 chemico-physical properties*

Peptide name	KRX29
Peptide sequence	KLLRrHDI
Chemical formula	$C_{46}H_{82}N_{18}O_9$
Peptide Molecular Weight, uma	1031.6
Peptide Molecular Weight +trifluoroacetic acid (TFA), uma	1601.6
Hydrophobic portion, %	38
Hydrophilic portion, %	62
Net charge at pH 7.0	+ 3
Isoelectric point (IET)	11.48

5.3.3.2 MLVs and SUVs preparation at different charge ratio

Multi lamellar vesicles (MLVs) were prepared by means of the Thin Film Hydration method followed by sonication in order to finally get suitable Small Unilamellar Vesicles (SUVs). The negative charged PG was used as one of the formulation component in order to electrostatically react with the positive charged KRX29 peptide. To this purpose, three different liposomal formulations were produced by changing the PG/KRX29 (-/+) charge ratio; in particular a 1:1, 7:1 and 13:1 (-/+) charge ratio formulations were prepared. Using the same lipid compositions, unloaded MLVs and SUVs were also produced in order to get a comparison with the loaded liposomal samples.

In short, for a 1:1 charge ratio formulation, PC (75 mg), CHO (9 mg) and PG (6.3 mg) at 11:3:1 (mol:mol) ratio were dissolved in 3 mL of chloroform/methanol 2:1 (vol/vol). Part of the solvent was removed by evaporation in a rotary evaporator (Heidolph, Laborota 4002 Control, Bergamo, Italy) under reduced pressure until a lipid film was produced. Then any traces of the solvent were removed by evaporation maintaining the sample under reduced pressure for 3 hours, at 50 °C. The dried lipid film was then hydrated at room temperature with 3 mL of pre-warmed deionized water containing 1 mg/ml of peptide KRX29 for loaded liposomes production and with pre-warmed deionized water without peptide for unloaded liposomes. Both the loaded and unloaded formulations were stirred in a continuous manner for 30 minutes at 60 rpm. MLVs produced starting from the 7:1 (-/+) and the 13:1 (-/+) charge ratio formulations were prepared as above described for the 1:1 (-/+) PG:KRX29 liposomes but varying the

lipids and peptide amounts used, as reported in Table 15. In particular, for the 7:1 (-/+) charge ratio formulation PC, CHO and PG were used at 4:1:3 (mol:mol) ratio while for the 13:1 (-/+) formulation, PC, CHO and PG were used at 2.5:1:2 (mol:mol) ratio.

Table 15. *Liposomal formulations for KRX29 encapsulation with different charge ratio (-/+)*

PG/KRX29 charge ratio	PC (mg/ml)	CHOL (mg/ml)	PG (mg/ml)	Peptide (mg/ml)
1:1	25	3	2.1	1
7:1	20	2.5	15	0.95
13:1	16	3	11	0.4

For all the formulations, the preparations containing MLVs were maintained at room temperature for 2 hours. Part of the unloaded and loaded liposome samples were used to characterized MLVs in terms of morphology and size; loaded MLVs were also characterized in terms of amount of peptide recovered, load and encapsulation efficiency. Most of the sample was then sonicated at 45% amplitude (treated volume: 1 mL) by applying a duty cycle consisting in 2 ten-second irradiation rounds (amplitude 45%), each followed by a twenty-second pause in order to prevent thermal vesicle disruption thus obtaining Large Unilamellar Vesicles (LUVs). The samples were stored overnight at 4 °C and protected from light. The samples were then sonicated at 45% amplitude (percentage of maximum deliverable power) for three more rounds in order to obtain SUVs (the duty cycle sonication protocol is in dept described in 4.1 section). The process parameters in MLV and SUV preparation are summarized in Table 16.

Table 16. *Process parameters adopted in Small Unilmellar Vesicles (SUVs) preparation, starting from Multilamellar Vesicles (MLVs)*

Process parameters	*From MLV to SUV*
Sonication duty cycle (s)	2 + 3 irradiation rounds
Fraction of maximum power (%)	45
Frequency (KHz)	20
Treated volume (mL)	1

5.3.3.3 MLVs and SUVs physicochemical characterization

Bright field imaging
Morphological and dimensional characterizations of unloaded and loaded MLVs, produced with the different formulations, were performed by optical microscopy (Axioplan 2- Image Zeiss, Jena, Germany) for bright field imaging. A 63 X objective was used to visualize the vesicles.

Particle sizes and zeta potential

The dimensional analysis of microscope images, performed with the software ImageJ, was combined with the Dynamic Light Scattering analysis for MLV and SUV. In particular, Dynamic Light Scattering analysis was performed by using the ZetasizerNano ZS (Malvern, UK) which incorporates noninvasive backscatter (NIBS) optics. A detection angle of 173 degrees was used to measure the particles size of the concentrated samples. For each formulation tested, the resulting particle size distribution was plotted as the number of liposomes versus size. Zeta potential was also determined in Light Scattering for both unloaded and loaded SUVs. All the measurements were performed in triplicate. The results were expressed as average values.

5.3.3.4 Determination of encapsulation efficiency, peptide KRX29 recovery and achieved loading

For each formulation tested, encapsulation efficiency, peptide recovery and load in liposomes were evaluated by Reversed Phase High Performance Liquid Chromatography (RP-HPLC) analysis. In brief, 150 µl of MLVs sample were centrifuged at 10500 rpm for 30 minutes at 4 °C and all supernatant was removed. The same was for SUVs, in this case 200 µl of sample were centrifuged at 30000 rpm overnight at 4 °C and all supernatant was removed. For both MLVs and SUVs samples, the recovered supernatants were diluted 1:3 v/v with 100 % ethanol and then injected into RP-HPLC. Subsequently, 300 µl and 400 µl of 100 % ethanol were added respectively to the MLVs and SUVs pellets. The samples were vortexed until the lipid pellets broke up and then analyzed by RP-HPLC. Peptide quantifications were carried out by external standard calibration with a satisfactory linearity (R^2 >0.998). The calibration curve was performed for peptide in distilled water, the retention time of peptide in ethanol and buffer solution was also analyzed resulting the same. High performance liquid chromatography was performed on a Shimadzu HPLC consisting of an autosampler, a dual wavelength absorbance UV detector, set to 215 nm. The mobile phases employed were: solvent A (water + 0.1% TFA) and solvent B (acetonitrile + 0.1% TFA); using a linear gradient from 5% to 90% B over 14 min, the separation was carried out using an Ascentis Express Peptide ES-C18 column 50 mm x 3.0 mm, 2.7µm (Supelco), at a flow rate of 0.800 mL/min.

For MLVs and SUVs formulations produced at the different charge ratio, the encapsulation efficiency (e.e.) was determined as the percentage of peptide encapsulated in liposomes to the initial amount of peptide included in the formulation and was calculated using the following equation:

$$\text{e. e.} \, (\%) = \left(\frac{encapsulated\ peptide,\ mg}{initial\ peptide\ amount,\ mg} \right) \times 100 \qquad (5.5)$$

where the amount of peptide encapsulated in liposome was calculated subtracting the amount of peptide present in the supernatant of the centrifuged sample from the total amount of peptide included in the formulation.

The effective loads of peptide into liposomes, ever for MLVs and SUVs formulations produced at the different charge ratio, were calculated as follows:

$$\text{load (\%)} = \left(\frac{encapsulated\ peptide,\ mg}{total\ mass\ of\ loaded\ liposomes,\ mg}\right) \times 100 \quad (5.6)$$

In particular, the theoretical load is referred to the initial amount of peptide included in the formulation (divided by the total mass); the effective one is referred to the assayed peptide amount (divided by the total mass).

The effective amount of peptide accounted for in MLVs and SUVs formulations after extraction was calculated as follows:

$$\text{recovery (\%)} = \left(\frac{peptide\ recovered,\ mg}{initial\ peptide\ amount,\ mg}\right) \times 100 \quad (5.7)$$

where peptide recovered is the total amount of peptide KRX29 extracted from supernatant and pellet of centrifuged samples.

5.3.3.5 MLVs at constant charge ratio but with different peptide concentration: preparation and characterization

In addition to the charge ratio, another key parameter affecting the encapsulation efficiency is the amount of peptide used in liposomes production. During the lipid film hydration the bilayer, getting in contact with the hydration solution containing the peptide, closes to form MLVs. During this process the amount of peptide that remains entrapped in the liposomes may changes on the basis on how concentrated the hydration solution is. In order to investigate the influence of the KRX29 concentration on the encapsulation efficiency another formulation was produced maintaining this time constant the PG/KRX29 charge ratio at 1:1 (-/+) but hydrating the lipid film with the double of peptide mass (2 mg/ml) as indicated in Table 17.

Table 17. *Composition of two 1:1 charge ratio formulations with different amount of peptide KRX29*

PG/KRX29 charge ratio (-/+)	PC (mg/ml)	CHOL (mg/ml)	PG (mg/ml)	Peptide (mg/ml)
1:1	25	3	2.1	1
1:1	22	3	4.2	2

The peptide amount was changed maintaining the same formulation charge ratio in order to observe the differences in encapsulation efficiency without the influence of electrostatic interactions, being this formulation characterized by a (-/+) charge balance. The final total lipids concentration was remained about the same (30 mg/ml) for both the formulations and MLVs were produced through the thin film hydration method as above described for the other formulations.

The final liposomes sample was characterized in terms of encapsulation efficiency, peptide recovery, load and stability evaluated by RP-HPLC analysis as before described for the other samples.

5.3.3.6 Stability test

Stability test of loaded liposomes was assayed in order to evaluate the ability of the nanoliposomes in retaining KRX29 at extracellular environment simulated conditions. Tris-buffered saline solution (TBS) was prepared dissolving Tris(hydroxymethyl)aminometane hydrochloride 0.01 M and sodium chloride 0.15 M in distilled water, obtaining a pH 7.4 TBS final solution. This solution was used as medium for the peptide-liposome complex stability test.

Release profile of peptide in Tris-HCl solution medium (pH 7.4) was thus studied testing the 1:1 (-/+) charge ratio formulation produced, containing 2 mg/ml of peptide. This formulation was choice for the stability test due to its higher peptide recovery efficiency (the amount of peptide accounted for (%)) respect to the 7:1 (-/+) and the 13:1 (-/+) charge ratio formulations.

In short, 850 µl of loaded liposomes sample were centrifuged at 10500 rpm for 30 min at 4 °C, subsequently the supernatant was carefully removed and replaced with the double of volume of Tris-HCl medium (1.7 ml). The sample was then putted in an incubator set at 37 °C with an orbital shaker and maintained in agitation at 60 rpm for 72 h. At predetermined intervals, 250 µl aliquots of loaded liposomes were taken from the sample and centrifuged at 10500 rpm for 30 min at 4 °C (Beckman Coulter Avanti J-25I, Ramsey, Minnesota, USA) to precipitate the liposomes. After each centrifugation the supernatants were collected for HPLC analysis. The 1:2 v/v dilution of the sample with Tris-HCl was taken into account during the peptide quantification. All the measurements were performed in triplicate. The percent of KRX29 released in the supernatant was calculated using the following equation:

$$\text{KRX29 released (\%)} = \left(\frac{peptide\ amount\ in\ supernatant,\ mg}{encapsulated\ peptide\ amount,\ mg} \right) \times 100 \quad (5.8)$$

where the peptide amount in supernatant is referred to the amount of KRX29 recovered at different times (after 45 minutes, 3 h, 24 h, 48 h and 72 h) in the

aliquots collected after centrifugation and the encapsulated peptide amount in liposome was calculated as described in 5.3.3.4 paragraph.

5.3.4 Results

5.3.4.1 MLVs and SUVs at different charge ratio

5.3.4.1a Physicochemical characterization

Bright field imaging

Bright field imaging was used to observe the structure of both unloaded and peptide KRX29 loaded MLVs, prepared starting from the different charge ratio formulations. As shown in Figure 25 spherical, separated and defined liposomes were obtained for the three different formulations tested.

| 1:1 (-/+) charge ratio | 7:1 (-/+) charge ratio | 13:1 (-/+) charge ratio |
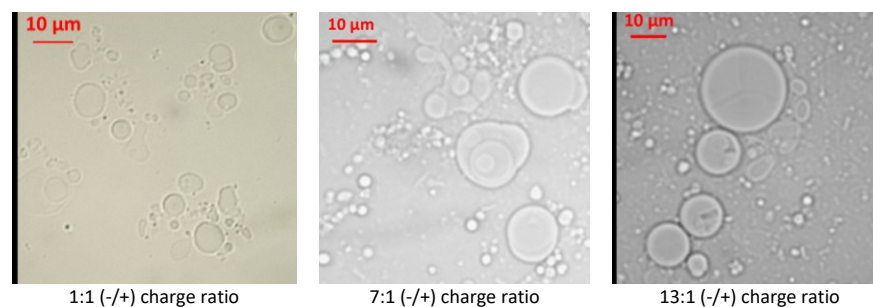
Figure 25. *Optical microscope pictures (in bright field, Obj. 63 X) of KRX29 loaded liposomes at the different tested charge ratios*

Unloaded and loaded MLVs and SUVs at different PG/KRX29 charge ratios were then analyzed for dimensional characterization. For all formulations, unloaded MLVs with a micrometric range size of 5 - 6.4 µm and KRX29 loaded MLVs with 7.2 - 11.7 µm range size were produced through the thin film hydration method.

Starting from MLVs, after five total sonication rounds, SUVs with nanometric size were achieved for both unloaded and peptide KRX29 loaded liposomes. Data taken from a numerical size distribution have showed a range size of 19 - 21 nm for unloaded vesicles while for loaded SUVs a 22 - 35 nm range size was observed. In Table 18 particles size results are summarized and presented along with polydispersity index (PDI) values. Results are expressed as average of three determinations with standard deviation.

Table 18. *Size of unloaded and loaded Multilamellar Vesicles (MLVs) and Small Unilamellar Vesicles (SUVs) at the different PG/KRX29 studied charge ratios. PDI is the polydispersity index. Results are expressed as average of three determinations with SD as standard deviation*

Sample charge ratio	Unloaded liposomes			KRX29 loaded liposomes		
	MLV (µm) ±SD	SUV (µm)± SD	PDI / ± SD	MLV (µm)±SD	SUV (µm) ±SD	PDI / ± SD
1:1 (-/+)	5 ± 1.9	0.019 ± 0.005	0.4 ± 0.008	7.2 ± 2	0.022 ± 0.002	0.5 ± 0.02
7:1 (-/+)	6.43 ± 2.5	0.02 ± 0.01	0.29 ± 0.002	10.19 ± 7.7	0.034 ± 0.01	0.24 ± 0.004
13:1 (-/+)	6.28 ± 1.72	0.021 ±0.007	0.3 ± 0.007	11.7 ± 5.9	0.035 ±0.008	0.37 ± 0.001

Zeta Potential

For all the different kinds of liposomal produced vectors, the DLS analysis showed, as attended, a negative zeta potential of unloaded and peptide loaded liposomes. In Table 19 all the results along with standard deviation are reported as average values of three determinations.

Table 19. *Zeta potential of unloaded and loaded Multilamellar Vesicles (MLVs) and Small Unilamellar Vesicles (SUVs) achieved using different PG/KRX29 charge ratios. Results are expressed as average of three determinations; SD is the standard deviation*

	1:1 (-/+)	7:1 (-/+)	13:1 (-/+)
Unloaded liposomes	-15.3 ± 0.6	-20.1 ± 1.62	- 41.9 ± 3.88
KRX29 loaded liposomes	-16.1 ± 0.37	-18.1 ± 3.51	-37.9 ± 0.4

5.3.4.1b Determination of encapsulation efficiency, peptide KRX29 recovery and achieved loading

Using the first 1:1 (-/+) charge ratio formulation, an encapsulation efficiency (e.e.) of 33.6 ± 0.32 % and of 37.7 ± 0.44 were obtained for MLVs and SUVs, respectively. With the same charge ratio formulation, peptide recoveries of 94.4 ± 0.78 % for MLVs and 80.6 ± 0.33 % for SUVs were also achieved.

Starting from the second formulation (7:1 (-/+) charge ratio) a significant increase in encapsulation efficiency was observed, obtaining an e.e. of 98.9 ± 1.53 %. and of 97.3 ± 0.34 % for MLVs and SUVs, respectively. On the contrary, peptide recoveries were reduced until to 46.6 ± 6.6 % for MLVs and 33.8 ± 12.5 % for SUVs.

A slight increase in the encapsulation efficiency was still visible using the last 13:1 (-/+) formulation with an e.e. of 100 ± 0 %. for MLVs and an 98.8 ± 1.4 % for SUVs, with a peptide recovery of 22.07 ± 1.85 % and 21.8 ± 0.64 % for MLVs and SUVs, respectively. All the results are summarized in Table 20**.**

Table 20. *Encapsulation efficiency and amount of peptide KRX29 accounted for in MLVs and SUVs loaded with KRX29 at the studied different charge ratios. Results are expressed as average of three determinations; SD is the standard deviation*

PG-KRX29 charge ratio	Encapsulation efficiency (%) and Standard Deviation (SD)		Amount of peptide KRX29 accounted for (%) and Standard Deviation (SD)	
	MLVs	SUVs	MLVs	SUVs
1:1 (-/+)	33.6 ± 0.32	37.7 ± 0.44	94.4 ± 0.78	80.6 ± 0.33
7:1 (-/+)	98.9 ± 1.53	97.3 ± 0.34	46.6 ± 6.6	33.8 ± 12.5
13:1 (-/+)	100 ± 0	98.8 ± 1.4	22.07 ± 1.85	21.8 ± 0.64

The results of theoretical and effective loads achieved for peptide KRX29, for small and large vesicles, are summarized in Table 21.

Table 21. *Theoretical load and effective load of MLVs and SUVs loaded with KRX29 at the studied different PG/KRX29 charge ratios. Results are expressed as average of three determinations; SD is the standard deviation*

PG-KRX29 charge ratio	Theoretical loading achieved(%)		Effective loading achieved (%) and Standard Deviation (SD)	
	MLVs	SUVs	MLVs	SUVs
1:1	3.37	3.37	1.16 ± 0.01	1.3 ± 0.01
7:1	2.23	2.23	2.21 ± 0.35	2.19 ± 0.38
13:1	1.3	1.3	1.27 ± 0	1.24 ± 0.004

Moreover in Table 22 the peptide mass balances, accurately determined by dedicated HPLC protocol, were reported for each formulation.

Table 22. *Mass balance of KRX29 loaded in MLVs and SUVs at the studied different charge ratios. Results are expressed as average of three determinations; SD is the standard deviation*

KRX29 Mass Balance in 1 ml sample	MLV	SUV
1:1 charge ratio formulation		
Total mass of peptide (mg) in supernatant and pellet ± SD	0.99 ± 0.008	0.84 ± 0.006
Mass of peptide (mg) in supernatant ± SD	0.7 ± 0.004	0.65 ± 0.004
Mass of peptide (mg) in pellet ± SD	0.29 ± 0.004	0.19 ± 0.002
7:1 charge ratio formulation		
Total mass of peptide (mg) in supernatant and pellet ± SD	0.40 ± 0.11	0.27 ± 0.06
Mass of peptide (mg) in supernatant ± SD	0.008 ±0.01	0.017 ±0.02
Mass of peptide (mg) in pellet ± SD	0.39 ± 0.12	0.26 ± 0.03
13:1 charge ratio formulation		
Total mass of peptide (mg) in supernatant and pellet ± SD	0.086 ± 0.002	0.084 ± 0.002
Mass of peptide (mg) in supernatant ± SD	0.0 ± 0.0	0.01 ± 0.001
Mass of peptide (mg) in pellet ± SD	0.086 ± 0.002	0.074 ± 0.001

5.3.4.2 MLVs at constant charge ratio and different peptide concentration

As it is shown in Table 23, using the 1:1 (-/+) charge ratio formulation with 2 mg/ml of KRX29, MLVs with an encapsulation efficiency of 57 ± 0.04 % were achieved respect to the 33.6 ± 0.32 % e. e. obtained by using 1 mg/ml of peptide at the same charge ratio.

Table 23. *Encapsulation efficiency and amount of peptide KRX29 accounted for in MLVs loaded with different amounts of KRX29 at the same PG/KRX29 charge ratio (1:1 -/+). Results are expressed as average of three determinations; SD is the standard deviation*

PG-KRX29 charge ratio (-/+)	Amount of KRX29 used for hydration (mg/ml)	Encapsulation efficiency (%) and SD	Amount of peptide KRX29 accounted for (%) and SD
1:1	1	33.6 ± 0.32	94.4 ± 0.78
1:1	2	57 ± 0.04	72.9 ± 0.06

Moreover, the amount of peptide accounted for was decreased with the last formulation (Table 23) while the effective load was increased (Table 24) if compared to the first formulation.

Table 24. *Theoretical load and effective load of MLVs loaded with different amounts of KRX29 at the same PG/KRX29 charge ratio (1:1 -/+). Results are expressed as average of three determinations; SD is the standard deviation*

PG-KRX29 charge ratio (-/+)	Amount of KRX29 used for hydration (mg/ml)	Theoretical loading achieved (%)	Effective loading achieved (%) and SD
1:1	1	3.37	1.16 ± 0.01
1:1	2	6.6	3.86 ± 0.002

The differences in encapsulation and extraction efficiencies can be also observed in Table 25 where the mass balances for the first and the last formulations were reported.

Table 25. *Mass balance of KRX29 loaded in MLVs at the two studied different KRX29 concentrations. Results are expressed as average of three determinations; SD is the standard deviation*

KRX29 Mass Balance in 1 ml sample	1 mg/ml peptide sample	2 mg/ml peptide sample
1:1 charge ratio formulation		
Total mass of peptide (mg) in supernatant and pellet $\pm$ SD	0.99 ± 0.008	1.5 ± 0.001
Mass of peptide (mg) in supernatant $\pm$ SD	0.7 ± 0.004	0.88 ± 0.001
Mass of peptide (mg) in pellet $\pm$ SD	0.29 ± 0.004	0.6 ± 0.0008

5.3.4.3 Stability test

Liposomes batches undergone to the stability test were found to be stable for 72 hours in stirred Tris-HCl solution at 37 °C. As it can be observed from Figure 26, after 3 h, a maximum of amount of peptide released was achieved.
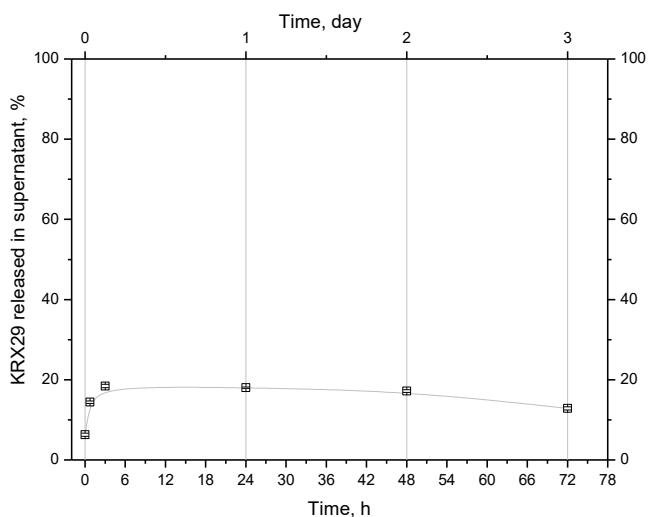
Figure 26. *Peptide release profile in Tris-HCl solution at 37°C*

The cumulative profile thus shows that only the 18 % of the encapsulated peptide was released. Indeed, after the 3 hours, only small differences in peptide amounts between the aliquots analyzed were assayed. These differences were reasonably due to the nature of the sample which being a suspension is not completely uniform in its liposomes content.

5.3.5 Discussion

As therapeutics agents, peptides could be used for the cure of a vast array of diseases but the lack of effective vectors limits their use (Tan et al., 2010). The awareness of the need of a delivery systems at first, and, then, the deeper understanding of the importance in having a tailored carriers, has led the scientific community to investigate about peptides encapsulation in different delivery systems (Belogurov et al., 2013, Mohan et al., 2015, Silva et al., 2013). In particular, in 2015, the results relative to a Phase IIB Trial of *BLP25 Liposome Vaccine* have been published. In their work, Butts and collaborators have produced BLP25 liposome vaccine consisting of BLP25 lipopeptide, immunoadjuvant monophosphoryl lipid A, and three lipids (cholesterol, dimyristoyl phosphatidylglycerol, and dipalmitoyl phosphatidylcholine) forming a liposomal product. They have evaluated the effect of their prepared loaded system on survival and toxicity in patients with stage IIIB and IV of non–small-cell lung cancer (NSCLC). They have demonstrated the safety of the developed preparation, suggesting a potential survival advantage for patients (Butts et al., 2005). Taking into account the potential and the possible various applications in medical field of peptides, it comes clear the crucial importance in projecting suitable delivery systems

considering peptide features and exploring the different possible lipid formulations. Consequently, becomes evident the necessity in using a versatile and reliable production technique, able to produce tailored carriers without affecting the peptide integrity and thus its final biological activity.

5.3.5.1 Effect of formulation

The design of liposome formulation has a crucial importance in tailored peptide-nanovectors production. Lipid type and concentration, amount of peptide to be used and presence of charged molecules are all parameters which affect the liposomal final features such as shape, size, zeta potential, stability as well as encapsulation efficiency and peptide loading. Moreover, for best results in encapsulation efficiency, if both charged lipids and active molecules are used, a design of the right (+/-) charge ratio in the final formulation should to be done.

In particular, in a work of Su and collaborators, it was underline the importance in take advantage of the charge ratio influence on liposomes-peptide bonds to produce peptides physically coating liposomes. They have showed that the coating was mainly driven by the electrostatic interaction between the cationic peptides and the anionic lipids and can be used as a versatile method to attach peptides on liposomal bilayer (Su et al., 2014). In this thesis it was exploited the effect of different lipid/peptide charge ratios to encapsulate a new small cyclic peptide to achieve the best formulation with the higher encapsulation efficiency without overlook the effects of this formulation parameter on all the other liposomes final features such as the size, the zeta potential and the peptide load and recovery efficiency.

5.3.5.1.a Effect of peptide/lipid charge ratio

Unloaded and loaded liposomes size
Numerous scientific studies have shown that the size and zeta potential of liposomes determine their in-vivo and ex-vivo performance, thus a good design first and a subsequent careful analysis of the data are fundamental steps in nanostructured vectors production (Mozafari, 2010, Chang et al., 2011).

Three peptide-liposomes formulations characterized by a different (-/+) charge ratio (1:1, 7:1, and 13:1 -/+) have been investigated in order to compare the obtained range size and zeta potential values. At first, for each formulation, unloaded MLVs and SUVs sizes were analyzed in order to compare the resulting range values with those obtained from KRX29 loaded small and large vesicles. A comparison between loaded and unloaded liposomes, maintaining constant the lipids type and their total concentration in the final formulation, is important to have an idea of peptide influence on the vesicles final size. First of all, it was observed that the use of negative charged PG in the formulation gives unloaded MLVs with a larger diameter

size. This can be visible by comparing the unloaded MLVs sizes obtained from the last two formulations (the 7:1 and the 13:1 -/+, whose diameter range size were respectively of 6.43 ± 2.5 μm and 6.28 ± 1.72 μm), with those obtained with the first formulation (1:1 -/+ sample with 5 ± 1.9 μm range size vesicles) where the amount of PG was drastically reduced. This can be explained due to the repulsive force generates between the charged lamellae: this condition involves the increase of the aqueous compartments and therefore the final vesicles diameter increases too (Sessa and Weissmann, 1968).

It is interesting to note that unloaded MLV diameter size was smaller than that found for MLVs loaded with KRX29 peptide and this was true for all the tested formulations. For example, in the first formulation, the diameter of unloaded MLVs was 5 ± 1.9 μm while for loaded vesicles was 7.2 ± 2 μm and it was possible to observe the same trend for all MLVs and SUVs samples (results are summarized in Table 18). For example, taking into account ever the 1:1 (-/+) formulation, the unloaded SUVs diameter size of 19 nm increases in the presence of peptide, becoming of 22 nm. The increasing in liposomes size can be explained due to the presence of peptide whose amphiphilic nature (KRX29 is constituted of 62 % hydrophilic and 38 % hydrophobic portions, see Table 14) allows it to be in part encapsulated in the aqueous core and in part entrapped in the lipid bilayer of liposomal structures. This leads to a global increasing in the final liposome volume. It is important to underline the relevance in producing loaded vesicles of nanoscale dimension, mostly if the formulation had to be used for intravenous injection. In numerous scientific works it was demonstrated that the liposomes ability to permeate through membrane fenestrations of diseased blood vessels can be associated to their nanoscale dimensions (Godin et al., 2010, Truran et al., 2014, Tsiklauri et al.). This can be very useful in the treatment of linked to heart failure disease states and other cardiovascular pathologies being characterized by diseased blood vessels (Khurana et al., 2005).

Zeta potential analysis of loaded liposomes

Another important feature is the final liposomes surface charge. This value is an index of liposomes stability and could influence liposomes transfection efficiency inside tissues and cells. It was recently demonstrated that, despite their negative charge, anionic formulations have provided challenges of self-assembly and transfection efficiency in the treatment of neuronal diseases. In particular, Tagalakis and collaborators have observed that anionic PEGylated siRNA nanocomplexes, unlike the cationic ones, were not only resistant to aggregation in the presence of serum but they also give a significant gene silencing when administered to rat brains (Tagalakis et al., 2014).

In this thesis, the zeta potential was analysed before and after peptide encapsulation in order to understand the effect of KRX29 on the total surface

charge. Zeta potential values of the unloaded formulations were strongly negative whereas those with peptide became less negative, denoting the influence of peptide content on the final surface charge. This can be explained due to the positive peptide amino acid sequences, which decrease the electrostatic field of the negatively charged phosphatidylglycerol head groups, thus diminishing the zeta potential values.

The total surface charge changed with about the same trend in the 7:1 (-/+) and 13:1(-/+) formulations, where a considerable amount of negative charged lipid was used and high encapsulation efficiency was also achieved. In particular, in the 7:1 (-/+) formulation the zeta potential decreases from -41.9 ± 3.88 mV of unloaded liposomes to -37.9 ± 0.4 mV for loaded liposomes and about the same decrease in zeta potential was assayed for the 13:1 (-/+) formulation, with a -20.1 ± 1.62 mV for the unloaded form and -18.1 ± 3.51 mV for the loaded one (see Table 19). No decrease in zeta potential was visible for the first 1:1 (-/+) formulation being this latter "neutral" since it was characterized by a charges balance between the negative PG and the positive KRX29. In this case only the phosphate groups of phosphatidylcholine give the weak negative charge (about -16 mV) to the final liposomes and the peptide, which is encapsulated with a low efficiency, has not influence.

The zeta potential analysis can be useful for the best formulation choice in order to achieve stable nanoparticles. Taking into account that liposomes are stable when have $|\zeta| > 30$ mV, for the 13:1 (-/+) loaded formulation a high zeta potential was achieved (-37.9 ± 0.4 mV), index of stable particles production. In this case, with the 13:1 (-/+) charge ratio it is possible to obtain the higher encapsulation efficiency (98.8 – 100 % e. e., see Table 20) with a favorable zeta potential.

Peptide recovery, encapsulation efficiency and load analysis

It has been shown that small differences in the spatial arrangement of amino acids can cause big changes in the interaction of peptides with lipid membranes, mostly affecting peptide orientation (Koller and Lohner, 2014). This can lead to a difficult recovery of the peptide from the final liposomal complex. Due to the different characteristics of peptides there is no a unique protocol for their extraction, on the contrary, this must be accurately studied according to the chemical nature of the amino acids which constituted the peptide sequence. In the work of Shariat et al., (Shariat et al., 2014) it was underline how the knowledge of the optimal methods for both encapsulation and peptide content determination in liposomes can accelerate the development of liposomal vaccine formulations. Indeed, they have explored the use of different encapsulation methods and different extraction methods for the delivery of a new designed peptide into liposomes, as an approach for breast cancer vaccine formulation. They found the maximal peptide recovery (92.6 ± 2.1 %) from liposomes using acidified isopropanol at 1:2 of sample to solvent ratio.

In this thesis, it was demonstrated that not only the solvent used but also the lipids/peptides charge ratio can influence peptide extraction helping to create more or less strong ties between the two molecules. By preliminary studies of peptide recovery, methanol and ethanol at different v/v ratio have been tested as extraction phase (data are not shown); at last ethanol as the extraction medium was selected in order to have the highest efficiency in peptide recovery from liposomes. In addition to the extraction solvent nature it was also demonstrated that the charge ratio strongly affected the peptide recovery: higher is the charge ratio between peptide and lipids, lower is the peptide extraction efficacy due to the strong electrostatic interaction (Figure 27).
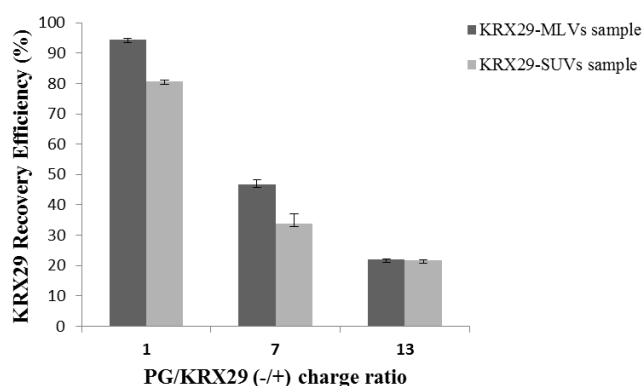
Figure 27. *Effect of PG/KRX29 (-/+) charge ratio on recovery efficiency*

On the contrary, higher is the charge ratio, higher is the encapsulation efficiency even if small differences were found in changing form the 7:1 (-/+) to the 13:1 (-/+) formulation (Figure 28).
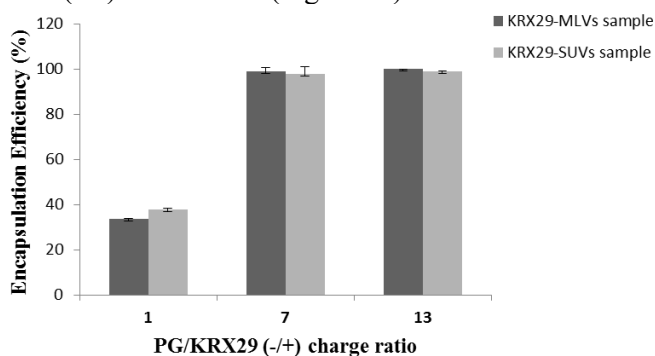
Figure 28. *Effect of PG/KRX29 (-/+) charge ratio on encapsulation efficiency*

In particular, as summarized in Table 20, taking into account the 7:1(-/+) formulation, the amount of peptide KRX29 recovered respect to the total

amount of used peptide was of 46.6 % for MLVs and of 33.8 % for SUVs corresponding to a 98.9 ± 1.53 % e. e. and 97.3 ± 0.34 % e.e. for MLVs and SUVs, respectively. When even more negative charges were used (13:1(-/+) formulation) the encapsulation efficiency was maxim, with a 100 % for MLVs and 98.8 ± 1.4 % e.e. for SUVs, but the amount of peptide KRX29 recovered (%) was drastically decreased (22.07 ± 1.85 % for MLVs and 21.8 ± 0.64 % for SUVs). When finally a 1:1 charge ratio was used low encapsulation efficiency was found, 33.6 ± 0.32 % for MLVs and 37.7 ± 0.44 % for SUVs (due to the neutralized charge) but almost the total amount of peptide used was recovered (94.4 ± 0.78 % from MLVs and 80.6 ± 0.33 % from SUVs). These results underline the crucial rule of charge ratio in peptides carriers design based on liposomal structures.

Theoretical and effective loads were also calculated for each formulation (results are summarized in Table 21) and a peptide mass balance was done for each formulation as reported in Table 22.

The high encapsulation efficiency found in both MLVs and SUVs and the effective loads achieved have demonstrated the great efficacy in using a 13:1 (-/+) charge ratio formulation. The use of an excess of thirteen negative charges respect to the positives one allows a very strong interaction between the phosphate groups of phosphatidylglycerol and the amine groups of peptide. This interaction can explain not only the elevated e.e. values but also limits in the peptide-lipids complex dissociation, resulting in a difficult peptide recovery.

5.3.5.1.b Effect of peptide concentration

As the charge ratio, also the peptide concentration should be carefully sought due to its influence on the liposomes encapsulation efficiency. In this thesis, starting from a neutral formulation (at 1:1 (-/+) charge ratio, negative PG and positive KRX29 charges are neutralized) it was demonstrated that when the peptide concentration is doubled the encapsulation efficiency (57 ± 0.04 % e.e.) increases of about 20 % respect to the 1 mg/ml peptide formulation (33.6 ± 0.32 % e. e.) (see Table 23). The explanation resides in a more concentrated solution, which gets in contact with the lipid film: when bilayer fragments start to close and form liposomes, a more concentrated solution remained entrapped inside the vesicles. This is true until a critical peptide/total lipids weigh ratio over that is not possible to further increase the encapsulation efficiency by increasing the peptide concentration because the quantity of phospholipids would not be enough to its full encapsulation. In that regard, Colletier and collaborators, have investigated the influence of the eggPC and POPC lipids concentration on the AChE protein encapsulation efficiency demonstrating that encapsulation is proportional to the number of lipids (Colletier et al., 2002). They have also demonstrated that encapsulation depends on electrostatic interactions between the enzyme peripheral surface and the polar head group of phospholipids. According to

this work and considering the results achieved, it was confirmed the crucial role played by the charge ratio in liposomes design that could help to increase encapsulation efficiency when the critical peptide/total lipids weigh ratio is already reached but is not enough to give the highest encapsulation efficiency.

5.3.5.2 Efficacy of ultrasound assisted technique in KRX29-liposomes production

As well as the formulation choice, also the production process is of crucial importance. The encapsulation efficiency of peptides into liposomal vesicles is generally low and common methods used for encapsulating peptides not help to achieve better results (Shariat et al., 2014). In particular, the sizing process often limits the successful preparation of SUVs loaded vesicles, using both the extrusion method (a certain amount of peptide can be lost on filters) and the traditional sonication one (peptides can aggregates each other during sonication treatment) (Shariat et al., 2014). Thus, the development of the appropriate technique and the study of the main process parameters, to optimize both production stages and loading/stability of nanovectors, are of crucial importance.

The ultrasound assisted Lipid Film Hydration technique was used for the production of MLVs and SUVs encapsulating KRX29 peptide. Starting from MLVs formulation, liposomes dimension has been related to the energy supply in order to obtain SUVs with the desired size, useful for peptides intravenous administration. As in depth described in 4.1 section for modeling studies, during the formation of smaller liposomes the ultrasonic energy used breaks the lipid bilayer of large vesicles (MLVs) into smaller pieces, then these pieces close themselves in spherical structures producing SUVs. As showed in Table 18, after five total irradiation rounds (the first two in order to get LUVs, then the other three after one night of vesicles stabilization) SUVs with a diameter range of 20-35 nm were produced.

The developed technique has allowed to obtain high encapsulation efficiency values in MLVs and SUVs, demonstrating the efficiency of both lipid hydration and size reduction steps. In that regard, vesicles exposed to a total of five duty cycle sonication rounds maintain intact their content and no significant differences in the encapsulation efficiency were observed between MLVs and SUVs for all the investigated formulations (see Table 20). It is important to underline that no peptide degradation products were visible through HPLC analysis after samples sonication steps, supporting the efficacy and the safety of the technique developed.

5.3.6 Remarks

In this thesis, with the aim to increase the potential therapeutic of the KRX29 peptide, tailored nanoliposomes as suitable delivery vectors were designed and produced.

The used thin lipidic film hydration/sonication technique has proved to be reliable and versatile to produce liposomal structure with tailored size, starting from several lipidic/peptide formulations. Indeed the adopted process parameters (ultrasonic frequency and amplitude, sonication time and rounds) and the use of different L-α Phosphatidyl - DL glycerol sodium salt concentrations have allowed to obtain stable nanostructured vectors having the desired features in terms of size and charge.

The effect of liposomes charge on both peptide encapsulation and recovery efficiencies was then studied, through a dedicated analytical HPLC protocol, showing, as expected, an antithetical behavior. The higher encapsulation efficiency (about 100%) was achieved (both in SUVs and MLVs), using the higher charge ratio formulation (13:1 (-/+)). Viceversa the ability to recover the entrapped peptide was obtained for loaded systems (both SUVs and MLVs) at the lower charge ratio formulation (1:1 (-/+)).

As the charge ratio, also the peptide concentration shows influence on the liposomes encapsulation efficiency. Finally, it has been demonstrated that when the peptide concentration is doubled the encapsulation efficiency increases of about 20% with respect to the used starting concentration of 1 mg peptide/ml (57% vs 34%).

Part of this work has been reported in:
Bochicchio S.; Sala M.; Spensiero A.; Scala M.C.;. Gomez-Monterrey I.M.; Lamberti G.; Barba A.A.; "On the design of tailored liposomes for peptide delivery", submitted

5.4 Nanoliposomes vectors for dsDNA delivery

5.4.1 Generalities

Nucleic Acid Based Drugs (NABDs) constitute a class of promising and powerful therapeutic new agents with limited side effects, potentially useable against a wide range of diseases, including cancer. Among them, the short interfering RNAs (siRNAs), represent very effective molecules. Despite their in vitro efficacy, the major drawback that limits siRNAs usage consists in a difficult delivery due to their very low stability in physiological fluids, and to their limited membrane-permeability through physiological barriers (see 2.2.1). On the other hand, liposomes represent interesting drug delivery systems (DDSs) which can be tailored in order to get the best performance in terms of load, vesicle size and transfection yield (Bochicchio et al., 2014).

In particular, cationic liposomes represent an advanced technology to deliver NABDs in gene therapy (Bochicchio et al., 2016b, Chien et al., 2005, Piazza et al., 2016). Characterized by cationic phospholipids, they are able to carry molecules with negatively charges with the conseguent improvement of both encapsulation efficiency and cellular uptake. In this thesis, in order to produce carriers for NABDs delivery, the experimental activity started exploring cationic liposome formulations able to encapsulate 21 bases-double stranded DNA (dsDNA), simulating siRNA molecule structure. After this preliminary tests siRNA sequences were effectively encapsulated in the produced vectors (next 5.5 section).

The dsDNA simulating siRNA was used for an economic reason (due to the high cost of siRNA structures) since for this experimental section it was necessary to simulate only the structure and not the biological activity of siRNA molecule. In particular, three different kind of lipid bilayers were projected including N-[1-(2,3-Dioleoyloxy)propyl]-N,N,N-trimethylammonium chloride (DOTAP) in the formulations, a positively charged lipid used to improve nucleic acids encapsulation, enhancing the interaction with the negatively charged dsDNA. In order to achieve the higher dsDNA encapsulation efficiency in the smaller carrier possible, the charge ratio (3:1, 5:1 and 7:1 (+/-)) between the positive DOTAP and the negative charged dsDNA was varyied. The dsDNA-SUVs complexes were characterized in terms of morphology, size, surface charge (zeta potential), encapsulation efficiency and stability (release properties) in PBS solution (pH 7.4) at 37°C, simulating physiological condition.

5.4.2 Materials

L-α-Phosphatidylcholine (PC) from egg yolk (CAS n. 8002-43-5), Cholesterol (CHO) (CAS n. 57-88-5), N-[1-(2,3-Dioleoyloxy)propyl]-

N,N,N-trimethylammonium chloride (DOTAP) (CAS n. 132172-61-3), Rhodamine B (CAS n. 81-88-9), potassium phosphate monobasic (CAS n. 7778-77-0), sodium hydroxide (CAS n. 1310-73-2), Tris(hydroxymethyl)aminometane hydrochloride (Tris), Boric acid (CAS 10043-35-3), Ethylenediaminetetraacetic acid (EDTA) (CAS 6381-92-6), Tetramethylethylenediamine (TEMED) (CAS 110-18-9) Ethidium Bromide (EtBr) (CAS n. 1239-45-8) and 100 bp DNA ladder (Product n. D5042) were purchased from Sigma Aldrich (Milan, Italy) as dried powders and used without further purification. Acrylamide/bis-acrylamide, 40% solution and Ammonium persulfate (APS) (Cat. 161-0700) were purchased from Biorad Laboratories. All the other chemicals and reagents such as chloroform (CAS n. 67-66-3), ethanol (CAS n. 64-17-5), methanol (CAS n. 67-56-1)(Sigma Aldrich- Milan, Italy) used were of analytical grade. 21 bases sense oligonucleotide (5'-CGT-ACG-CGG-AAT-ACT-TCG-ATT-3') and antisense (5'-TCG-AAG-TAT-TCC-GCG-TAC-GTT-3') were purchased from Eurogentec.

5.4.3 Methodology and sperimental set-up

5.4.3.1 Phosphate buffer solution preparation

A phosphate buffer solution (PBS) was prepared by dissolving potassium phosphate monobasic 0.2 M and sodium hydroxide 0.2 M in distilled water thus obtaining a pH 7.4 PBS final solution. This buffer solution was used for carrying out liposome production and dsDNA load and stability tests.

5.4.3.2 Tris-buffered saline solution (TBS) preparation

Tris-buffered saline solution (TBS) was prepared dissolving Tris(hydroxymethyl)aminometane hydrochloride 50 mM and sodium chloride 100 mM in distilled water, obtaining a pH 7.5 TBS final solution used for the annealing of sense and antisense DNA sequences.

5.4.3.3 Duplex-DNA generation

A 21 base pair double-stranded DNA was prepared annealing 5'-CGT-ACG-CGG-AAT-ACT-TCG-ATT-3' sense strand with 5'-TCG-AAG-TAT-TCC-GCG-TAC-GTT-3' antisense strand.
Sense and antisense oligonucleotides, in lyophilized powder form, were resuspended in MilliQ water to a final concentration of 1000 μM for both oligonucleotides, and stored at -20 °C. 300 μl of each oligonucleotide was annealed in 150 μl of TBS buffer (pH 7.5) by heating at 95 °C; after 2 minutes, the heating block was switched off and allowed to slowly cool down to obtain dsDNA.

To evaluate DNA purity, absorbance measures at 280 nm and 260 nm were performed to detect the possible presence of proteic contaminants. The A_{260}/A_{280} absorbance ratio was calculated. Good-quality DNA must have a A_{260}/A_{280} ratio of 1.7–2.0.

5.4.3.4 dsDNA PolyAcrylamide Gel Electrophoresis (PAGE) analysis

After the duplex generation and prior to its encapsulation in liposomal structures, dsDNA integrity was demonstrated through native Polyacrylamide gel Electrophoresis.

The acrylamide/TBE gel was prepared by mixing 2 ml of Tris/Borate/EDTA buffer (TBE) 5 M, 3 ml of acrylamide stock solution at 40 %, 5 ml of distilled water, 70 µl of APS (150 mg/ml stock solution) and 10 µl of TEMED.

dsDNA (2 µg) and 100 bp DNA ladder were loaded into individual wells and subjected to electrophoresis on 12 % acrylamide gel (30 minutes at 80 V) in Tris/Borate/EDTA buffer (TBE) 1 M containing 90 mM Tris (pH 7.6), 90 mM boric acid and 2 mM EDTA. After staining with ethidium bromide (0.5 µg/ml), gels were viewed with UltraBright LED Transilluminator (Maestrogen, USA) at 470 nm.

5.4.3.5 Preparation of cationic SUVs containing dsDNA

dsDNA-SUVs first formulation

Small Unilamellar liposome Vesicles were prepared by means of the Thin Film Hydration method followed by sonication. Briefly, PC (40 mg), CHO (2 mg) and DOTAP (20 mg) at 10:1:5 (mol:mol) ratio were dissolved in 1 mL of chloroform/methanol 2:1 (vol/vol). The solvent was removed by evaporation in a rotary evaporator (Heidolph, Laborota 4002 Control) and the lipid film produced was vacuum-dried for 3 hours at 50°C in a water bath.

The dried lipid film was then hydrated at room temperature with 2 mL of PBS (pH 7.5), pre-warmed, containing dsDNA (2.8 mg) under adequate stirring. The ratio of dsDNA to the total amount of lipids was 1:20 (w/w) with a DOTAP/DNA charge ratio of 3:1 (+/-).

The sample was then sonicated at 45% amplitude (treated volume: 1 mL) by applying the duty cycle protocol previously described (4.1 section). The sample was stored overnight at 4°C and protected from light and was then sonicated at 45% amplitude (percentage of maximum deliverable power) for four more rounds in order to obtain SUVs.

DOTAP, positively charged, was included in the formulation to improve encapsulation enhancing the interaction with negatively charged dsDNA.

dsDNA-SUVs second formulation
Small unilamellar vesicles were prepared by the same Thin Film Hydration method followed by sonication described above but changing the formulation, in order to achieve an improved encapsulation efficiency. In this case PC (45 mg), CHO (2 mg) and DOTAP (15 mg) at 11:1:4 (mol:mol) ratio were used. The weight ratio of dsDNA (1.3 mg) to the total amount of lipids was 1:50 (w/w) and the charge ratio of DOTAP to dsDNA was 5:1 (+/-). All the process parameters and steps used were the same describe above for the first formulation.

dsDNA-SUVs third formulation
Small unilamellar liposome vesicles were prepared again by using PC (40 mg), CHO (2 mg) and DOTAP (20 mg) at 10:1:5 (mol:mol) ratio. The weight ratio of dsDNA (1.35 mg) to the total amount of lipids was 1:50 (w/w) and the charge ratio of DOTAP to dsDNA was 7:1 (+/-). All the process parameter and steps used were the same describe above for the first and second formulations.

5.4.3.6 Physicochemical characterization of vesicles

Bright field imaging and fluorescence imaging
The morphological and dimensional characterizations of MLVs were performed with optical microscopy (Axioplan 2- Image Zeiss) for bright field and fluorescence imaging. A 100 X oil immersion objective was used to visualize the vesicles taking advantage of the fluorochromes Rhodamine B, to label and visualize the vesicles, and 4',6-diamidino-2-phenylindole (DAPI) for label and visualize DNA sequences.

Particle sizes
A dimensional analysis of microscope images, performed with the software ImageJ was combined with a Dynamic Light Scattering analysis for MLV and SUV dimensional characterization. In particular, Dynamic Light Scattering analysis were performed by using the ZetasizerNano ZS (Malvern, UK) which incorporates noninvasive backscatter (NIBS) optics. The detection angle of 173 degrees was used. The resulting particle size distribution was plotted as the number of liposomes versus size. All the measurements were performed in triplicate. The results were expressed as average values.

Zeta Potential
In order to evaluate liposome carriers stability, their zeta potential was misured through Dynamic Light Scattering analysis, performed by using the ZetasizerNano ZS (Malvern, UK). As discussed for all the previously applications, the zeta potential is an important stability index of liposomes

which should be taken into account during liposomes bilayer formulation. Liposomes are stable when have $|\zeta| > 30$ mV.

5.4.3.7 Evaluation of dsDNA load and stability test

Determination of SUVs encapsulated dsDNA

For each sample, dsDNA load in SUVs was determined by UV spectrophotometric assay (λ=260 nm). Liposomes were centrifuged at 25000 rpm for 2 h at 4 °C (Beckman Coulter Avanti J-25I, Ramsey, Minnesota, USA). The pellet containing vesicles was lysed with ethanol, and dsDNA was precipitated and resuspended in PBS for spectrophotometric assay (λ=260 nm, PBS as blank) in order to determine the initial amount of dsDNA prior to release.

For all formulations, encapsulation efficiency (e.e.) was determined as the percentage of detected encapsulated dsDNA in liposomes to the initial amount of dsDNA included in the formulation; it was calculated using the following equation:

$$\text{e.e.} (\%) = \left(\frac{encapsulated\ dsDNA,\ mg}{initial\ dsDNA\ amount, mg} \right) \times 100 \qquad (5.9)$$

dsDNA loads were determined through the ratio:

$$\text{load} (\%) = \left(\frac{encapsulated\ dsDNA,\ mg}{total\ mass\ of\ loaded\ liposomes,\ mg} \right) \times 100 \quad (5.10)$$

In particular, the theoretical load is referred to the initial amount of dsDNA included in the formulation (divided by the total mass); the effective one is referred to the assayed dsDNA amount (divided by the total mass).

Stability test and evaluation dsDNA release

dsDNA release studies were performed in PBS solution (pH 7.5) at 37°C. Release profile has been evaluated during 10 days. Briefly, 125 μl aliquots of the sample were removed at given times and centrifuged to precipitate the liposomes. Liposomes (pellets) were lysated with ethanol and centrifuged again, after dsDNA precipitation ethanol was evaporated and the dsDNA was resuspended in PBS. dsDNA in supernatant and pellet was determined via UV spectrophotometric analysis (λ=260 nm, PBS as blank).

5.4.4 Results

5.4.4.1 dsDNA purity and integrity

The A260/A280 ratio found for dsDNA was higher than 1.8, index of no proteins contamination of the sample. Moreover, the PAGE analysis showed an intact dsDNA as visible in Figure 29, where the DNA band is perfectly visible without any traces of smear or other degradation signs.
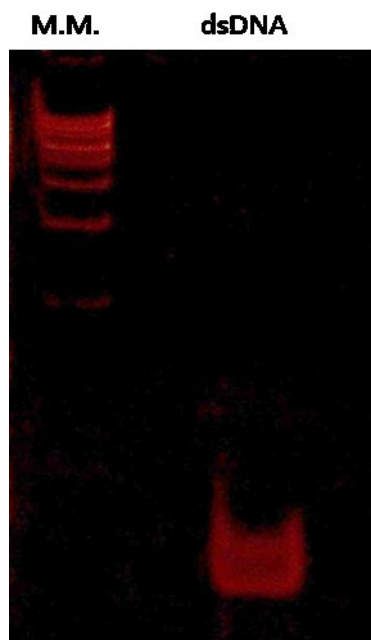
Figure 29. *Native PAGE of dsDNA. In the first lane a 100 bp ladder molecular weight, in the second lane 2 μg of 21 bp dsDNA molecule (simulating "Homo sapiens siRNA probe Luciferase", 12833.4 g/mol). The relative band is well visible*

5.4.4.2 Cationic liposomes: loading and characteristics of the tree formulations

Physicochemical characterization of vesicles
Bright field and fluorescence imaging were used in the present study to clarify the structure of cationic liposome formulations and the related dsDNA-liposomes complexes. As showed in Figure 30, spherical, separated and defined liposomes were achieved from each formulation.
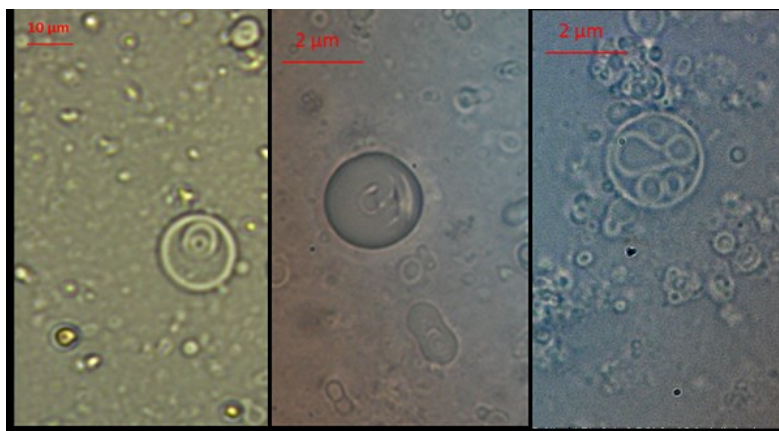
Figure 30 *Optical microscope pictures (in bright field, Obj. 63 X and 100 X) of dsDNA loaded Multilamellar Vesicles (MLVs), achieved respectively from the first, second and third formulation*

The fluorescence visualization by using the DAPI-Rhodamine B double labeling technique, for the simulataneuos visualization of dsDNA and nanoliposomes, has shown the successful formation of nanometric complexes (Figure 31) even if aggregates and/or large vesicles produced together with SUVs are visible in the captured images.
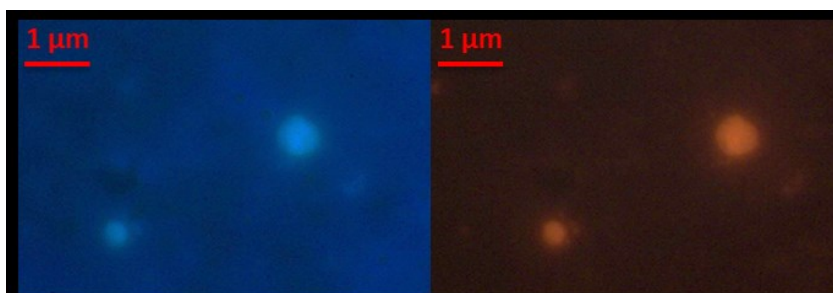
Figure 31. *Fluorescence microscope picture of dsDNA liposome vesicles (Obj 100X). DAPI-labeled dsDNA at left; Rhodamine B-labeled liposomes at right*

Particles size
For each formulation prepared, the dimensional analysis of microscope images prior to vesicle sonication has shown micrometric MLVs. In particular the diameter size was 2.9 ± 0.3 μm, 2.2 ± 3.2 μm and 2.3 ± 3.5 respectively for the fist, the second and the third formulation. A Dynamic Light Scattering analysis, carried out after six total sonication rounds, showed nanometric SUVs with diameter size of 0.056 ± 0.004 μm, 0.028 ± 0.005 μm and 0.029 ± 0.01 μm respectively for the 3:1, 5:1 and 7:1 (+/-) charge ratio formulation.

The obtained results for both MLVs and SUVs are summarized in Table 26.

Table 26. *Loaded Multilamellar Vesicles (MLVs) and Small Unilamellar Vesicles (SUVs) dimensional characterization at different DOTAP/dsDNA charge ratio; Results are expressed as average of three determinations; SD is the standard deviation*

dsDNA-liposomes samples	1st formuation	2nd formulation	3rd formulation
DOTAP/dsDNA charge ratio	3:1	5:1	7:1
MLVs size [μm] ± SD	2.9 ± 0.3	2.2 ± 3.2	2.3 ± 3.5
SUVs size [μm] ± SD	0.056 ± 0.004	0.028 ± 0.005	0.029 ± 0.01
SUVs PDI ± SD	0.30 ± 0.81	0.40 ± 0.02	0.30 ± 0.04

Zeta Potential
Dynamic Light Scattering analysis, performed by using the ZetasizerNano ZS (Malvern, UK), has shown a zeta potential of 52.8 ± 1.58 mV for the 3:1 charge ratio formulation, and a zeta potential of 68 ± 4.01 mV and 48 ± 1.7 mV respectively for the 5:1 and the 7:1 charge ratio formulations, demonstrating high particles stability in all the three cases. Results are summarized in Table 27.

Table 27. *Zeta potential and encapsulation efficiency of dsDNA-liposomes complexes formulated starting from different DOTAP/dsDNA charge ratio; Results are expressed as average of three determinations; SD is the standard deviation*

Complex samples	1st formuation	2nd formulation	3rd formulation	
DOTAP/dsDNA charge ratio	3:1	5:1	7:1	
Zeta Potential [mV] ± SD	52.8 ± 1.58	68 ± 4.01	48 ± 1.7	
Encapsulation efficieny(%)±SD	SUVs 54.0 ± 1.2	SUVs 61.5 ± 6.7	SUVs 64 ± 1.4	MLVs 100 ± 0

Determination of SUVs encapsulated ds-DNA
For all formulations high effective loads were obtained. The results of SUVs loads determination are reported in Table 28.

Table 28 *Theoretical and effective loads (%) in Small Unilamellar Vesicles (SUVs) at different DOTAP/dsDNA charge ratio; for the third formulation also Multilamellar Vesicles (MLVs) loads are reported. Results are expressed as average of three determinations; SD is the standard deviation*

dsDNA-liposomes formulations	DOTAP/dsDNA charge ratio (+/-)	Theoretical load (%)	Effective load achieved (%) and Standard Deviation (SD)
SUVs 1st	3:1	4.27	2.30 ± 0.04 %
SUVs 2nd	5:1	2.0	1.23 ± 0.01 %
SUVs 3rd	7:1	2.13	1.36 ± 0.03 %
MLVs 3rd	7:1	2.13	2.13 ± 0.00 %

The encapsulation efficiency achieved for SUVs was 54.0 ± 1.2 % for the first formulation, 61.5 ± 6.7 % for the second formulation and 64 ± 1.4 % for the last formulation. The MLVs produced using the third formulation showed an encapsulation efficiency of 100 %. The results of SUVs encapsulation efficiency (and MLVs for the last formulation) are summarized in Table 27.

Stability test and evaluation ds-DNA release
Liposomes loaded with dsDNA underwent a stability test to evaluate their loading efficiency and the timing of drug release, in conditions similar to the intracellular environment. As shown in Figure 32, liposomes were found to be stable at 37°C in PBS (pH 7.4) media release for a ten days period.
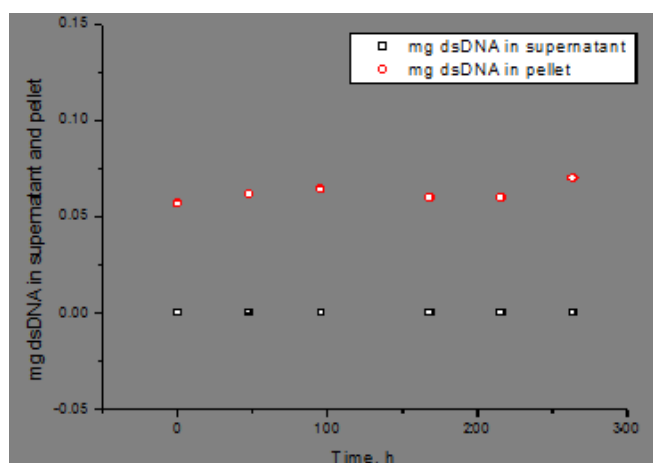
Figure 32. *dsDNA retention in Small Unilamellar Vesicles (SUVs) and release in PBS: circles symbols are referred to dsDNA retained in the pellet; squares symbols are referred to dsDNA lost in phosphate buffer solution*

5.4.5 Discussion

5.4.5.1 Ultrasound assited technique in dsDNA-liposomes production

The ultrasound assited technique used was indicated to encapsulate dsDNA, a molecule characterized by high degradability. In particular, according to the modelling study (see 4.1 section), through the dedicated duty cycles protocol, nano-liposomal vesicles were achieved in the expected diameter range and with a polydispersity index less than 0.4 (see Table 26). Staring from MLVs with 2.9 - 2.2 μm range size, after six total sonication rounds, SUVs with 56 - 28 nm range size were achieved. The advantages in using the ultrasound assisted technique were well described in the previous sections of chapter 5 for stable, highly loaded vitamins, ferrous sulfate and peptide liposomes preparation.

Moreover, ever referring to the technique used, the effect of duty cycle sonication on the encapsulation efficiency and DNA loads is visible in the last formulation, comparing the results obtained for MLVs with those obtained for SUVs.

For the 7:1 (+/-) formulation the theoretical load, expressed in percent value, was of 2.13 % for both micro and nanoliposomes (SUVs sample is produced from MLVs sample) and the effective loads achieved were 2.13 % and 1.36 % respectively for MLVs and SUVs.

Encapsulation efficiency was 100 % for MLVs and 64 % for SUVs. The different levels of DNA incorporation efficiency between MLVs and SUVs can be explained as an effect of the sonication process on the vesicles. The ultrasound assisted technique, inducing a cyclic opening and closing of liposomal bilayer, involves DNA losses in the sonication bulk.

Results are in accordance with what already observed for MLVs loaded with vitamins and subjected to sonication, in particular the effect of sonication on DNA loss is similar to what seen for vitamin B12 (being highly soluble molecule and encapsulated in the aqueous core of liposomes such DNA).

5.4.5.2 Including DOTAP in liposomes formulation

Projecting the liposomes bilayer, taking into account the molecule nature to be encapsulated, has a great relevance in the final features of drug-carrier complexes. In particular, drug encapsulation efficiency (thus its effective load) and the zeta potential values of the carrier systems change in a manner that depends on the initial formulation ingredients. In particular, the advantages in inserting cationic lipids into liposomes bilayer, to be used as delivery systems for NABDs, allows both an optimization of the cellular uptake and a nucleic acids encapsulation efficiency. The cellular uptake of liposomal carriers is facilitated for cationic liposomes due to the interaction between their positive charge with the negative once of the cell membrane.

This successful interaction in the presence of DOTAP was demonstrated for in vivo and/or ex vivo experiments including many type of cell, such as monocytic leukemia cells and different cancer cell line (Pires et al., 1999, Campbell et al., 2001, Porteous et al., 1997, Lu et al., 2012). Moreover, being DNA and RNA negative charged molecules which can be neutralized by cationic lipids, positively charged liposomes are particularly valid nucleic acids carriers, ensuring their controlled drug-delivery and improving their internalization and expression (Ying, 2010, Li et al., 2011).

In many works, it was demonstrated that DOTAP safety is tightly linked to its amount used in the formulation (Lu et al., 2012, Brgles et al., 2012). In a Phase I Clinical Trial of systemically administered TUSC2(FUS1) nanoparticles in humans, the toxicity of DOTAP was studied. Patients with recurrent and/or metastatic lung cancer, previously treated with platinum based chemotherapy, were treated with escalating doses of intravenous DOTAP:cholesterol nanoparticles encapsulating a TUSC2 expression plasmid (*DOTAP:cholTUSC2*) every 3 weeks. The MTD was determined to be 0.06 mg/kg. In particular, nanoparticles stock solution was prepared starting with a concentration of 20 mM DOTAP, the diluted plasmid DNA and the diluted nanoparticle stock were mixed in equal volumes to a final concentration of 4 mM DOTAP and 0.5 mg/ml of DNA. Prior to the treatment the assigned dose was diluted in 100 ml of 5% (w/v) dextrose water.

Lu and collaborators have concluded that DOTAP:chol*TUSC2* can be safely administered intravenously in lung cancer patients resulting in a successful gene uptake by human primary and metastatic tumors (Lu et al., 2012).

In this thesis the DOTAP concentration was maintained in a safety range (the maximum DOTAP concentration used in the stock solution was 14 mM, which can be diluted to a final concentration of 4 mM containing 0.225 mg/ml of DNA for in vivo experiment). Moreover, considering that the knowledge of the right DOTAP/DNA ratio is of crucial importance to achieve a safety and smart final lipoplex, the effect in changing the amount of DOTAP on liposomes final features was studied.

5.4.5.3 Effect in changing DOTAP/DNA charge ratio on liposomes final features

Effect on liposomes shape, size and zeta potential

Liposomes shape, diameter and size dispersity are important parameters in drug delivery applications.

First of all, it was demonstrated that changing the amount of DOTAP respect to the total mass of DNA not affects the dsDNA-nanoliposomes shape which ever mantain its spherical and defined conformation. Is interesting to note that increasing the (+/-) charge ratio, liposomes size decreases and it is visible in both MLVs and SUVs preparations, especially switching from the first to the second formulation. Increasing the charge ratio from 3:1 to 5:1

(+/-), MLVs diameter size changes from 2.9 µm to 2.2 µm while remains mostly constant (2.3 µm) in the last (7:1 charge ratio) formulation (see Table 26). The same effect was observed for SUVs samples presenting a diameter size of 56 nm when 3:1 (+/-) charge ratio formulation is used and a reduced diameter size of 28 nm for 5:1 (+/-) charge ratio formulation. Also in this case the size (29 nm) doesn't change in a relevant manner when 7:1 (+/-) charge ratio is used.

Results are in accordance with a work of Marija Brgles and collaborators (Brgles et al., 2012) who have analized the trend in liposome size respect to DOTAP/DNA (+/-) charge ratio demonstrating that an increase in the charge ratio results in a decrease in liposome/DNA complex size. Moreover, they have demonstrated how liposomes size and charge of liposome/DNA complexes are considered key features for the transfection efficiency of formulation.

In a work of Campbell and collaborators, QLS (Quasi-elastic Light Scattering) was used to determine the effect of DOTAP on the size distribution of liposomes as a function of phospholipid acyl chain length, degree of unsaturation, and concentration of DOTAP. They observed that DOTAP reduces the mean diameter of PC-containing multilamellar liposomes, in particular regardless of the phospholipid chain length and degree of unsaturation (Campbell et al., 2001).

Again, Xiu and collaborators have demonstrated that at cationic lipid/DNA charge ratios between 1:1 and 2:1, the complexes have the largest diameter. Higher or lower charge ratios result in lipoplexes with smaller diameters (Xu et al., 1999).

The chemico-physical interactions and the DOTAP-induced alterations occurring during the changes in liposomes bilayer fluidity and size are the subjects of many studies. The reduction in size can be explained by the DOTAP ability in facilitating head group electrostatic interactions which decrease the bilayer radius of curvature as a result of phospholipid-cationic head group contact (Campbell et al., 2001). In particular, in their work, Zuidam and collaborators have suggested that the quaternary amine of DOTAP and the phosphate group of the phospholipid DOPC may form a salt bridge decreasing the bilayer radius of curvature (Zuidam and Barenholz, 1997).

Regarding the external surface charge of nanoparticles, the zeta potential (ζ) is an important stability index of liposomes which should take into account during their bilayer formulation. As discussed for all the other applications, liposomes are stable when have $|\zeta| > 30$ mV.

Here, for all the three formulations tested, an high zeta potential was achieved, index of stable particles production. In particular, for the last formulation, due to the increased dsDNA loads (and their negative charges), the zeta potential was slightly reduced with respect to the other formulations,

ever mantaining a large excess of positive charge in the final vesicles (see Table 27).

This reduction in external positive charge together with an increasing in DNA encapsulation efficiency is an interesting result if we consider that NABDs have to reach the cell nucleus dissociating from liposomes and overcoming the endosomes barriers. Indeed, for a successful transfection, a reduction in surface charge may be beneficial to allow appropriate DNA dissociation from the lipoplex after cellular uptake and for the endosomal escape thus allowing the NABDs to exert their biological function.

Effect on liposomes encapsulation efficiency and loads

It is important to note as increasing the DOTAP/dsDNA (+/-) charge ratio, the encapsulation efficiency also increases due to the presence of a greater amount of positive charges attracting the DNA negative once more strongly. Being the lipid film formulated with an increasing amount of DOTAP lipids, infact, more amine positive groups will interact with the negative phosphate groups by which the double stranded DNA (or siRNA) is composed. In the last formulation, increasing the DOTAP/DNA charge ratio (the 7:1 (+/-) sample), an encapsulation efficiency of 100% in MLVs and of 64% in SUVs has been obtained; this values of e.e. was higher than those obtained from the previous investigated formulations (Table 27).

Considering the effective loads achieved (Table 28) and comparing this results with the theoretical loads obtained for each sample, it can be observed that the last formulation presents also the highest load. For the 7:1 (+/-) charge ratio, the loads were 1.36 % for SUVs and 2.13 % for MLVs, considering a theoretical load of 2.13 %.

Furthermore, for all the three formulations, SUVs were found to be stable at 37 °C in PBS media release for a ten days period; load and structure are remained unaltered after this period.

5.4.6 Remarks

The performed activities have confirmed the versatility of the ultrasound assisted technique developed for producing lipid vectors encapsulating NABDs. The charge ratio (+/-) variation from 3:1 to 7:1 (+/-) by changing the amount of positive lipid (DOTAP) used during liposome preparation have allowed to an improved e.e. by passing from the first to the second up to the third formulation. Moreover, the stability test has shown that the produced vesicles can keep intact DNA molecules for more than 10 days if incubated in intracellular environment similar conditions (PBS solution at 37 °C). The study demonstrated the successful preparation of a stable, highly loaded SUVs formulations containing dsDNA simulating siRNA, to yield the basis for an improved nucleic acid based drugs shelf life for gene therapies. Studies of dsDNA entrapment within liposomes have indeed given

the bases for siRNA encapsulation and transfection in cell/tissues, subsequently carried out and described in the next section.

Part of this work has been reported in:
Bochicchio S.; Dalmoro A.; Barba A.A.; D'Amore M.; Lamberti G.; "New preparative approaches of micro and nano drug delivery carriers"; *Current Drug Delivery*, 2017, 14 (2), 203-215.

5.5 Nanoliposomes vectors for siRNAs delivery

Part of this research activity has been performed at Cattinara hospital, in Trieste, for the in vitro experimantation on cell lines and at San Giovanni di Dio e Ruggi D'Aragona hospital, in Salerno, for the ex-vivo testing on colon mucosa tissues.

5.5.1 Generalities

The recent discovery of RNA interference (RNAi) mechanism, and its effector molecule, the short interfering RNA (siRNA), has led to an increased interest in the development of innovative therapies, able to target disease components, at genetic level, that are considered 'undruggable' with the conventional medicines.

RNA interference (RNAi) is a natural mechanism to silence gene expression post-transcriptionally (Figure 33). It is based on a sequence-specific RNA degradation, as described for the first time by Fire and co-workers in 1998 (Fire et al., 1998), who found out that in the nematode Caenorhabditis elegans there were dsRNA molecules able to silence gene expression (Andrew Z. Fire and Craig C. Mello won the 2006 Nobel Prize in Physiology or Medicine, for their discovery of RNA interference, -RNAi-gene silencing by dsRNA).
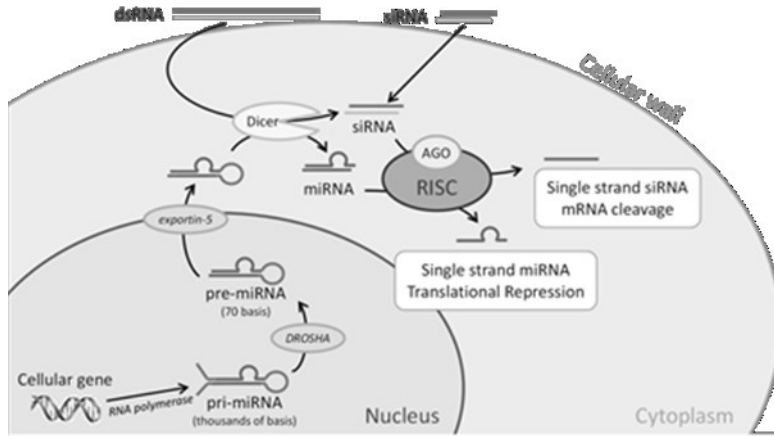
Figure 33. *RNA interference mechanism. Double-stranded RNAs (dsRNAs) are processed by a complex consisting of Dicer and other protein activators and kinase into small interfering RNAs (siRNAs), which are loaded into Argonaute 2 (AGO2) and RNA-induced Silencing Complex (RISC). siRNAs are denatured and become single-strand molecules. The RISC is then active and, using the incorporated single-strand siRNA as template, recognizes the target mRNA to degrade (mRNA cleavage). RISC analyzes mRNAs and identifies as targets only the one with sequences perfect complementary to the 21-22 nucleotides of the siRNA, thus silencing their expression*

However, while searches over new siRNA sequences, more and more specific for the target mRNAs, go on, the scientific community is busily focused on the development of suitable drug delivery systems (DDSs) able to vehicle this powerful molecules, otherwise not useable in their naked form. Due to their low stability in physiological fluids, low membrane-permeability and their short half-life in the circulatory system, Nucleic Acid Based Drugs (NABDs) require to be encapsulated in suitable carriers (see 2.2.1 paragraph). In general, the versatility and the easiness of carriers modification in terms of size, charge, lipid composition and linkage with cell-targeting molecules, are all factors affecting the successful siRNA delivery into the target cells/tissue (Bochicchio et al., 2014, Barba et al., 2015). Because of their ability in meeting all of these features, liposomes seem to be the ideal candidates for siRNAs incorporation, solving their delivery issues. Liposomes on nanometric scale, known as Small Unilamellar Vesicles (SUVs), are particularly desired; indeed it was demonstrated that, due to the Enhanced Permeability and Retention (EPR) effect (Bregoli et al., 2016), liposomes with small dimensions can permeate through membrane fenestrations of diseased blood vessels penetrating into the tumor tissue (Kibria et al., 2016). Moreover, a positively charged vesicles are preferable to enhance the interaction with both the negatively charged siRNA, improving its encapsulation efficiency, and the cell plasmatic membrane, also negatively charged, improving siRNA incorporation in the target cells (Ibraheem et al., 2014, Kim et al., 2010).

For all the above stated reasons, in the last few years, liposomes encapsulating siRNAs have been increasingly investigated for their key role in the development of new potential strategies for the treatment of different type of cancer, obesity, diabetes, neurological disorders, inflammations and other disabling diseases (Guo et al., 2016, Golkar et al., 2016, Wei et al., 2016, Ryther et al., 2005, Dunckley et al., 2005, Kigasawa et al., 2010, Ran et al., 2014). Among these latter, Inflammatory Bowel Diseases (IBDs), including different pathological states such as Crohn's Disease (CD) and Colitis Ulcerosa (UC), are auto-immune disorders whose origin is unknown and whose incidence is increasing in almost every region in the world, affecting 2.5-3 million Europeans, with a direct healthcare cost of 4.6-5.6 bn Euros/year (Burisch et al., 2013, Kaistha and Levine, 2014). The important cost for society are related with an high rate of sick leave, permanent work disability and unemployment due to the high risk of colorectal cancer, several times increased if compared to the healthy control population (Nikolaus and Schreiber, 2007, Burisch and Munkholm, 2015, Farraye et al., 2010). The great risk in developing cancer in patients with UC and CD has led to search more about the genetic changes that occur as IBD progresses from benign mucosa to dysplasia, up to invasive colorectal cancer (Kanaan et al., 2012). The promoter factor that initiates cancer pathways is unknown and different are the molecules investigated, especially those involved in the

pRb-E2F1 pathway (Ying et al., 2007). In particular, E2F1 is a transcription factor that has a key role in the promotion of the cell cycle, its high level in the late G1 phase of the cell growth cycle results in the expression of numerous factors for DNA synthesis, and thus the progression towards the following S phase (Ertosun et al., 2016). Being an important regulator of the growth and the cells proliferation, E2F1 gene overexpression is related to neoplastic development in several cancerous cell lines, including gastric and colorectal carcinomas (Mega et al., 2005). It was demonstrated that E2F1 promotes the aggressiveness of human colorectal cancer by activating the ribonucleotide reductase small subunit M2 whose high expression induces cancer and contributes to tumor growth and invasion (Fang et al., 2015).

Due to the observed correlation, in this work the inhibition of E2F1 expression was studied as a potential way to treat cancer associated to IBD diseases. With the aim to investigate the possibility in reducing E2F1 expression levels, two kinds of siRNA sequences direct against E2F1 (si-E2F1-1117 and siE2F1-1324), at different concentrations, were encapsulated in cationic nanoliposomes suitably designed and produced by the technique based on lipid Thin Film Hydration/sonication process developed in this thesis. The loaded nanoliposomes were then transfected in suitable human cell line and in intestinal human biopsy fragments (collected from healthy and IBD donors during lower endoscopy performed for colonic cancer screening) to investigate in vitro and ex vivo silencing activity. In particular, in order to evaluate the effective efficacy of carriers in siRNA delivery, nanoliposomes uptake studies and siRNA-nanoliposomes transfections were accomplished in both HT29 human colon adenocarcinoma cell line, where conditions are more reproducible, and in cultured human biopsies, in which the cell–cell interactions, thus the human intestinal mucosa cytoarchitecture, are preserved unlike isolated cell cultures.

5.5.2 Materials and methods

5.5.2.1 Unloaded and siRNA loaded vesicles preparation

Nanoliposomes design

Nanoliposomes loaded with two different siRNA sequences for E2F1 expression inhibition were designed and produced. At first the liposomes bilayer was designed in order to achieve a positive charged complex able to cross the negative plasma membrane thus to enter in the cells. In that regard the cationic DOTAP phospholipid, which is also able to electrostatically interact with the negative siRNA molecules, was chosen as well to promote siRNA encapsulation inside the lipid vesicles. The charge ratio between DOTAP and siRNA sequences used was 8.5:1 (+/-) and was calculated counting 1 positive charge for each DOTAP molecule and 42 negative

charges for each 21 bp siRNA molecule. This ratio was chosen on the basis of previous work in which the effect of different DOTAP/dsDNA charge ratios on dsDNA encapsulation efficiency was studied (see the previous section) (Bochicchio et al., 2016b). The ratio was selected in order to obtain the highest siRNA encapsulation efficiency simultaneously getting an excess of positive charge on the final siRNA-SUV complex for a better cellular uptake.

Nanoliposomes production

For unloaded and siRNA-loaded vesicles production, Cholesterol (CAS 57-88-5), L-α-phosphatidylcholine (PC) from egg yolk (CAS 8002-43-5) and dioleoyloxypropyl-N,N,N-trimethylammoniumpropane (DOTAP) (CAS 132172-63-1, >99 % pure) were purchased from Sigma-Aldrich (Milan, Italy). The experimental siRNA sequences direct against E2F1, siE2F1-1117 (sense sequence 5'-GAGGAGUUCAUCAGCCUUUdTdT-3') and siE2F1-1324 (5'-GCCACCAUAGUGUCACCACdTdT-3' sense sequence) were selected according to previously reported guidelines from Poliseno and collaborators (Dapas et al., 2009, Poliseno et al., 2004) and were chemically synthesized, together with luciferase mRNA GL2 siRNA control, by Eurofins Genomics (Ebersberg, Germany). The GAPDH siRNA positive control (Cat. 4457288) and the negative control siRNA (Cat. 4457287) sequences were obtained from Ambion®, Thermo Fisher (Waltham, MA, USA). Nuclease free water (CAS 129114) was purchased from Qiagen (Hilden, Germany), chloroform (CAS 67-66-3), methanol (CAS 67-56-1) and all the other reagents were of analytical grade and were purchased from Sigma-Aldrich (Milan, Italy).

siE2F1-SUVs complexes were produced using the Thin Film Hydration method followed by duty cycle sonication through the ultrasound based size reduction method developed in this thesis and previously described (4.1 section). Briefly PC, DOTAP and CHOL at 3:0.3:1 (mol:mol) ratio were dissolved in 1 mL of chloroform/methanol at 2:1 (vol/vol). The solvent was removed by evaporation in a rotary evaporator (Heidolph, Laborota 4002 Control) and the produced lipid film was vacuum-dried for 3 hours at 50 °C in a water bath, rotating at 30 rpm. The dried lipid film was then hydrated at room temperature with 500 μl of phosphate buffer solution (PBS; potassium phosphate monobasic 0.2 M, sodium hydroxide 0.2 M - pH 7.4) containing siE2F1-1324 at 8 μM. The sample was mixed for 30 minutes by the rotary evaporator (60 rpm; room temperature). The process was repeated in an identical manner for siE2F1-1117, siRNA positive controls (GADPH and GL2 inhibitors) and siRNA negative control (scramble siRNA) encapsulation. Finally, the above described steps were followed for unloaded liposomes production with the only difference in the hydration solution which was pure PBS not containing siRNA sequences.

At the end of the process a total of six samples containing Multilamellar Vesicles (MLVs) were achieved, maintained at room temperature for 2 hours, and then diluted to a final volume of 1 mL by adding 500 µl of PBS pH 7.4 thus obtaining a siRNA concentration of 4 µM for the loaded samples with a 1:260 (w/w) siRNA/total lipids ratio.

In order to get liposomes of nanometric size, samples were sonicated at 45% amplitude (treated volume: 1 mL) applying a duty cycle consisting of 2 irradiation rounds of 10 seconds, each followed by 20 seconds of pause to prevent thermal vesicle disruption, obtaining Large Unilamellar Vesicles (LUVs). The samples were stored at 4 °C for one night, protected from light, and were then sonicated at 45% amplitude for four more rounds in order to achieve SUVs. The VCX 130 PB Ultrasonic Processors of Sonics & Materials Inc. USA instrument was used (maximum power 130 W, frequency 20 kHz; sonotrode tip length 137 mm; sonotrode tip diameter 3 mm) as for all the other applications (5.1; 5.2; 5.3; 5.4 sections).

5.5.2.2 Unloaded and siRNA loaded vesicles characterization

Morphology

The morphological characterizations of unloaded and siRNA loaded liposomes were performed with optical microscope in fluorescence field (Axioplan 2- Image Zeiss, Jena, Germany) equipped with a software to capture the images. The Rhodamine B dye (CAS 83-68-9-Sigma-Aldrich, Milan, Italy) was used to visualize lipid vesicles. DAPI dye (4'6-diamidino-2-phenylindole-Thermo Fisher Scientific, Waltham, MA, USA) was used to visualize siRNA molecules in the liposomes aqueous core. A 100 X oil immersion objective was used.

Size and zeta potential

A dimensional analysis of MLVs microscope images, performed with the software *ImageJ,* was combined with a Dynamic Light Scattering analysis for unloaded LUV, SUV and siRNA-SUV characterization. Size and zeta potential determinations were performed by using the ZetasizerNano ZS (Malvern, UK) with noninvasive backscatter (NIBS) optics. The detection angle of 173 degrees was used. The resulting particle size distribution was plotted as the number of liposomes versus size. All the measurements were performed in triplicate. The results were expressed as average values.

Encapsulation efficiency (EE) by spectrophotometric and electrophoretic assay

After removing an aliquot for the Electrophoretic assay in order to measure the unencapsulated siRNA, siE2F1-1117-SUVs and siE2F1-1324-SUVs samples were centrifuged overnight at 30000 rpm (Beckman Optima L-90K

Ultacentrifuge, SW 55 Ti rotor). The released siRNA was examined by submitting the recovered supernatants of the two samples to an UV spectrophotometric assay performed using Lambda 25 UV/VIS Spectrophotometer. An absorption spectrum from 200 nm to 300 nm was investigated for both the samples and the maximal wavelength for RNA molecules, 260 nm, was considered. The encapsulation efficiency (EE) was determined as the percentage of siRNA encapsulated in liposomes to the initial amount of siRNA included in the formulation and was calculated using the equation:

$$\text{EE (\%)} = \left(\frac{encapsulated\ siRNA,\ \mu g}{initial\ siRNA\ amount,\ \mu g} \right) \times 100 \qquad (5.11)$$

where the amount of siRNA encapsulated in liposome was calculated subtracting the amount of siRNA presents in the supernatant of the centrifuged sample from the total amount of siRNA included in the formulation.

An electrophoretic assay on 1.5 % agarose (Cat. A7002, ≥99 % pure, Sigma-Aldrich) gel was performed to evaluate the eventual not encapsulated amount of siRNA invisible at the spectrophotometric assay. For the agar gel a Tris/Borate/EDTA buffer (TBE - 0.5 X) was used and 25 µl of ethidium bromide (0.5 mg/ml) were added to the solution to visualize siRNA in the UV-spectrum. The gel was loaded with a 123 bp molecular marker (M.M., Cat. D5042, Sigma-Aldrich), and with both siE2F1-1117-SUV and siE2F1-1324-SUV complexes. The naked forms of siE2F1-1117 and siRNA-1324 were also loaded and used as control samples. Sample volumes equivalent to 1 µg of siRNA were disposed in each well. The electrophoresis run was performed for 30 minutes at 80 V, using the same 0.5 X TBE solution as previously done for the gel preparation. The result of the electrophoresis was detected with UltraBright LED Transilluminator (Maestrogen).

5.5.2.3 Cell culture condition

The human colorectal adenocarcinoma cell lines HT29 and LoVo-109 were cultured in low glucose Dulbecco's modified Eagle's medium (DMEM) and RPMI medium respectively. Both medium were supplemented with 10% fetal bovine serum (FBS), 2 mM L-glutamine, 100 U/ml penicillin and 100 µg/ml streptomycin (Euroclone, Milan, Italy).

5.5.2.4 Colon tissue culture condition

Biopsies of human colon, isolated from six different donors, were collected during a lower endoscopy. For tissue culture, fragments, with the epithelium facing upward, were placed on a stainless-steel mesh positioned over the central well of an organ-culture dish containing Dulbecco's modified eagle's medium (F-12 HAM), HEPES, NaHCO3, pyridoxine and L-glutamine (Sigma-Aldrich). The dish was placed in a modular incubator chamber,

gassed with 5% CO2 and 95% O2, and then incubated at 37°C for 24 h (Piazza et al., 2016). By using this setting, one tissue biopsy was incubated with unloaded Rhodamine B-SUVs, to test their cellular uptake, and the other five were transfected with siRNA-SUVs complexes, to test their ability in E2F1 silencing. All clinical investigations have been conducted according to the declaration of Helsinki principles. Patient's consent for participation in this study was registered. Local Ethical committee approved the study protocol.

5.5.2.5 Uptake study in tissue biopsies

To test liposomes uptake in colon tissues, biopsy fragments of a female patient were incubated with unloaded liposomes labelled with Rhodamine B. For this purpose, unloaded Rhodamine B-labelled SUVs were prepared. Briefly, a 500 µl aliquot of unloaded SUVs sample was taken and marked with 1.5 µL of 5 mg/mL Rhodamine B-solution. After 2 h of incubation at room temperature, the excess of Rhodamine B was removed by centrifugation for 1.5 h at 9000 rpm (Beckman Coulter Avanti J-25I Centrifuge, JA2550 rotor). The sample was washed two times with PBS and re-centrifuged, then the supernatant, carefully removed, was put away and the pellet resuspended in 500 µl of PBS and 60 µl aliquots were used to overly cultured biopsies in the presence of culture medium. After 24 hours of incubation at 37 °C the culture medium was removed and the tissue fragments were frozen. The frozen tissue fragments were put in Cryostat Embedding Medium (05-9801 Killik Bio-Optica- Milan, Italy), in order to achieve tissue sections through the use of a cryostat (Leica CM1950, Wetzlar, Germany). DAPI (1:1000 diluited) was added to the sections, to visualize the cell nuclei composing the colon tissues. The sections were studied under a fluorescence microscope with a 20 X objective.

5.5.2.6 siRNA-SUVs transfection in cells

The sequences of the siRNAs directed against the transcription factor E2F1 mRNA (siE2F1 1324, siE2F1 1117) and the luciferase mRNA (siGL2, control) have been previously described (Dapas et al., 2009) and reported in 5.5.2.1 paragraph together with siRNAs-SUVs complexes preparation.
To study the effects of siRNA-SUVs on cell number and on E2F1 mRNA, 8×10^4 HT29 cells were seeded in 12 well-plates in the presence of 1 ml of 10% fetal calf serum-containing medium. The day after seeding, cell transfection was conducted in 400 µl of serum-free medium by using 1.3 µg of the siRNA-SUVs complexes or 1.3 µg of siRNA mixed with Lipofectamine®2000 (1 mg/ml) (Invitrogen, Carlsbad, CA, USA) at a weight ratio siRNA-transfectant of 1:1 (w/w). siRNA concentration corresponded to 220 nmol/L. After 3 hours at 37°C, transfection medium was removed, cells were washed with PBS and then 1 ml of complete

medium was added to the cells. The effect of the siRNA-SUVs were evaluated three days after transfection. To evaluate the effects of siRNA-SUVs on E2F1 mRNA levels, total RNA was extracted from cells, quantified and then quality evaluated as described (Baiz et al., 2009). Reverse transcription was performed using 500 ng of total RNA in the presence of random hexamers and MuLv reverse transcriptase (Applied Biosystem, Foster City, CA, USA). Real time PCR was performed with the 7900/HT Detection System (Applied Biosystems) and all amplification reactions were conducted in triplicate, utilizing SYBER Green Master mix solution (Applied Biosystems). The primers and the real-time amplification conditions were previously described (Farra et al., 2011). The relative amounts of each target mRNA were normalized by 28S rRNA content according to Pfaffl (Pfaffl, 2004).

To study the effects of siRNA-SUVs on cell viability, 5×10^3 HT29 cells or LoVo-109 were seeded in 96 microplate in 200 μl of complete medium/well. Three days after transfection of 220 nM siRNA-SUVs and siRNA-Lipofectamine®2000 complexes, 3-(4,5-dimethylthiazol-2-yl)-2,5-diphenyl-tetrazolium bromide (MTT, Sigma-Aldrich, St Louis, MO, USA) test was conducted according to standard procedure (Farra et al., 2011).

5.5.2.7 siRNA-SUVs transfection in colon tissue

Tissue cultures from 5 donor were transfected with three different siRNA concentrations: 50 nM, 100 nM and 200 nM. At first the intermediate 100 nM concentration was used. Afterwards, the concentration was doubled and halved.

Transfection of 100 nM siRNA-SUV complexes in donor 1

The biopsy was obtained during the colonoscopy of a 27 years old male donor, suffering from Irritable Bowel Syndrome. The tissue fragments were prepared as described for colon tissue culture (5.5.2.4 paragraph) and were transfected with the siE2F1-SUVs complexes. Furthermore, in order to study the eventual E2F1 expression changes in presence of inflammation, siRNA-liposome complexes were transfected with and without the presence of lipopolysaccharides from Escherichia Coli (EC-LPS), used as inflammatory agent. In total, 8 fragments were incubated and the experiment was set as follow: one fragment was treated only with a culture medium (basal sample) and another one with the culture medium containing 2 μl of EC-LPS. The other 6 fragments were transfected respectively with siE2F1-1117-SUVs cultured in a pure medium; siE2F1-1117-SUV cultured in a medium containing EC-LPS; siE2F1-1324-SUV cultured in a pure medium; siE2F1-1324-SUV cultured in medium containing EC-LPS; siRNA positive control-SUV; siRNA negative control-SUV. The latter two were both cultured in a medium without EC-LPS. In order to obtain a concentration of 100 nM

siRNA in the culture medium, a volume of 30 µl was transfected for all the samples. The plates were incubated at 37°C. After 24 hours, the transfection was stopped, the culture medium was removed, the tissues were recovered and the E2F1 expression was examined by Western blot technique.

Transfection of 200 nM siRNA-SUV complex in donors 2 and 3

Donor 2, a 54 years old female, had a colorectal cancer screening that it was found to be in the standards and donor 3 was a 36 years old male, suffering from Morbus Crohn. In total 4 fragments of colon tissue for each donors were treated and, for both, the transfection was set as follows: one fragment was treated only with a culture medium (basal sample) and the other three fragments were transfected respectively with siE2F1-1324-SUVs, siRNA positive control-SUVs and siRNA negative control-SUVs complexes. The volume of siRNA-SUVs samples transfected was 60 µL for all the plates, thus obtaining a final siRNA concentration of 200 nM. Transfections were executed in the same conditions above described.

In the sight of the results obtained from donor 1, siE2F1-1117-SUVs complexes together with the EC-LPS treatments were excluded from this and from the subsequent experiments. siE2F1-1117-SUVs and EC-LPS treatments seemed to have no influence on the expression of E2F1 (see 5.5.3.4 results section) and thus were not further studied.

Transfection of 200 nM and 50 nM siRNA-SUV complex in donors 4 and 5

Patient 4, a 24 years old male, was a donor suffering from Ulcerative Colitis and patient 5, a 27 years old male, was a donor suffering from ileal Morbus Crohn. In this case, in order to find a correlation between siRNA concentration transfected in tissue and E2F1 expression inhibition, fragments of the same patient were treated with two different concentrations: 200 nM and 50 nM. In total, for both donors, 7 fragments of colon tissue were cultured. One fragment was the basal sample (treated only with culture medium) and the other 6 fragments were treated as described for patients 2 and 3 but using the two siRNA concentrations.

5.5.2.8 Evaluation of E2F1 protein expression after transfection in tissue: Western blot

Total proteins were isolated by colon specimen lysis in a buffer composed of 50 mmol/L Tris-HCl (pH 8.0), 150 mmol/L NaCl, 0.1% SDS, 1% NP40 (Sigma-Aldrich) supplemented with protease and phosphatase inhibitors (CalbioChem). After samples centrifugation, the proteins present in supernatants were quantified with the Bradford method (Bradford, 1976). 40 µg of total proteins extract from colon tissue were separated by 10% sodium dodecyl sulfate/polyacrylamide gel electrophoresis (SDS-PAGE) and then transferred to nitrocellulose membrane (Biorad). Blotting membranes were

incubated with blocking solution with 5% non-fat dried milk powder dissolved in Tris-Buffered Saline Tween-20 (TBST) buffer (pH 7.5) composed of 10 mmol∕L Tris–HCl, 150 mmol∕L NaCl, and 0.1% Tween20, for 1 h at room temperature, washed three times, and then incubated with rabbit polyclonal anti E2F1 (1:300 dilution) (Proteintech –Cat. Numb. 12171-1-AP) overnight at 4 °C. After three washes with TBST buffer, the membranes were incubated for 1 hr with horseradish peroxidase–linked goat anti rabbit secondary antibody (1:2000 dilution) (Immunoreagents). Internal controls were carried out using β-Actin rabbit antibody (1:1000 dilution) (ABM) and Glyceraldehyde 3 phosphate dehydrogenase (GAPDH) antibody (1:5000 dilution) (Biorbyt).

The membranes were then processed by using ImageQuant[TM] LAS 4000 Biomolecular Imager (GE Healthcare Bio-sciences, Little Chalfont, United Kingdom) by treating with enhanced chemiluminescence western blotting detection reagents (Clarity Western ECL Substrate, Biorad, cat. 170-5060). Following films scanning, bands intensities were measured by densitometry analysis using the ImageJ software.

5.5.3 Results and discussion

5.5.3.1 Unloaded and siRNA loaded vesicles

Nanoparticles formulation and production

The production process (formulation and manufacturing) is of crucial importance in preparing siRNA-liposomes complexes with the desired size without affecting siRNAs integrity. The ultrasound assisted method adopted, described, modelled and applied in previous section (Chapter 4) (Barba et al., 2014) has been successfully used to produce stable siRNA-SUVs complexes on nanometric scale, useful for the EPR effect which involves carriers extravasation through tumor vascular fenestrations of 50 – 100 nm range size.

Considering the high degradability of siRNA molecules, thus the difficulty in preserving them during all production steps, one of the main goal was to produce liposomes on nanometric size ensuring the integrity of siRNAs molecular structure at the end of the process as well as preserving their biological activity.

In particular, in the developed process, the ultrasonic energy provided in duty cycle, was used to break the lipid bilayer of large vesicles (MLVs) into smaller pieces, then these pieces close themselves in spherical structures producing SUVs still containing the starting totally RNA molecules. The high encapsulation efficiency obtained together with the vesicles nanometric size achieved showed efficacy and safety of the developed technique.

Morphology

Liposomes shape is the first factor affecting carriers uptake in the cellular compartment. Spherical nanoparticles uptake in mammalian cells was demonstrated to be 3.75-5 times more than rod-shape nanoparticles, indicating that carriers curvature can affect the entry in the plasma membrane (Chithrani and Chan, 2007). In that regard, the morphological properties of the unloaded liposomes achieved during our production process were studied. As shown in Figure 34 spherical MLVs, LUVs and SUVs were obtained respectively after the hydration step, after 2 rounds of duty cycle sonication and after 6 total rounds of the size reduction process. For all the samples spherical vesicles were obtained with the loss of multiple layers moving from MLVs to LUVs and SUVs.
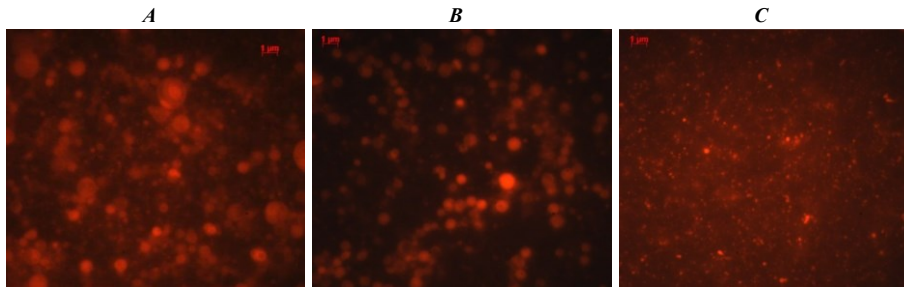
Figure 34. *Fluorescence microscopy images of merged lipid vesicles labelled with Rhodamine B dye and visualized with a 100 X objective. A) Multilamellar Vesicles (MLVs) not subjected to the size reduction process; B) Large Vesicles (LVs) after two rounds of duty cycle sonication; C) Small Vesicles (SUVs) after six rounds of duty cycle sonication*

Formation of siRNA loaded liposomes was also investigated in fluorescence microscopy. As visible in Figure 35 siRNA-SUVs complexes were obtained. Vesicles labelled with the two different dyes, the red one for liposomes and the green one for siRNA visualization, are in the same location and have the same spherical shape, implying that the siRNA molecules were successful complexed with the liposomes. The small complexes obtained are called SUVs for the presumable presence of just one lipid bilayer surrounding the aqueous core.
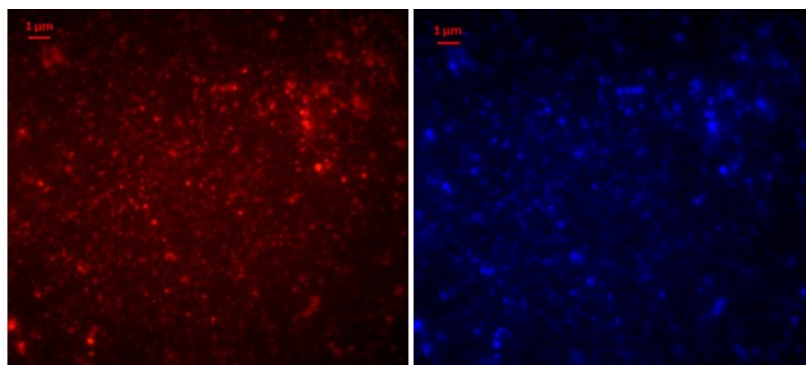
Figure 35. *Fluorescence images of siRNA loaded nanometric vesicles labelled with Rhodamine B (on the left) and siRNA DAPI labelled (on the right) visualized with a 100 X objective*

Size and zeta potential

The carriers size is a key factor affecting liposomes performance as drug delivery systems during the diffusion-mediated transport into the diseased tissue. For this reason, one of the main liposomes relevant features resides in the easy way by which their dimensions can be modified. The diameter size of unloaded liposomes produced was analyzed and the obtained values are summarized in Table 29, presented as average of three determinations. After two rounds of duty cycle sonication, MLVs (2.66 ± 1.24 μm) are turned into LUVs, vesicles which are still of micrometric size (1.76 ± 0.66 μm) but containing only one lipid bilayer. After four more rounds of sonication, SUVs were achieved of nanometric size (24.86 nm ± 5.8).

Table 29. *Size of produced unloaded Multilamellar Vesicles (MLVs), Large Unilamellar Vesicles (LUVs) and Small Unilamellar Vesicles (SUVs). Results are expressed as average of three determinations with SD as standard deviation*

Unloaded liposomes sample	Size (μm) ± SD
MLVs	2.66 ± 1.24
LUVs	1.76 ± 0.66
SUVs	0.025 ± 0.006

In general, the lipid composition affects the dimensions of MLVs. As already discussed in the 5.4 section, in the case of cationic liposomes it has been demonstrated that the diameter is influenced by the amount of DOTAP in the lipid membranes: the quaternary amine groups of the cationic lipid DOTAP and the phosphate group of PC, interact with each other. This strong interaction makes the membrane more stable and compact, and causes a

smaller particle size than could be expected without the interaction. The salt bridge between the functional groups of the two constitutive lipids results in a smaller bilayer radius of curvature which increases the stability and the encapsulation efficiency of the liposomes that contain drugs (Campbell et al., 2001). The size obtained moving from MLVs to the nanometric liposomes instead depends from the reduction process applied. It is important to point out that the transition from multilamellar to unilamellar vesicles takes only few seconds using the ultrasound based sizing technique described. The technique was modelled by Barba and collaborators in order to predict the size of spherical liposomes as an effect of the ultrasound application (Barba et al., 2014).

In Table 30 it is possible to note that the loaded liposomes diameter value (33-38 nm range size) is higher than that found for the unloaded ones (25 nm). This can be due to the fact that the liposomes have encapsulated large siRNA molecules, while the unloaded liposomes only contain PBS hydration solution. The sizes of the loaded liposomes, even when larger than those of the unloaded one, is still considered optimal being smaller than the dimensions of the expected fenestrations in the EPR effect. These fenestrations are typically 50 – 100 nm in size and the passive mechanism of permeation through the vessel gaps is an important pathway for nanoparticle accumulation into to the diseased tissue (Steichen et al., 2013).

Table 30. *Size, PDI and zeta potential of siE2F1-1117 and siE2F1-1324 produced loaded Small Unilamellar Vesicles (SUVs). Results are expressed as average of three determinations with SD as standard deviation*

siRNA-SUVs sample	*Size (nm) ± SD*	*PDI ± SD*	*Zeta Potential (mV) ± SD*
siE2F1-1117 SUVs	32.91 ± 4.82	0.32 ± 0.04	8.70 ± 1.60
siE2F1-1324 SUVs	38.11 ± 5.57	0.43 ± 0.017	18.02 ± 1.07
unloaded SUVs	24.86 ± 5.8	0.26 ± 0.005	27.90 ± 1.60

Also the PDI is higher in both loaded samples than in the unloaded one, suggesting a broader distribution of the sizes of the loaded particles; even if the sample is not really monodisperse, PDI value remains low.

Another important feature is the surface charge of liposomes. Zeta potential (ζ) was analyzed for both unloaded and SUVs encapsulating siRNAs samples, the results are presented in Table 30. The zeta-potential was positive for all the samples making the produced liposomes applicable for the encapsulation of negative siRNA molecules. The positive zeta-potential also promotes the fusion with the negatively charged cell membrane. In

particular, the ζ of siRNA loaded liposomes (about 9-18 mV range) is lower than that of the unloaded one (28 mV). This can be ascribed to the partially neutralization of DOTAP charges by the negative siRNA molecules after the complexation, making liposomes less positively charged. It can be observed that the ζ value of the siE2F1-1324-SUVs liposomes (18.02 ± 1.07 mV) appears to be significantly higher than the zeta-potential of the siE2F1-1117-SUVs sample (8.70 ± 1.60 mV). This can be explained considering that when liposomes are formed, the largest part of the negatively charged hydrophilic siRNA is encapsulated in the aqueous core, however, a small part of the siRNA molecule can have an electrostatics interaction with the DOTAP molecules at the outer of the liposomes surface. For siE2F1-1117-SUVs sample it is possible that a strong complexation and a less core encapsulation occurred.

Encapsulation efficiency (EE) by spectrophotometric and electrophoretic assay

The result of the UV-analysis shows no siRNA presence in the supernatants for siRNA-SUVs thus suggesting that under our condition the encapsulation rate is close to 100 %. This result indicates the optimal DOTAP/siRNA (+/-) charge ratio used and, more generally, the efficacy of liposomal bilayer design as well that of the production technique used. The result of the electrophoretic assay is given in Figure 36.
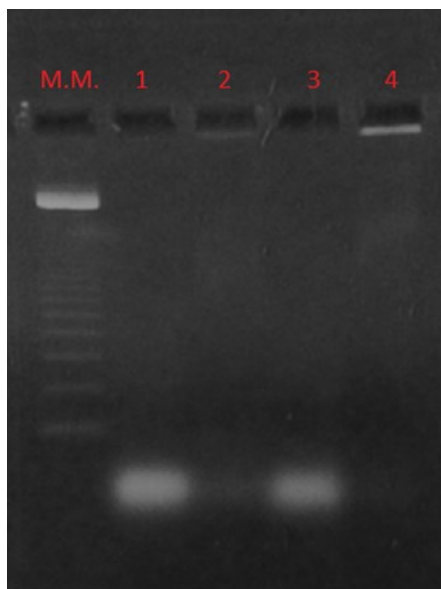
Figure 36. *UV-image of the agar gel after the electrophoretic assay. Following the order: M.M., DNA 123 bp; Lane 1, Naked siE2F1-1117; Lane 2, Nanoliposomes-siE2F1-1117; Lane 3, Naked siE2F1-1324; Lane 4, Nanoliposomes-siE2F1-1324*

The absence of bands in the lanes 2 and 4 shows no detectable amounts of unloaded siRNA confirming the 100 % siRNA encapsulation efficiency in the liposomes and also showing the high stability of the formed complexes since no decomplexation under the electric field was observed. Complex stability is a very important parameter to take into account due to the high degradability and toxicity of free siRNA. Moreover, this result indicates the success of the ultrasound assisted technique used which allows to preserve siRNA integrity since no evidence of nucleic acids degradation were visible on the gel.

5.5.3.2 Effects of siRNA-nanoliposomes on the vitality of human colon carcinoma cell lines

Based on the promising physical characterization of SUVs above reported, their delivery properties were investigated in a commonly used model of colon cells, *i.e.* the cell line HT29. As siRNA, a siRNA directed against the transcription factor E2F1 (siE2F1) was used, which was previously demonstrated to be able to reduce the vitality and growth of different cultured human cells (Dapas et al., 2009).

Three days post transfection, siE2F1- SUVs were able to significantly reduce the vitality of the colon carcinoma cell line HT29, compared to SUVs loaded by a control siRNA (siGL2- SUVs) (Figure 37 A, white columns). This result was comparable to that obtained delivering siE2F1 by a commonly used commercial transfection reagent (siE2F1- Lipofectamine®2000) (Figure 37 A, grey columns), thus proving the effectiveness of our SUVs.

The un-specific toxicity of SUVs in relation to Lipofectamine®2000 was then investigated. To this purpose, the un-specific effects on cell viability of each of the carriers either alone or loaded by the control siGL2 were compared. Data (Figure 37 B) clearly indicate that SUVs are far less toxic (Figure 37 B) than Lipofectamine®2000. This is a desirable property for a delivery agent, which should leave to the carried molecule all the biological effects without introducing its own un-specific toxicity. Indeed, an un-specific toxicity of the carrier can confound the determination of the biological effect(s) of a given drug making the evaluation of its therapeutic potential very problematic.

The decrease in cell vitality observed for siE2F1- SUVs in HT29 was confirmed by a reduction in cell counting (Figure 37 C). This proves the ability of the prepared SUVs to properly delivering siE2F1, which is expected to down regulate cell growth. To further confirm the functional delivery, we also show that siE2F1- SUVs were able to significantly reduce the mRNA level of E2F1 (Figure 37 D) compared to the control siGL2-SUVs.

Finally, to exclude that the delivery efficacy of our SUVs might be cell type dependent, the effects in a different human colon-carcinoma cell line, *i.e.* LoVo109 were explored. Results (Figure 37 E) indicate that also in the

LoVo109 cell line siE2F1-SUVs can reduce cell vitality, proving the general delivery effectiveness of siE2F1-SUVs in colon cells.

Together the presented data indicate the efficacy of the delevoped SUVs in the delivery of siE2F1 with negligible un-specific toxic effects, at least in the human cell line considered. This is a relevant feature for any novel anti-cancer approach, which should overcome the well-known un-specific toxicity of available anticancer approaches. Based on these encouraging results, it was moved to the evaluation of SUVs delivery effectiveness in a more complex model, *i.e.* colon tissue cultures, as below detailed.
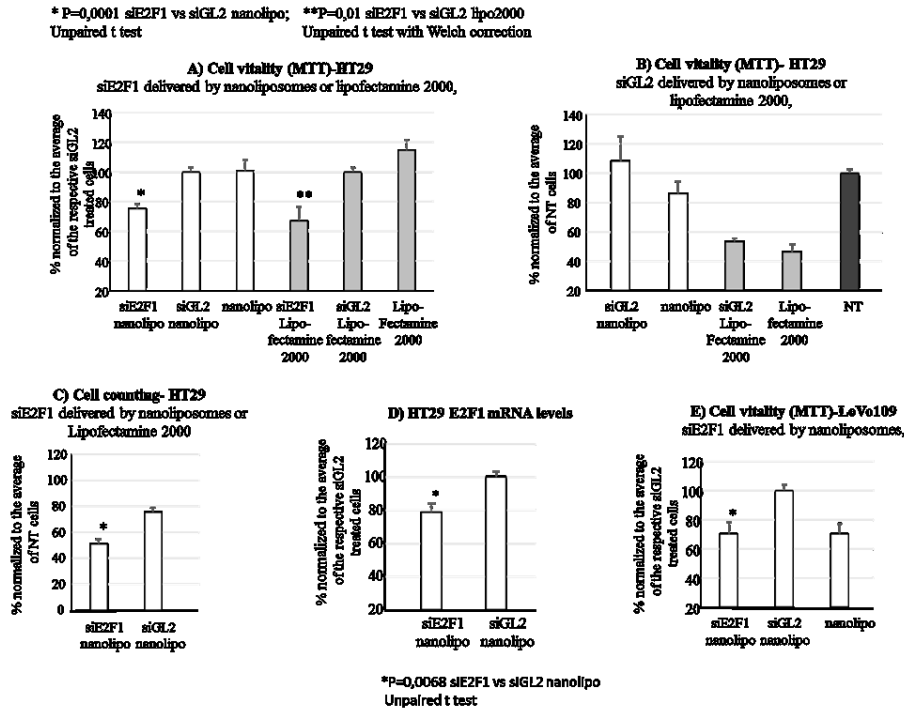
Figure 37. *A) siE2F1-nanoliposome complexes and siE2F1-Lipofectamine® 2000 effects on HT29 cell vitality (*P=0.0001 siE2F1 vs siGL2 nanolipo, Unpaired t test; **P=0.01 siE2F1 vs siGL2 lipo2000, Unpaired t test with Welch correction); B) Un-specific effects on cell of nanoliposomes and Lipofectamine®2000 alone or loaded by the control siGL2; C) Cell counting after siE2F1-nanoliposomes transfection in HT29 cell line; D) E2F1 mRNA levels after siE2F1 –nanoliposomes transfection in HT29 cells (*P=0.0068 siE2F1 vs siGL2 nanolipo, Unpaired t test); E) siE2F1-nanoliposome complexes effects on LoVo109 cell vitality. All data are reported as mean ± SEM*

145

5.5.3.3 Uptake study in colon tissue cultures

The above reported data strongly support the effectiveness of the prepared SUVs. However, the delivery efficacy can significantly vary in more complex scenario such as that represented by an organized tissue. Here, cell-cell interaction as well as the presence of the extracellular matrix can affect particle uptake. Thus, the ability of the produced SUVs to penetrate the colon mucosa tissue was tested. To this end, SUVs were marked by a red die and the distribution within the colon mucosa was analysed (Figure 38); tissue cell architecture was visualized by DAPI staining of the nuclei. Data indicate the presence of SUVs spread all over the colon tissue suggesting an effective tissue penetration including non-easy-to reach regions such as the villi and the intestinal crypts. Notably, no evident signs of cell damage were observed thus confirming the absence of any significant toxicity as observed in vitro.
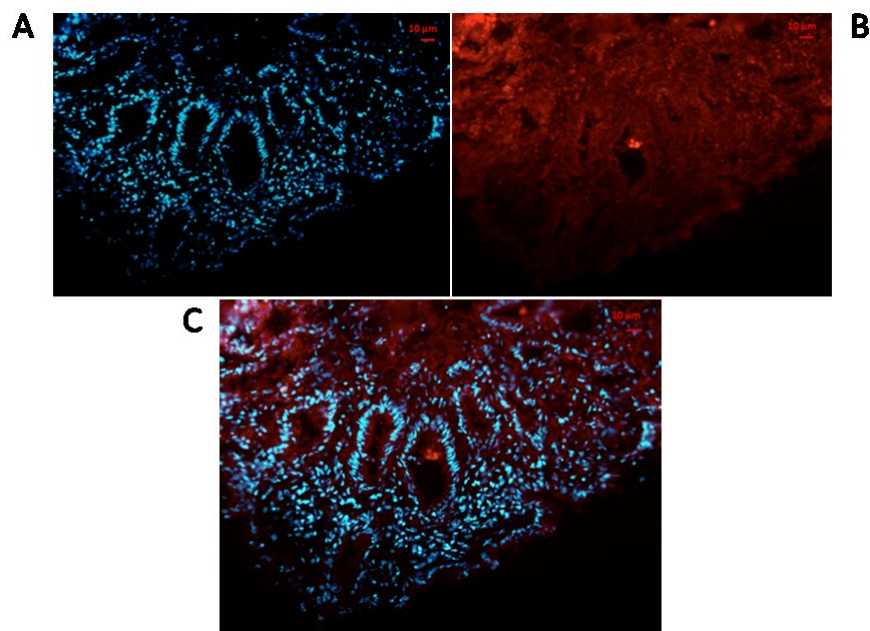
Figure 38. *Fluorescence microscope images of colon tissue section after 24 h of incubation with liposomes; 20 X objective. A) cell nuclei were visualized with DAPI, B) unloaded liposomes were Rhodamine B-labelled, C) cell nuclei and labelled liposomes images merge*

5.5.3.4 Evaluation of E2F1 protein expression after transfection in tissue: Western blot

After siE2F1-1324 nanoliposomes transfection, an inhibition of E2F1 expression level was observed in four of five donor's biopsy analysed, delineating a successful result obtained also in a dynamic human model. In particular, the E2F1 inhibition was observed at 100 nM siRNA concentration and also at 200 nM siRNA achieving a silencing effect till 80.5 %. No reduction effects were observed using 50 nM siRNA concentration. Differences in E2F1 expression levels between different donor's tissues after siRNA transfections have highlighted a patient-dependent effect (Piazza et al., 2016). Moreover, differences in proteins expression levels between the same biopsy fragments after siRNA transfections were also found as expected for a dynamic human model which, if on one side represents a great way to overcome the limits of cell cultures, being these just a small part of the entire tissue architecture, on the other side can be less controllable due to the different basal characteristics of the fragments. In fact, the constituent types of cells can differ from one tissue fragment to another, a tissue portion can, for example, be more superficial and thus mostly composed of epithelial cells, another portion, being less superficial, can be constituted from epithelial, blood and lamina cells. This has to be taken into account for this kind of transfection experiments whose results are below, patient to patient, detailed.

siRNA-SUV complexes (100 nM) transfected in donor mucosa 1

The first transfection was done in colon tissue biopsy of donor mucosa 1 as described in materials and methods, using a concentration of siE2F1-1117 and siE2F1-1324 of 100 nM. All the silencing values of E2F1 and GAPDH were normalized for both the basal sample and the negative control sample. As shown in Figure 39, the addition of the pro-inflammatory factor EC-LPS had no effect on E2F1 expression without increasing its levels as can be expected, therefore was left out of the subsequent experiments. Also the inhibition of E2F1 expression after siE2F1-1117-nanoliposomes transfection was considered not significant thus liposomes loaded with siE2F1-1117 were left out of the subsequent transfections. The inhibition of E2F1 expression with siE2F1-1324 loaded liposomes, normalized for both the control untreated sample (Figure 39 A) and the positive control sample (Figure 39 B), was of 20 %. The silencing of E2F1 expression with siE2F1-1324 loaded liposomes in tissue treated also with EC-LPS was of 65 % compared to the tissue treated with only EC-LPS. This result was considered interesting and siE2F1-1324-SUV sample was taken for further transfections to verify the expression values obtained after liposomes treatments without EC-LPS. The expression of GAPDH was also evaluated as positive control. As seen in Figure 39, the expression of GAPDH was inhibited significantly only in the sample transfected with the siRNA-SUVs positive control, with a 43.6 % of

inhibition normalizing for the basal sample, confirming the successful transfection. Moreover, the negative control did not show inhibition of E2F1 or GAPDH expressions, demonstrating the absence of random silencing effects.
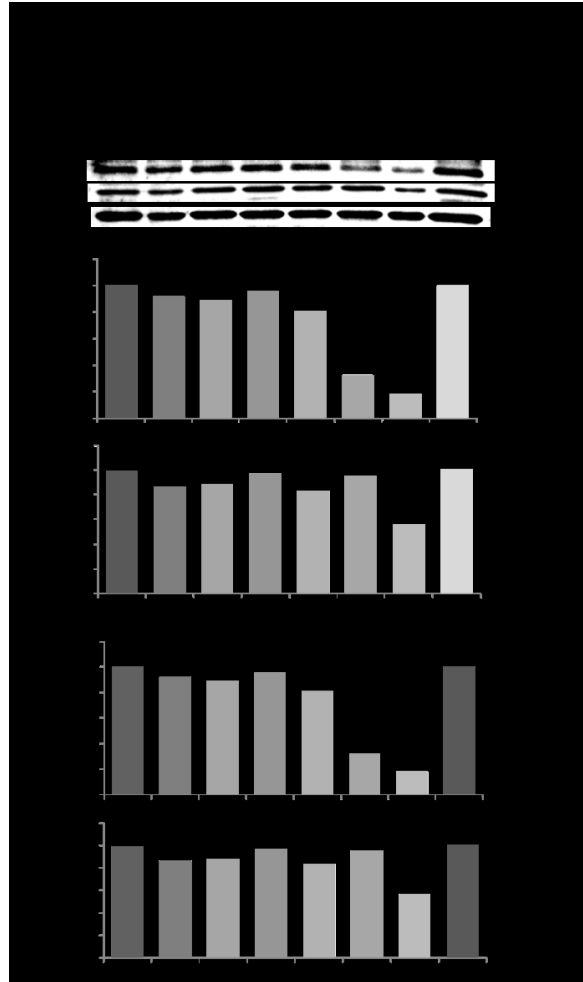
Figure 39. *E2F1 and GAPDH expressions in donor 1 after siRNA-nanoliposome transfection at 100 nM. The proteins band quantification is normalized to Actin. The order of the analyzed samples is: Tissue incubated in 1. Only medium; 2. Medium with EC-LPS; Tissue transfected with: 3. siE2F1-1117 nanoliposomes; 4. siE2F1-1117 nanoliposomes in medium with EC-LPS; 5. siE2F1-1324 nanoliposomes; 6. siE2F1-1324 in medium with EC-LPS; 7. Positive control nanoliposomes and 8. Negative control nanoliposomes. Figures A are referred to E2F1 expression levels normalized respect to the not treated (NT) or basal sample. Figures B are referred to E2F1 expression levels normalized respect to the siRNA negative control (CTRL – siRNA) treated sample*

siRNA-SUV complex (200 nM) transfected in donors mucosa 2 and 3

The results of the Western Blot analysis for patients 2 and 3 are shown in Figure 40. As can be seen in the first graph of Figure 40 A, relatively to the patient 2, the expression of E2F1, normalized to the basal (not treated) sample, is inhibited of 43.2 % and of about the 37 % normalizing for the scramble siRNA negative control treated tissue (second graph of Figure 40 A). The expression of GAPDH does not appear to be silenced after the transfection of the siRNA-positive control-nanoliposomes. This result can be explained by the fact that, being colon tissue biopsies not completely comparable with one another (they can differ for the nature and amount of cells they are made from, for their weight which is not exactly equal, for a different enzymatic activity), the transfection process can go in a different manner also between fragments of the same patient. For example if the tissue fragment in which the positive control-nanoliposomes is transfected contains more cells than the fragment transfected with siE2F1-1324 complexes, liposomes will reach a smaller fraction of the total cell nuclei and the siRNA concentration will be insufficient to lower the proteins expression levels. This might have caused a lower inhibition of GAPDH expression in patient 2 and no inhibition of E2F1 expression in patient 3 in which anyway the expression of GAPDH was inhibited of 38 % after positive control nanoliposomes transfection normalizing for both the not treated and the negative control samples (Figure 40 B), confirming the liposomes ability in enter the cells and release siRNAs molecule as well as the successful transfection. The negative control was valid for all the transfections done and, for both the patients, no significant inhibition of E2F1 and GAPDH expression was found in the presence of a scramble sequences, demonstrating, once more, the absence of random silencing effects.
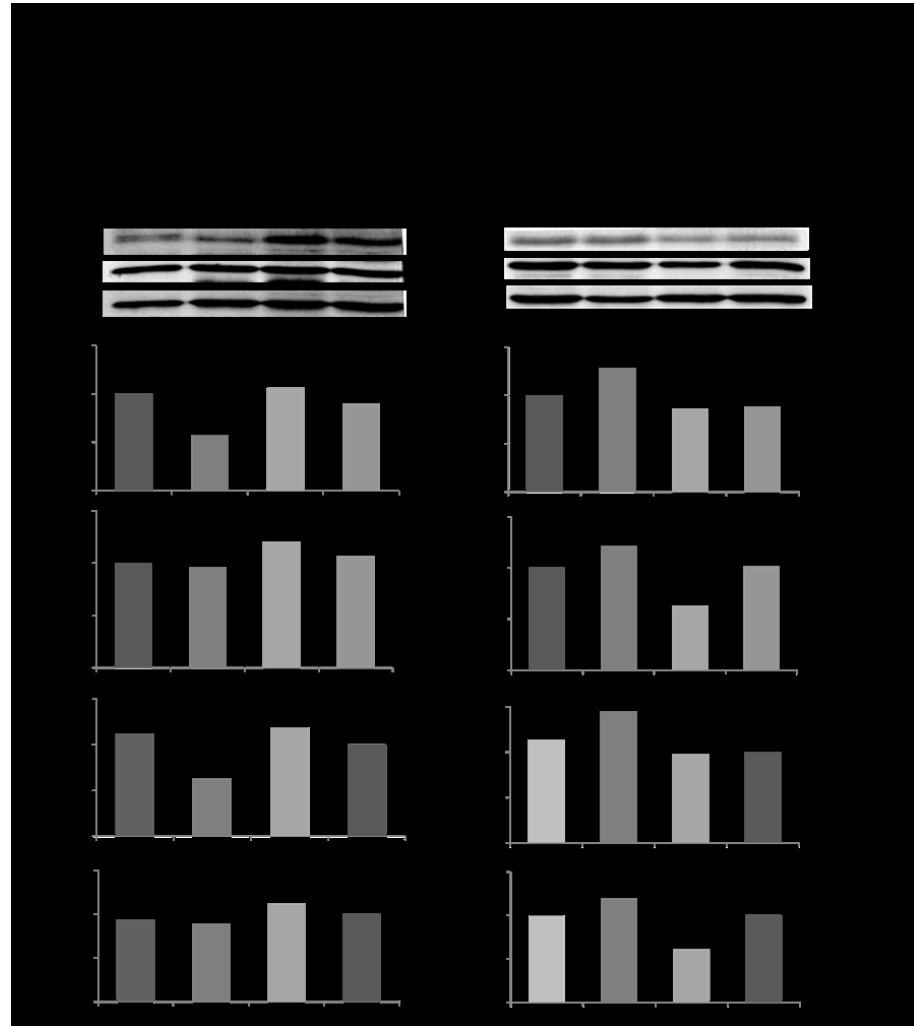
Figure 40. *E2F1 and GAPDH expressions in donors 2 (A) and 3 (B) after siRNA-nanoliposome transfection at 200 nM. The proteins band quantification is normalized to Actin. The order of the analyzed samples is: 1. Tissue fragment incubated in medium; Tissue fragments transfected with: 2. siE2F1-1324 nanoliposomes; 3. Positive control nanoliposomes; and 4. Negative control nanoliposomes. E2F1 expression levels are normalized respect to the basal (not treated) sample and respect to the siRNA negative control (CTRL – siRNA) treated sample*

siRNA-SUV complex (200 nM and 50 nM) transfected in donors mucosa 4 and 5

E2F1 and GADPH expression levels after 50 nM and 200 nM siRNA-nanoliposomes transfections were determined for patients 4 and 5. Normalizing for the basal sample no significative inhibitions of E2F1 and GAPDH expressions were found for both the patients when siRNAs were used at 50 nM (Figure 41 A-B). Instead, at 200 nM siE2F1-1324 nanoliposomes a significant inhibition was observed in both patients 4 and 5. In particular, in patient 4, the E2F1 expression level was decreased by 80.5 % respect to the basal tissue (Figure 41 A) and by the 40.3 % in patient 5 (Figure 41 B) ever normalizing to the not treated tissue. Normalizing for siRNA negative control treated sample, E2F1 inhibition percentages don't change in a significant manner confirming the absence of random effects. Regarding the GAPDH expression this was not reduced in patient 4 (Figure 41 A) but significantly reduced in patient 5 decreasing of the 64.3 % respect to the basal tissue (Figure 41 B), thus confirming that differences in biopsy fragments structures, weight and cells composition can affect transfection process which, anyway, has proved to be efficient in silencing E2F1 in both the last two patients with the explored liposomal delivery systems.

Data indicate the ability of the produced nanoliposomes in encapsulating the siRNA molecules in an effective manner, in delivering them excellently into the colon cell line and human colon tissue studied and in their ability in release their content once inside the endosome compartment. Moreover, E2F1 protein level reduction indicates the successful siRNA entrance in the cell nuclei and the selectivity of the used siRNA-1324 sequence against E2F1 mRNA. All this finding suggests a promising potential of the developed nanoliposomes-siRNA complexes for the treatment of diseases in which the pathophysiology is characterized by an excessive expression of E2F1 transcription factor as cancer forms associated to IBDs.
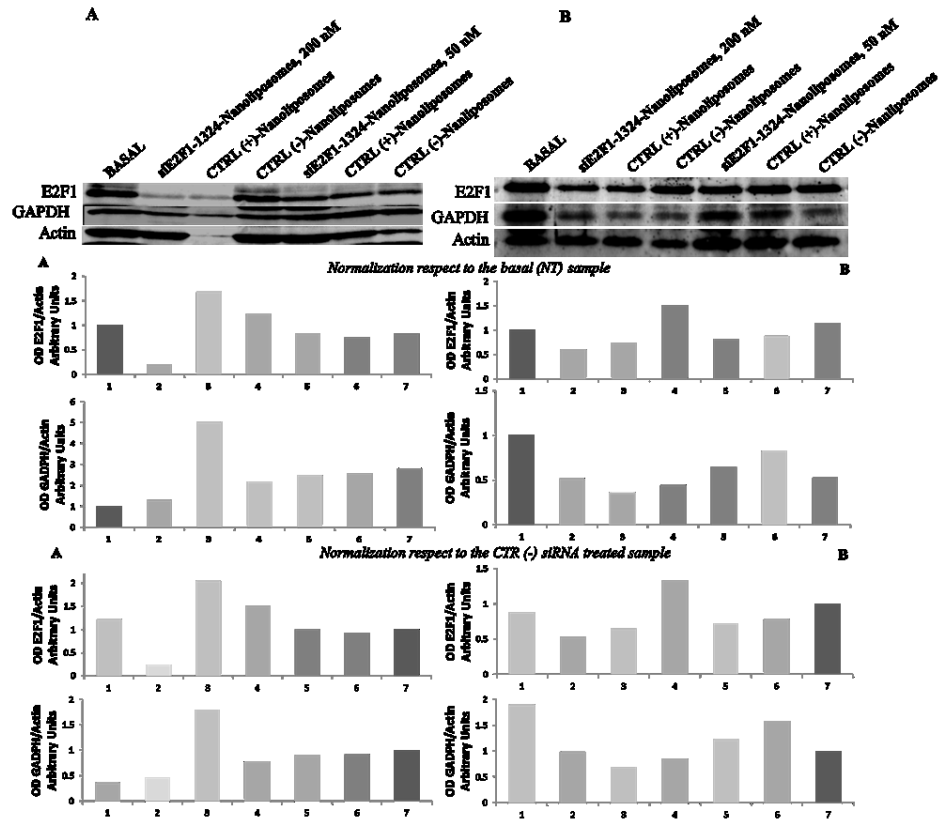
Figure 41. *E2F1 and GAPDH expressions in donors 4 (A) and 5 (B) after siRNA-nanoliposome transfection at 200 nM and 50 nM. The proteins band quantification is normalized to Actin. The order of the analyzed samples is: 1. Tissue fragment incubated in medium; Tissue fragments transfected with: 2. siE2F1-1324 nanoliposomes; 3. Positive control nanoliposomes; and 4. Negative control nanoliposomes. E2F1 expression levels are normalized respect to the basal (not treated) sample and respect to the siRNA negative control (CTRL – siRNA) treated sample*

5.5.4 Remarks

In this thesis, taylored designed SUVs loaded with an anti E2F1 siRNA have been produced and tested in vitro and ex vivo models of colon tissue.

To produce SUVs the lipidic thin film hydration combined with a size reduction process via sonication in duty cycle was used. This developed preparative protocol is far less complex and more rapid than the one usually adopted for liposomes size reduction. The produced liposomes are in the nanometric size range and thus can take advantage of the EPR effect. Moreover, nanoliposomes have shown high degree of size homogeneity, relevant feature that can guarantee a uniform behavior in terms of delivery properties, and the siRNA encapsulation rate reaches almost 100% indicating a remarkable capability of siRNA loading.

Together, the characteristics of the designed SUVs resulted in a low unspecific toxicity in cultured colon cells compared to commonly used transfection reagents. This is a desirable property for a delivery agent, which should leave to the carried molecule all the biological effects without introducing its own un-specific toxicity. Moreover, SUVs loaded by siE2F1 were effective in the down regulation of the target in cultured cells and in the consequent reduction of cell growth. Finally, a remarkable uptake and target silencing efficiencies were observed in cultured human biopsy of colon mucosa.

In conclusion, whereas further studies in more complex models are required, the developed SUVs have the potential to contribute to the development of novel effective anti-colorectal cancer therapies for a future personalized medicine.

Part of this work has been reported in:

Bochicchio S.; Dalmoro A.; Barba A.A.; Grassi G.; Lamberti G.; "Liposomes as siRNA delivery vectors"; *Current Drug Metabolism*, 2015, 15, 882-892

Bochicchio S.; Dapas B.; Russo I.; Ciacci C.; Piazza O.; De Smedt S.; Pottie E.; Barba A.A.; Grassi G.; "In vitro and ex vivo delivery of tailored siRNA-nanoliposomes for E2F1 silencing as a potential therapy for colorectal cancer", IJP - International Journal of Pharmaceutics, 2017, in press

6. Concluding Remarks

In this chapter the work done is resumed and the main results are highlighted.

Liposomes engineering has revolutionized active molecules delivery by providing new tools to customize therapeutics for specific clinical application and to enhance micronutrients controlled release in nutraceutical field thus solving the major drawbacks of bioactive compounds linked to their low stability, limited membrane-permeability, short half-life and low bioavailability.

In this PhD thesis lipid nanostructured vectors with tailored features to be used for both nutraceutical and pharmaceutical applications were realized through the design of novel production processes, expressly developed in order to overcome the limits of conventional methods. To date, one of the major drawback of the processes used for liposomes production resides in the impossibility to manufacture large volumes of product in output despite the high energy consumption, long times of production together with the use of toxic solvents and other process drastic conditions.

Therefore, in order to respond to the needs of a better process performance, improving the efficiency and cutting down energy consumption, two novel techniques, sharing the ultrasound technology as process intensification tool used in particles size reduction and homogenization operations, were designed and developed.

Starting with the use of the ultrasounds as alternative energy, a particles size reduction process was developed and coupled with the bench scale conventional Thin Film Hydration (TFH) technique. In this method, after solvents evaporation through the use of a rotary evaporator, a lipid film is formed and then hydrated, spontaneously producing micrometric vesicles characterized by the presence of several bilayers. In order to produce, in a versatile manner structures with modulable dimension (micro or nano), the method was revisited by adding the duty cycle sonication treatment.

A dynamic model able to describe the curvature of a lipid bilayer under the effect of ultrasonic energy was then proposed and tested and the phenomenological aspects involved in vectors constitution were investigated. In particular, starting from micrometric vesicles, the energy is used to break the lipid bilayer into smaller pieces, then these pieces close themselves in spherical structures producing small liposomes.

Due to its easiness, reliability, versatility and its great potential in reducing time spent, the ultrasound intensification tool was also used for liposomes homogenization operation during vesicles production through the simil-microfluidic approach. In particular, a new simil-microfluidic bench scale apparatus able to produce lipid vectors directly on nanometric scale was designed and fabricated.

Through the use of constructive expedients (millimetric diameter tubes, peristaltic pumps, injection needle) it was possible to reproduce the phenomenology connected to the vesicles formation through a microfluidic approach. In particular, liposomes formation is governed by the molecular

diffusion between two phases: the lipids/organic solvent and the water; this latter simultaneously diffuses into the organic solvent in order to reduce its concentration below the critical value required for the lipids solubilization. Liposomes formation happens at the interfaces between the alcoholic and water phases, when they start to interdiffuse in a direction normal to the liquid flow stream, changes in flow conditions result in a size variations of the insertion section of the organic phase reflecting on the vesicles dimensional features. For instance, it was shown that the liposomes dimensional distibution increases as increasing the ratio between the water volumetric flow rate to the lipids-ethanol volumetric flow rate; on contrary, ultrasonic energy enhances the homogenization of the hydroalcoholic bulk and its duty cycle application efficaciously promoted a better vesicles dimensional distribution. This result was also confirmed by working at equal flow rates but at different lipid concentrations.

In general, it is important to underline that while making the large scale nanoliposomes production a safe and low cost process (working at room conditions and in absence of toxic solvents) the developed simil-microfluidic apparatus is also highly productive due to the use of ultrasound, a scalable tool for process intensification.

Several active molecules were successfully encapsulated in different classes of lipid nanostructured vectors (neuter, cationic and anionic) by using the ultrasound assisted tool at first coupled with the conventional THF method and subsequently used as integrant part of the homogenization section of the simil-microfluidic bench scale apparatus. For nutraceutical applications, nanoliposomes containing vitamins with different hydrophobicity (α-tocopherol, ergocalciferol, vitamin B12) and ferrous sulfate, with highly interesting features for supplements market, were produced trought the use of ultrasound assisted TFH method and the simil-microfluidic apparatus, respectively.

Micro liposomal vesicles containing vitamins with tailored dimensions (2.9 μm - 5.7 μm range size) were produced, obtaining, after sonication in duty cycle, small vesicles (40 nm - 51 nm range size). High encapsulation efficiency was obtained in both large vesicles (72.0 ± 00 % e.e., vitamin B12; 95.0 ± 7.07 % e.e., α-tocopherol; 81.5 ± 2.12 %, ergocalciferol) and small liposomes (56.2 ± 8.51 %, vitamin B12; 76.3 ± 14.02 %, α-tocopherol; 57.5 ± 13.9 %, ergocalciferol). An increase of encapsulation efficiency in small vesicles from 40% to 56.2 % between vitamin B12 encapsulated with the developed technique or by breaking unloaded preformed liposomes (conventional approach), has been achieved.

Through the simil-microfluidic method it was possible to produce ferrous sulfate-nanoliposomes with high encapsulation efficiencies (a 97% e.e. was achieved using the last formulation tested) and good dimensional features (127-135 nm, not sonicated vesicles; 48-76 nm, sonicated vesicles) to be used for the cure of iron deficiencies related diseases, such anemia.

Elevated process yield if compared to the THF and Ethanol Injection classical bench scale techniques was achieved without the use of drastic conditions.

The efficiency and sustainability of the developed process could will have a great impacts on the nutraceutical-processing industries thus drastically reducing process time and costs finally making iron-nanoliposomal based nutraceutical products cheaper.

Nanoliposomes containing KRX29, a new synthetized peptide for a not conventional heart failures therapy and nucleic acids based drugs (NABDs), therapeutic agents used in gene therapy, were successfully produced for pharmaceutical purposes.

Through the use of the developed ultrasound assisted process KRX29-nanoliposomes were successfully produced. Starting from micrometric vesicles (7.2 - 11.7 μm range size) nanoliposomes (22 - 35 nm range size) were obtained and the effect of their surface charge on both peptide encapsulation and recovery efficiency was studied. By using the higher charge ratio formulation (13:1 (-/+)) the highest encapsulation efficiency (about 100%) was achieved in both large and small vesicles while at the lower charge ratio formulation (1:1 (-/+)) the best ability to recover the entrapped peptide was obtained.

Preliminary experiments in which dsDNA was used to simulate the structure of siRNA molecule have confirmed the versatility of the ultrasound assisted technique for producing micro (2.2 - 2.9 μm) and nano lipid vectors (28 - 56 nm) encapsulating NABDs. By varying the charge ratio from 3:1 to 7:1 (+/-DOTAP/dsDNA) it was shown that an high encapsulation efficiency (64 % e.e. in nanoliposomes and 100 % e.e. in large vesicles) was possible by using the 7:1 (+/-) charge ratio.

In the light of these results, siRNAs-nanoliposomes complexes for E2F1 protein expression inhibition were successfully produced to potentially treat cancer associated to Inflammatory Bowel Diseases. Nanoliposomes (33-38 nm range size) characterized by an high siRNA encapsulation efficiency (100 %) and a very low cytotoxicity in cells when compared with the commercial transfection agent Lipofectamine® 2000, were obtained through the TFH/sonication technique. Moreover, the produced complexes have shown an excellent uptake in the cultured human colon mucosa tissues and a remarkable anti-E2F1 expression effect after siE2F1-1324-nanoliposomes transfection with a clear tendency to respond in a patient-dependent way.

In this thesis the formulative and chemical engineering approaches have allowed to achieve nanostructured vectors, able to deliver, in a controlled manner, different active molecules, with the desired features (tailored on the application of interest), produced through safe and inexpensive processes purposely developed and potentially of industrial interest.

Appendix

In this appendix details of the pubblications inherent the Ph.D. project are presented together with a short description.

Pubblications

International Journals

1.

In vitro and ex vivo delivery of tailored siRNA-nanoliposomes for E2F1 silencing as a potential therapy for colorectal cancer

Sabrina Bochicchio[a,b,1], Barbara Dapas[c,1], Ilaria Russo[d,1], Carolina Ciacci[d], Ornella Piazza[d], Stefaan De Smedt[e], Eline Pottie[e], Anna Angela Barba[a,*], Gabriele Grassi[c,f]

[a] *Dipartimento di Farmacia, University of Salerno, Fisciano, SA, Italy*
[b] *Dipartimento di Ingegneria Industriale, University of Salerno, Fisciano, SA, Italy*
[c] *Dipartimento di Scienze della Vita, University of Trieste, Italy*
[d] *Dipartimento di Medicina, Chirurgia e Odontoiatria "Scuola Medica Salernitana", University of Salerno, Fisciano, SA, Italy*
[e] *Department of Pharmaceutics, University of Gent, Belgium*
[f] *Dipartimento di Scienze Mediche, Chirurgiche e della Salute, Ospedale di Cattinara, University of Trieste, Italy*

Abstract

Tailored developed nanoliposomes loaded with a siRNA against the transcription factor E2F1 (siE2F1), were produced and delivered to human colorectal adenocarcinoma cell lines and to intestinal human biopsies. siE2F1 loaded nanoliposomes were produced through a dedicated ultrasound assisted technique producing particles with about 40 nm size (Small Unilamellar Vesicles, SUVs) and 100% siRNA encapsulation efficiency. Compared to other production methods, the one proposed here can easily produce particles in the nanometric scale by suitable ultrasonic duty cycle treatments. Furthermore, SUVs have a high degree of size homogeneity, a relevant feature for uniform delivery behaviour.

siE2F1-loaded SUVs demonstrated a very low cytotoxicity in cells when compared to a commercial transfection agent. Moreover, SUVs loaded with siE2F1 were effective in the down regulation of the target in cultured colon carcinoma cells and in the consequent reduction of cell growth. Finally, a remarkable uptake and target silencing efficiencies were observed in cultured human biopsy of colonic mucosa. In conclusion, whereas further studies in more complex models are required, the siE2F1-SUVs generated have the potential to contribute to the development of novel effective inflammatory bowel diseases-associated colorectal cancer therapies for a future personalized medicine.

Special issue

"New trends in gene therapy: multidisciplinary approaches to siRNAs controlled delivery"

Online version 2016

Print 2017

2. **Bochicchio S.**; Dalmoro A.; Barba A.A.; D'Amore M., Lamberti G.; "New preparative approaches of micro and nano drug delivery carriers" Current Drug Delivery, 2017 - online 2016

Abstract

The full success of pharmacological therapies is strongly depending from the use of suitable, efficient and smart drug delivery systems (DDSs). Thus DDSs development is one of the main challenges in pharmaceutical industry both to achieve tailored carrier systems based on drug features and to promote manufacturing innovations to reduce energetic resources, emissions, wastes and risks. Main functions of an ideal DDS are: to protect loaded active molecules from degradation in physiological environments; to deliver them in a controlled manner and towards a specific organ or tissue, to allow the maintenance of the drug level in the body within therapeutic window. Smart features, such as those able to induce active molecule release upon the occurrence of specific physiological stimuli, are also desirable. Under the manufacturing point of view, the current industrial scenery is obliged to respond to the increasing market requirements and to the mandatory rules in sustainable productions such as raw material and energy savings. In this work a general framework on drug delivery systems preparation techniques is presented. In particular two sections on innovation in preparative approaches carried out are detailed. These latter involve the use of microwave and ultrasonic energy applied in the production of polymeric and lipidic delivery systems on micro- and nanometric scale. The novelties of

these preparative approaches are emphasized and examples of developed drug delivery carriers, loaded with vitamins and drug mimicking siRNA, are shown.

3. Dalmoro A.; Abrami M.; Galzerano B.; **Bochicchio S.**; Barba A.A.; Grassi M.;Larobina D.; "Injectable chitosan/b-glycerophosphate system for sustained release: gelation study, structural investigation, and erosion tests"- Current Drug Delivery, 2017- online 2016

Abstract

Hydrogels can constitute reliable delivery systems of drugs, including those based on nucleic acids (NABDs) such as small interfering ribonucleic acid (siRNA). Their nature, structure, and response to physiological or external stimuli strongly influence the delivery mechanisms of entrapped active molecules, and, in turns, their possible uses in pharmacological and biomedical applications. In this study a thermo-gelling chitosan/β-glycero-phosphate system has been optimized in order to assess its use as injectable system able to: i) gelling at physiological pH and temperature, and ii) modulate the release of included active ingredients. To this aim we first analyzed the effect of acetic acid concentration on the gelation temperature. We then found the "optimized composition", namely, the one in which the Tgel is equal to the physiological temperature. The resulting gel was tested, by low field nuclear magnetic resonance (LF-NMR), to evaluate its average mesh-size, which can affect release kinetics of loaded drug. Finally, films of gelled chitosan, loaded with a model drug, have been tested in vitro to monitor their characteristic times, i.e. diffusion and erosion time, when they are exposed to a medium mimicking a physiological environment (buffer solution at pH 7.4). Results display that the optimized system is deemed to be an ideal candidate as injectable gelling material for a sustained release.

4. Piazza O.; Russo I.; **Bochicchio S.**; Barba A. A.; Lamberti G.; Zeppa P.; Di Crescenzo V.; Carrizzo A.; Vecchione C.; Ciacci C.; "Cyclin D1 Gene Silencing by siRNA in ex vivo human tissues cultures" Current Drug Delivery, 2017- online 2016

Abstract

Short interfering RNAs (siRNAs) are double-stranded RNA molecules able to specifically targeting genes products responsible for human diseases. Cyclin D1 (CyD1) is a cell cycle-regulatory molecule, up-regulated at sites of inflammation in several tissues. CyD1 is a very interesting potential target in lung and colon inflammatory diseases.
Objective. The aim of this paper was testing CyD1 expression in human lung and colon tissues after the application of an inflammatory stimulus, and verifying its gene silencing by using siRNA for CyD1 (siCyD1).

Method. Colon and pulmonary biopsies were treated with siCyD1 by using two different transfection carriers: a) invivofectamine and b) ad hoc produced nanoliposomes. After 24 hours of incubation with nanoliposomes encapsulating siRNA or invivofectamine-CyD1siRNA, in presence or absence of EC-LPS, we analysed the protein expression of CyD1 through Western-Blotting.

Results. After EC-LPS treatment, in both colon and pulmonary biopsies, an overexpression of CyD1was found (about 64% and 40% respectively). Invivofectamine-CyD1 siRNA reduced the expression of CyD1 approximately by 46% compared to the basal condition, and by around 65% compared to EC-LPS treated colon samples. In lung, following invivofectamine siRNA silencing in the presence of EC-LPS, no reduction was observed. Ad hoc nanoliposomes were able to enter colon and lung tissues, but CyD1 silencing was reported in 2 colon samples out of 4 and no efficacy was demonstrated in the only lung sample we studied.

Conclusion. It is possible to silencing Cyclin D1 expression in vitro "organ culture" model. Our preliminary results encourage further investigations, using different siRNA concentrations delivered by nanoliposomes.

5. D'Apolito R.; **Bochicchio S.**; Dalmoro A.; Barba A. A.; Guido S.; Tomaiuolo G.; "Microfluidic investigation of the effect of liposome surface charge on drug delivery in microcirculation "Current Drug Delivery, 2017 – online 2016

Abstract

Nano-carrier drug transport in blood microcirculation is one of the hotspots of current research in drug development due to many advantages over traditional therapies, such as reduced side-effects, target delivery, controlled release, improved pharmacokinetics and therapeutic index. Despite the substantial efforts made in the design of nanotherapeutics, the big majority of the used strategies failed to overcome the biological barriers to drug transport encountered in human microvasculature, such as transport by blood flow via the microcirculatory network and margination, the mechanism according to which particles migrate along vessel radius to the wall. In fact, drug transport efficiency in microvasculature is affected by both the particulate nature of blood and drug carrier properties, such as size, shape and surface charge. In this work, the effect of the surface charge of liposomes on their margination in blood flow in microcapillaries was experimentally evaluated. By high-speed video microscopy and image analysis it was found that the two custom-made liposomes (one neuter and the other positively charged) tend to drift laterally, moving towards the wall and accumulating in the cell-free layer. In particular, neuter and cationic liposomes showed a comparable margination propensity, suggesting that the

presence of blood cells governs the flow behavior independently on liposome surface charge.

6.

Vitamin delivery: Carriers based on nanoliposomes produced via ultrasonic irradiation

Sabrina Bochicchio [a, d], Anna Angela Barba [a, *], Gabriele Grassi [b, c], Gaetano Lamberti [d]

[a] Dipartimento di Farmacia, Università degli Studi di Salerno, via Giovanni Paolo II, 132-84084 Fisciano, SA, Italy
[b] Dipartimento di Scienze della Vita, Università di Trieste, Via L. Giorgieri, 1-34128 Trieste, Italy
[c] Dipartimento di Scienze Mediche, Chirurgiche e della Salute, Università degli Studi di Trieste, Ospedale di Cattinara, Strada di Fiume, 447-34100 Trieste, Italy
[d] Dipartimento di Ingegneria Industriale, Università degli Studi di Salerno, Via Giovanni Paolo II, 132-84084 Fisciano, SA, Italy

Abstract

In recent years much attention has been focused on using lipid carriers as potential delivery systems for bioactive molecules due to their favorable properties such as high biocompatibility, size and composition versatility. In this paper formulation, preparation and characterization of liposomes, a class of powerfully versatile lipidic carriers, produced by means of an innovative ultrasound-assisted approach based on the thin-film hydration method, are presented and discussed. The main aim of this study is to obtain nanostructures (Small Unilamellar Vesicles, SUVs), less than 100 nm in size, loaded with different vitamins (B12, tocopherol and ergocalciferol), starting from lipidic microstructures (Multilamellar Large Vesicles, MLVs). Suitable formulations, sonication protocols and nanoliposomes were pointed out. SUVs with diameter size ranging from 40 nm to 51 nm were achieved starting from MLVs with a diameter range of 2.9–5.7 μm. Starting from MLVs with higher encapsulation efficiency for all kind of vitamins, SUVs with an encapsulation efficiency of 56% for vitamin B12, 76% for α-tocopherol and 57% for ergocalciferol were obtained. Stability tests have shown that the used lipid composition allows to keep intact the nanovesicles and their content for more than 10 days if incubated at simulated extracellular environment conditions.

7.

Liposomes as siRNA Delivery Vectors

Sabrina Bochicchio[1,2], Annalisa Dalmoro[1], Anna Angela Barba[1,*], Gabriele Grassi[3,4] and Gaetano Lamberti[2]

[1]*Dipartimento di Farmacia, Università degli Studi di Salerno, Via Giovanni Paolo II, 132, 84084 Fisciano (SA) – Italy;* [2]*Dipartimento di Ingegneria Industriale, Università degli Studi di Salerno, Via Giovanni Paolo II, 132, 84084 Fisciano (SA) – Italy;* [3]*Dipartimento di Scienze della Vita, Università di Trieste, Via L. Giorgieri 1, 34128 Trieste, Italy;* [4]*Dipartimento di Scienze Mediche, Chirurgiche e della Salute, Università degli Studi di Trieste, Ospedale di Cattinara, Strada di Fiume 447, 34100 Trieste,- Italy*

Abstract

Nucleic Acid Based Drugs (NABDs) constitute a class of promising and powerful therapeutic new agents with limited side effects, potentially useable against a wide range of diseases, including cancer. Among them, the short interfering RNAs (siRNAs), represent very effective molecules. Despite their *in vitro* efficacy, the major drawback that limits siRNAs usage consists in a difficult delivery due to their very low stability in physiological fluids, and to their limited membrane-permeability through physiological barriers. On the other hand, the liposomes (lipid bilayers closed in vesicles of various sizes) represent interesting drug delivery systems (DDSs) which can be tailored in order to get the best performance in terms of load, vesicle size and transfection yield. In this work, the current state of study in these two fields, and the connections between them, are briefly summarized.

8.

Soft Matter

PAPER

Ultrasonic energy in liposome production: process modelling and size calculation

A. A. Barba,[a] S. Bochicchio,[a] G. Lamberti[*b] and A. Dalmoro[a]

Abstract

The use of liposomes in several fields of biotechnology, as well as in pharmaceutical and food sciences is continuously increasing. Liposomes can be used as carriers for drugs and other active molecules. Among other characteristics, one of the main features relevant to their target applications is the liposome size. The size of liposomes, which is determined during the production process, decreases due to the addition of energy. The energy is used to break the lipid bilayer into smaller pieces, then these pieces close themselves in spherical structures. In this work, the mechanisms of rupture

of the lipid bilayer and the formation of spheres were modelled, accounting for how the energy, supplied by ultrasonic radiation, is stored within the layers, as the elastic energy due to the curvature and as the tension energy due to the edge, and to account for the kinetics of the bending phenomenon. An algorithm to solve the model equations was designed and the relative calculation code was written. A dedicated preparation protocol, which involves active periods during which the energy is supplied and passive periods during which the energy supply is set to zero, was defined and applied. The model predictions compare well with the experimental results, by using the energy supply rate and the time constant as fitting parameters. Working with liposomes of different sizes as the starting point of the experiments, the key parameter is the ratio between the energy supply rate and the initial surface area.

- *National Journals*

9.

Home › Le riviste › ICF - Rivista dell'industria chimica e farmaceutica › ICF – RIVISTA DELL'INDUSTRIA CHIMICA E FARMACEUTICA N°2 APRILE/MAGGIO 2016

Le riviste | ICF - Rivista dell'industria chimica e farmaceutica

ICF

ICF – RIVISTA DELL'INDUSTRIA CHIMICA E FARMACEUTICA N°2 APRILE/MAGGIO 2016

Media Kit
Inserzionisti
Fiere & Eventi
Archivio Sfogliabile
News

Nanovettori per il rilascio di farmaci antitumorali a base di acidi nucleici

Sabrina Bochicchio

Abstract

The development of gene therapy along with advances in nanotechnology have opened one of the most promising frontiers for the treatment of cancer allowing effective and customizable treatments. In the controlled release of new therapeutic agents based on nucleic acids, a key role is played by delivery systems, able to carry not only a protective function but also a smart release activity. From here, the new challenges of scientific research.

10.

Abstract

In the pharmaceutical/nutraceutical field the methods concerning the encapsulation of active molecules in polymeric and lipid materials are constantly evolving. Of particular interest are those based on the so-called "Process Intensification". Examples of innovative approaches relate to the exploitation of some effective tools of process intensification are microwave and ultrasound, used for the energy supply in an unconventional way.

- *Book chapter*

11.
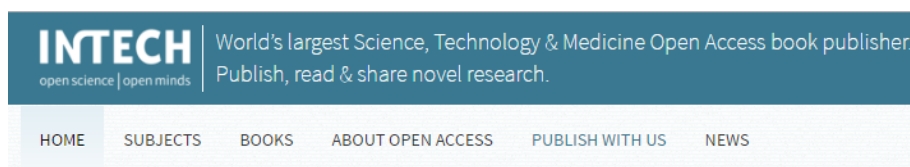
Bochicchio S.; Lamberti; Barba A.A.; "Phenomenological and formulation aspects in tailored nanoliposomes production" chapter in book Liposomes, InTech Ed., 2016, in press

Abstract

Liposomes as cell-mimetic system have attracted wide attention of researchers in various branches of the drug delivery topic as they can be highly functionalized and personalized thus solving the major drawbacks of bioactive molecules linked to their low stability, limited membrane permeability, short half-life and low bioavailability. The development of sustainable processes able to produce ad hoc liposomes in a rapid manner through the use of not labored techniques, avoiding drastic conditions, is of great relevance for the industrial sector. In this chapter two novel liposomes production processes, the Ultrasound assisted Thin Film Hydration and the simil-microfluidic techniques sharing the same size

reduction/homogenization preparative step are presented. The phenomenological aspects involved in vectors constitution through the duty cycle sonication process (bilayer rupture/vesicles formation mechanisms) and through the simil-microfluidic approach (intubated flows interdiffusion mechanisms) are described. Finally, two applications as case histories involving the use of the developed techniques for relevant classes of active molecule delivery are described. In particular a pharmaceutical application concerns the encapsulation of siRNA molecule, used for gene therapy, inside cationic nanoliposomes, and a nutraceutical application consists in the production of ferrous sulphate anionic liposomal formulations with improved features compared to those already present on the market.

References

ABBASI, S. & AZARI, S. 2011. Efficiency of novel iron microencapsulation techniques: fortification of milk. *International Journal of Food Science & Technology,* 46**,** 1927-1933.

ABEYSINGHE, A. & BARAKAT, S. 2016. The Paris Agreement.

ABRAMOV, O. V. 1999. *High-intensity ultrasonics: theory and industrial applications*, CRC Press.

ADRIAN, J. E., WOLF, A., STEINBACH, A., RÖSSLER, J. & SÜSS, R. 2011. Targeted delivery to neuroblastoma of novel siRNA-anti-GD2-liposomes prepared by dual asymmetric centrifugation and sterol-based post-insertion method. *Pharmaceutical research,* 28**,** 2261-2272.

ATHERTON, E. 1989. Solid phase peptide synthesis. *A practical approach*.

ATTAMA, A. A., MOMOH, M. A. & BUILDERS, P. F. 2012. Lipid nanoparticulate drug delivery systems: a revolution in dosage form design and development. *InTech, Croatia***,** 107-140.

AVVARU, B., PATIL, M. N., GOGATE, P. R. & PANDIT, A. B. 2006. Ultrasonic atomization: effect of liquid phase properties. *Ultrasonics,* 44**,** 146-158.

AZEVEDO, M. A., CERQUEIRA, M. Â. & VICENTE, A. A. Development of biopolymer based-nanosystems for vitamins delivery. The European Symposium of Biopolymers, 2013 Lisbon, Portugal. 144.

BAIZ, D., POZZATO, G., DAPAS, B., FARRA, R., SCAGGIANTE, B., GRASSI, M., UXA, L., GIANSANTE, C., ZENNARO, C. & GUARNIERI, G. 2009. Bortezomib arrests the proliferation of hepatocellular carcinoma cells HepG2 and JHH6 by differentially affecting E2F1, p21 and p27 levels. *Biochimie,* 91**,** 373-382.

BANGHAM, A. D. & HORNE, R. 1964. Negative staining of phospholipids and their structural modification by surface-active agents as observed in the electron microscope. *Journal of molecular biology,* 8**,** 660-IN10.

BANSODE, S., BANARJEE, S., GAIKWAD, D., JADHAV, S. & THORAT, R. 2010. Microencapsulation: a review. *International journal of pharmaceutical sciences review and research,* 1**,** 38-43.

BARBA, A. A., BOCHICCHIO, S., LAMBERTI, G. & DALMORO, A. 2014. Ultrasonic energy in liposome production: process modelling and size calculation. *Soft Matter*.

BARBA, A. A., DALMORO, A., D'AMORE, M. & LAMBERTI, G. 2013. In vitro dissolution of pH sensitive microparticles for colon-specific drug delivery. *Pharmaceutical development and technology,* 18**,** 1399-1406.

BARBA, A. A., LAMBERTI, G., SARDO, C., DAPAS, B., ABRAMI, M., GRASSI, M., FARRA, R., TONON, F., FORTE, G. & MUSIANI, F. 2015. Novel Lipid and Polymeric Materials as Delivery Systems for Nucleic Acid Based Drugs. *Current drug metabolism,* 16**,** 427-452.

BARNADAS-RODRíGUEZ, R. & SABÉS, M. 2001. Factors involved in the production of liposomes with a high-pressure homogenizer. *International journal of pharmaceutics,* 213**,** 175-186.

BATTAGLIA, L., GALLARATE, M., PANCIANI, P. P., UGAZIO, E., SAPINO, S., PEIRA, E. & CHIRIO, D. 2014. Techniques for the Preparation of Solid Lipid Nano and Microparticles.

BATZRI, S. & KORN, E. D. 1973. Single bilayer liposomes prepared without sonication. *Biochimica et Biophysica Acta (BBA)-Biomembranes,* 298**,** 1015-1019.

BELOGUROV, A. A., STEPANOV, A. V., SMIRNOV, I. V., MELAMED, D., BACON, A., MAMEDOV, A. E., BOITSOV, V. M., SASHCHENKO, L. P., PONOMARENKO, N. A. & SHARANOVA, S. N. 2013. Liposome-encapsulated peptides protect against experimental allergic encephalitis. *The FASEB Journal,* 27**,** 222-231.

BENITA, S. 2006. *Microencapsulation: methods and industrial applications*, Informa HealthCare.

BIRD, R. B., STEWART, W. E. & LIGHTFOOT, E. N. 2007. *Transport phenomena*, John Wiley & Sons.

BLEVE, M., PAVANETTO, F. & PERUGINI, P. 2011. Solid Lipid Nanoparticles: Technological Developments and in Vivo Techniques to Evaluate Their Interaction with the Skin. *Progress in Molecular and Environmental Bioengineering– From Analysis and Modeling to Technology Applications*.

BOCHICCHIO, S., BARBA, A. A., GRASSI, G. & LAMBERTI, G. 2016a. Vitamin delivery: Carriers based on nanoliposomes produced via ultrasonic irradiation. *LWT-Food Science and Technology,* 69**,** 9-16.

BOCHICCHIO, S., DALMORO, A., BARBA, A., D'AMORE, M. & LAMBERTI, G. 2016b. New Preparative Approaches for Micro and Nano Drug Delivery Carriers. *Current drug delivery*.

BOCHICCHIO, S., DALMORO, A., BARBA, A. A., GRASSI, G. & LAMBERTI, G. 2014. Liposomes as siRNA Delivery Vectors. *Current drug metabolism,* 15**,** 882-892.

BOUCHEMAL, K., BRIANÇON, S., PERRIER, E. & FESSI, H. 2004. Nano-emulsion formulation using spontaneous emulsification: solvent, oil and surfactant optimisation. *International Journal of Pharmaceutics,* 280**,** 241-251.

BRADFORD, M. M. 1976. A rapid and sensitive method for the quantitation of microgram quantities of protein utilizing the principle of protein-dye binding. *Analytical biochemistry,* 72**,** 248-254.

BREGOLI, L., MOVIA, D., GAVIGAN-IMEDIO, J. D., LYSAGHT, J., REYNOLDS, J. & PRINA-MELLO, A. 2016. Nanomedicine applied to translational oncology: a future perspective on cancer treatment. *Nanomedicine: Nanotechnology, Biology and Medicine,* 12**,** 81-103.

BRGLES, M., ŠANTAK, M., HALASSY, B., FORCIC, D. & TOMAŠIĆ, J. 2012. Influence of charge ratio of liposome/DNA complexes on their size after extrusion and transfection efficiency. *International journal of nanomedicine,* 7**,** 393.

BURCK, J., BALS, C. & ROSSOW, V. 2014. *The Climate Change Performance Index: Results 2015*, Germanwatch Berlin.

BURISCH, J., JESS, T., MARTINATO, M. & LAKATOS, P. L. 2013. The burden of inflammatory bowel disease in Europe. *Journal of Crohn's and Colitis,* 7**,** 322-337.

BURISCH, J. & MUNKHOLM, P. 2015. The epidemiology of inflammatory bowel disease. *Scandinavian journal of gastroenterology,* 50**,** 942-951.

BUTTS, C., MURRAY, N., MAKSYMIUK, A., GOSS, G., MARSHALL, E., SOULIÈRES, D., CORMIER, Y., ELLIS, P., PRICE, A. & SAWHNEY, R. 2005. Randomized phase IIB trial of BLP25 liposome vaccine in stage IIIB and IV non–small-cell lung cancer. *Journal of Clinical Oncology,* 23**,** 6674-6681.

CAMPBELL, R. B., BALASUBRAMANIAN, S. V. & STRAUBINGER, R. M. 2001. Phospholipid-cationic lipid interactions: influences on membrane and vesicle properties. *Biochimica et Biophysica Acta (BBA)-Biomembranes,* 1512**,** 27-39.

CANOVA-DAVIS, E., REDEMANN, C. T., VOLLMER, Y. P. & KUNG, V. T. 1986. Use of a reversed-phase evaporation vesicle formulation for a homogeneous liposome immunoassay. *Clinical chemistry,* 32**,** 1687-1691.

CAROTENUTO, A., CIPOLLETTA, E., GOMEZ-MONTERREY, I., SALA, M., VERNIERI, E., LIMATOLA, A., BERTAMINO, A., MUSELLA, S., SORRIENTO, D. & GRIECO, P. 2013. Design, synthesis and efficacy of novel G protein-coupled receptor kinase 2 inhibitors. *European journal of medicinal chemistry,* 69**,** 384-392.

CARTER, P. J. 2011. Introduction to current and future protein therapeutics: a protein engineering perspective. *Experimental cell research,* 317**,** 1261-1269.

CASCONE, S., LAMBERTI, G., TITOMANLIO, G., BARBA, A. A. & D'AMORE, M. 2012. Microencapsulation effectiveness of small active molecules in biopolymer by ultrasonic atomization technique. *Drug development and industrial pharmacy,* 38**,** 1486-1493.

CHANG, W.-K., TAI, Y.-J., CHIANG, C.-H., HU, C.-S., HONG, P.-D. & YEH, M.-K. 2011. The comparison of protein-entrapped liposomes and lipoparticles: preparation, characterization, and efficacy of cellular uptake. *International journal of nanomedicine,* 6**,** 2403.

CHATURVEDI, S. & KUMAR, V. 2012. Production techniques of lipid nanoparticles: A review. *RJPBCS,* 3**,** 525-41.

CHEN, C., HAN, D., CAI, C. & TANG, X. 2010. An overview of liposome lyophilization and its future potential. *Journal of Controlled Release,* 142**,** 299-311.

CHIEN, P.-Y., WANG, J., CARBONARO, D., LEI, S., MILLER, B., SHEIKH, S., ALI, S. M., AHMAD, M. U. & AHMAD, I. 2005. Novel cationic cardiolipin analogue-based liposome for efficient DNA and small interfering RNA delivery in vitro and in vivo. *Cancer gene therapy,* 12**,** 321-328.

CHITHRANI, B. D. & CHAN, W. C. 2007. Elucidating the mechanism of cellular uptake and removal of protein-coated gold nanoparticles of different sizes and shapes. *Nano letters,* 7**,** 1542-1550.

CHO, N.-J., HWANG, L. Y., SOLANDT, J. J. & FRANK, C. W. 2013. Comparison of extruded and sonicated vesicles for planar bilayer self-assembly. *Materials,* 6**,** 3294-3308.

COELHO, J. F., FERREIRA, P. C., ALVES, P., CORDEIRO, R., FONSECA, A. C., GÓIS, J. R. & GIL, M. H. 2010. Drug delivery systems: Advanced technologies potentially applicable in personalized treatments. *The EPMA journal,* 1**,** 164-209.

COLLETIER, J.-P., CHAIZE, B., WINTERHALTER, M. & FOURNIER, D. 2002. Protein encapsulation in liposomes: efficiency depends on interactions between protein and phospholipid bilayer. *BMC biotechnology,* 2**,** 1.

DALMORO, A., BARBA, A. A., D'AMORE, M. & LAMBERTI, G. 2014. Single-Pot Semicontinuous Bench Scale Apparatus To Produce Microparticles. *Industrial & Engineering Chemistry Research,* 53**,** 2771-2780.

DALMORO, A., BARBA, A. A., LAMBERTI, G., GRASSI, M. & D'AMORE, M. 2012. Pharmaceutical applications of biocompatible polymer blends containing sodium alginate. *Advances in Polymer Technology,* 31**,** 219-230.

DALMORO, A., LAMBERTI, G., TITOMANLIO, G., BARBA, A. A. & D'AMORE, M. 2010. Enteric micro-particles for targeted oral drug delivery. *Aaps Pharmscitech,* 11**,** 1500-1507.

DANINO, D., LIVNEY, Y. D., RAMON, O., PORTNOY, I. & COGAN, U. 2014. Beta-casein assemblies for enrichment of food and beverages and methods of preparation thereof. Google Patents.

DAPAS, B., FARRA, R., GRASSI, M., GIANSANTE, C., FIOTTI, N., UXA, L., RAINALDI, G., MERCATANTI, A., COLOMBATTI, A. & SPESSOTTO, P. 2009. Role of E2F1–Cyclin E1-Cyclin E2 Circuit in Human Coronary Smooth Muscle Cell Proliferation and Therapeutic Potential of Its Downregulation by siRNAs. *Molecular Medicine,* 15**,** 297.

DARY, O. & HURRELL, R. Guidelines on food fortification with micronutrients.

DAS, K. & KINSELLA, J. 1990. Stability of food emulsions: physicochemical role of protein and nonprotein emulsifiers. *Advances in food and nutrition research,* 34**,** 81-201.

DAVID, S., RESNIER, P., GUILLOT, A., PITARD, B., BENOIT, J.-P. & PASSIRANI, C. 2012. siRNA LNCs–A novel platform of lipid nanocapsules for systemic siRNA administration. *European Journal of Pharmaceutics and Biopharmaceutics,* 81**,** 448-452.

DE PAOLI, T. & HAGER, A. A. 1996. Liposomes containing bioavailable iron (II) and process for obtaining them. Google Patents.

DEASSIS, L. M., MACHADO, A. R., DA MOTTA, A. D. S., COSTA, J. A. V. & DE SOUZA-SOARES, L. A. 2014. Development and Characterization of Nanovesicles Containing Phenolic Compounds of Microalgae Spirulina Strain LEB-18 and Chlorella pyrenoidosa. *Advances in Materials Physics and Chemistry,* 4**,** 6.

DEASSIS, L. M., ZAVAREZE, E. D. R., PRENTICE-HERNÁNDEZ, C. & DE SOUZA-SOARES, L. A. D. 2012. Review: characteristics of nanoparticles and their potential applications in foods. *Brazilian Journal of Food Technology,* 15**,** 99-109.

DESAI, M. P., LABHASETWAR, V., AMIDON, G. L. & LEVY, R. J. 1996. Gastrointestinal uptake of biodegradable microparticles: effect of particle size. *Pharmaceutical research,* 13**,** 1838-1845.

DESHPANDE, P. P., BISWAS, S. & TORCHILIN, V. P. 2013. Current trends in the use of liposomes for tumor targeting. *Nanomedicine,* 8**,** 1509-1528.

DUA, J., RANA, A. & BHANDARI, A. 2012. Liposome: methods of preparation and applications. *Int J Pharm Stud Res,* 3**,** 14-20.

DUBEY, R. 2009. Microencapsulation technology and applications. *Defence Science Journal,* 59**,** 82-95.

DUNCKLEY, T., COON, K. D. & STEPHAN, D. A. 2005. Discovery and development of biomarkers of neurological disease. *Drug discovery today,* 10**,** 326-334.

DWIVEDI, C., SAHU, R., TIWARI, S. P., SATAPATHY, T. & ROY, A. 2014. ROLE OF LIPOSOME IN NOVEL DRUG DELIVERY SYSTEM. *Journal of Drug Delivery and Therapeutics,* 4.

DWIVEDI, C. & VERMA, S. Review on Preparation and Characterization of Liposomes with Application.

EMAMIFAR, A., KADIVAR, M., SHAHEDI, M. & SOLEIMANIAN-ZAD, S. 2010. Evaluation of nanocomposite packaging containing Ag and ZnO on shelf life of fresh orange juice. *Innovative Food Science & Emerging Technologies,* 11**,** 742-748.

ERTOSUN, M. G., HAPIL, F. Z. & NIDAI, O. O. 2016. E2F1 transcription factor and its impact on growth factor and cytokine signaling. *Cytokine & growth factor reviews*.

FANG, Z., GONG, C., LIU, H., ZHANG, X., MEI, L., SONG, M., QIU, L., LUO, S., ZHU, Z. & ZHANG, R. 2015. E2F1 promote the aggressiveness of human colorectal cancer by activating the ribonucleotide reductase small subunit M2. *Biochemical and biophysical research communications,* 464**,** 407-415.

FARRA, R., DAPAS, B., POZZATO, G., SCAGGIANTE, B., AGOSTINI, F., ZENNARO, C., GRASSI, M., ROSSO, N., GIANSANTE, C., FIOTTI, N. & GRASSI, G. 2011. Effects of E2F1–cyclin E1–E2 circuit down regulation in hepatocellular carcinoma cells. *Digestive and Liver Disease,* 43**,** 1006-1014.

FARRAYE, F. A., ODZE, R. D., EADEN, J. & ITZKOWITZ, S. H. 2010. AGA medical position statement on the diagnosis and management of colorectal neoplasia in inflammatory bowel disease. *Gastroenterology,* 138**,** 738-745.

FERNÁNDEZ-GARCÍA, E., MÍNGUEZ-MOSQUERA, M. I. & PÉREZ-GÁLVEZ, A. 2007. Changes in composition of the lipid matrix produce a differential incorporation of carotenoids in micelles. Interaction effect of cholesterol and oil. *Innovative food science & emerging technologies,* 8**,** 379-384.

FIRE, A., XU, S., MONTGOMERY, M. K., KOSTAS, S. A., DRIVER, S. E. & MELLO, C. C. 1998. Potent and specific genetic interference by double-stranded RNA in Caenorhabditis elegans. *nature,* 391**,** 806-811.

FOOD, I. & BOARD, N. 2002. Dietary Reference Intakes: Vitamin A. *Vitamin K, Arsenic, Boron, Chromium, Copper, Iodine, Iron, Manganese, Molybdenum, Nickel, Silicon, Vanadium and Zinc. Washington, DC: National Academy Press.[PubMed]*.

FOSGERAU, K. & HOFFMANN, T. 2015. Peptide therapeutics: current status and future directions. *Drug discovery today,* 20**,** 122-128.

FREDERIKSEN, L., ANTON, K., HOOGEVEST, P. V., KELLER, H. R. & LEUENBERGER, H. 1997. Preparation of liposomes encapsulating water-soluble compounds using supercritical carbon dioxide. *Journal of pharmaceutical sciences,* 86**,** 921-928.

FROMHERZ, P. 1983. Lipid-vesicle structure: size control by edge-active agents. *Chemical Physics Letters,* 94**,** 259-266.

FUNKE, S. A. & WILLBOLD, D. 2012. Peptides for therapy and diagnosis of Alzheimer's disease. *Current pharmaceutical design,* 18**,** 755.

GASCO, M. R. 1993. Method for producing solid lipid microspheres having a narrow size distribution. Google Patents.

GODIN, B., SAKAMOTO, J. H., SERDA, R. E., GRATTONI, A., BOUAMRANI, A. & FERRARI, M. 2010. Emerging applications of nanomedicine for the diagnosis and treatment of cardiovascular diseases. *Trends in pharmacological sciences,* 31**,** 199-205.

GOLKAR, N., SAMANI, S. M. & TAMADDON, A. M. 2016. Modulated cellular delivery of anti-VEGF siRNA (bevasiranib) by incorporating supramolecular assemblies of hydrophobically modified polyamidoamine dendrimer in stealth liposomes. *International Journal of Pharmaceutics*.

GRIECO, P., GITU, P. & HRUBY, V. 2001. Preparation of 'side-chain-to-side-chain'cyclic peptides by Allyl and Alloc strategy: potential for library synthesis. *The Journal of Peptide Research,* 57**,** 250-256.

GUO, J., O'DRISCOLL, C. M., HOLMES, J. D. & RAHME, K. 2016. Bioconjugated gold nanoparticles enhance cellular uptake: A proof of concept study for siRNA delivery in prostate cancer cells. *International journal of pharmaceutics,* 509**,** 16-27.

GUPTA, S. & ABU-GHANNAM, N. 2011. Recent developments in the application of seaweeds or seaweed extracts as a means for

enhancing the safety and quality attributes of foods. *Innovative Food Science & Emerging Technologies,* 12**,** 600-609.

HADINOTO, K., SUNDARESAN, A. & CHEOW, W. S. 2013. Lipid–polymer hybrid nanoparticles as a new generation therapeutic delivery platform: a review. *European Journal of Pharmaceutics and Biopharmaceutics,* 85**,** 427-443.

HARDING, V. B., JONES, L. R., LEFKOWITZ, R. J., KOCH, W. J. & ROCKMAN, H. A. 2001. Cardiac βARK1 inhibition prolongs survival and augments β blocker therapy in a mouse model of severe heart failure. *Proceedings of the National Academy of Sciences,* 98**,** 5809-5814.

HAUSCHILD, S., LIPPRANDT, U., RUMPLECKER, A., BORCHERT, U., RANK, A., SCHUBERT, R. & FÖRSTER, S. 2005. Direct preparation and loading of lipid and polymer vesicles using inkjets. *Small,* 1**,** 1177-1180.

HELFRICH, W. 1973. Elastic properties of lipid bilayers: theory and possible experiments. *Zeitschrift für Naturforschung. Teil C: Biochemie, Biophysik, Biologie, Virologie,* 28**,** 693.

HELFRICH, W. 1974. The size of bilayer vesicles generated by sonication. *Physics Letters A,* 50**,** 115-116.

HEURTAULT, B., SAULNIER, P., PECH, B., PROUST, J.-E. & BENOIT, J.-P. 2002. A novel phase inversion-based process for the preparation of lipid nanocarriers. *Pharmaceutical research,* 19**,** 875-880.

HIRSCH, M., ZIROLI, V., HELM, M. & MASSING, U. 2009. Preparation of small amounts of sterile siRNA-liposomes with high entrapping efficiency by dual asymmetric centrifugation (DAC). *Journal of Controlled Release,* 135**,** 80-88.

HOAR, T. & SCHULMAN, J. 1943. Transparent water-in-oil dispersions: the oleopathic hydro-micelle. *Nature,* 152**,** 102-103.

HOOD, R. R., DEVOE, D. L., ATENCIA, J., VREELAND, W. N. & OMIATEK, D. M. 2014. A facile route to the synthesis of monodisperse nanoscale liposomes using 3D microfluidic hydrodynamic focusing in a concentric capillary array. *Lab on a chip*.

HOPE, M. J., NAYAR, R., MAYER, L. D. & CULLIS, P. 1993. Reduction of liposome size and preparation of unilamellar vesicles by extrusion techniques. *Liposome technology,* 1**,** 123-139.

HOW, C. W., ABDULLAH, R. & ABBASALIPOURKABIR, R. 2013. Physicochemical properties of nanostructured lipid carriers as colloidal carrier system stabilized with polysorbate 20 and polysorbate 80. *African Journal of Biotechnology,* 10**,** 1684-1689.

HUANG, Q. 2012. *Nanotechnology in the food, beverage and nutraceutical industries*, Elsevier.

HUANG, X., CADDELL, R., YU, B., XU, S., THEOBALD, B., LEE, L. J. & LEE, R. J. 2010. Ultrasound-enhanced microfluidic synthesis of liposomes. *Anticancer research,* 30**,** 463-466.

HUANG, Y.-Y. & WANG, C.-H. 2006. Pulmonary delivery of insulin by liposomal carriers. *Journal of controlled release,* 113**,** 9-14.

HUSSAIN, N., JAITLEY, V. & FLORENCE, A. T. 2001. Recent advances in the understanding of uptake of microparticulates across the gastrointestinal lymphatics. *Advanced drug delivery reviews,* 50**,** 107-142.

HUYNH, N., PASSIRANI, C., SAULNIER, P. & BENOIT, J. 2009. Lipid nanocapsules: a new platform for nanomedicine. *International journal of pharmaceutics,* 379**,** 201-209.

IACCARINO, G., BARBATO, E., CIPOLLETTA, E., DE AMICIS, V., MARGULIES, K. B., LEOSCO, D., TRIMARCO, B. & KOCH, W. J. 2005. Elevated myocardial and lymphocyte GRK2 expression and activity in human heart failure. *European heart journal,* 26**,** 1752-1758.

IBRAHEEM, D., ELAISSARI, A. & FESSI, H. 2014. Gene therapy and DNA delivery systems. *International journal of pharmaceutics,* 459**,** 70-83.

IMMORDINO, M. L., DOSIO, F. & CATTEL, L. 2006. Stealth liposomes: review of the basic science, rationale, and clinical applications, existing and potential. *International journal of nanomedicine,* 1**,** 297.

ISAILOVIĆ, B. D., KOSTIĆ, I. T., ZVONAR, A., ĐORĐEVIĆ, V. B., GAŠPERLIN, M., NEDOVIĆ, V. A. & BUGARSKI, B. M. 2013. Resveratrol loaded liposomes produced by different techniques. *Innovative Food Science & Emerging Technologies,* 19**,** 181-189.

JAAFAR-MAALEJ, C., CHARCOSSET, C. & FESSI, H. 2011. A new method for liposome preparation using a membrane contactor. *Journal of liposome research,* 21**,** 213-220.

JAHN, A., VREELAND, W. N., DEVOE, D. L., LOCASCIO, L. E. & GAITAN, M. 2007. Microfluidic directed formation of liposomes of controlled size. *Langmuir,* 23**,** 6289-6293.

JAHN, A., VREELAND, W. N., GAITAN, M. & LOCASCIO, L. E. 2004. Controlled vesicle self-assembly in microfluidic channels with hydrodynamic focusing. *Journal of the American Chemical Society,* 126**,** 2674-2675.

KAISTHA, A. & LEVINE, J. 2014. Inflammatory bowel disease: the classic gastrointestinal autoimmune disease. *Current problems in pediatric and adolescent health care,* 44**,** 328-334.

KANAAN, Z., RAI, S. N., EICHENBERGER, M. R., BARNES, C., DWORKIN, A. M., WELLER, C., COHEN, E., ROBERTS, H., KESKEY, B. & PETRAS, R. E. 2012. Differential MicroRNA expression tracks neoplastic progression in inflammatory bowel disease-associated colorectal cancer. *Human mutation,* 33**,** 551-560.

KARADAG, A., ÖZÇELIK, B., SRAMEK, M., GIBIS, M., KOHLUS, R. & WEISS, J. 2013. Presence of Electrostatically Adsorbed Polysaccharides Improves Spray Drying of Liposomes. *Journal of food science,* 78**,** E206-E221.

KHURANA, R., SIMONS, M., MARTIN, J. F. & ZACHARY, I. C. 2005. Role of angiogenesis in cardiovascular disease a critical appraisal. *Circulation,* 112**,** 1813-1824.

KIBRIA, G., HATAKEYAMA, H., SATO, Y. & HARASHIMA, H. 2016. Anti-Tumor Effect via Passive Anti-angiogenesis of PEGylated Liposomes Encapsulating Doxorubicin in Drug Resistant Tumors. *International journal of pharmaceutics*.

KIGASAWA, K., KAJIMOTO, K., HAMA, S., SAITO, A., KANAMURA, K. & KOGURE, K. 2010. Noninvasive delivery of siRNA into the epidermis by iontophoresis using an atopic dermatitis-like model rat. *International journal of pharmaceutics,* 383**,** 157-160.

KIM, H.-K., DAVAA, E., MYUNG, C.-S. & PARK, J.-S. 2010. Enhanced siRNA delivery using cationic liposomes with new polyarginine-conjugated PEG-lipid. *International journal of pharmaceutics,* 392**,** 141-147.

KOLLER, D. & LOHNER, K. 2014. The role of spontaneous lipid curvature in the interaction of interfacially active peptides with membranes. *Biochimica et Biophysica Acta (BBA)-Biomembranes,* 1838**,** 2250-2259.

KOSARAJU, S. L., TRAN, C. & LAWRENCE, A. 2006. Liposomal delivery systems for encapsulation of ferrous sulfate: preparation and characterization. *Journal of liposome research,* 16**,** 347-358.

KREMER, J., VAN DER ESKER, M., PATHMAMANOHARAN, C. & WIERSEMA, P. 1977. Vesicles of variable diameter prepared by a modified injection method. *Biochemistry,* 16**,** 3932-3935.

KULL, H.-J. 1991. Theory of the Rayleigh-Taylor instability. *Physics Reports,* 206**,** 197-325.

KWAK, H.-S. 2014. Nano-and Microencapsulation for Foods. Wiley Online Library.

LAMOUNIER, J. A., CAPANEMA, F. D., DA SILVA ROCHA, D., DE OLIVEIRA, J. E. D., DA SILVA, M. C. & DE ALMEIDA, C. A. N. 2010. Iron fortification strategies for the control of childhood anemia in Brazil. *Journal of tropical pediatrics***,** fmq001.

LAOUINI, A., JAAFAR-MAALEJ, C., GANDOURA-SFAR, S., CHARCOSSET, C. & FESSI, H. 2012a. Spironolactone-loaded liposomes produced using a membrane contactor method: An improvement of the ethanol injection technique. *UK Colloids 2011.* Springer.

LAOUINI, A., JAAFAR-MAALEJ, C., LIMAYEM-BLOUZA, I., SFAR, S., CHARCOSSET, C. & FESSI, H. 2012b. Preparation, characterization and applications of liposomes: state of the art. *Journal of Colloid Science and Biotechnology,* 1**,** 147-168.

LASIC, D. D. & PAPAHADJOPOULOS, D. 1998. *Medical applications of liposomes*, Elsevier.

LAYRISSE, M., CHAVES, J. F., BOSCH, V., TROPPER, E., BASTARDO, B. & GONZALEZ, E. 1996. Early response to the effect of iron fortification in the Venezuelan population. *The American journal of clinical nutrition,* 64**,** 903-907.

LI, C. & DENG, Y. 2004. A novel method for the preparation of liposomes: freeze drying of monophase solutions. *Journal of pharmaceutical sciences,* 93**,** 1403-1414.

LI, P., NIELSEN, H. M. & MÜLLERTZ, A. 2012. Oral delivery of peptides and proteins using lipid-based drug delivery systems. *Expert opinion on drug delivery,* 9**,** 1289-1304.

LI, Y., WANG, J., GAO, Y., ZHU, J., WIENTJES, M. G. & AU, J. L.-S. 2011. Relationships between liposome properties, cell

membrane binding, intracellular processing, and intracellular bioavailability. *The AAPS journal,* 13**,** 585-597.

LIU, C., YE, A., LIU, W., LIU, C. & SINGH, H. 2013. Liposomes as food ingredients and nutraceutical delivery systems. *AGRO FOOD INDUSTRY HI-TECH,* 24**,** 68-71.

LIU, N. & PARK, H.-J. 2010. Factors effect on the loading efficiency of Vitamin C loaded chitosan-coated nanoliposomes. *Colloids and Surfaces B: Biointerfaces,* 76**,** 16-19.

LOPEZ-RUBIO, A., GAVARA, R. & LAGARON, J. M. 2006. Bioactive packaging: turning foods into healthier foods through biomaterials. *Trends in Food Science & Technology,* 17**,** 567-575.

LU, C., STEWART, D. J., LEE, J. J., JI, L., RAMESH, R., JAYACHANDRAN, G., NUNEZ, M. I., WISTUBA, I. I., ERASMUS, J. J. & HICKS, M. E. 2012. Phase I clinical trial of systemically administered TUSC2 (FUS1)-nanoparticles mediating functional gene transfer in humans. *PLoS One,* 7**,** e34833.

LYNCH, S. R. & STOLTZFUS, R. J. 2003. Iron and ascorbic acid: proposed fortification levels and recommended iron compounds. *The Journal of nutrition,* 133**,** 2978S-2984S.

MAITANI, Y., IGARASHI, S., SATO, M. & HATTORI, Y. 2007. Cationic liposome (DC-Chol/DOPE= 1: 2) and a modified ethanol injection method to prepare liposomes, increased gene expression. *International journal of pharmaceutics,* 342**,** 33-39.

MAITANI, Y., SOEDA, H., JUNPING, W. & TAKAYAMA, K. 2001. Modified ethanol injection method for liposomes containing β-sitosterol β-D-glucoside. *Journal of liposome research,* 11**,** 115-125.

MASSING, U., CICKO, S. & ZIROLI, V. 2008. Dual asymmetric centrifugation (DAC)—A new technique for liposome preparation. *Journal of Controlled Release,* 125**,** 16-24.

MEGA, S., MIYAMOTO, M., EBIHARA, Y., TAKAHASHI, R., HASE, R., LI, L., SHICHINOHE, T., KAWARADA, Y., UEHARA, H. & KANEKO, H. 2005. Cyclin D1, E2F1 expression levels are associated with characteristics and prognosis of esophageal squamous cell carcinoma. *Diseases of the Esophagus,* 18**,** 109-113.

MEHANSHO, H. 2006. Iron fortification technology development: new approaches. *The Journal of nutrition,* 136**,** 1059-1063.

MEHNERT, W. & MÄDER, K. 2001. Solid lipid nanoparticles: production, characterization and applications. *Advanced drug delivery reviews,* 47**,** 165-196.

MELLICAN, R. I., LI, J., MEHANSHO, H. & NIELSEN, S. S. 2003. The role of iron and the factors affecting off-color development of polyphenols. *Journal of agricultural and food chemistry,* 51**,** 2304-2316.

MEURE, L. A., FOSTER, N. R. & DEHGHANI, F. 2008. Conventional and dense gas techniques for the production of liposomes: a review. *Aaps Pharmscitech,* 9**,** 798-809.

MIELE, E., SPINELLI, G. P., MIELE, E., DI FABRIZIO, E., FERRETTI, E., TOMAO, S. & GULINO, A. 2012. Nanoparticle-based delivery of small interfering RNA: challenges for cancer therapy. *International journal of nanomedicine,* 7**,** 3637.

MOHAMMADI, M., GHANBARZADEH, B. & HAMISHEHKAR, H. 2014. Formulation of Nanoliposomal Vitamin D3 for Potential Application in Beverage Fortification. *Advanced pharmaceutical bulletin,* 4**,** 569.

MOHAN, A., RAJENDRAN, S. R., HE, Q. S., BAZINET, L. & UDENIGWE, C. C. 2015. Encapsulation of food protein hydrolysates and peptides: a review. *Rsc Advances,* 5**,** 79270-79278.

MORA, J. O. 2002. Iron supplementation: overcoming technical and practical barriers. *The Journal of nutrition,* 132**,** 853S-855S.

MOZAFARI, M. 2010. Nanoliposomes: preparation and analysis. *Liposomes.* Springer.

MOZAFARI, M. R. 2005. Liposomes: an overview of manufacturing techniques. *Cellular and Molecular Biology Letters,* 10**,** 711.

MOZAFARI, M. R., REED, C. J., ROSTRON, C., KOCUM, C. & PISKIN, E. 2002. Formation and characterisation of non-toxic anionic liposomes for delivery of therapeutic agents to the pulmonary airways. *Cellular and Molecular Biology Letters,* 7**,** 243-244.

MUKHERJEE, S., RAY, S. & THAKUR, R. 2009. Solid lipid nanoparticles: a modern formulation approach in drug delivery system. *Indian journal of pharmaceutical sciences,* 71**,** 349.

NACK, H. 1970. Microencapsulation techniques applications and problems. *J. Soc. Cosmetic Chemists,* 21**,** 85-98.

NIKOLAUS, S. & SCHREIBER, S. 2007. Diagnostics of inflammatory bowel disease. *Gastroenterology,* 133**,** 1670-1689.

OLIVEIRA, C. B., RIGO, L. A., ROSA, L. D., GRESSLER, L. T., ZIMMERMANN, C. E. P., OURIQUE, A. F., DA SILVA, A. S., MILETTI, L. C., BECK, R. C. R. & MONTEIRO, S. G. 2014. Liposomes produced by reverse phase evaporation: in vitro and in vivo efficacy of diminazene aceturate against Trypanosoma evansi. *Parasitology,* 141**,** 761-769.

ORIVE, G., HERNÁNDEZ, R. M., GASCÓN, A. R. & PEDRAZ, J. L. 2005. Micro and nano drug delivery systems in cancer therapy. *Cancer Therapy,* 3**,** 131-138.

OTAKE, K., IMURA, T., YODA, S., TAKEBAYASHI, Y., SUGETA, T., NAKAZAWA, N., SAKAI, H. & ABE, M. Formation and physicochemical properties of liposomes using a supercritical reverse phase evaporation method. 6th International Symposium on Supercritical Fluids, 2003.

PARHI, R., SURESH, P. & PRADESH, I. SUPERCRITICAL FLUID TECHNOLOGY: A REVIEW.

PARK, S.-J., CHOI, S. G., DAVAA, E. & PARK, J.-S. 2011. Encapsulation enhancement and stabilization of insulin in cationic liposomes. *International journal of pharmaceutics,* 415**,** 267-272.

PATEL, A., CHOLKAR, K. & MITRA, A. K. 2014a. Recent developments in protein and peptide parenteral delivery approaches. *Therapeutic delivery,* 5**,** 337-365.

PATEL, A., PATEL, M., YANG, X. & MITRA, A. K. 2014b. Recent advances in protein and peptide drug delivery: a special emphasis on polymeric nanoparticles. *Protein and peptide letters,* 21**,** 1102.

PEER, D., KARP, J. M., HONG, S., FAROKHZAD, O. C., MARGALIT, R. & LANGER, R. 2007. Nanocarriers as an emerging platform for cancer therapy. *Nature nanotechnology,* 2**,** 751-760.

PFAFFL, M. W. 2004. Quantification strategies in real-time PCR. *AZ of quantitative PCR,* 1**,** 89-113.

PHAPAL, S. M. & SUNTHAR, P. 2013. Influence of micro-mixing on the size of liposomes self-assembled from miscible liquid phases. *Chemistry and physics of lipids,* 172**,** 20-30.

PIAZZA, O., RUSSO, I., BOCCHICCHIO, S., BARBA, A., LAMBERTI, G., ZEPPA, P., DI CRESCENZO, V.,

CARRIZZO, A., VECCHIONE, C. & CIACCI, C. 2016. Cyclin D1 Gene Silencing by siRNA in ex vivo human tissue cultures. *Current drug delivery.*

PIDGEON, C., MCNEELY, S., SCHMIDT, T. & JOHNSON, J. E. 1987. Multilayered vesicles prepared by reverse-phase evaporation: liposome structure and optimum solute entrapment. *Biochemistry,* 26**,** 17-29.

PIRES, P., SIMÕES, S., NIR, S., GASPAR, R., DÜZGÜNES, N. & DE LIMA, M. C. P. 1999. Interaction of cationic liposomes and their DNA complexes with monocytic leukemia cells. *Biochimica et Biophysica Acta (BBA)-Biomembranes,* 1418**,** 71-84.

PISAL, D. S., KOSLOSKI, M. P. & BALU-IYER, S. V. 2010. Delivery of therapeutic proteins. *Journal of pharmaceutical sciences,* 99**,** 2557-2575.

POLISENO, L., EVANGELISTA, M., MERCATANTI, A., MARIANI, L., CITTI, L. & RAINALDI, G. 2004. The energy profiling of short interfering RNAs is highly predictive of their activity. *Oligonucleotides,* 14**,** 227-232.

PONS, M., FORADADA, M. & ESTELRICH, J. 1993. Liposomes obtained by the ethanol injection method. *International journal of pharmaceutics,* 95**,** 51-56.

PORTEOUS, D. J., DORIN, J. R., MCLACHLAN, G., DAVIDSON-SMITH, H., DAVIDSON, H., STEVENSON, B., CAROTHERS, A., WALLACE, W., MORALEE, S. & HOENES, C. 1997. Evidence for safety and efficacy of DOTAP cationic liposome mediated CFTR gene transfer to the nasal epithelium of patients with cystic fibrosis. *Gene therapy,* 4**,** 210-218.

PRADHAN, P., GUAN, J., LU, D., WANG, P. G., LEE, L. J. & LEE, R. J. 2008. A facile microfluidic method for production of liposomes. *Anticancer research,* 28**,** 943-947.

PUPO, E., PADRÓN, A., SANTANA, E., SOTOLONGO, J., QUINTANA, D., DUEÑAS, S., DUARTE, C., DE LA ROSA, M. C. & HARDY, E. 2005. Preparation of plasmid DNA-containing liposomes using a high-pressure homogenization–extrusion technique. *Journal of controlled release,* 104**,** 379-396.

PUTHETI, S. 2015. Application of nanotechnology in food nutraceuticals and Pharmaceuticals. *Journal of science and technology,* 2**,** 17-23.

RAJASEKARAN, A., SIVAGNANAM, G. & XAVIER, R. 2008. Nutraceuticals as therapeutic agents: A Review. *Research Journal of Pharmacy and Technology,* 1**,** 328-340.

RAN, R., LIU, Y., GAO, H., KUANG, Q., ZHANG, Q., TANG, J., HUANG, K., CHEN, X., ZHANG, Z. & HE, Q. 2014. Enhanced gene delivery efficiency of cationic liposomes coated with PEGylated hyaluronic acid for anti P-glycoprotein siRNA: A potential candidate for overcoming multi-drug resistance. *International journal of pharmaceutics,* 477**,** 590-600.

RAN, Y. & YALKOWSKY, S. H. 2003. Halothane, a novel solvent for the preparation of liposomes containing 2-4′-amino-3′-methylphenyl benzothiazole (AMPB), an anticancer drug: A technical note. *AAPS PharmSciTech,* 4**,** 70-74.

REZA MOZAFARI, M., JOHNSON, C., HATZIANTONIOU, S. & DEMETZOS, C. 2008. Nanoliposomes and their applications in food nanotechnology. *Journal of liposome research,* 18**,** 309-327.

RIAZ, M. 1996. Liposomes preparation methods. *Pakistan journal of pharmaceutical sciences,* 9**,** 65-77.

RIGAUD, J.-L., PITARD, B. & LEVY, D. 1995. Reconstitution of membrane proteins into liposomes: application to energy-transducing membrane proteins. *Biochimica et Biophysica Acta (BBA)-Bioenergetics,* 1231**,** 223-246.

ROVOLI, M., GORTZI, O., LALAS, S. & KONTOPIDIS, G. 2013. β-Lactoglobulin improves liposome's encapsulation properties for vitamin E delivery. *Journal of liposome research***,** 1-8.

RUYSSCHAERT, T., MARQUE, A., DUTEYRAT, J.-L., LESIEUR, S., WINTERHALTER, M. & FOURNIER, D. 2005. Liposome retention in size exclusion chromatography. *BMC biotechnology,* 5**,** 11.

RYTHER, R., FLYNT, A., PHILLIPS, J. & PATTON, J. 2005. siRNA therapeutics: big potential from small RNAs. *Gene therapy,* 12**,** 5-11.

SAMAD, A., SULTANA, Y. & AQIL, M. 2007. Liposomal drug delivery systems: an update review. *Current drug delivery,* 4**,** 297-305.

SANGUANSRI, P. & AUGUSTIN, M. A. 2006. Nanoscale materials development–a food industry perspective. *Trends in Food Science & Technology,* 17**,** 547-556.

SANTIAGO, P. 2012. Ferrous versus ferric oral iron formulations for the treatment of iron deficiency: a clinical overview. *The Scientific World Journal,* 2012.

SAWANT, R. R. & TORCHILIN, V. P. 2012. Challenges in development of targeted liposomal therapeutics. *The AAPS journal,* 14**,** 303-315.

SCHATZLEIN, A. 2013. Fundamentals of Pharmaceutical Nanoscience.

SCHUBERT, R. 2002. Liposome preparation by detergent removal. *Methods in enzymology,* 367**,** 46-70.

SEKHON, B. S. 2010. Supercritical fluid technology: an overview of pharmaceutical applications. *International Journal of PharmTech Research,* 2**,** 810-826.

SESSA, G. & WEISSMANN, G. 1968. Phospholipid spherules (liposomes) as a model for biological membranes. *Journal of lipid research,* 9**,** 310-318.

SHAH, R., ELDRIDGE, D., PALOMBO, E. & HARDING, I. 2015. Lipid Nanoparticles: Production, Characterization and Stability. *SpringerBriefs in Pharmaceutical Science & Drug Development (*

SHAJI, J. & BHATIA, V. 2013. Proliposomes: a brief overview of novel delivery system. *Int J Pharm Biosci,* 4**,** 150-160.

SHARIAT, S., BADIEE, A., JAAFARI, M. R. & MORTAZAVI, S. A. 2014. Optimization of a method to prepare liposomes containing HER2/Neu-derived peptide as a vaccine delivery system for breast cancer. *Iranian journal of pharmaceutical research: IJPR,* 13**,** 15.

SHINODA, K. & ARAI, H. 1964. The correlation between phase inversion temperature in emulsion and cloud point in solution of nonionic emulsifier. *The Journal of Physical Chemistry,* 68**,** 3485-3490.

SHUM, H. C., LEE, D., YOON, I., KODGER, T. & WEITZ, D. A. 2008. Double emulsion templated monodisperse phospholipid vesicles. *Langmuir,* 24**,** 7651-7653.

SIEKMANN, B. & WESTESEN, K. 1992. Submicron-sized parenteral carrier systems based on solid lipids. *Pharm. Pharmacol. Lett,* 1**,** 123-126.

SILVA, A., ROSALIA, R., SAZAK, A., CARSTENS, M., OSSENDORP, F., OOSTENDORP, J. & JISKOOT, W. 2013. Optimization of encapsulation of a synthetic long peptide in PLGA nanoparticles: low-burst release is crucial for efficient

CD8+ T cell activation. *European Journal of Pharmaceutics and Biopharmaceutics,* 83**,** 338-345.

SILVA, C., MORAES, M., CARVALHO, J. & PINHO, S. Characterization of spray-dried phospholipid particles for the production of beta-carotene-loaded liposomes.

SINGH, H. 2016. Nanotechnology Applications in Functional Foods; Opportunities and Challenges. *Preventive nutrition and food science,* 21**,** 1.

SINGHAL, G. B., PATEL, R. P., PRAJAPATI, B. & PATEL, N. A. 2011. Solid lipid nanoparticles and nano lipid carriers: as novel solid lipid based drug carrier. *Int Res J Pharm,* 2**,** 20-52.

SJÖSTRÖM, B. & BERGENSTÅHL, B. 1992. Preparation of submicron drug particles in lecithin-stabilized o/w emulsions I. Model studies of the precipitation of cholesteryl acetate. *International journal of pharmaceutics,* 88**,** 53-62.

SMITH, J., ZHANG, Y. & NIVEN, R. 1997. Toward development of a non-viral gene therapeutic. *Advanced drug delivery reviews,* 26**,** 135-150.

SOOTTITANTAWAT, A., TAKAYAMA, K., OKAMURA, K., MURANAKA, D., YOSHII, H., FURUTA, T., OHKAWARA, M. & LINKO, P. 2005. Microencapsulation of *l*-menthol by spray drying and its release characteristics. *Innovative Food Science & Emerging Technologies,* 6**,** 163-170.

SRINIVAS, P. R., PHILBERT, M., VU, T. Q., HUANG, Q., KOKINI, J. L., SAOS, E., CHEN, H., PETERSON, C. M., FRIEDL, K. E. & MCDADE-NGUTTER, C. 2010. Nanotechnology research: applications in nutritional sciences. *The journal of nutrition,* 140**,** 119-124.

STEICHEN, S. D., CALDORERA-MOORE, M. & PEPPAS, N. A. 2013. A review of current nanoparticle and targeting moieties for the delivery of cancer therapeutics. *European Journal of Pharmaceutical Sciences,* 48**,** 416-427.

STEKEL, A., MONCKEBERG, F. & BEYDA, V. 1986a. Combating iron deficiency in Chile: a case study.

STEKEL, A., OLIVARES, M., PIZARRO, F., CHADUD, P., LOPEZ, I. & AMAR, M. 1986b. Absorption of fortification iron from milk formulas in infants. *The American journal of clinical nutrition,* 43**,** 917-922.

SU, C., XIA, Y., SUN, J., WANG, N., ZHU, L., CHEN, T., HUANG, Y. & LIANG, D. 2014. Liposomes Physically Coated with

Peptides: Preparation and Characterization. *Langmuir,* 30**,** 6219-6227.

SWEENEY, L. G., WANG, Z., LOEBENBERG, R., WONG, J. P., LANGE, C. F. & FINLAY, W. H. 2005. Spray-freeze-dried liposomal ciprofloxacin powder for inhaled aerosol drug delivery. *International journal of pharmaceutics,* 305**,** 180-185.

SZOKA, F. & PAPAHADJOPOULOS, D. 1978. Procedure for preparation of liposomes with large internal aqueous space and high capture by reverse-phase evaporation. *Proceedings of the National Academy of Sciences,* 75**,** 4194-4198.

TABANDEH, H. & MORTAZAVI, S. A. 2013. An Investigation into Some Effective Factors on Encapsulation Efficiency of Alpha-Tocopherol in MLvs and the Release Profile from the Corresponding Liposomal Gel. *Iranian journal of pharmaceutical research: IJPR,* 12**,** 21.

TAGALAKIS, A. D., DO HYANG, D. L., BIENEMANN, A. S., ZHOU, H., MUNYE, M. M., SARAIVA, L., MCCARTHY, D., DU, Z., VINK, C. A. & MAESHIMA, R. 2014. Multifunctional, self-assembling anionic peptide-lipid nanocomplexes for targeted siRNA delivery. *Biomaterials,* 35**,** 8406-8415.

TAN, M. L., CHOONG, P. F. & DASS, C. R. 2010. Recent developments in liposomes, microparticles and nanoparticles for protein and peptide drug delivery. *Peptides,* 31**,** 184-193.

TAN, Y.-C., CRISTINI, V. & LEE, A. P. 2006. Monodispersed microfluidic droplet generation by shear focusing microfluidic device. *Sensors and Actuators B: Chemical,* 114**,** 350-356.

TEIXEIRA, M. L., DOS SANTOS, J., SILVEIRA, N. P. & BRANDELLI, A. 2008. Phospholipid nanovesicles containing a bacteriocin-like substance for control of< i> Listeria monocytogenes</i>. *Innovative food science & emerging technologies,* 9**,** 49-53.

TONIAZZO, T., BERBEL, I. F., CHO, S., FÁVARO-TRINDADE, C. S., MORAES, I. C. F. & PINHO, S. C. 2014. β-carotene-loaded liposome dispersions stabilized with xanthan and guar gums: Physico-chemical stability and feasibility of application in yogurt. *LWT - Food Science and Technology,* 59**,** 1265-1273.

TORRES, M. A., LOBO, N. F., SATO, K. & QUEIROZ, S. D. S. 1996. Fortification of fluid milk for the prevention and

treatment of iron defficiency anemia in children under 4 years of age. *Revista de Saúde Pública,* 30**,** 350-357.

TRURAN, S., WEISSIG, V., RAMIREZ-ALVARADO, M., FRANCO, D. A., BURCIU, C., GEORGES, J., MURARKA, S., OKOTH, W. A., SCHWAB, S. & HARI, P. 2014. Nanoliposomes protect against AL amyloid light chain protein-induced endothelial injury. *Journal of liposome research,* 24**,** 69-73.

TSIKLAURI, L., DAYYOUB, E., TSAGAREISHVILI, G., VACHNADZE, V. & BAKOWSKY, U. OP 7. PEGYLATED HERBAL LOADED NANOSTRUCTURED LIPID CARRIERS FOR THE THERAPY OF CARDIOVASCULAR DESEASE. 3rd INTERNATIONAL CONFERENCE on PHARMACEUTICAL SCIENCES. 34.

ULRICH, A. S. 2002. Biophysical aspects of using liposomes as delivery vehicles. *Bioscience Reports,* 22**,** 129-150.

ÜNER, M. 2006. Preparation, characterization and physico-chemical properties of solid lipid nanoparticles (SLN) and nanostructured lipid carriers (NLC): their benefits as colloidal drug carrier systems. *Die Pharmazie-An International Journal of Pharmaceutical Sciences,* 61**,** 375-386.

VAN DER MEEL, R., FENS, M. H., VADER, P., VAN SOLINGE, W. W., ENIOLA-ADEFESO, O. & SCHIFFELERS, R. M. 2014. Extracellular vesicles as drug delivery systems: lessons from the liposome field. *Journal of Controlled Release,* 195**,** 72-85.

WAGNER, A. & VORAUER-UHL, K. 2010. Liposome technology for industrial purposes. *Journal of drug delivery,* 2011.

WAGNER, A., VORAUER-UHL, K. & KATINGER, H. 2002a. Liposomes produced in a pilot scale: production, purification and efficiency aspects. *European journal of pharmaceutics and biopharmaceutics,* 54**,** 213-219.

WAGNER, A., VORAUER-UHL, K., KREISMAYR, G. & KATINGER, H. 2002b. The crossflow injection technique: an improvement of the ethanol injection method. *Journal of liposome research,* 12**,** 259-270.

WALLACE, S. J., LI, J., NATION, R. L. & BOYD, B. J. 2012. Drug release from nanomedicines: selection of appropriate encapsulation and release methodology. *Drug delivery and translational research,* 2**,** 284-292.

WANG, T., DENG, Y., GENG, Y., GAO, Z., ZOU, J. & WANG, Z. 2006. Preparation of submicron unilamellar liposomes by freeze-drying double emulsions. *Biochimica et Biophysica Acta (BBA)-Biomembranes,* 1758**,** 222-231.

WEBER, S., ZIMMER, A. & PARDEIKE, J. 2014. Solid Lipid Nanoparticles (SLN) and Nanostructured Lipid Carriers (NLC) for pulmonary application: A review of the state of the art. *European Journal of Pharmaceutics and Biopharmaceutics,* 86**,** 7-22.

WEI, L., GUO, X.-Y., YANG, T., YU, M.-Z., CHEN, D.-W. & WANG, J.-C. 2016. Brain tumor-targeted therapy by systemic delivery of siRNA with Transferrin receptor-mediated core-shell nanoparticles. *International Journal of Pharmaceutics,* 510**,** 394-405.

WOODBURY, D. J., RICHARDSON, E. S., GRIGG, A. W., WELLING, R. D. & KNUDSON, B. H. 2006. Reducing liposome size with ultrasound: bimodal size distributions. *Journal of liposome research,* 16**,** 57-80.

XIA, S. & XU, S. 2005. Ferrous sulfate liposomes: preparation, stability and application in fluid milk. *Food research international,* 38**,** 289-296.

XU, Y., HUI, S.-W., FREDERIK, P. & SZOKA, F. C. 1999. Physicochemical characterization and purification of cationic lipoplexes. *Biophysical journal,* 77**,** 341-353.

YASSIN, A. E. B., ANWER, M. K., MOWAFY, H. A., EL-BAGORY, I. M., BAYOMI, M. A. & ALSARRA, I. A. 2010. Optimization of 5-flurouracil solid-lipid nanoparticles: a preliminary study to treat colon cancer. *International journal of medical sciences,* 7**,** 398.

YILDIRIMER, L., THANH, N. T., LOIZIDOU, M. & SEIFALIAN, A. M. 2011. Toxicology and clinical potential of nanoparticles. *Nano today,* 6**,** 585-607.

YIN, F., GUO, S., GAN, Y. & ZHANG, X. 2014. Preparation of redispersible liposomal dry powder using an ultrasonic spray freeze-drying technique for transdermal delivery of human epithelial growth factor. *International journal of nanomedicine,* 9**,** 1665.

YING, B. 2010. siRNA-loaded cationic liposomes for cancer therapy: development, characterization and efficacy evaluation. *Pharmaceutical Science Dissertations*.

YING, L., HOFSETH, A. B., BROWNING, D. D., NAGARKATTI, M., NAGARKATTI, P. S. & HOFSETH, L. J. 2007. Nitric oxide inactivates the retinoblastoma pathway in chronic inflammation. *Cancer research,* 67**,** 9286-9293.

YU, B., LEE, R. J. & LEE, L. J. 2009. Microfluidic methods for production of liposomes. *Methods in enzymology,* 465**,** 129-141.

ZHAO, Y., XIA, F. & JIN, H. PREPARATION OF LIPOSOME PRECURSORS BY SUPERCRITICAL ANTI-SOLVENT TECHNIQUES.

ZHENG, S., ZHENG, Y., BEISSINGER, R. & FRESCO, R. 1994. Microencapsulation of hemoglobin in liposomes using a double emulsion, film dehydration/rehydration approach. *Biochimica et Biophysica Acta (BBA)-Biomembranes,* 1196**,** 123-130.

ZUIDAM, N. J. & BARENHOLZ, Y. 1997. Electrostatic parameters of cationic liposomes commonly used for gene delivery as determined by 4-heptadecyl-7-hydroxycoumarin. *Biochimica et Biophysica Acta (BBA)-Biomembranes,* 1329**,** 211-222.

Acknowledgments

Finally I would like to acknowledge the most important people in my life.

I warmly thank Massimiliano, my love mate, whose presence has been crucial in all aspects of my PhD career. Thank you for always understood and supported my choices with great respect, love and sacrifice, for sharing with me these unruly years traveling around Italy, for being a constant source of strength and inspiration in my life.

Thanks to my acquired sister Francesca for sharing with me tears and joys, bills and pizzas (sometimes both too salty), for paying with me the gym and never go. Thanks for your great positivity, sensibility and your support for reaching towards my goal. Simply thanks for always have been there for me.

Thanks to my lifetime-friend Chiara, who even thousands of miles away has been always present during this years with the same good tips ever and her formidable aptitude in instantly understanding me.
Thank you for always believing in me!

Words cannot express how I immensely thank my family.

I thank my mother for her untiring dedication to every aspects of my life, for her essential support during each step, for having always motivated me to give my best.

I thank my father for his constant encouragement, for never having lost a single stride of my research activity, for his unique ability to play down and laugh about it.

I thank my sister, Alessia, my life – landmark, for the support during these years, for our phone calls which always relieved me from all the uncertainties. Thank you and Gianluca for the loving hospitality, without I could not go on in these years.

I thank my brother, Massimiliano, for his presence and fresh life perspective, for the moral support and especially for our weekends full of nonsense laughter which have always given me the energy to face on Mondays. Thanks for being so crazy!